Studies of Lipid Peroxidation, its Link to Human Pathologies, and Isotopic Reinforcement of Polyunsaturated Fatty Acids as a Strategy to Reduce Oxidative Damage

By

Connor Reid Lamberson

Dissertation

Submitted to the Faculty of the

Graduate School of Vanderbilt University

in partial fulfillment of the requirements

for the degree of

DOCTOR OF PHILOSOPHY

in

Chemistry

May 31, 2017

Nashville, Tennessee

Approved:

Ned A. Porter, Ph.D.

Lawrence J. Marnett, Ph.D.

John A. McLean, Ph.D.

Brian O. Bachmann, Ph.D.

For Grandpa.

Thank you for the memories and wisdom you imparted on me.

ACKNOWLEDGEMENTS

This work was made possible by generous support from the National Science Foundation grant, the National Institute of Health grant, funding from Retrotope, Inc., the Vanderbilt Institute for Chemical Biology and Vanderbilt University College of Arts and Science.

First and foremost, I would like to extend my thanks and gratitude to my Ph.D. advisor, Professor Ned A. Porter. He provided the framework, support, and freedom for me to pursue my scientific interests over the past five years. He has been an excellent scientific mentor as well as a tremendous role model. His career exudes passion and drive, traits which have undoubtedly rubbed off on myself and countless other students over the years.

I would also like to thank my dissertation committee members Dr. Lawrence J. Marnett, Dr. John A. McLean, and Dr. Brian O. Bachmann. They have all provided valuable suggestions and guidance through committee meetings as well as course work. All have at one time or another opened up their labs to me as well, allowing me to expand my scientific knowledge and skill all while broadening my horizons.

I have been fortunate to work with a number of wonderful people who have provided both mentorship and friendship. Dr. Libin Xu was an invaluable resource and friend. He was an excellent mentor, and his work ethic left a lasting impression on me – I will be forever grateful for his help and friendship. The rest of the lab – Dr. Keri Tallman, Dr. Hye-Young Kim, Dr. Wei Liu, and Dr. Hubert Muchalski – have also been excellent friends and coworkers. They were always friendly, helpful, and continually dropped what they were doing to answer my questions or shoot the breeze. I'll miss their daily companionship as I move on into the next chapter of my career.

I would also like to extend a special thank you to Misha Shchepinov and Retrotope, Inc. for providing me with deuterated fatty acids, funding, and stimulating conversations. I admire the drive and passion that Misha has for his ideas and passions, and truly appreciate all of the help and support he provided over the years.

Beyond my lab mates, I would like to say a sincere thank you to Dr. Rafael Montenegro. He provided instrumental support for a number of my projects in spite of all of the work he was doing pursuing his Ph.D. More importantly, he was an excellent friend and roommate. He expanded my world view through insightful discussions and his been there for me during my highest and lowest moments. I also want to extend a special thank you to Dr. William N. Beavers, Dr. James Galligan, Michelle Mitchner, and James Wepy, all of the Marnett lab. They provided valuable support over the last two years as I dove headfirst into the macrophage world. They also proved to be excellent friends.

Finally, I would like to thank my family. Their love and support over the years has been astounding, and I will be forever thankful for them. My new wife, Kimberly, has also been wonderful over the past five years. She provided me with not only love and support, but reminded me of the important things in life whenever I lost sight of them. Her companionship kept me going when things became difficult, and her thoughtful and caring personality continually brought me smiles when I needed them.

TABLE OF CONTENTS

LIST OF TABLES

LIST OF FIGURES

LIST OF ABBREVIATIONS/NOMENCLATURE/SYMBOLS

‡	Transition state
θ'	Secondary dihedral angle
κ	Force constant
μ	Reduced mass
τ	Time (s)
υ	Fundamental vibrational frequency
7α-OH	7α-hydroxycholesterol
7β-OH	7β-hydroxycholesterol
7α-OOH	7α-hydroperoxycholesterol
7β-OOH	7β-hydroperoxycholesterol
7-DHC	7-Dehydrocholesterol
7-keto-chol	7-Ketocholesterol
8-DHC	8-Dehydrocholesterol
11-D_1-Lnn	11-D_1-Linolenic acid
11,11-D_2-Lnn	11,11-D_2-Linolenic acid
14,14-D_2-Lnn	14,14-D_2-Linolenic acid
AA	Arachidonic acid
aAA	Alkynyl arachidonic acid
aBiotin	Alkynyl biotin
aHNE	Alkynyl 4-hydroxy-2-nonenal
aLA	Alkynyl linoleic acid

AAPH	2,2'-Azobis(amidinopropane) dihydrochloride
AIBN	2,2'-Azobis-isobutyrylnitrile
AMVN	2,2'-Azobis(2,4-dimethylvaleronitrile)
APCI	Atmospheric pressure chemical ionization
ARE	Antioxidant response element
BDE	Bond dissociation enthalpy
BHT	Butylated hydroxytoluene
BRPRA	British Rubber Producers Research Association
CAT	Catalase
$CoQH_2$	Ubiquinol
COX	Cyclooxygenase
COX1	Cyclooxygenase-1
COX2	Cyclooxygenase-2
$cPLA_2$	Cytosolic phospholipase A_2
Cys	Cysteine
D	Deuterium
D_1-LA	11-D_1-Linoleic acid
D_2-LA	11,11-D_2-Linoleic acid
D_4-LA	11,11,14,14-D_4-Linoleic acid
D-PUFA	Deuterated polyunsaturated fatty acid
Da	Dalton
DHA	Docosahexaenoic acid
DHCEO	3β,5α-dihydroxy-cholest-7-en-6-one

DHCR7	7-Dehydrocholesterol reductase
DHCR24	24-Dehydrocholesterol reductase
E_a	Activation energy
EPR	Electron paramagnetic resonance
ERG	Electron releasing groups
EWG	Electron withdrawing groups
H	Hydrogen
h	Plank’s constant
HETE	Hydroxyeicosatetraenoic acid
His	Histidine
HODE	Hydroxyoctadecadienoic acid
HpETE	Hydroperoxyeicosatetraenoic acid
HPLC	High performance liquid chromatography
HpODE	Hydroperoxyoctadecadienoic acid
HNE	4-Hydroxy-2-nonenal
HRMS	High resolution mass spectrometry
iNOS	Inducible nitric oxide synthase
KIE	Kinetic isotope effect
KLA	Kdo2-Lipid A
k_p	Propagation rate constant
LA	Linoleic acid
LDL	Human low-density lipoprotein
Lnn	Linolenic acid

LOX	Lipoxygenase
LPS	Lipopolysaccharide
Lys	Lysine
MDA	Malondialdehyde
MeOAMVN	2,2’-Azobis(4-methoxy-2-dimethylvaleronitrile)
MS	Mass spectrometry
m/z	Mass-to-charge ratio
N_3-Biotin	Azido biotin
NMR	Nuclear magnetic resonance
NO	Nitric oxide
NO_2^-	Nitrite
ONE	4-oxo-2-nonenal
R_i	Rate of initiation
S. cerevisiae	*Saccharomyces cerevisiae*
SDS-PAGE	Tris-glycine polyacrylamide gels
SOD	Superoxide dismutase
PAMPs	Pathogen-associated molecular patterns
PD	Parkinson’s disease
PGs	Prostaglandins
PGH_2	Prostaglandin H_2
PMHC	2,2,5,7,8-Pentamethyl-6-chromanol
POPC	1-Palmitoyl-2-oleoyl-*sn*-glycero-phosphocholine
PPh_3	Triphenylphosphine

PUFA	Polyunsaturated fatty acid
RNS	Reactive nitrogen species
ROS	Reactive oxygen species
SLOS	Smith-Lemli-Opitz syndrome
SOMO	Semioccupied molecular orbital
TLR4	Toll-like receptor 4
TMP	Tocopherol-mediated peroxidation
TocH	α-Tocopherol
Toc·	Tocopheryl radical
Tyr	Tyrosine
UV	Ultraviolet
ZPE	Zero point energy

Chapter I

FREE RADICALS, LIPID PEROXIDATION, AND THE LINK TO HUMAN PATHOLOGIES

1.1. Introduction

Lipids are loosely defined as a group of naturally occurring organic compounds which are hydrophobic or amphipathic in nature, but which are also readily soluble in organic solvents.[1] These solubility features are present in an extremely heterogeneous collection of molecules such as fatty acids, phospholipids, eicosanoids, and sterols.[2] Some selected structures are shown in Figure 1.

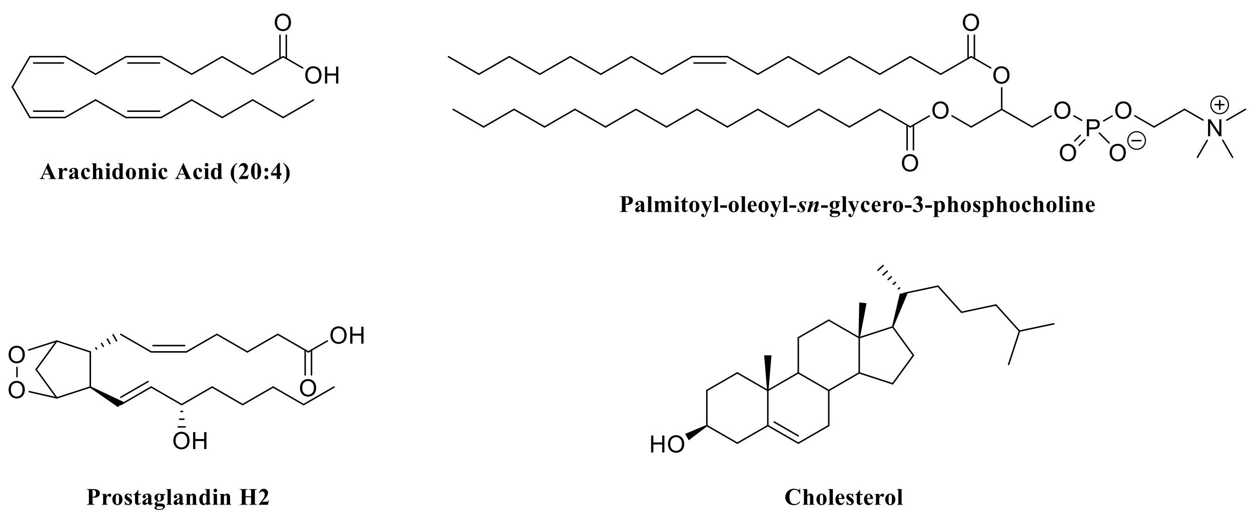

Figure 1. Selected lipids.

The functions of various lipids are as diverse as their structure (Figure 1). For instance, arachidonic acid is a polyunsaturated fatty acid (PUFA) that can be found in a variety of phospholipids and that plays an important role in cellular signaling.[3] It is also a substrate for cyclooxygenase-2 (COX2) which synthesizes prostaglandin H_2 (PGH_2) in response to environmental stress.[4,5,6] 1-Palmitoyl-2-oleoyl-*sn*-glycero-phosphocholine (POPC) is a member of the phosphatidylcholine class, which is a major component of biological membranes. Cholesterol is an essential component of animal cell membranes, providing structural integrity and fluidity; it also serves as a precursor to the biosynthesis of bile acids and steroid hormones.[7]

Many lipids are susceptible to free radical oxidation and degradation in the presence of reactive oxygen species (ROS)[8] and reactive nitrogen species (RNS).[9] The oxidation of lipids has physiological consequences ranging from the breakdown of lipid bilayers to inflammation and the progression of human disease states such as Parkinson's disease (PD)[10, 11] and atherosclerosis.[12,13]

The aim of this introductory chapter is to provide an overview of free radicals, the free radical oxidation of lipids, and a description of how the rate constants for these processes are measured. The links between the oxidation of lipids and the progression of various human pathologies will also be discussed.

1.2. Historical Background

Around the year 1800, Swiss chemist Theodore de Saussure conducted the first recorded experiments concerning lipid oxidation. Armed with a primitive mercury manometer, de Saussure was able to observe a layer of walnut oil absorb nearly 150 times its own volume of oxygen over a one year period.[14] This was the first instance in which oxygen was implicated in a reaction with some constituent of the oil. However, its involvement in free radical mediated processes was at least a century away from being fully understood.

Evidence for the existence of the free radical species was first reported in the literature in 1900 by Gomberg in his article in the *Journal of the American Chemical Society* outlining the existence of the triphenylmethyl radical.[15] The discovery came about during attempts to synthesize hexaphenylethane with the intent to study stereochemical aspects attached to the compound.

Gomberg made a number of experimental observations that ultimately pointed to the existence of the triphenylmethyl radical:

1. Zinc abstracts the halogen atom from the precursor triphenylchloromethane to give the carbon centered radical;
2. The formed radical is stable in both solution and dry crystalline state for weeks under an inert atmosphere;
3. Oxygen adds to triphenylmethane to give a peroxide;
4. Triphenyliodomethane is formed from triphenylchloromethane in the presence of iodine;

Gomberg unequivocally reserved the field for himself at the end of the article, and he would eventually come to be known as the father of organic free radical chemistry.

Nearly twenty years after Gomberg's landmark paper, many aspects of peroxidation began to emerge. It was found that linoleic acid (LA) oxidized at a higher rate than oleic acid,[16] and two years later that linolenic acid oxidized faster than LA.[17] The mechanism of oxidation continued to be explored in the years after Stephens' successful isolation of a cyclohexene derived peroxide.[18]

1.3. Free Radicals

As it is understood today, a free radical is an atom, molecule, or ion that has an unpaired valence electron residing in one of its electronic orbitals. According to the Pauli principle, this lone electron has a magnetic moment that can be expressed by a quantum number of + ½ or – ½, making the radical paramagnetic in nature. The stability of carbon free radicals mirrors that of carbocations, with a stability hierarchy of 3˚ > 2˚ > 1˚, with conjugation resulting in further stabilization. Relative stability for various organic compounds may also be discerned by studying bond dissociation enthalpy (BDE) (Figure 2). In general, as the BDE of the bond being broken increases, the stability of the resulting radical decreases.[19]

$$\text{R-H} \xrightarrow{\Delta H} \text{R}\bullet + \text{H}\bullet \qquad \Delta H = \text{BDE (kcal/mol)}$$

Figure 2. Bond Dissocation Enthalpy

Free radicals can be formed through a homolysis (bond breaking event) in which the pair of electrons comprising the bond are split evenly and each fragment retains one electron (Figure 2). An electron transfer can also occur to give a radical species and a charged species. This can be spontaneous in nature as some compounds are inherently unstable, but more often an external perturbation is required for the generation. These events can include irradiation, heat, natural biological processes (i.e. electron transport chain),[20] or a biological response to various environmental stimuli.[21,22,23,24]

1.3.1. Free Radical Oxidation

As the 20th century progressed, production-line assembly of vehicles and two world wars spurred the West's appetite for rubber. The British Rubber Producers Research Association (BRPRA) was born out of these unique pressures. Bolland and Gee carried out a number of studies on the oxidation of polyunsaturated fatty acids and other related isoprenoids at the BRPRA during the '40s and early '50s.[25] Their work on ethyl linoleate outlined a mechanism for the autoxidation of this compound in which a hydrogen atom is abstracted from the center carbon flanked on either side by an olefin, a process resulting in a conjugated pentadienyl radical with three resonance structures. Molecular oxygen from the atmosphere adds to this radical to give conjugated peroxyl radicals which then propagate the chain reaction through another hydrogen atom transfer as shown in Figure 3.[26]

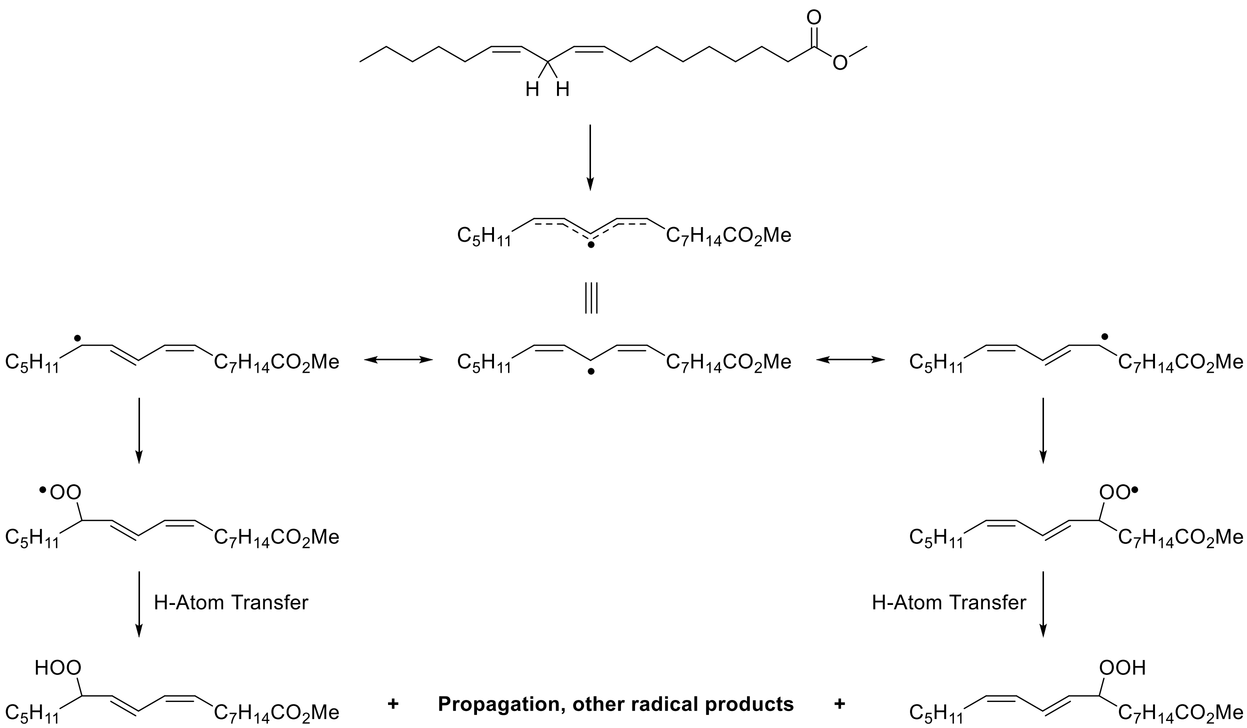

Figure 3. Autoxidation of methyl linoleate.

Interest in the free radical oxidation of lipids increased in the last five decades as scientists began to discover the role of free radicals in various areas of biological interest[27] including radical production by enzymes,[28] photosynthesis,[29,30] and the superoxide anion radical.[31,32] Lipid peroxidation has been intrinsically linked to human pathologies such as heart disease,[33,34] environmental exposures,[35] neurodegenerative disorders,[36,37] cancer,[38,39] and diabetes.[40]

The autoxidation of lipids and other organic compounds results in the buildup of peroxides which can initiate chain reactions under certain conditions, a process that leads to the consumption of oxygen as further peroxide products are formed. The process follows three separate steps: initiation, propagation, and termination (Figure 4).

Initiation: $R{-}H + In\cdot \longrightarrow R\cdot$

Propagation: $R\cdot + O_2 \longrightarrow R{-}OO\cdot$

$R{-}OO\cdot + R{-}H \xrightarrow{k_p} R{-}OOH + R\cdot$

Termination: $R\ 2{-}OO\cdot \longrightarrow$ nonradical products (ketones, alcohols)

Figure 4. General scheme for the autoxidation of lipids

1.3.2. Initiation of Autoxidation

The first step of free radical chain oxidation is initiation, in which a carbon centered radical is formed. In biological systems, the initiation event can occur through a variety of environmental events. These include UV-light, ionizing radiation, or chemical species found in air pollution. The initiating event may also be sparked via enzymatic means such as cytochrome P450s, xanthine oxidase, or a variety of other enzymes.

In order to study these mechanistically complex reactions, solution oxidations have been carried out to remove or control variables associated with initiation events. Under these controlled laboratory conditions, it is desirable to generate a consistent stream of free radicals at a well defined rate for the reaction being studied. Azo initiators have filled this role for the following reasons:

1. Azo initiators decompose by first-order kinetics under most conditions
2. Water and lipid soluble initiators are widely available
3. Initiators can be tailored to fit particular temperature regimes
4. Peroxyl or alkoxyl radical species are produced

Azo initiators decompose thermally to give molecular nitrogen and a pair of radicals (Figure 5A). The radical formed after decomposition may be carbon centered, as is the case with AAPH, AMVN, AIBN, and MeOAMVN (Figure 5B). Once decomposition occurs, the resulting carbon-centered alkyl radicals readily add molecular oxygen to give two peroxyl radicals. These peroxyl radicals then initiate the free radical chain reaction by abstracting hydrogen from neighboring organic compounds to give new carbon centered radicals.

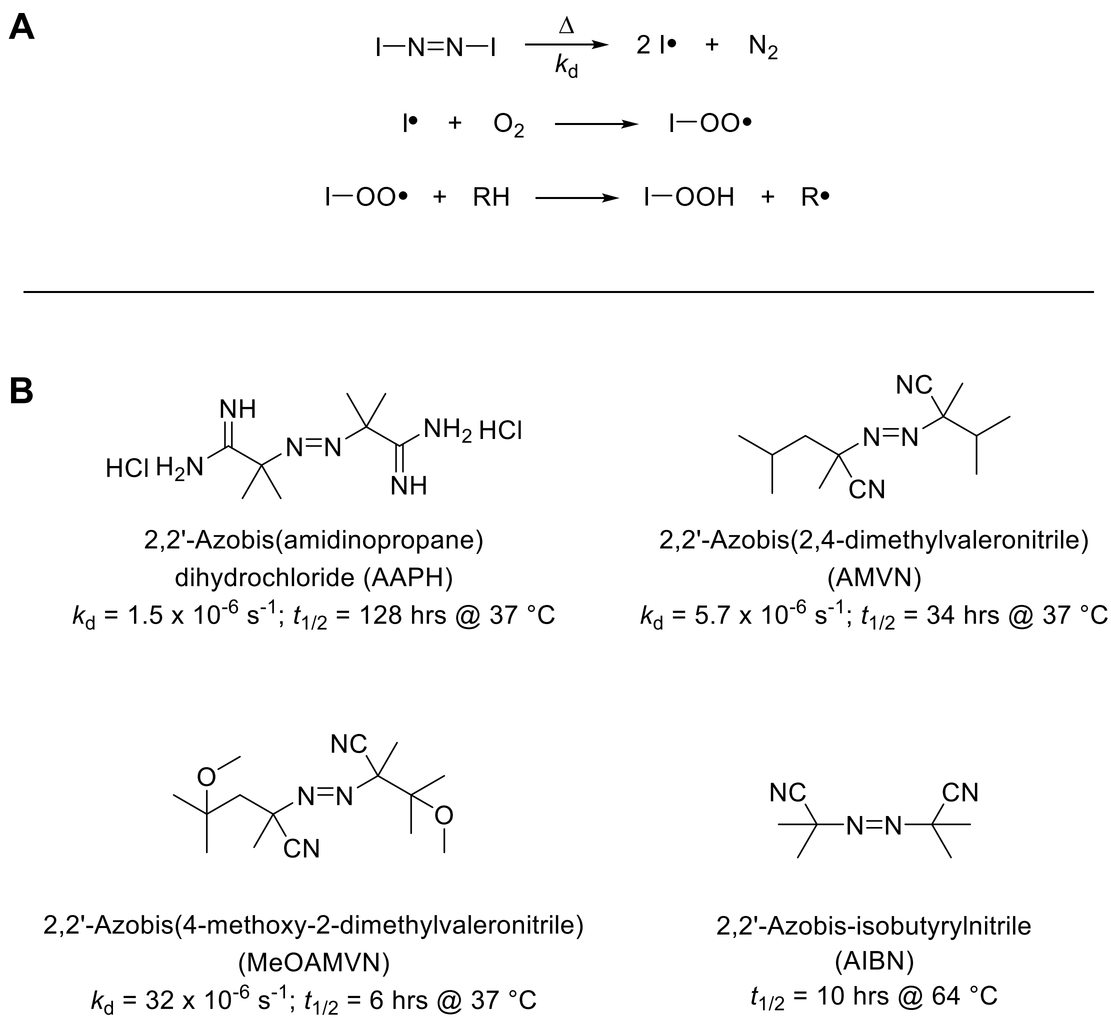

Figure 5. Azo initiators are used to generate a consistent stream of free radicals at a well-defined rate and are commonly used in solution oxidations of organic compounds. **A.** Scheme for decomposition of azo initiators; **B.** Selected azo initiators.

1.3.3. Propagation of Autoxidation

Once a carbon-centered radical is formed, propagation usually occurs through the two steps shown in Figure 6. In the first step molecular oxygen adds to the newly formed carbon-centered radical to give a peroxyl radical. This addition occurs at the diffusion controlled rate constant when oxygen pressures are above 100 mmHg.[41] Subsequent steps occur at rates slower than oxygen addition, thus the peroxyl radical is the predominant radical species present during autoxidation.[42]

The second step in propagation occurs when the newly formed peroxyl radical abstracts hydrogen from a reactive molecule. This step is bound by parameters that result in a much slower reaction rate when compared to the addition of oxygen to the carbon centered radical. Thus, H-atom abstraction is considered to be the rate-determining step for the peroxidation process. Measurement of the propagation rate constant (k_p) provides insight to the oxidizability of the compound being interrogated.

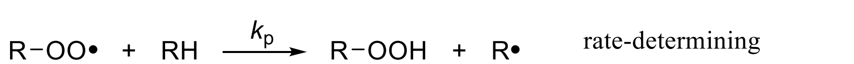

Figure 6. Peroxyl radical formation and hydrogen atom abstraction (k_p) occurring during propagation.

Peroxyl radicals can also undergo addition to carbon-carbon double bonds as shown in Figure 7. Once the peroxyl radical adds, a new carbon centered radical is formed to which oxygen can rapidly add to generate a new peroxyl radical. This type of reaction is commonplace in copolymerizations of compounds such as styrene and oxygen.[40,43]

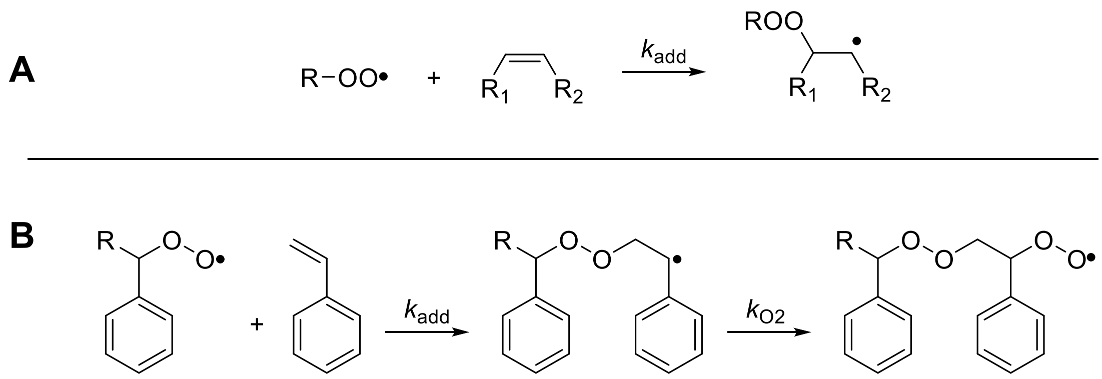

Figure 7. A. Addition of a peroxyl radical to a double bond; B. Copolymerization of Styrene with Oxygen.[39,40,41,43]

1.3.4. Termination of Autoxidation

Generally, termination involves the coupling or disproportionation of two radicals in solution to generate non-radical products. This can occur through a stepwise Vaughan termination[42] or a cyclic, concerted reaction of an intermediate tetroxide known as a Russell termination,[43] both shown in Figure 8.

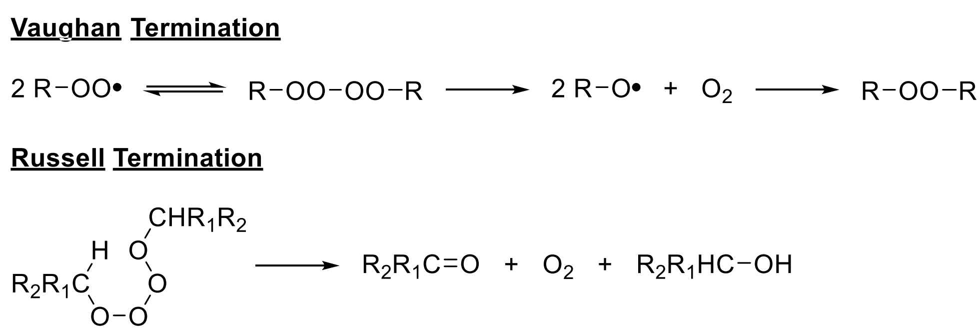

Figure 8. Schemes for Vaughan and Russell Termination.[42,43]

1.4. Lipid Peroxidation

Lipid peroxidation is defined as the autoxidation of any lipid species. Compounds containing weak C-H bonds undergo rapid autoxidation.[44] Thus, PUFAs are very susceptible to radical attack due to the presence of homo-conjugated double bonds (or bis-allylic methylene groups).[45] Radical attack preferentially occurs at these sites due to the low bond dissociation enthalpy (BDE) of the bis-allylic methylene C-H bond (75 kcal/mol) compared to an allyl (≈ 88 kcal/mol) C-H bond.[46] This lower BDE is a consequence of the formation of a stabilized pentadienyl radical in which the radical is delocalized across five carbon atoms. Certain sterols are also prone to peroxidation. The primary examples are 7-dehydrocholesterol[47] (7-DHC) and 8-dehydrocholesterol[39] (8-DHC), both of which give highly stabilized pentadienyl radicals after hydrogen atom abstraction (Figure 9).

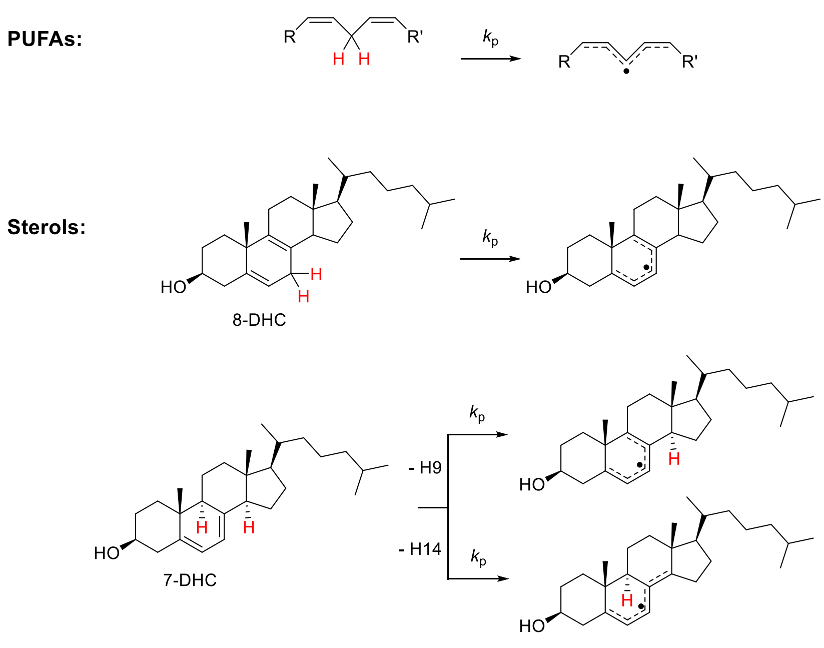

Figure 9. Pentadienyl radical formation for PUFAs and sterols 7-DHC and 8-DHC.

1.4.1. Rate Constant Measurements

Determination of rate constants has been critical in the understanding and advancement of free radical chemistry. Rate constants for the reaction of oxygen centered radicals - particularly peroxyl radicals - are of interest since they are the main species present during the autoxidation of organic compounds or the peroxidation of lipids. Thus, determining peroxyl radical reaction rates has been a focus of chemists for over fifty years.

Direct Measurement

Direct determination of rate constants may be achieved through the use of techniques, including the rotating sector method and flash photolysis. The rotating sector method was first used in 1937 to measure the mean lifetime of radicals in the polymerization of gaseous methyl methacrylate.[48] The technique was carried out by interrupting the exciting light produced by a water-cooled mercury arc lamp using a rotating slotted disk.[48,49] Spinning the disk at a controlled speed yields equal periods of light and darkness.[49] The overall rate of polymerization depends on the sector speed which allows for determination of the average lifetime of free radicals.[49] The method can be used to measure rate constants in the gaseous or liquid phase[50] of any chain reaction in which the kinetic chains are broken by a bimolecular reaction between the chain carrying species.[49]

Indirect Measurement – Radical Clocks

The indirect measurement of rate constants can be achieved through the use of radical clocks.[51,52,53] This type of experiment utilizes a unimolecular radical reaction having a known rate constant to determine a bimolecular radical reaction with an unknown rate constant. An example of a radical clock is the 5-hexeny radical cyclization shown in Figure 10. The 5-hexenyl radical cyclization clock utilizes a competition between a 5-*exo-trig* cyclization (k_R) and hydrogen atom abstraction from some substrate A-H (k_H). Kinetic analysis of the mechanism leads to the conclusion that the ratio of the products [**1**]/[**2**] is proportional to k_H/k_R. Thus, if k_R for the unimolecular 5-*exo-trig* cyclization and the concentration of A-H is known, the rate constant (k_H) can be determined. In general, the radical clock is very useful for determining rate constants for reactions involving carbon centered radicals. A number of clocks have been reported for measuring rate constants in the range of 10^{-1} to 10^{12} M^{-1} s^{-1}.[51,52,53]

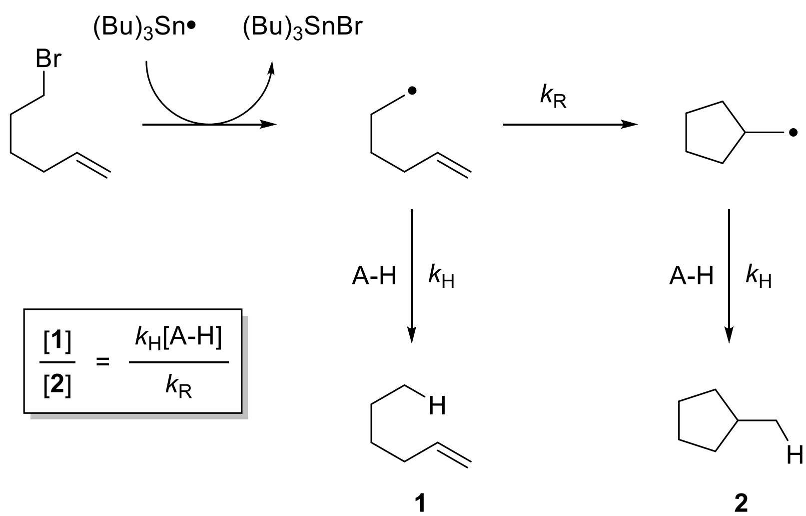

Figure 10. 5-Hexenyl radical cyclization clock.

Peroxyl Radical Clocks

The work reported in this dissertation relies heavily on the peroxyl radical clock developed by Roschek *et al*.[54] The clock was developed and calibrated based on the competition between intramolecular β-fragmentation (k_β) and intermolecular hydrogen atom abstraction from a donor molecule (k_H). The clock was based on the autoxidation of methyl linoleate, the mechanism of which is shown in Figure 12. It was calibrated with both methyl linoleate and α-tocopherol (Figure 11), both of which have well established rate constants for their reaction with peroxyl radicals (k_H;

linoleate = 62 M^{-1} s^{-1}, tocopherol = 3.5 x 10^6 M^{-1} s^{-1}).[55,56,57,58] These two calibration points have made the clock applicable to rate constants in the range of 10^0 to 10^7 M^{-1} s^{-1}.[54]

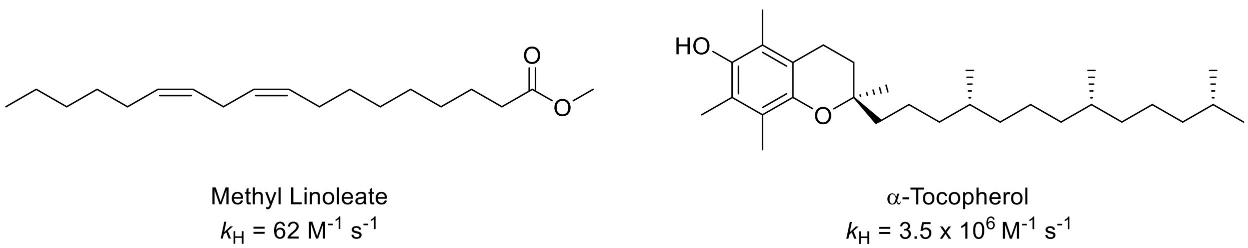

Figure 11. Structures and rate constants for methyl linoleate[55,56] and α-tocopherol[57,58].

The autoxidation of methyl linoleate results in the buildup of four distinct hydroperoxyoctadecadienoic acids, or HpODEs (Figure 12, Compounds **6**, **9**, **11**, **14**). These hydroperoxides can be classified as the kinetically favored *cis,trans*-isomers and the thermodynamically more stable *trans,trans*-isomers. The distribution of the kinetic and thermodynamic products is dependent on the concentration and reactivity of hydrogen atom donors present in solution.

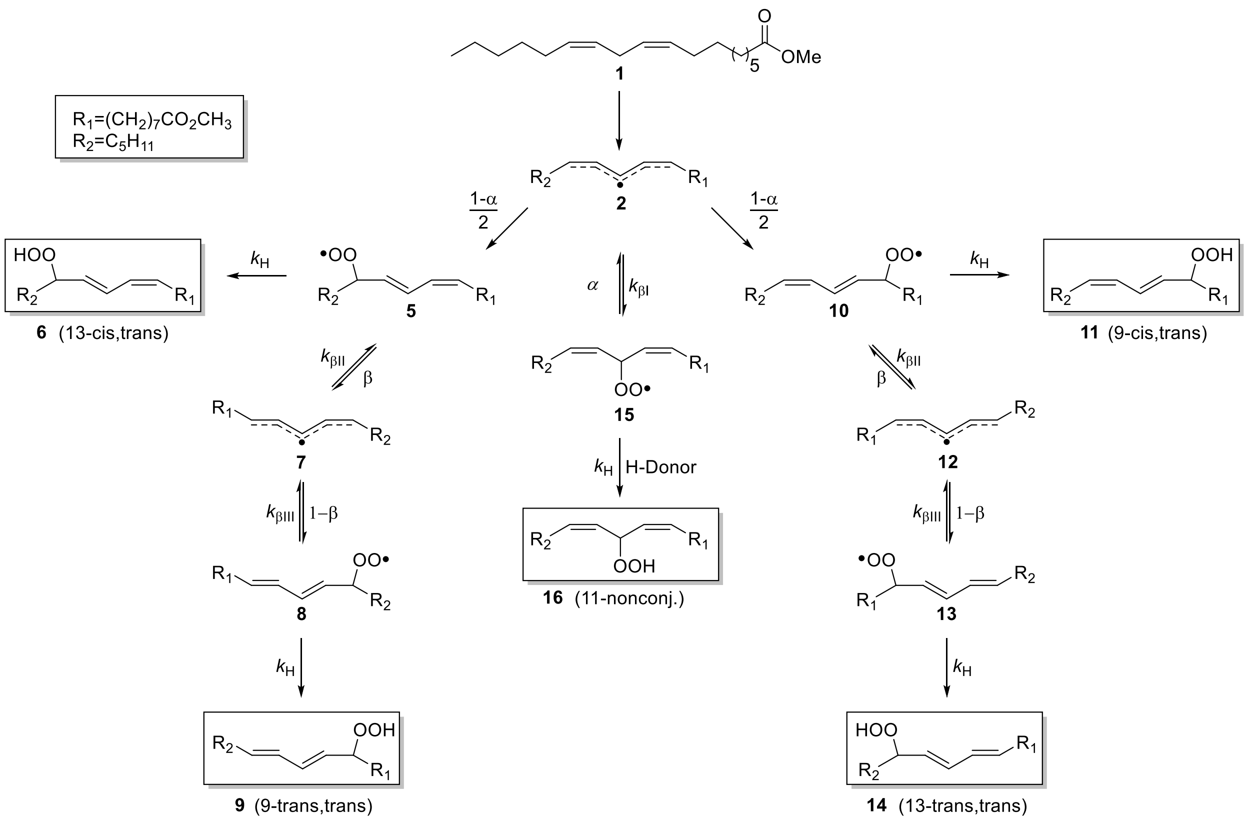

Figure 12. The mechanism for autoxidation of methyl linoleate that forms the basis of the Linoleate Peroxyl Radical Clock.[54]

Methyl Linoleate Clock

The first-formed carbon radical in the autoxidation of linoleate is the delocalized pentadienyl radical (**2**, Figure 12). Oxygen partitions itself across this radical to give the kinetically favored nonconjugated (**15**) and *cis*,*trans*-conjugated peroxyl radicals (**5** and **10**). The nonconjugated peroxyl radical (**15**) undergoes rapid β-fragmentation ($k_{\beta I}$). In the absence of an excellent hydrogen atom donor such as an antioxidant (i.e. TocH) this fragmentation occurs at a rate much faster than hydrogen atom donation (k_H), rendering it kinetically invisible.

Once **5** or **10** are formed, multiple pathways are accessible depending on the hydrogen donating capability of the molecules present in solution. The peroxyl radical can abstract a hydrogen atom from another molecule (k_H) to give the corresponding kinetically favored *cis*,*trans*-conjugated hydroperoxide. Alternatively, peroxyl radical **5** or **10** can undergo bond rotation followed by β-fragmentation ($k_{\beta III}$ in Figure 12) to form a new pentadienyl radical (**7** or **12**) that has a *cis*,*trans*-configuration. Oxygen can then partition across the transoid or cisoid ends of either **7** or **12** to give the *cis*,*trans*- or *trans*,*trans*-peroxyl radicals (**5** and **10** or **8** and **13**) with partition coefficients of β and 1-β, respectively. Hydrogen atom abstraction by these peroxyl radical gives the corresponding hydroperoxide. Ultimately, the competition outlined above between bimolecular hydrogen atom abstraction/transfer (k_H) and uniolecular β-fragmentation of the peroxyl radical forms the basis of the peroxyl radical clock.

Steady state analysis of the autoxidation of linoleate (Figure 12) leads to Equation 1, in which the product distribution (*cis*,*trans*- vs. *trans*,*trans-HpODEs*) is described as a function of oxygen partitioning (β), β-fragmentation ($k_{\beta II}$ and $k_{\beta III}$), and the concentration of H-atom donor ([H-donor]).[54]

$$\frac{[trans,cis]}{[trans,trans]} = \frac{[\mathbf{6+11}]}{[\mathbf{9+14}]} = \frac{k_H[H-Donor]}{k_{\beta II}(1-\beta)} + \frac{k_{\beta III}}{k_{\beta II}}\left(\frac{\beta}{1-\beta}\right) \qquad (1)$$

The methyl linoleate clock was calibrated using methyl linoleate itself, whose β-fragmentation rate constants and partition coefficients have been determined.[54, 59] This allows for the use of a simplified kinetic expression given in Equation 2 which relates the *trans*,*cis*/*trans*,*trans*-product ratio and kinetic rate (or propagation rate) constants.[47]

$$\frac{trans,cis}{trans,trans} = \frac{k_p^1[R_1-H]}{214\ s^{-1}} + \frac{k_p^2[R_2-H]}{214\ s^{-1}} + \frac{k_p^3[R_3-H]}{214\ s^{-1}} + \cdots + 0.16 \qquad (2)$$

Where k_p^n and $[R_n\text{-}H]$ are the propagation rate constants and concentrations, respectively, for any H-atom donor in solution. Equation 2 can be further simplified to give the master Equation 3.

$$\boxed{\frac{trans,cis}{trans,trans} = \sum_{i=1-n} \frac{k_p^i[R_i-H]}{214\ s^{-1}} + 0.16} \qquad (3)$$

As k_p[R-H] approaches zero, the boundary limit of Equation 2 represents oxidation conditions under thermodynamic control. The *trans*,*cis*/*trans*,*trans*-product ratio approaches 0.16 in this instance.[47]

The formation of both *trans*,*cis*- and *trans*,*trans*-products results in the accumulation of these UV active compounds that can be separated using normal phased high performance liquid chromatography. If the ratio of *trans*,*cis*/*trans*,*trans*-products is plotted versus the concentration of H-atom donor present in solution, the slope of the resulting plot is proportional to k_p[R-H], which can be used to solve for the propagation rate constant.

Oxygen Consumption and Oxidizability

Another method used for the indirect measurement of peroxidation rate constants involves the measurement of oxygen consumption. The method relies on the fact that as autoxidation of a compound occurs, molecular oxygen will be 'transferred' from the surrounding medium to the forming peroxides. This consumption of oxygen is measured through the use of a Clark electrode that contains a catalytic platinum surface where the partial pressure of oxygen (pO_2) is measured via Equation 4 below:

$$O_2 + 4\,e^- + 2\,H_2O \rightarrow 4\,OH^- \qquad (4)$$

The apparatus contains two bulbs in which Clark electrodes are inserted. One acts as the reaction vessel, the second as the reference cell. Both contain atmospheric pressures of O_2. The bulbs are submerged in a water bath which is held at a constant temperature and shaken vigorously. The change in pO_2 is reported using an integrator and is indicative of oxygen consumption. A schematic for the instrument can be seen in Figure 13.

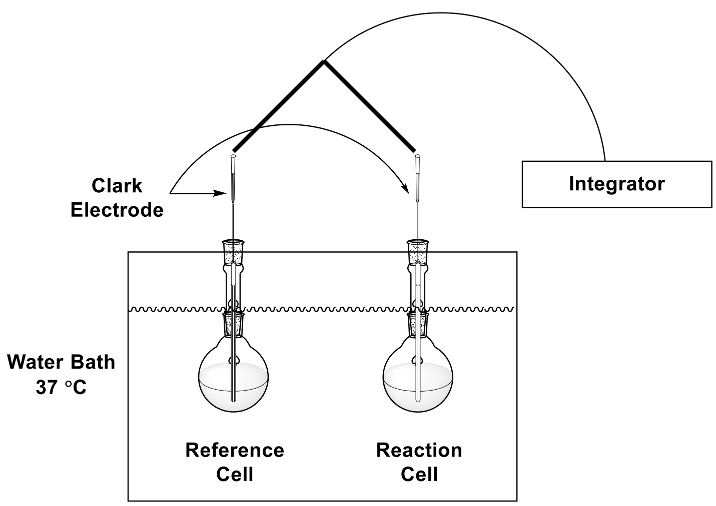

Figure 13. Oxygen consumption apparatus.

Under steady state analysis of the autoxidation of a PUFA of interest, the rate of oxygen consumption is given by Equation 5:

$$\frac{-d[O_2]}{dt} = \left\{\frac{k_p}{\sqrt{2k_t}}\right\}[RH]\sqrt{R_i} \qquad \textbf{(5)}$$

Where k_p is the propagation rate constant, k_t is the rate of termination, [RH] is the concentration of the PUFA or other compound of interest, and R_i is the rate of initiation.[56]

In order to quantitatively study autoxidation kinetics, the rate of initiation must be known and controlled throughout the course of the experiment. Similar to the methyl linoleate clock described previously, thermally labile azo-intiators (Figure 5B) are used as they decompose at a known rate (k_d) to give two separate radicals (Figure 5A).

The rate of initiation is governed by both the rate of decomposition of the initiator (k_D) and the efficiency in which the initial carbon centered radical I• is able to escape the solvent cage of its genesis. The R_i is generally measured by monitoring an 'induction period'[60] for the consumption of a phenolic antioxidant, the equation for which is shown below (Equation 6):

$$R_i = \frac{n[ArOH]}{\tau} \qquad \textbf{(6)}$$

Where *n* is the number of radicals trapped by the phenolic antioxidant being used (for example, TocH and its analogs have *n* values of 2), and τ is the time over which oxygen uptake is inhibited. The value for τ can be calculated as long as *n* is known.[56]

Data from these experiments are typically visualized by plotting oxygen consumption versus time. The induction period method is used to measure R_i. To obtain these plots, known amounts of antioxidant and the PUFA to be oxidized are added to the reaction vessel. After temperature equilibration, known amounts of initiator are added. The induction period (or period in which oxygen uptake is inhibited) is determined by tracing the slope for parts A (induction) and B (oxidation). The intercept between the two slopes marks the time at which induction ends and oxidation begins, and corresponds to the value of τ. From this determination, R_i is calculated and the oxidizability of the PUFA under study is readily calculated using Equation 5.[56] A typical oxygen consumption plot demonstrating these characteristics is shown in Figure 14.

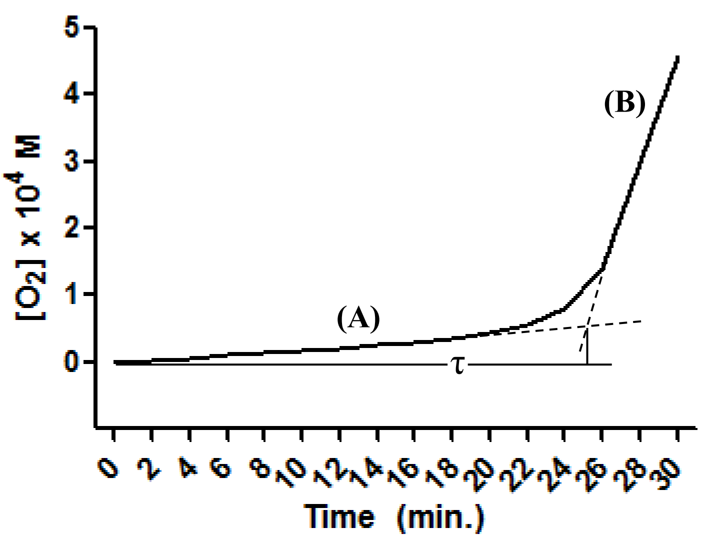

Figure 15: Typical oxygen consumption plot of methyl linoleate. (A) indicates the induction period, and (B) shows the oxidation period.

1.4.2. *Structure-Reactivity and Propagation Rate Constants*

The propagation rate constant (k_p) for most free radical oxidations involves hydrogen atom transfer from an organic substrate to a chain carrying peroxyl radical. This transfer is typically slower than all other steps that occur during autoxidation, making it the rate limiting (or rate determining) step for the process as a whole. Numerous k_p values have been determined for organic substrates undergoing autoxidation using classical rotating sector techniques discussed above.[55] These experiments form the basic understanding of the mechanistic framework of free radical chain oxidations. Selected propagation rate constants from these experiments are given in Table 1.[44 61 62]

Compound	k_p (M^{-1} s^{-1})
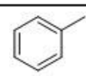	0.24
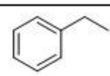	1.3
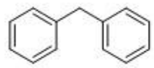	4.8
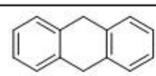	88
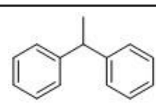	0.34
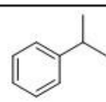	0.18
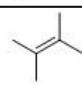	1.68
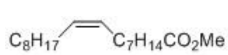	0.88
	14
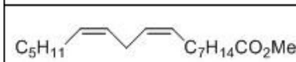	62

Table 1. Selected autoxidation propagation rate constants (k_p) for organic compounds.[44,61,62]

The compounds shown in Table 1 have a substantial spread in structural features with an equally large distribution of measured propagation rate constants. The difference in rates can be understood by looking at the bond dissociation enthalpy (BDE), or the change in enthalpy associated with breaking a C-H bond during propagation. Substituent groups, levels of substitution, and delocalization present on the structure of the molecule with the reactive C-H bond will factor into the value of the BDE.

Radical stability follows the order shown below in Figure 15, with tertiary radicals being the most stable. The converse is applicable with respect to the reactivity towards hydrogen atom abstraction. The ultimate stability and reactivity of the particular radical species is dependent on the BDE of the bond which is being broken in the propagation step. Typically, as the substitution on the radical center increases the corresponding parent C-H bond BDE decreases.[62]

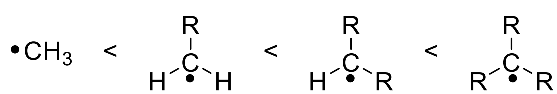

Figure 16. Relative radical stability.

Substituents surrounding the radical also play an important role in reactivity, specifically concerning its delocalization capabilities. Delocalization occurs when the free radical is no longer confined to the original carbon atom on which it was formed. In the frame of reference of a free radical, nearly every substituent can act as a source of stabilization. These include electron withdrawing groups (EWG) such as carbonyls and electron releasing groups (ERG) like methoxy substituents. The overall ability to provide stabilization for the radical can be illustrated in terms of resonance structures analogous to the allyl radical in Figure 16. Generally, increasing stabilization results in lower BDE for the C-H bond being broken.[44]

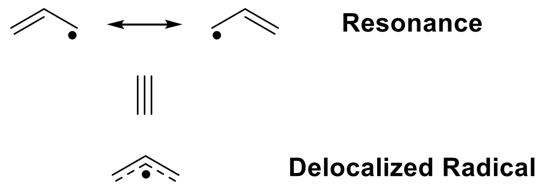

Figure 17. Resonance and delocalization of the allyl radical.

1.4.3. Autoxidation of Polyunsaturated Fatty Acids

The benchmark rate constant used to establish the peroxyl radical clock is that of methyl linoleate (18:2). Its autoxidation has been studied in depth by several independent laboratories, and the consensus propagation rate constant is 62 M^{-1} s^{-1} at 30 °C.[55,56] Linoleate is an ω-6 fatty acid that is 18 carbons long and contains two units of unsaturation, separated by a singular methylene group to give a homo-conjugated system. Under oxidative conditions, the methylene carbon (or *bis*-allylic carbon) is subject to hydrogen atom abstraction due to the lower BDE at this location (75 kcal/mol) in comparison to the mono-allylic carbons (88 kcal/mol) on either side of the double bonds (Figure 17).[63]

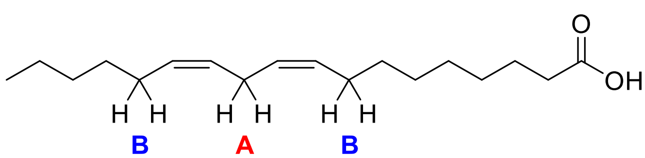

Carbon	C-H BDE (kcal/mol)
A	75
B	88

Figure 18. C-H BDEs for sites of possible hydrogen atom abstraction during methyl linoleate autoxidation.[46]

In general, propagation rate constants for PUFAs are related to the number of units of unsaturation present in the respective PUFAs structure as shown in Figure 18.[47] Oleic acid (18:1) is a monounsaturated fatty acid and has a k_p of less than 1 M^{-1} s^{-1}, a rate that is much smaller than that of linoleate. Arachidonic acid (20:4) has two more units of unsaturation than linoleate and it has a k_p of 201 ± 12 M^{-1} s^{-1}, 3.2 times that of linoleate. Both eicosapentaenoic acid (20:5; 249 ± 14 M^{-1} s^{-1}), and docosahexaenoic acid (22:6; 321 ± 32 M^{-1} s^{-1}) show similar increases in k_p (4.0 and 5.4 times greater than linoleate, respectively). This assortment of PUFAs are all targets of peroxyl radicals, and their relative rates of hydrogen atom transfer or propagation are clearly dependent on the number of *bis*-allylic methylene groups present – 1, 3, 4, and 5 for 18:2, 20:4, 20:5, and 22:6 respectively.[47]

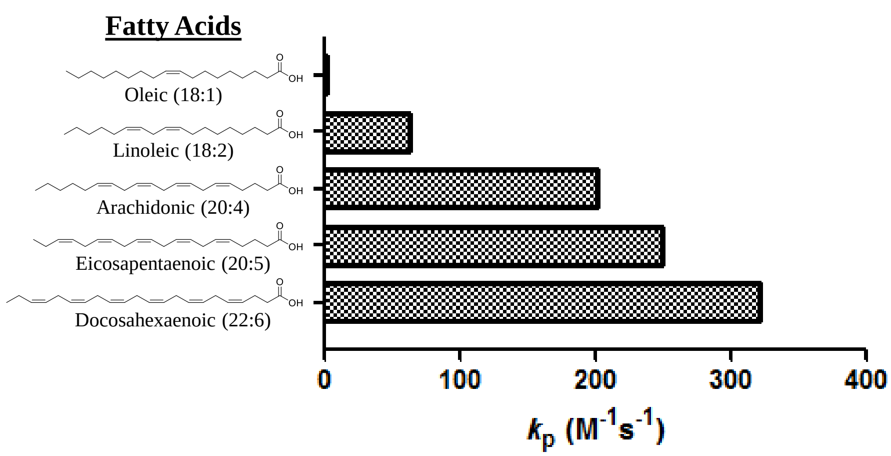

Figure 19. Propagation Rate Constants (k_p) for Common PUFAs.

1.4.4. Sterol Autoxidation

Sterols are also targets of peroxyl radicals, and propagation rate constants for these compounds also show the important link between structure and reactivity. Cholesterol, like oleate, has one double bond and four allylic hydrogen atoms. However, its k_p of 11 M^{-1} s^{-1} is over 10 fold that of oleate (0.9 M^{-1} s^{-1}, Table 1). In general, cyclic alkenes are better hydrogen atom donors than comparable straight-chain molecules due to the allylic C-H bonds being oriented in such a way that allows the radical to be readily delocalized with minimal structural distortion. This can be attributed to maximum overlap between the alkene π bond and the developing radical from H-atom abstraction.[47] Furthermore, the cholesteryl radical is highly substituted (disubstituted at C-5, monosubstituded at C-7) in comparison to oleate (Figure 19).

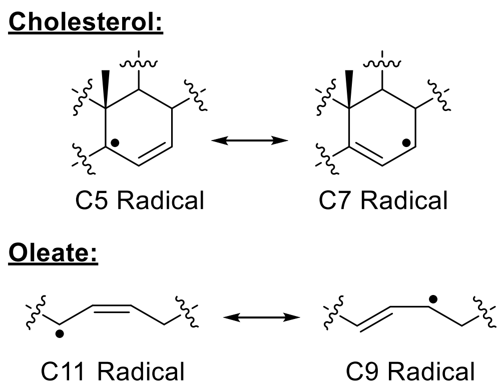

Figure 19. Comparison of substitution for the Cholesterol allyl radical and Oleate allyl radical.

Cholesterol is ubiquitous in cellular plasma membranes.[64] It plays an important role in maintaining plasma membrane integrity,[65,66] lipid-raft-mediated cell signaling,[67] myelin formation,[68] and brain development.[69] Cholesterol can be taken up through the diet, or it can be biosynthesized via squalene-2,3-epoxide. Lanosterol is the first sterol formed from this epoxide and depending on whether its C24 double bond is reduced early or late by 3β-hydroxysterol-Δ^{24}-reductase (DHCR24), the pathways followed are either the Kandutsch-Russell pathway[70] or Bloch pathway,[71] respectively (Figure 20).

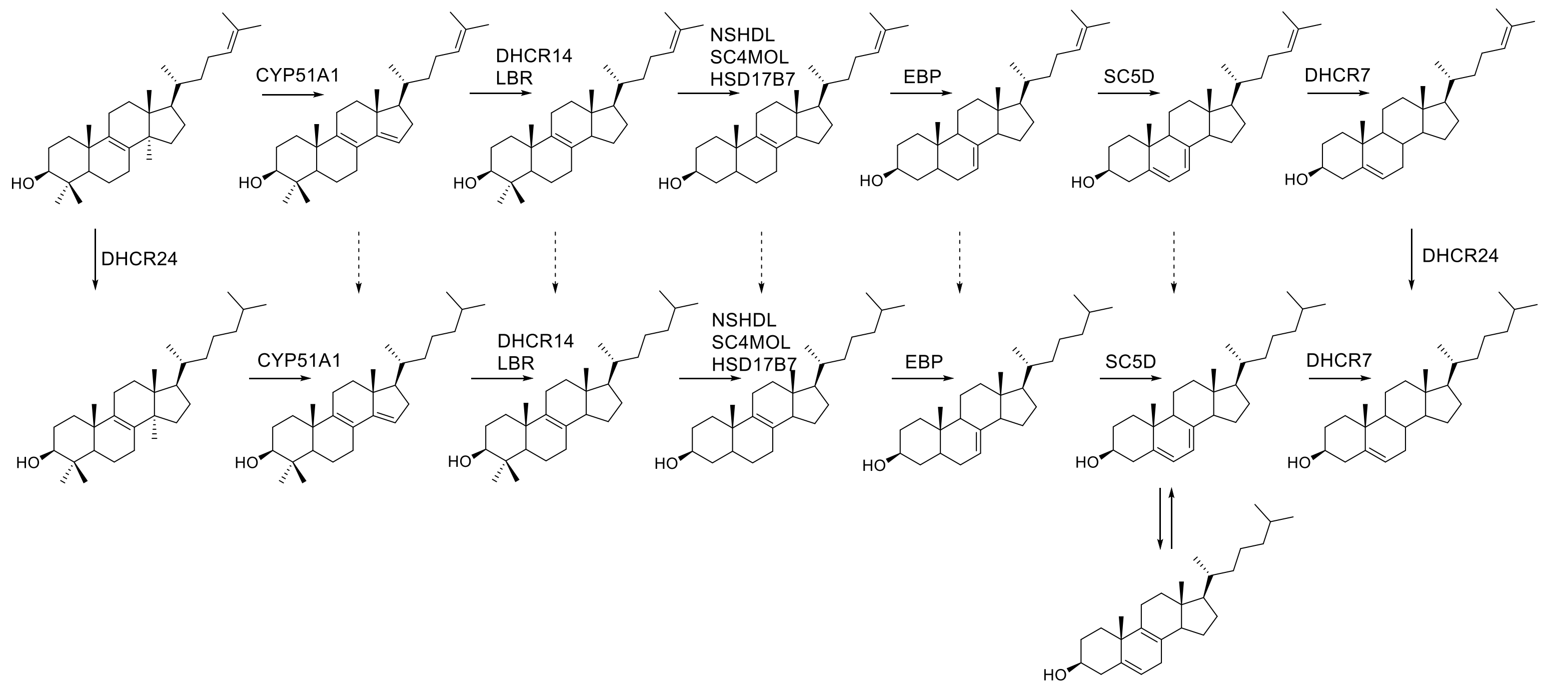

Figure 20. Pathways for the biosynthesis of cholesterol. The Bloch pathway (top) and Kandutsch-Russell pathway (bottom) are separated by a singular enzymatic reduction of the unsaturation located at C24-C25 of the sterol side chain by 24-dehydrocholesterol reductase. This step can presumably occur at any point during biosynthesis, starting from lanosterol and ending with desmosterol.

The free radical oxidation of cholesterol has been implicated in a variety of degenerative diseases including atherosclerosis,[72] Alzheimer's disease,[73] and retinal degeneration.[74] Oxysterols, the products formed during free radical oxidation of sterols, have been extensively studied.[72] Some of these products are shown in Figure 21. In 1973, scientists reported that 7-ketocholesterol, 7α-hydroxycholesterol, and 7β-hydroxycholesterol inhibited sterol biosynthesis.[75] Since then, a large body of work has been completed concerning the important biological activity of oxysterols.[76,77]

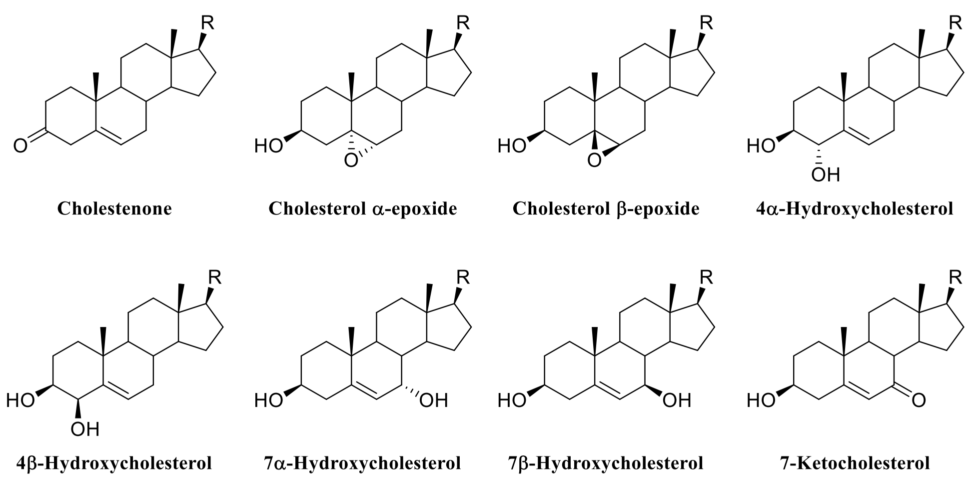

Figure 21. Free radical oxidation of cholesterol leads to the formation of oxysterols. Commonly encountered oxysterols are shown above. All are known to originate from non-enzymatic free radical oxidations except for 7α-hydroxycholesterol (which can come from enzymatic or non-enzymatic oxidation) and cholestenone (principally formed enzymatically).[72]

At low temperatures, peroxyl radicals primarily abstract hydrogen atoms from cholesterol at C7[78] resulting in an allylic radical with two resonance contributors at C5 and C7 as seen in Figure 22A. Radicals at both positions can be trapped by oxygen. However, the 5α- or 5β-hydroperoxides are typically not found in the product mixture. The 5α- and 5β- peroxyl radicals have been calculated to be 3 to 6 kcal/mol less stable, respectively, than their counterpart peroxyl radicals formed at C7 and are expected to undergo rapid β-fragmentation (k_β). Recent work has shown that under kinetically controlled conditions in the presence of a good H-atom donor such as α-Tocopherol (TocH) the 5α-peroxyl radical may be trapped. The k_β for the 5α-peroxyl radical was calculated to be 5.6 x 10^5 s^{-1},[79] explaining why the 5α-hydroperoxide is only observed under conditions in which TocH is present.

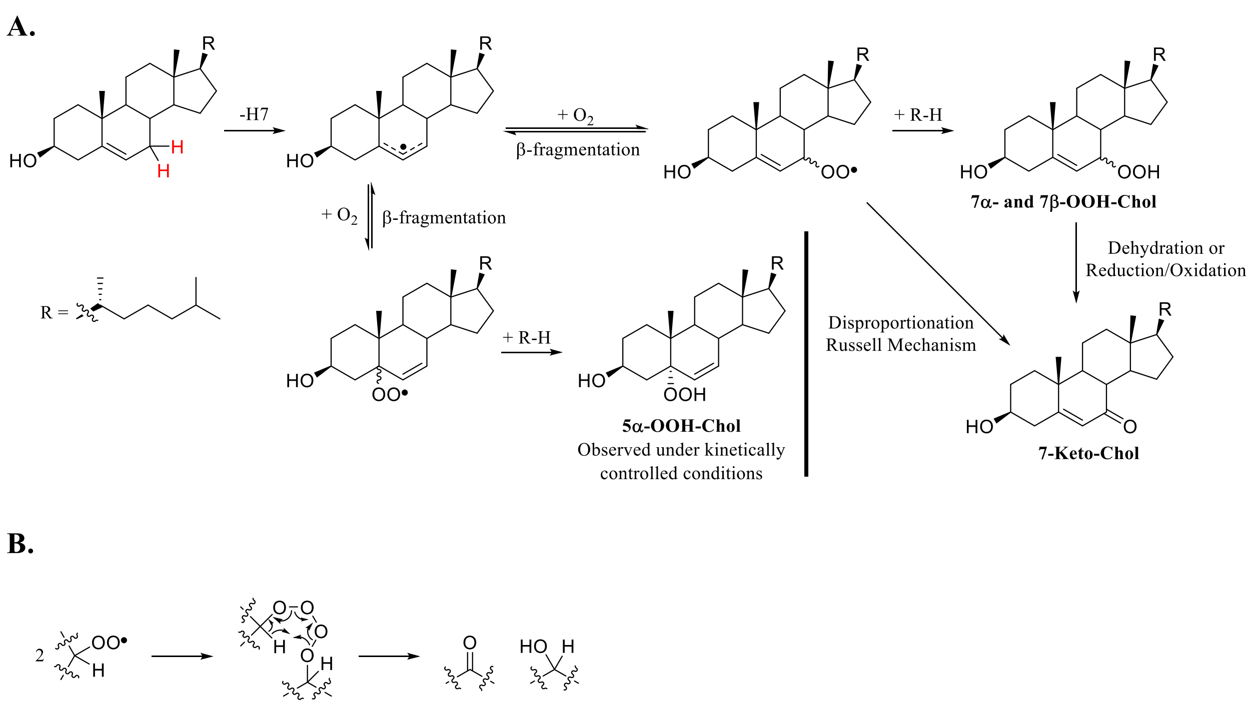

Figure 22. A. Autoxidation of cholesterol after H7 abstraction, resulting in the formation of oxysterols 5α-OOH-Chol, 7α- and 7β-OOH-Chol (and corresponding hydroxides), and 7-Keto-Chol;[39] **B.** Mechanism of Russell fragmentation for sec-butyl peroxyl radicals.[83]

Oxygen can add to the allylic radical at C7 shown in Figure 22A on both faces of the molecule (α and β) to give 7α- or 7β-hydroperoxycholesterol (7α-OOH-chol and 7β-OOH-chol). Both may be reduced by agents present in the biological environment, including peroxidase[80] or Fe^{2+},[81] to give the corresponding 7α- or 7β-hydroxycholesterol (7α-OH-chol and 7β-OH-chol, Figure 21). Both 7α-OH-chol and 7β-OH-chol as well as 7-ketocholesterol (7-keto-chol), can also be formed from a disproportionation reaction of 7α-OOH-chol and 7β-OOH-chol.[78] Furthermore, 7-keto-chol can also be formed by dehydration of 7α- or 7β-OOH-chol[82] or by decomposition of a tetroxide intermediate formed during termination reactions between 7α- or 7β-peroxyl radicals known as the Russell mechanism (Figure 22B).[83]

Cholesterol may also undergo free radical oxidation through allylic H-atom abstraction at C4. This pathway results in the formation of 4α-OOH-Chol, 4β-OOH-Chol, 6α-OOH-Chol and 6β-OOH-Chol (Figure 23A), and further downstream oxidation products. Peroxyl radical addition can also occur at the double bond to form the 5α,6α- and 5β,6β-epoxides are formed. An alkoxyl radical is formed as a byproduct during epoxide formation, and this radical can further propagate chain sequences (Figure 23B).[39]

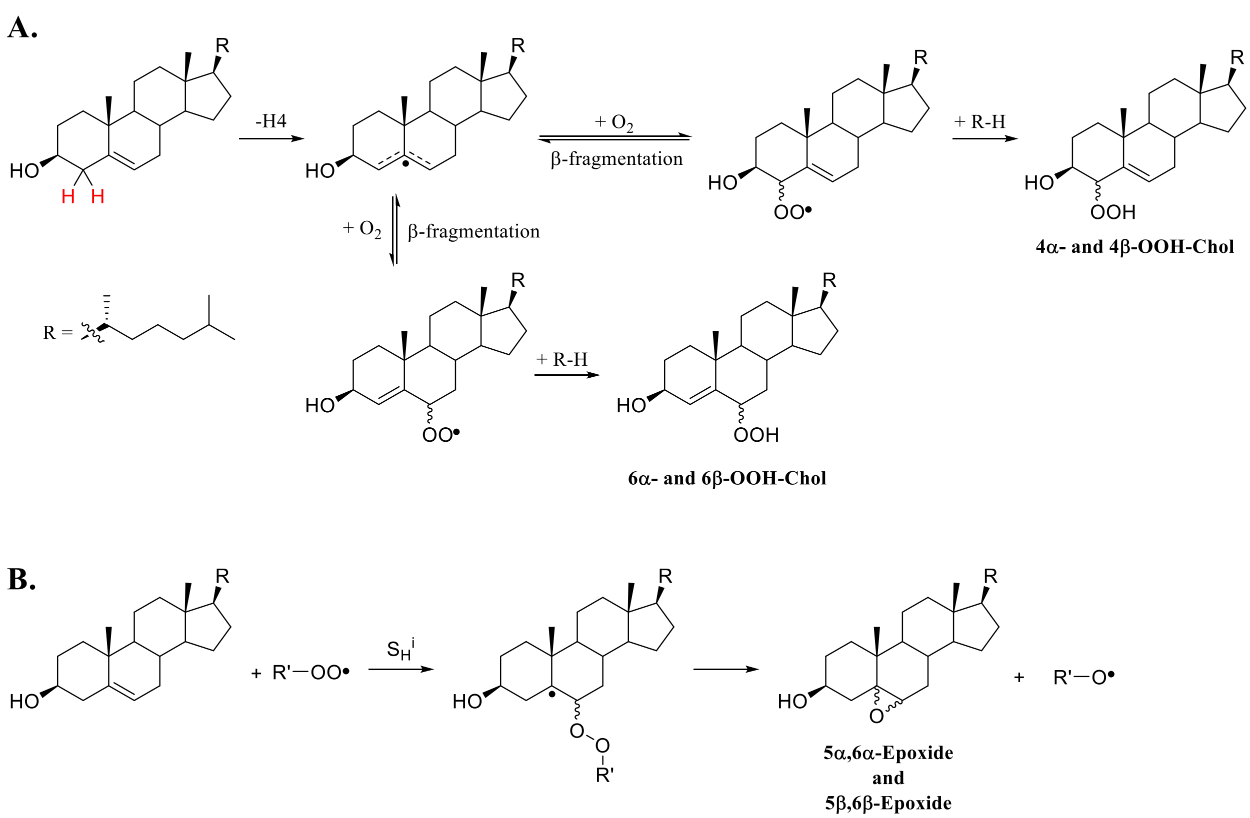

Figure 23. A. Free radical oxidation of cholesterol after H4-abstraction, producing 4α-OOH-Chol, 4β-OOH-Chol, 6α-OOH-Chol, and 6β-OOH-Chol oxysterols; **B.** Peroxyl radical addition via $S_H{}^i$ mechanism to generate the 5α,6α-epoxide and 5β,6β-epoxide.[39]

Other than their necessity in the biosynthesis of cholesterol, other intermediate sterols in the Bloch and Kandustch-Russell have interesting biological functions. For instance, 7-Dehydrocholesterol (7-DHC) is the biosynthetic precursor to a number of sterols and other biologically important molecules other than cholesterol. The enzyme 3β-hydroxysterol-Δ7-reductase (DHCR7) is responsible for reducing the C7-C8 double bond to give cholesterol. 7-DHC is also the precursor to 8-dehydrocholesterol (8-DHC) through the enzyme 3β-hydroxysteroid-Δ8,Δ7-isomerase. Finally, 7-DHC is converted to previtamin D_3 upon exposure to UV irradiation.[84] All of these transformations are shown in Figure 24.

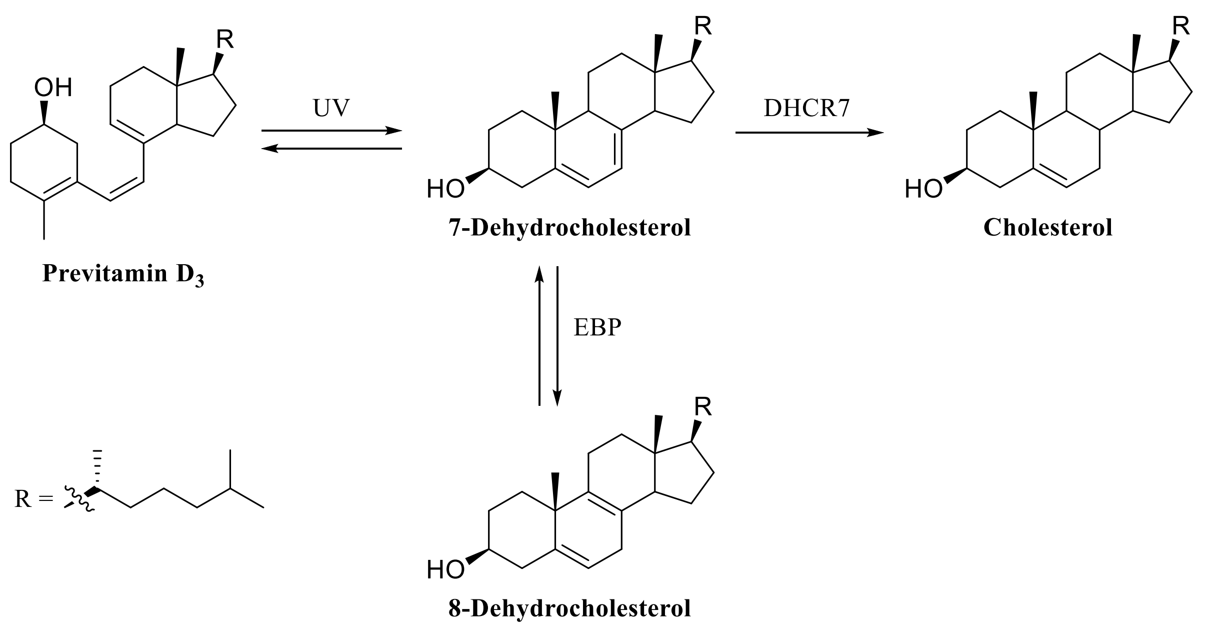

Figure 24. Transformations of 7-DHC into 8-DHC, cholesterol, and previtamin D_3.

Even though 7-DHC is vital for the biosynthesis of cholesterol and other biologically important molecules, it is the most oxidizable lipid known with a propagation rate constant of 2260 $M^{-1}\ s^{-1}$.[47] This sterol has a conjugated diene in the B-ring, and four abstractable allylic hydrogen atoms distributed at C4, C9, and C14. Molecular mechanics calculations suggest that hydrogen atoms at C9 and C14 are both well positioned for abstraction by peroxyl radicals, with dihedral angles for both C7-C8-C9-H9 and C7-C8-C14-H14 close to 90˚ as seen in Figure 25.[47]

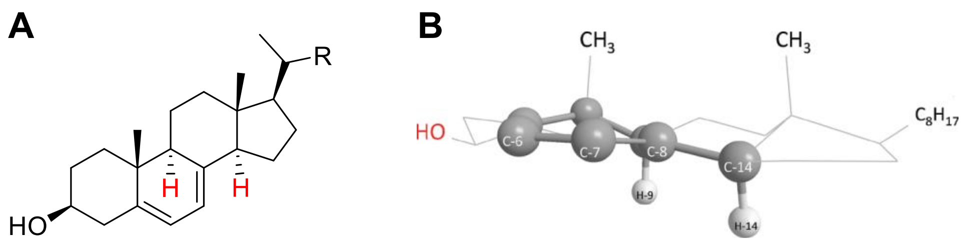

Figure 25. A. 7-Dehycholesterol with H-9 and H-14 highlighted in red; **B.** 7-Dehydrocholesterol low-energy conformation (MM2) showing reactive H-9 and H-14 and the B-ring conjugated diene frame.[47]

The pentadienyl radical resulting from hydrogen atom abstraction at either C9 and C14 (Figure 26) are also highly substituted, adding to their stability.[47] With the availability of two highly reactive hydrogen atoms as well as two highly substituted pentadienyl radicals formed after hydrogen atom abstraction, the mechanisms for the autoxidation of 7-DHC is complex, as are the oxysterols which can be formed.

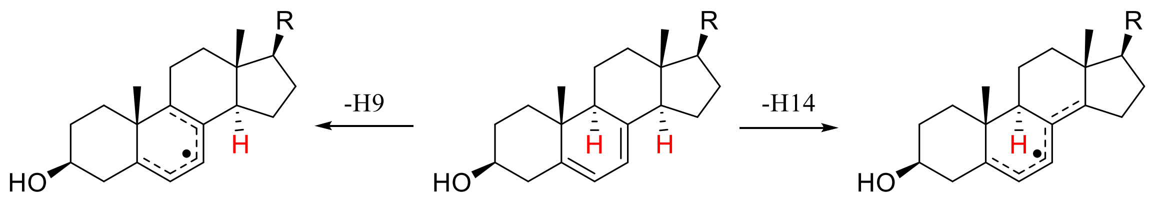

Figure 26. Hydrogen atom abstraction of either H9 or H14 yields highly substituted pentadienyl radicals.

Abstraction of H9 results in a pentadienyl radical spanning carbons C5-C6-C7-C8-C9. Oxygen can add to form either the C5 or C9-peroxyl radical (Figure 27). These peroxyl radicals can form the 5- or 9-hydroperoxides, or undergo a 5-*exo*-cyclization to give the endoperoxide shown in the box in Figure 28. This intermediate oxysterol can undergo a number of further transformations, which are shown in detail in the same figure.[39]

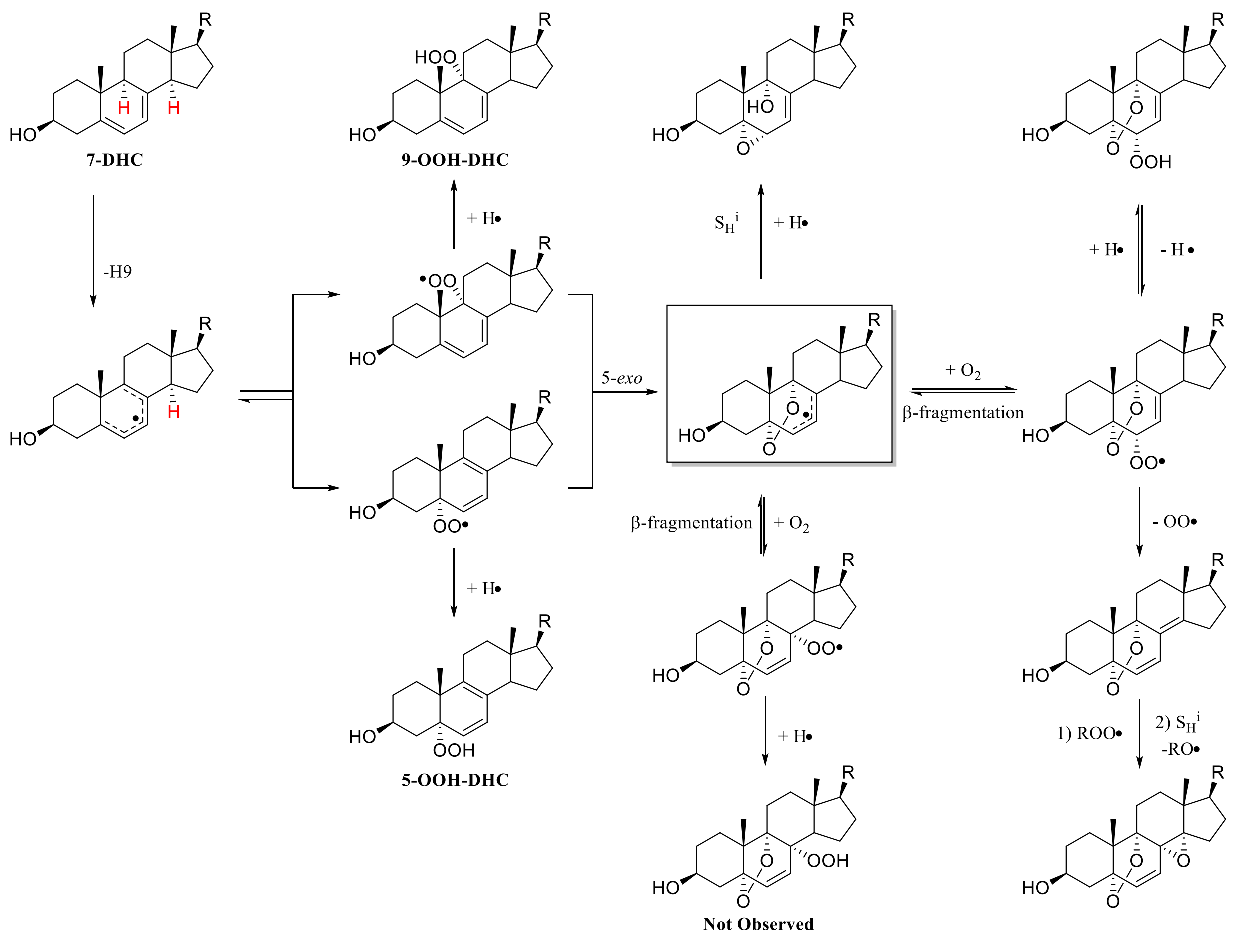

Figure 27. Mechanism for free radical oxidation of 7-DHC after H9 abstraction.[39]

Abstraction of H14 leads to the pentadienyl radical spanning carbons C5-C6-C7-C8-C14 (Figure 28). Oxygen addition to give the 5- or 14-peroxyl radical can be followed by H-atom transfer to give the corresponding hydroperoxides (5-OOH-DHC and 14-OOH-DHC, respectively). In contrast to the H-9 mechanism, the diene framework after H14 abstraction spans both B and C rings and is unfavorable for 5-*exo*-cyclization. Still, further reactions are possible after 5- and 14-OOH-DHC formation due to the remaining reactivity in the molecule. These reactions could include a β-scission of the hydroperoxide (-OH•) followed by an S_H^i reaction to ultimately give an epoxy hydroperoxide. If 14-OOH-DHC is formed, H9 is vulnerable to further oxidation, leading to more complex products.[39]

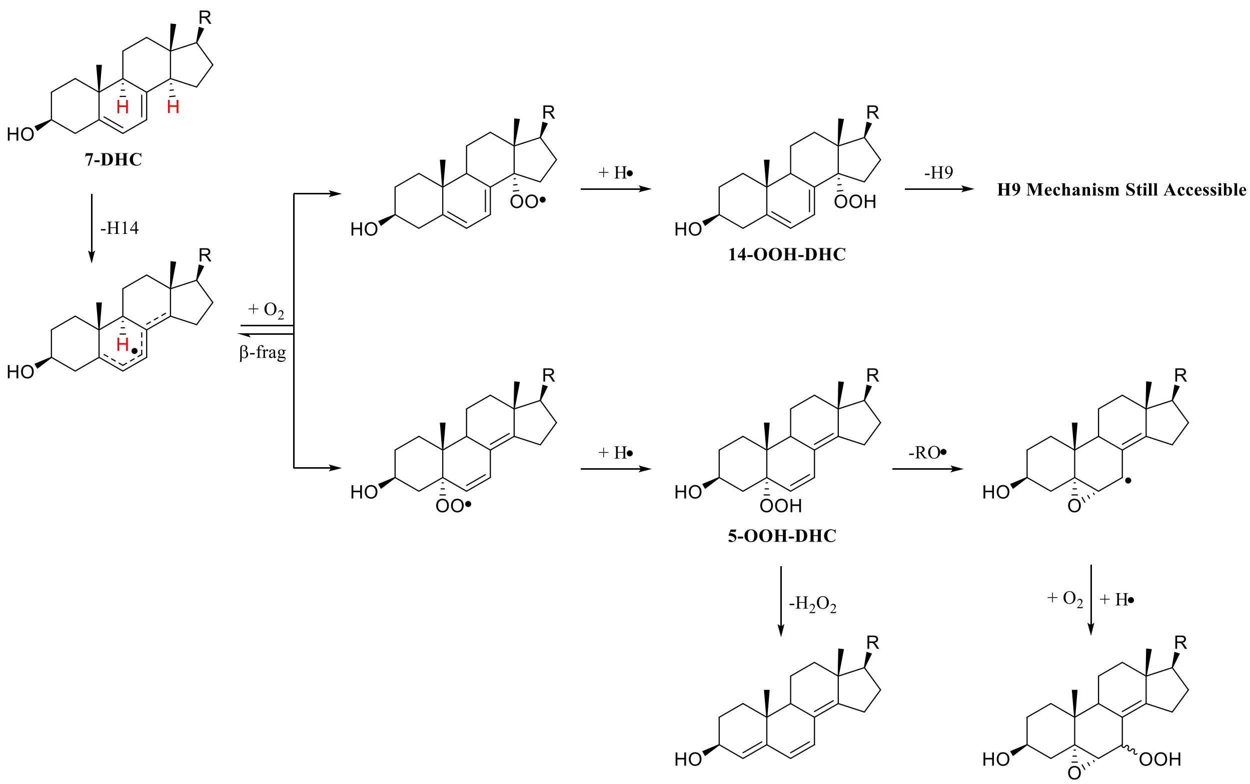

Figure 28. Mechanism for free radical oxidation of 7-DHC after H14 abstraction.[39]

7-DHC can also undergo addition reactions with peroxyl radicals to form the 7-DHC-5α,6α-epoxide (Figure 29).[85] This reactive epoxide can undergo ring opening and further oxidation to give 3β,5α-dihydroxy-cholest-7-en-6-one (DHCEO), which is a major oxysterol observed in both cell and animal models for SLOS as a biomarker for the peroxidation of 7-DHC.[86,87,85]

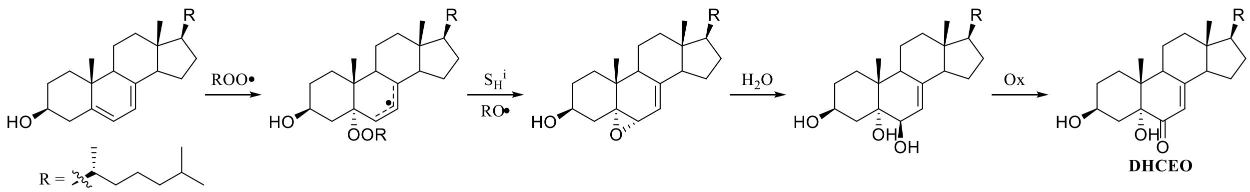

Figure 29. S_H^i reaction of a peroxyl radical and 7-DHC to give DHCEO, a major biomarker for peroxidation of 7-DHC.

Another highly oxidizable sterol is 8-DHC, having a propagation rate constant of 990 M^{-1} s^{-1}.[88] 8-DHC has a homo-conjugated diene in its B-ring and six reactive hydrogen atoms (4 allylic, 2 *bis*-allylic). Abstraction of one of the *bis*-allylic hydrogen atoms at C7 yields a pentadienyl radical identical to that of 7-DHC after H9 abstraction. Thus, it is expected that free radical oxidation of 8-DHC will follow the H9 mechanism for 7-DHC shown in Figure 30.[39]

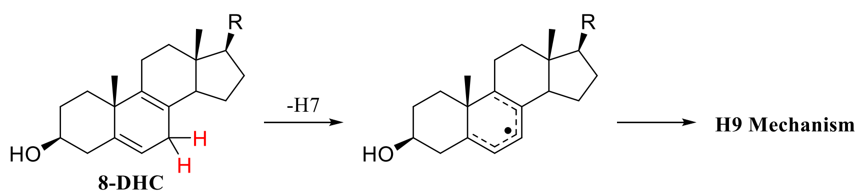

Figure 30. Free radical oxidation of 8-DHC follows the H9 mechanism for 7-DHC.[39]

As one can see, the autoxidation of sterols is very complex regardless of the propagation rate constant the particular molecule is able to sustain. The complexity of products, coupled with the propensity of sterols such as 7-DHC and 8-DHC to propagate free radical oxidations at extremely high rates, creates a situation in which the buildup of these sterols can quickly become detrimental in lipid-rich biological systems. Table 2 gives a brief recap of the three sterols discussed at length in this section, showing their structure and reactive hydrogen atoms, the conjugated radicals formed after hydrogen atom abstraction, and the measured propagation rate constants for each.

Sterol	Delocalization	k_p (M^{-1} s^{-1})
R = C_6H_{13} 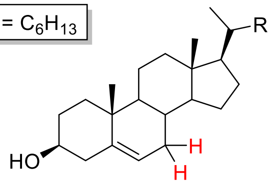 Cholesterol	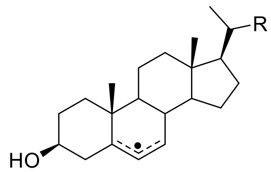	11 ± 1 M^{-1} s^{-1}
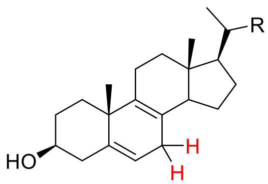 8-Dehydrocholesterol	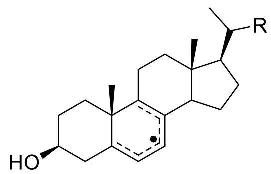	994 ± 33 M^{-1} s^{-1}
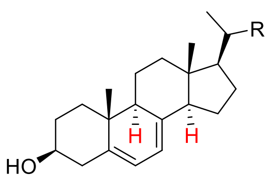 7-Dehydrocholesterol	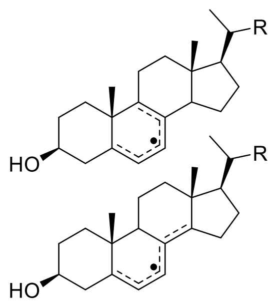	2260 ± 40 M^{-1} s^{-1}

Table 2. Structure, delocalized radicals, and k_p for Cholesterol, 8-DHC, and 7-DHC.

1.4.5. Antioxidants

Peroxidation can be inhibited or halted when a peroxyl radical encounters an antioxidant capable of breaking the chain reaction. The chain breaking process generally occurs through the H-atom abstraction reaction shown in Figure 31 (**1**).

(**1**) $R{-}OO\bullet + X{-}H \longrightarrow R{-}OOH + X\bullet$

(**2**) $R{-}OO\bullet + X\bullet \longrightarrow R{-}OO{-}X$

(**3**) $X\bullet + X\bullet \longrightarrow X{-}X$

Figure 31. Mechanism of phenolic antioxidants.

Chain-breaking antioxidants are typically phenolic in nature,[89] therefore the radical generated (X•) after H-atom abstraction by the peroxyl radical is highly stabilized through resonance delocalization. The radical (X·) is unsuited to continue the chain oxidation, hence the term ‘chain-breaking’. Eventually the phenolic radical will be destroyed through reaction with another radical, be it another peroxyl radical or disproportionation with another phenolic radical (Figure 31, **2** and **3**).[90]

One of the most efficient and prevalent antioxidants in Nature is tocopherol, commonly referred to as Vitamin E. This antioxidant exists as four different structures which are shown in Figure 32. Each member of the tocopherol series is an excellent chain breaking antioxidant, however α-tocopherol (TocH) has the largest inhibition rate constant (k_{inh}=3.5 x 10^6 M^{-1} s^{-1}) for H-atom donation to a peroxyl radical than the rest of the series.[91]

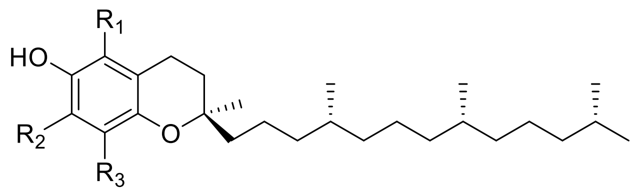

α-Tocopherol : R_1=R_2=R_3=CH_3

β-Tocopherol : R_1=R_3=CH_3; R_2=H

γ-Tocopherol : R_1=R_2=CH_3; R_3=H

δ-Tocopherol : R_1=CH_3; R_2=R_3=H

Figure 32. α, β, γ, and δ-Tocopherols.

Efforts to understand the effectiveness of TocH as a chain-breaking antioxidant and the search for equal or better antioxidants has been has been a major focus for some time. Howard and Ingold carried out a number of structure-activity relationship studies to understand the relationship between rates of inhibition (Equation 1, Figure 31) of simple phenols and the substituents located on the phenyl ring.[92,93,94,95] They found that optimal inhibition rates were achieved when a phenol contains a methoxy substituent group at the *para*- (or 4-) position to the phenol, with the remaining positions methylated. Therefore, the logically superior antioxidant should be 4-methoxy-2,3,5,6-tetramethylphenol (Figure 34A). But the inhibition rate constant for this phenol was determined to be 3.9×10^5 M^{-1} s^{-1},[91] much less than TocH (3.5×10^6 M^{-1} s^{-1}).

Steric hindrance to the abstraction of the phenolic O-H hydrogen atom is likely to be similar for both TocH and 4-methoxy-2,3,5,6-tetramethylphenol. The remaining explanation for the difference in rates of inhibition for the two antioxidants lies in thermodynamic differences – i.e. the O-H bond in TocH must be weaker than that of 4-methoxy-2,3,5,6-tetramethylphenol. This means that the phenoxyl radical from TocH must be more stabilized than the same radical from 4-methoxy-2,3,5,6-tetramethylphenol.[89]

This stabilization will be dependent on the orientation of the oxygen atom *para-* to the phenolic O-H group, as it is able to stabilize the phenoxyl radical by conjugative electron delocalization.[89] The extent of overlap between the p-type orbital and the semioccupied molecular orbital (SOMO) of the radical will depend on the dihedral angle θ between the p-type orbital overlap on O_1 and a perpendicular from the aromatic plane (Figure 33B). This particular dihedral should be equal to a secondary dihedral angle (θ') between the O_1-C_2 bond and the aromatic plane.

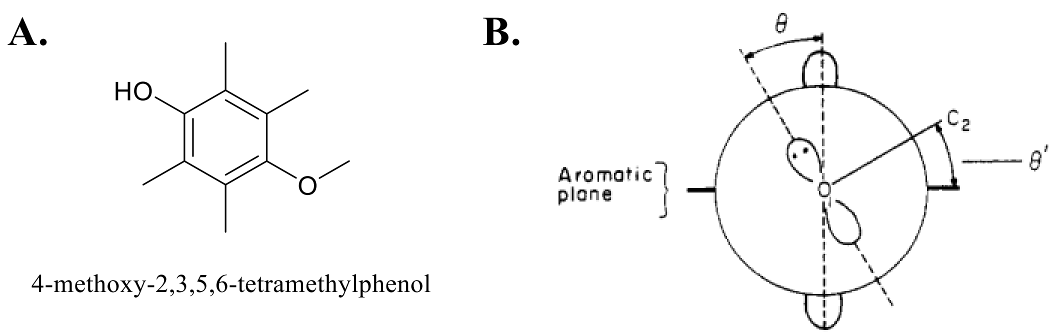

Figure 33. A. 4-methoxy-2,3,5,6-tetramethylphenol, a simple phenolic compound containing features found to be optimal for chain-breaking antioxidant activity. **B.** Schematic showing dihedral angles θ (O_1 p-orbital and perpendicular to aromatic plane) and θ' (O_1-C_2 bond and the aromatic plane). As θ' decreases, orbital overlap between the p-orbital on O_1 and SOMO of the phenoxyl radical increases, resulting in higher rates of inhibition.[73]

Therefore, as θ' decreases to 0˚, overlap between the p-type orbital and SOMO should be maximized and inhibition rate constants should increase.[89] This trend was confirmed through obtaining x-ray crystal structures for a number of phenols and TocH.[91,57] The θ' for TocH (17˚) is much lower than that of 4-methoxy-2,3,5,6-tetramethylphenol (89˚), suggesting that stereoelectronics are ultimately responsible for the excellent chain-breaking antioxidant activity of TocH.

Despite being an excellent chain-breaking antioxidant, Bowry and Stocker reported that the tocopheryl radical may also maintain a chain sequence by abstracting hydrogen from lipid substrates if the rate of initiation is low and the concentration of tocopherol is high.[96] This finding was the result of increased interest in the oxidative modification of human low-densitiy lipoprotein (LDL) and the involvement of this process in the development of atherosclerotic lesions. The major antioxidant present in LDL particles is TocH, and much research had been done with respect to the ability of TocH to disrupt the oxidative modification of LDL and as an epidemiological marker for ischaemic heart disease.

Initial experiments demonstrated that peroxidation of lipids within the LDL particle continue in the presence of over 90% of the original TocH in the particle.[97] Further studies revealed that under mild free-radical initiated conditions using water soluble azo initiators, the presence of TocH actually accelerated lipid peroxidation. Increasing TocH under these conditions further increased the rate at which peroxidation occurred.[98] This led to kinetic arguments which suggest that the apparent prooxidant activity of TocH under certain circumstances is due to the tocopheryl radical's ability to attack and abstract active L-H bonds of PUFAs (Figure 34, k_{TMP}).[99]

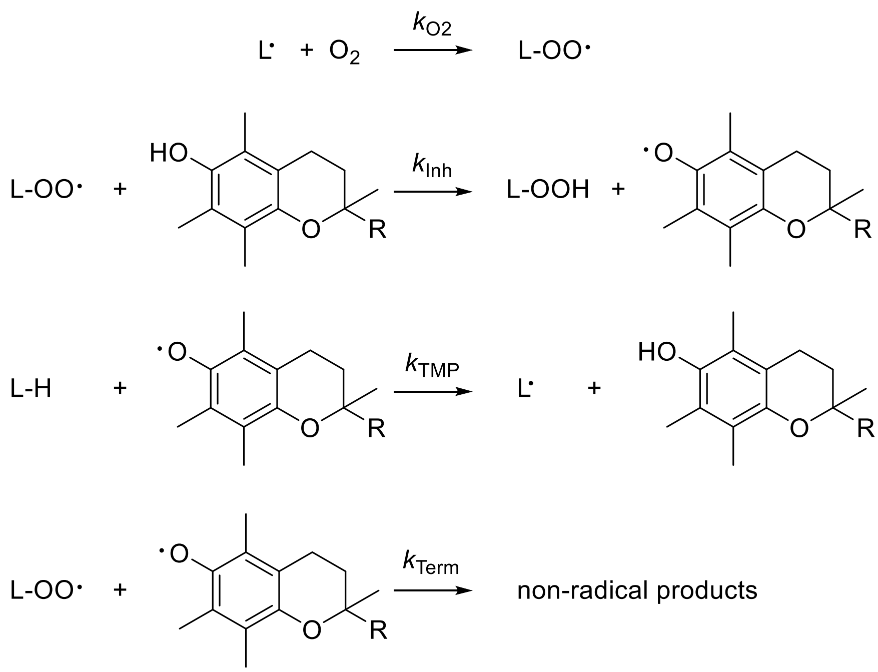

Figure 34. Tocopherol Mediated Peroxidation.[83]

1.4.6. Kinetic Isotope Effects

A kinetic isotope effect (KIE) is observed if the replacement of an atom central to a mechanistic pathway by one of its isotopes (e.g. ^{1}H to ^{2}H or ^{3}H, ^{12}C to ^{13}C, etc.) results in a change in the rate of a reaction. Isotopic substitution will usually have no effect on the qualitative chemical reactivity of a molecule but it can in some circumstances have a measurable effect on the rate of the reaction and lead to a kinetic isotope effect (KIE). When the bond broken during the reaction is isotopically substituted (i.e. C-H to C-D), any measurable change in rate is due to a primary KIE. The H/D KIE for a reaction can be calculated using Equation 7, where k_H and k_D are reaction rates for the H and D compounds, respectively.

$$KIE = \frac{k_H}{k_D} \qquad (7)$$

The largest differences in rate are typically observed when a hydrogen atom is replaced with one of its isotopes. The underlying reason for this is due to the fact that the zero-point energy (ZPE) of the bond being broken is an important determinant in the rate of the reaction. Each C-H(D) bond has a characteristic vibration with some ZPE that is a consequence of quantized vibrational levels. The ZPE is directly linked to the mass of the atom by Equation 8, where E_n is the energy of ZPE, *h* is Plank's constant, and *v* is the fundamental vibrational frequency.

$$E_n = \left(n + \frac{1}{2}\right) hv \qquad (8)$$

The vibrational freqnecy (v) is calculated using Equation 9, where κ is the force constant of the bond being broken.

$$\upsilon = \frac{1}{2\pi}\sqrt{\frac{k}{\mu}} \qquad (9)$$

Finally, the denominator in Equation 9 is μ, the reduced mass of the atom being abstracted. The reduced mass is calculated using Equation 10.

$$\mu = \frac{m_1 \times m_2}{m_1 + m_2} \qquad (10)$$

Note that as the mass of the atom abstracted increases, that atom vibrates at a lower frequency and contributes less to the ZPE of the bond being broken. Thus, the ZPE is lowered for the heavier isotopes (C-^{2}H; 2100 cm^{-1}, 3.0 kcal mol^{-1}) in comparison to the ZPE for the lighter atom (C-^{1}H; 2900 cm^{-1}, 4.15 kcal mol^{-1}). This difference results in a larger activation energy (ΔG=1.15 kcal mol^{-1}) needed to reach the transition state (‡) for the heavier atoms, ultimately affecting the rate at which the reaction proceeds (Figure 35). At room temperature, the difference in activation energies corresponds to a measurable difference in the rate of reaction *if and only if* breaking the bond to hydrogen or deuterium is directly involved in the formation of the transition state .[100]

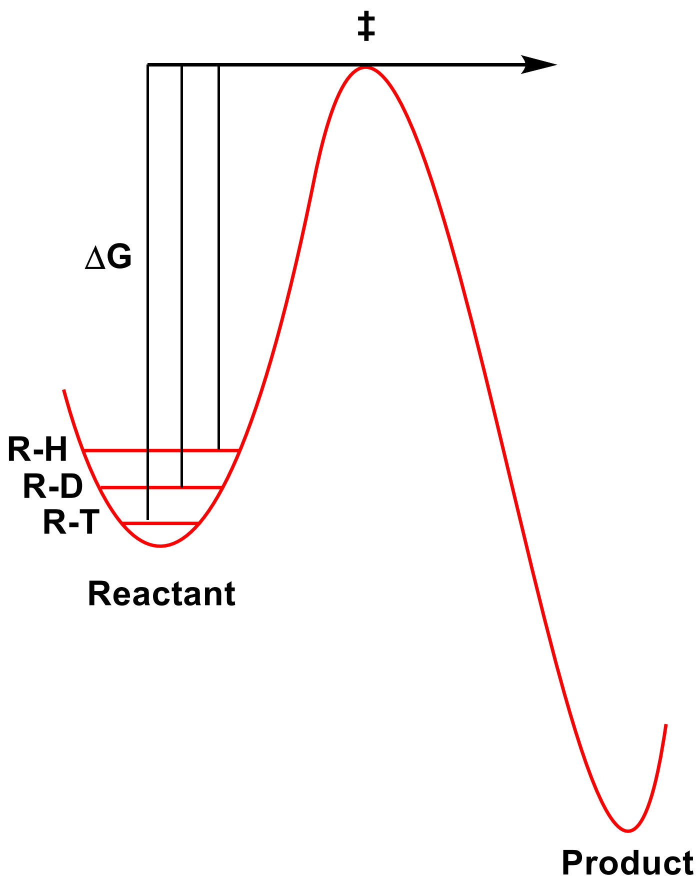

Figure 35. Reaction energy diagram outlining differing zero-point energies associated with isotopic substitution of hydrogen (^{1}H) with deuterium (^{2}H) and tritium (^{3}H).

The rate of a particular reaction (k) or activation energy (E_a) associated with a transformation can be determined using the Arrhenius equation as shown in Equation 11. In this equation A is the Arrhenius constant, k_B is the Boltzmann constant, and T is temperature.

$$k = Ae^{-\frac{E_a}{k_B T}} \qquad \textbf{(11)}$$

Therefore, the KIE for the breaking of a hydrogen atom bond may also be described in terms of the Arrhenius equation as shown in Equation 12. For hydrogen atom abstraction occurring at 300 K (27 ˚C), the maximum H/D KIE is 7 using this equation.[100]

$$\frac{k_H}{k_D} = e^{-\frac{E_a^H - E_a^D}{2k_B T}} \qquad \textbf{(12)}$$

1.5. Enzymatic Oxidation

Lipids may be oxidized by enzymes that selectively abstract hydrogen atoms and direct oxygen addition to the intermediate carbon radicals to generate products having defined stereochemistry. The products of enzymatic oxidation are diverse, with many of those products acting as signaling molecules for various cellular functions.

1.5.1. Cyclooxygenases

The cyclooxygenase (COX) family is comprised of cyclooxygenase 1 (COX1), the constitutively expressed species,[4] and cyclooxygenase 2 (COX2), which is expressed in response to an inflammatory burst or attack.[101] Both enzymes utilize a tyrosyl radical in the active site to abstract hydrogen from arachidonic acid (AA),[102] and both oxygenate LA and AA[103] as well as other ω-3 and ω-6 PUFAs.[104]

Oxygenation of PUFAs by the COX family results in an array of signaling molecules that modulate cellular function such as vascular relaxation and constriction, platelet aggregation, and mucosal regeneration.[105] Commensurate to the array of signaling molecules generated by the family, its expression has also been linked to a number of human pathologies including cancer,[106] cardiovascular disease,[107] and neurodegenerative disorders.[108]

The COX family of enzymes are structural homodimers that act as functional heterodimers to *bis*-oxygenate and cyclize AA which has been released from the lipid bilayer by cytosolic phospholipase A_2 ($cPLA_2$).[109,110] Once AA is brought into the active site, the pro-*S* hydrogen atom situated on *bis*-allylic C-13 is abstracted by Tyr385-O•, after which oxygenation occurs at C-11 and is followed by cyclization to give PGG_2. This peroxide is reduced by the peroxidase active site to give PGH_2, which is the precursor to other eicosanoid signaling molecules (via their respective synthases) of PGE_2, PGD_2, $PGF_{2\alpha}$, PGI_2, and thromboxane A_2 (TXA_2) (Figure 36).[102] Monooxygenated species are also generated by the COX family, including 11(*R*)-HETE and 15(*S*)-HETE.[111]

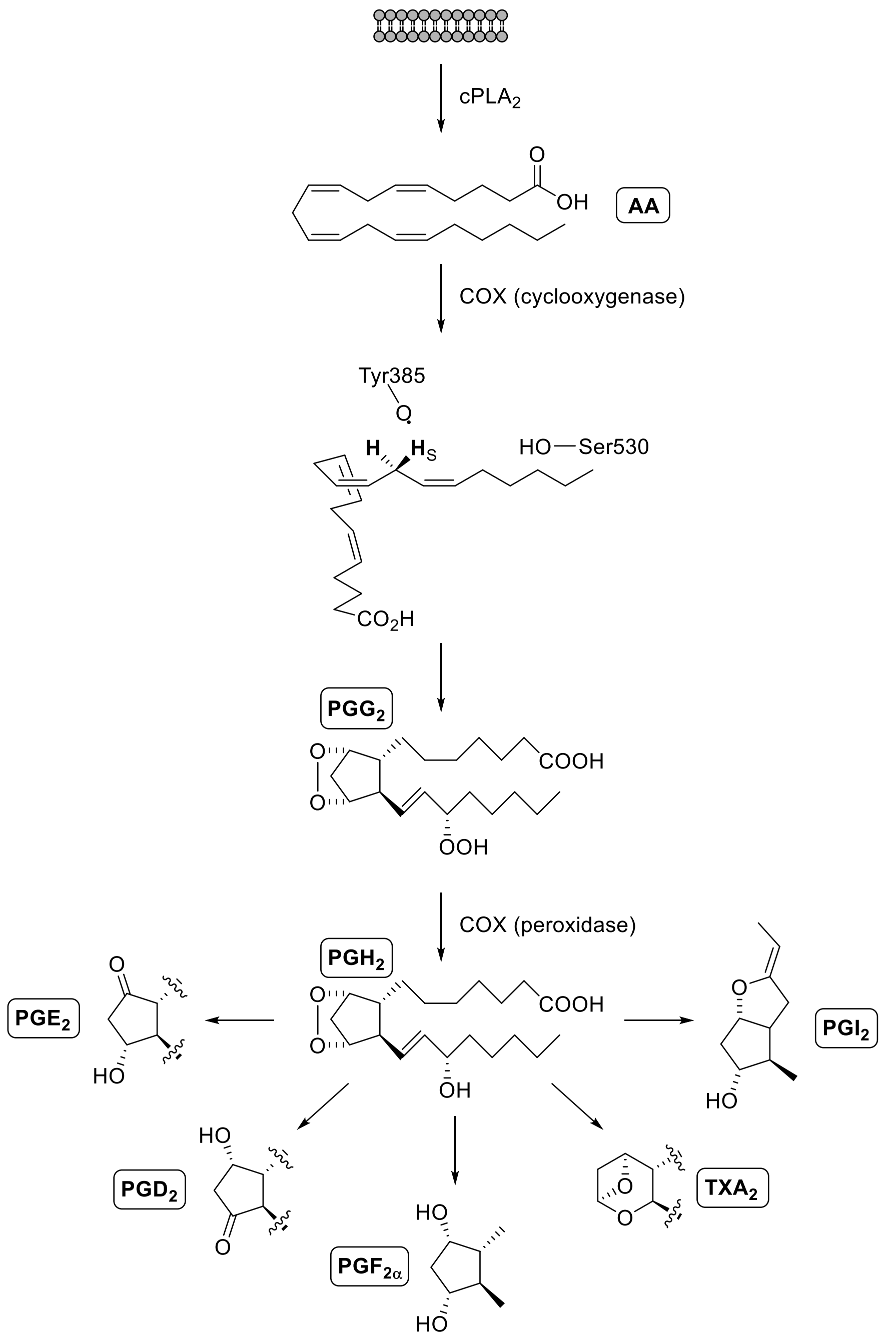

Figure 36. COX metabolism of AA. AA is released from the lipid bilayer by $cPLA_2$. Once in the active site, Tyr385-O• abstracts the pro-S hydrogen atom from C-13. Oxygenation and cyclization results in the formation of PGG_2, and the formation of alcohol PGH_2 is catalyzed by the peroxidase. PGG_2 serves as a precursor for the other eicosanoids shown.[86]

1.5.2. Lipoxygenases

Lipoxygenases (LOXs) belong to a separate family of enzymes capable of controlled oxygenation of both LA and AA in either the free or esterified state.[112,113] The LOX family enzymes are named depending on the lipid products formed in the oxidation. For instance, 9-LOX and 13-LOX catalyze the oxygenation of LA to form 9-HpODE and 13-HpODE, respectively.[114] Similarly, the LOX's responsible for oxygenation of AA to give the hydroperoxyeicosatetraenoic acids (HpETEs) – 5-HpETE, 8-HpETE, 12-HpETE, or 15-HpETE (Figure 37) – are named based upon the preferred product (5-LOX, 8-LOX, etc.).[115]

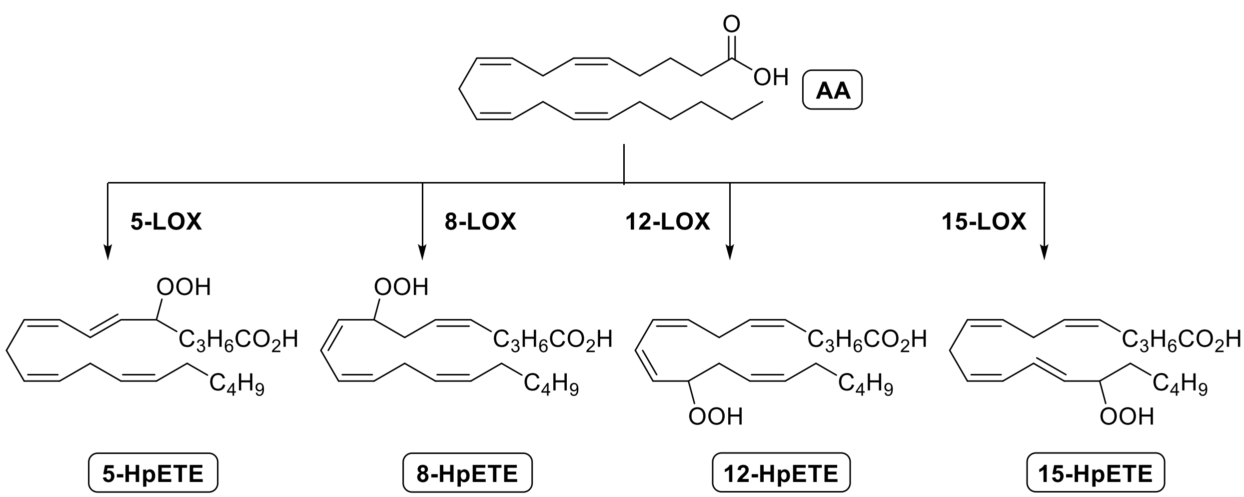

Figure 37. Oxygenation of AA to form HpETEs by members of the Lipoxygenase family.[99]

1.6. Conclusions

The autoxidation of lipids has been extensively studied and linked to a number of cellular disruptions and human pathologies such as cardiovascular disease,[116,117,118,119,120] Parkinson's disease,[121,122] and Alzheimer's disease.[34,123] It is clear that ROS can facilitate a broad spectrum of damage within different classes of lipids, and diminishing these reactions is key to controlling the downstream effects of oxidative damage. The aim of this dissertation is to expand on the ideas and findings discussed in this introductory chapter, focusing on kinetic studies of sterol autoxidation as well as physical studies surrounding a strategy to diminish lipid peroxidation *in vivo* through the use of isotopically reinforced PUFAs. Deuterium is substituted for hydrogen at the reactive *bis*-allylic centers in these synthetic lipids.[124] The following work will be presented:

1. Measurement of propagation rate constants for natural and isotopically reinforced PUFAs.
2. Competition experiments to assess the effects of D-PUFAs on the rate of peroxide formation.
3. Determination of rate constants for peroxidation of sterols important in the biosynthesis of cholesterol using the methyl linoleate clock.
4. An examination of tocopherol-mediated oxidation of PUFAs and deuterated derivatives.
5. A study of the effects of deuterated PUFAs in RAW 264.7 macrophages, a prototypical cell line used extensively in the study of lipid metabolism.

1.7. References

1. Smith, A. D., *Oxford Dictionary of Biochemistry and Molecular Biology, Rev. Ed.* Oxford University Press: Oxford, 2000.

2. Fahy, E.; Cotter, D.; Sud, M.; Subramaniam, S., Lipid classification, structures and tools. *Biochim. Biophys. Acta* **2011,** *1811*, 637-647.

3. Piomelli, D., Arachidonic acid in cell signaling. *Curr. Opin. Cell Biol.* **1993,** *5*, 274-280.

4. Hamberg, M.; Samuelsson, B., Detection and isolation of an endoperoxide intermediate in prostaglandin biosynthesis. *Proc. Natl. Acad. Sci. U.S.A.* **1973,** *70*, 899-903.

5. Nugteren, D. H.; Hazelhof, E., Isolation and properties of intermediates in prostaglandin biosynthesis. *Biochim. Biophys. Acta* **1973,** *326*, 448-461.

6. Hamberg, M.; Svensson, J.; Wakabayashi, T.; Samuelsson, B., Isolation and structure of two prostaglandin endoperoxides that cause platelet aggregation. *Proc. Natl. Acad. Sci. U.S.A.* **1974,** *71*, 345-349.

7. Herman, G. E., Disorders of cholesterol biosynthesis: prototypic metabolic malformation syndromes. *Hum. Molec. Genet.* **2003,** *12*, R75-R88.

8. Esterbauer, H., Cytotoxicity and Genotoxicity of Lipid-Oxidation Products. *Am. J. Clin. Nut.* **1993,** *57*, S779-S786.

9. Radi, R.; Beckman, J. S.; Bush, K. M.; Freeman, B. A., Peroxynitrite-induced membrane lipid peroxidation: the cytotoxic potential of superoxide and nitric oxide. *Arch. Biochem. Biophys.* **1991,** *288*, 481-487.

10. McGeer, P. L.; McGeer, E. G., Inflammation and neurodegeneration in Parkinson's disease. *Parkinsonism Relat. Disord.* **2004,** *10*, S3-S7.

11. Dexter, D. T.; Carter, C. J.; Wells, F. R.; Javoy-Agid, F.; Agid, Y.; Lees, A.; Jenner, P.; Marsden, C. D., Basal lipid peroxidation in substantia nigra is increased in Parkinson's disease. *J. Neurochem.* **1989,** *52*, 381-389.

12. Berliner, J. A.; Heinecke, J. W., The role of oxidized lipoproteins in atherogenesis. *Free Radic. Biol. Med.* **1996,** *20*, 707-727.

13. Berliner, J. A.; Leitinger, N.; Tsimikas, S., The role of oxidized phospholipids in atherosclerosis. *J. Lipid Res.* **2009,** *50*, S207-S212.

14. de Saussure, T., *Recherches chimiques sure la vegetation*. Paris, 1804.

15. Gomberg, M., An instance of trivalent carbon: triphenylmethyl. *J. Am. Chem. Soc.* **1900,** *22*, 757-771.

16. Holm, G. E.; Greenbank, G. R.; Deysher, E. F., Susceptibility of fats to autoxidation. *Ind. Eng. Chem.* **1927,** *19*, 156-158.

17. Kuhn, R.; Meyer, K. Z., *Physiol. Chem.* **1929,** *185*, 193-199.

18. Stephens, N. H., Studies in auto-oxidation. I. Cyclohexene peroxide. *J. Am. Chem. Soc.* **1928,** *50*, 568-571.

19. March, J., *Advanced Organic Chemistry: Reactions, Mechanisms, and Structure*. 1 ed.; McGraw-Hill: New York, 1968; p 153-158.

20. Murphy, M. P., How mitochondria produce reactive oxygen species. *Biochem. J.* **2009,** *417*, 1-13.

21. MacMicking, J. D.; North, R. J.; LaCourse, R.; Mudgett, J. S.; Shah, S. K.; Nathan, C. F., Identification of nitric oxide synthase as a protective locus against tuberculosis. *Proc. Natl. Acad. Sci. U.S.A.* **1997,** *94*, 5243-5248.

22. Park, J. S.; Svetkauskaite, D.; He, Q.; Kim, J. Y.; Strassheim, D.; Ishizaka, A.; Abraham, E., Involvement of toll-like receptors 2 and 4 in cellular activation by high mobility group box 1 protein. *J. Biol. Chem.* **2004,** *279*, 7370-7377.

23. West, A. P.; Koblansky, A. A.; Ghosh, S., Recognition and signaling by toll-like receptors. *Annu. Rev. Cell Dev. Biol.* **2006,** *22*, 409-437.

24. West, A. P.; Brodsky, I. E.; Rahner, C.; Woo, D. K.; Erdjument-Bromage, H.; Tempst, P.; Walsh, M. C.; Choi, Y.; Shadel, G. S.; Ghosh, S., TLR signalling augments macrophage bactericidal activity through mitochondrial ROS. *Nature* **2011,** *472*, 476-480.

25. Bolland, J. L.; Gee, G., Kinetic studies in the chemistry of rubber and related materials. II. The kinetics of oxidation of unconjugated olefins. *Trans. Faraday Soc.* **1946,** *42*, 236-243.

26. Bolland, J. L.; Gee, G., Kinetic Studies in the Chemistry of Rubber and Related Materials. II. The Kinetics of Oxidation of Unconjugated Olefins. *Transactions of the Faraday Society* **1946,** *42*, 236-243.

27. Pryor, W. A., *The Role of Free Radical Reactions in Biological Systems*. Academic Press: New York, 1976; Vol. 1, p 287.

28. Arnold, W.; Clayton, R. K., The first step in photosynthesis: evidence for its electronic nature. *Proc. Natl. Acad. Sci. U.S.A.* **1960,** *46*, 769-776.

29. Kohl, D. H.; Townsend, J.; Commoner, B.; Crespi, H. L.; Dougherty, R. C.; Katz, J. J., Effects of isotopic substitution on electron spin resonance signals in photosynthetic organisms. *Nature* **1965,** *206*, 1105-1110.

30. Babior, B. M.; Kipnes, R. S.; Curnutte, J. T., Biological defense mechanisms. The production by leukocytes of superoxide, a potential bactericidal agent. *J. Clin. Invest.* **1973,** *52*, 741-744.

31. Greenberg, M. E.; Li, X. M.; Gugiu, B. G.; Gu, X. D.; Qin, J.; Salomon, R. G.; Hazen, S. L., The lipid whisker model of the structure of oxidized cell membranes. *J. Biol. Chem.* **2008,** *283*, 2385-2396.

32. Murphy, R. C.; Johnson, K. M., Cholesterol, reactive oxygen species, and the formation of biologically active mediators. *J. Biol. Chem.* **2008,** *283*, 15521-15525.

33. Zhu, X.; Tang, X.; Anderson, V. E.; Sayre, L. M., Mass spectrometric characterization of protein modification by the products of nonenzymatic oxidation of linoleic acid. *Chem. Res. Toxicol.* **2009,** *22*, 1386-1397.

34. Montine, T. J.; Peskind, E. R.; Quinn, J. F.; Wilson, A. M.; Montine, K. S.; Galasko, D., Increased cerebrospinal fluid F2-isoprostanes are associated with aging and latent Alzheimer's disease as identified by biomarkers. *Neuromol. Med.* **2011,** *13*, 37-43.

35. Hammad, L. A.; Wu, G. X.; Saleh, M. M.; Klouckova, I.; Dobrolecki, L. E.; Hickey, R. J.; Schnaper, L.; Novotny, M. V.; Mechref, Y., Elevated levels of hydroxylated phosphocholine lipids in the blood serum of breast cancer patients. *Rapid Commun. Mass Spectrom.* **2009,** *23*, 863-876.

36. Wu, R. P.; Hayashi, T.; Cottam, H. B.; Jin, G.; Yao, S.; Wu, C. C.; Rosenbach, M. D.; Corr, M.; Schwab, R. B.; Carson, D. A., Nrf2 responses and the therapeutic selectivity of electrophilic compounds in chronic lymphocytic leukemia. *Proc. Natl. Acad. Sci. U.S.A.* **2010,** *107*, 7479-7484.

37. Silverstein, R. L.; Febbraio, M., CD36, a scavenger receptor involved in immunity, metabolism, angiogenesis, and behavior. *Sci. Signal.* **2009,** *2*, 1-16.

38. Hammad, L.; Wu, G.; Saleh, M.; Klouckova, I.; Dobrolecki, L.; Hickey, R.; Schnaper, L.; Novotny, M.; Mechref, Y., Elevated levels of hydroxylated phosphocholine lipids in the blood serum of breast cancer patients. *Rapid Communications in Mass Spectrometry* **2009,** *23* (6), 863-876.

39. Yin, H.; Xu, L.; Porter, N. A., Free radical lipid peroxidation: mechanisms and analysis. *Chem. Rev.* **2011,** *111*, 5944-5972.

40. Mayo, F. R.; Miller, A. A., Oxidation of unsaturated compounds. II. Reactions of styrene peroxide. *J. Am. Chem. Soc.* **1956,** *78*, 1023-1034.

41. Mayo, F. R., The oxidation of unsaturated compounds. V. The effect of oxygen pressure on the oxidation of styrene. *J. Am. Chem. Soc.* **1958,** *80*, 2465-2480.

42. Bell, E. R.; Raley, J. H.; Rust, F. F.; Seubold, F. H.; Vaughan, W. E., Reactions of free radicals associated with low temperature oxidation of paraffins. *Discuss. Faraday Soc.* **1951,** *10*, 242-249.

43. Russell, G. A., Deuterium-isotope effects in the autoxidation of aralkyl hydrocarbons. Mechanism of the interaction of peroxy radicals. *J. Am. Chem. Soc.* **1957,** *79*, 3871-3877.

44. Howard, J. A.; Ingold, K. U., Absolute rate constants for hydrocarbon autoxidation. V. The hydroperoxy radical in chain propagation and termination. *Can. J. Chem.* **1967,** *45*, 785-792.

45. Porter, N. A., Mechanisms for the autoxidation of polyunsaturated lipids. *Acc. Chem. Res.* **1986,** *19*, 262-268.

46. Gardner, H. W., Oxygen radical chemistry of polyunsaturated fatty acids. *Free Radic. Biol. Med.* **1989,** *7*, 65-86.

47. Xu, L.; Davis, T. A.; Porter, N. A., Rate constants for peroxidation of polyunsaturated fatty acids and sterols in solution and in liposomes. *J. Am. Chem. Soc.* **2009,** *131*, 13037-13044.

48. Melville, H. W., The photochemical polymerization of methyl methacrylate vapour. *Proc. Roy. Soc. A* **1937,** *163*, 511-542.

49. Swain, C. G.; Bartlett, P. D., Rate constants of the steps in addition polymerization. II. Use of the rotating-sector method on liquid vinyl acetate. *J. Am. Chem. Soc.* **1946,** *68*, 2381-2386.

50. Jones, T. T.; Melville, H. W., The determination of the lifetime of active polymeric molecules. *Proc. Roy. Soc. A* **1940,** *175*, 392-409.

51. Newcomb, M., Competition methods and scales for alkyl-radical reaction kinetics. *Tetrahedron* **1993,** *49*, 1151-1176.

52. Griller, D.; Ingold, K. U., Free-radical clocks. *Acc. Chem. Res.* **1980,** *13*, 317-323.

53. Newcomb, M.; Toy, P. H., Hypersensitive radical probes and the mechanisms of cytochrome P450-catalyzed hydroxylation reactions. *Acc. Chem. Res.* **2000,** *33*, 449-455.

54. Roschek, B.; Tallman, K.; Rector, C.; Gillmore, J.; Pratt, D.; Punta, C.; Porter, N., Peroxyl radical clocks. *J. Org. Chem.* **2006,** *71*, 3527-3532.

55. Howard, J. A.; Ingold, K. U., Absolute rate constants for hydrocarbon autoxidation. VI. Alkyl aromatic and olefinic hydrocarbons. *Can. J. Chem.* **1967,** *45*, 793-802.

56. Cosgrove, J. P.; Church, D. F.; Pryor, W. A., The kinetics of the autoxidation of polyunsaturated fatty acids. *Lipids* **1987,** *22*, 299-304.

57. Burton, G. W.; Doba, T.; Gabe, E. J.; Hughes, L.; Lee, F. L.; Prasad, L.; Ingold, K. U., Autoxidation of biological molecules. IV. Maximizing the antioxidant activity of phenols. *J. Am. Chem. Soc.* **1985,** *107*, 7053-7065.

58. Pratt, D. A.; DiLabio, G. A.; Brigati, G.; Pedulli, G. F.; Valgimigli, L., 5-Pyrimidinols: novel chain-breaking antioxidants more effective than phenols. *J. Am. Chem. Soc.* **2001,** *123*, 4625-4626.

59. Davis, T. A.; Gao, L.; Yin, H.; Morrow, J. D.; Porter, N. A., In vivo and in vitro lipid peroxidation of arachidonate esters: The effects of fish oil w-3 lipids on product distribution. *J. Am. Chem. Soc.* **2006,** *128*, 14897-14904.

60. Boozer, C. E.; Hammond, G. S.; Hamilton, C. E.; Sen, J. N., Air oxidation of hydrocarbons. II. The stoichiometry and fate of inhibitors in benzene and chlorobenzene. *J. Am. Chem. Soc.* **1955,** *77*, 3233-3237.

61. Howard, J. A.; Ingold, K. U., Absolute rate constants for hydrocarbon autoxidation. IV. Tetralin, cyclohexene, diphenylmethane, ethylbenzene, and allylbenzene. *Can. J. Chem.* **1966,** *44*, 1119-1130.

62. Carey, F. A.; Sundberg, R. J., *Advanced Organic Chemistry Part A: Structure and Mechanisms*. 5th ed.; Springer: New York, NY, 2007.

63. Gardner, H. W., Oxygen radical chemistry of polyunsaturated fatty acids. *Free Radic. Biol. Med.* **1989,** *7*, 65-86.

64. van Meer, G.; Voelker, D. R.; Feigenson, G. W., Membrane lipids: where they are and how they behave. *Nat. Rev. Mol. Cell Biol.* **2008,** *9* (2), 112-124.

65. Shrivastava, S.; Paila, Y. D.; Dutta, A.; Chattopadhyay, A., Differential Effects of Cholesterol and its Immediate Biosynthetic Precursors on Membrane Organization. *Biochemistry* **2008,** *47* (20), 5668-5677.

66. Rog, T.; Vattulainen, I.; Jansen, M.; Ikonen, E.; Karttunen, M., Comparison of cholesterol and its direct precursors along the biosynthetic pathway: Effects of cholesterol, desmosterol and 7-dehydrocholesterol on saturated and unsaturated lipid bilayers. *J. Chem. Phys.* **2008,** *129*, 154508.

67. Brown, D. A.; London, E., Functions of Lipid Rafts in Biological Membranes. *Annu. Rev. Cell Dev. Biol.* **1998,** *14*, 111-136.

68. Jurevics, H.; Morell, P., Cholesterol for Synthesis of Myelin is Made Locally, Not Imported into Brain. *J. Neurochem.* **1995,** *64*, 895-901.

69. Dietschy, J. M., Central nervous system: cholesterol turnover, brain development and neurodegeneration. *Biol. Chem.* **2009,** *390*, 287-293.

70. Kandutsch, A. A.; Russell, A. E., Preputial gland tumor sterols. 3. A metabolic pathway from lanosterol to cholesterol. *J. Biol. Chem.* **1960,** *235*, 2256-2261.

71. Bloch, K., Sterol molecule: structure, biosynthesis, and function. *Steroids* **1992,** *57*, 378-383.

72. Brown, A. J.; Jessup, W., Oxysterols and atherosclerosis. *Atherosclerosis* **1999,** *142*, 1-28.

73. Vaya, J.; Schipper, H. M., Oxysterols, cholesterol homeostasis, and Alzheimer disease. *J. Neurochem.* **2007,** *102*, 1727-1737.

74. Rodriguez, I. R.; Fliesler, S. J., Photodamage generates 7-keto- and 7-hydroxycholesterol in the rat retina via a free radical-mediated mechanism. *Photochem. Photobiol.* **2009,** *85*, 1116-1125.

75. Kandutsch, A. A.; Chen, H. W., Inhibition of Sterol Synthesis in Cultured Mouse Cells by 7α-Hydroxycholesterol, 7β-Hydroxycholesterol, and 7-Ketocholesterol. *J. Biol. Chem.* **1973,** *248*, 8408-8417.

76. Smith, L. L.; Johnson, B. H., Biological activities of oxysterols. *Free Radic. Biol. Med.* **1989,** *7*, 285-332.

77. Javitt, N. B., Oxysterols: novel biologic roles for the 21st century. *Steroids* **2008,** *73*, 149-157.

78. Smith, L. L., Cholesterol Autoxidation 1981-1986. *Chem. Phys. Lipids* **1987,** *44*, 87-125.

79. Zielinski, Z. A.; Pratt, D. A., Cholesterol autoxidation revisited: Debunking the dogma associated with the most vilified of lipids. *J. Am. Chem. Soc.* **2016,** *138*, 6932-6935.

80. Ursini, F.; Maiorino, M.; Gregolin, C., The selenoenzyme phospholipid hydroperoxide glutathione peroxidase. *Biochim. Biophys. Acta* **1985,** *839*, 62-70.

81. Girotti, A. W., Lipid hydroperoxide generation, turnover, and effector action in biological systems. *J. Lipid Res.* **1998,** *39*, 1529-1542.

82. Chang, Y. H.; Abdalla, D. S. P.; Sevanian, A., Characterization of Cholesterol Oxidation Products Formed by Oxidative Modification of Low Density Lipoprotein. *Free Radic. Biol. Med.* **1997,** *23*, 202-214

83. Howard, J. A.; Ingold, K. U., Self-reaction of sec-butylperoxy radicals. Confirmation of the Russell mechanism. *J. Am. Chem. Soc.* **1968,** *90*, 1056-1058.

84. Holick, M. F.; Frommer, J. E.; McNeill, S. C.; Richtand, N. M.; Henley, J. W.; Potts, J. T. J., Photometabolism of 7-dehydrocholesterol to previtamin D_3 in skin. *Biochem. Biophys. Res. Commun.* **1977,** *76*, 107-114.

85. Xu, L.; Korade, Z.; Rosado, D. A.; Liu, W.; Lamberson, C. R.; Porter, N. A., An oxysterol biomarker for 7-dehydrocholesterol oxidation in cell/mouse models for Smith-Lemli-Opitz syndrome. *J. Lipid Res.* **2011,** *52*, 1222-1233.

86. Korade, Z.; Xu, L.; Shelton, R.; Porter, N. A., Biological activities of 7-dehydrocholesterol-derived oxysterols: implications for Smith-Lemli-Opitz syndrome. *J. Lipid Res.* **2010,** *51*, 3259-3269.

87. Xu, L.; Korade, Z.; Porter, N. A., Oxysterols from free radical chain oxidation of 7-dehydrocholesterol: Product and mechanistic studies. *J. Am. Chem. Soc.* **2010,** *132*, 2222-2232.

88. Xu, L.; Porter, N. A., Unpublished results. 2011.

89. Burton, G. W.; Ingold, K. U., Vitamin E: Application of the principles of physical organic chemistry to the exploration of its structure and function. *Acc. Chem. Res.* **1986,** *19*, 194-201.

90. Ingold, K. U., Inhibition of the autoxidation of organic substances in the liquid phase. *Chem. Rev.* **1961,** *61*, 563-589.

91. Burton, G. W.; Ingold, K. U., Autoxidation of biological molecules. I. The antioxidant activity of vitamin-E and related chain-breaking phenolic antioxidants in vitro. *J. Am. Chem. Soc.* **1981,** *103*, 6472-6477.

92. Howard, J. A.; Ingold, K. U., The inhibited autoxidation of styrene: Part I. The deuterium isotope effect for inhibition by 2,6-di-*tert*-butyl-4-methoxyphenol. *Can. J. Chem.* **1962,** *40*, 1851-1864.

93. Howard, J. A.; Ingold, K. U., The inhibited autoxidation of styrene: Part II. The relative inhibiting efficiencies of meta- and para-substituted phenols. *Can. J. Chem.* **1963,** *41*, 1744-1751.

94. Howard, J. A.; Ingold, K. U., The inhibited autoxidation of styrene: Part III. The relative inhibiting efficiencies of ortho-alkyl phenols. *Can. J. Chem.* **1963,** *41*, 2800-2806.

95. Howard, J. A.; Ingold, K. U., The inhibited autoxidation of styrene: Part IV. Solvent effects. *Can. J. Chem.* **1964,** *42*, 1044-1056.

96. Bowry, V. W.; Stocker, R., Tocopherol-mediated peroxidation. The prooxidant effect of vitamin-E on the radical-initiated oxidation of human low-density lipoprotein. *J. Am. Chem. Soc.* **1993,** *115*, 6029-6044.

97. Stocker, R.; Bowry, V. W.; Frei, B., Ubiquinol-10 protects human low-density lipoprotein more efficiently against lipid-peroxidation than does alpha-tocopherol. *Proc. Natl. Acad. Sci. U.S.A.* **1991,** *88*, 1646-1650.

98. Bowry, V. W.; Ingold, K. U.; Stocker, R., Vitamin-E in human low-density lipoprotein - When and how this antioxidant becomes a prooxidant. *Biochem. J.* **1992,** *288*, 341-344.

99. Ingold, K. U.; Bowry, V. W.; Stocker, R.; Walling, C., Autoxidation of lipids and antioxidation by alpha-tocopherol and ubiquinol in homogenous solution and in aqueous dispersions of lipids: Unrecognized consequences of lipid particle size as exemplified by oxidation of human low density lipoprotein. *Proc. Natl. Acad. Sci. U.S.A.* **1993,** *90*, 45-49.

100. Westheimer, F. H., The magnitude of the primary kinetic isotope effect for compounds of hydrogen and deuterium. *Chem. Rev.* **1961,** *61*, 265-273.

101. Fu, J. Y.; Masferrer, J. L.; Seibert, K.; Raz, A.; Needleman, P., The induction and suppression of prostaglandin-H2 synthase (cyclooxygenase) in human monocytes. *J. Biol. Chem.* **1990,** *265*, 16737-16740.

102. Rouzer, C. A.; Marnett, L. J., Mechanism of free radical oxygenation of polyunsaturated fatty acids by cyclooxygenases. *Chem. Rev.* **2003,** *103*, 2239-2304.

103. Hubbard, W. C.; Hough, A. J.; Brash, A. R.; Watson, J. T.; Oates, J. A., Metabolism of linoleic and arachidonic acids in VX2 carcinoma tissue - Identification of monohydroxy octadecadienoic acids and monohydroxy eicosatetraenoic acids. *Prostaglandins* **1980,** *20*, 431-447.

104. Groeger, A. L.; Cipollina, C.; Cole, M. P.; Woodcock, S. R.; Bonacci, G.; Rudolph, T. K.; Rudolph, V.; Freeman, B. A.; Schopfer, F. J., Cyclooxygenase-2 generates anti-inflammatory mediators from omega-3 fatty acids. *Nat. Chem. Biol.* **2010,** *6*, 433-441.

105. Stables, M. J.; Gilroy, D. W., Old and new generation lipid mediators in acute inflammation and resolution. *Prog. Lipid Res.* **2011,** *50*, 35-51.

106. Sano, H.; Kawahito, Y.; Wilder, R. L.; Hashiramoto, A.; Mukai, S.; Asai, K.; Kimura, S.; Kato, H.; Kondo, M.; Hla, T., Expression of cyclooxygenase-1 and cyclooxygenase-2 in human colorectal-cancer. *Cancer Res.* **1995,** *55*, 3785-3789.

107. Schonbeck, U.; Sukhova, G. K.; Graber, P.; Coulter, S.; Libby, P., Augmented expression of cyclooxygenase-2 in human atherosclerotic lesions. *Am. J. Pathol.* **1999,** *155*, 1281-1291.

108. Teismann, P.; Tieu, K.; Choi, D. K.; Wu, D. C.; Naini, A.; Hunot, S.; Vila, M.; Jackson-Lewis, V.; Przedborski, S., Cyclooxygenase-2 is instrumental in Parkinson's disease neurodegeneration. *Proc. Natl. Acad. Sci. U.S.A.* **2003,** *100*, 5473-5478.

109. Dong, L.; Vecchio, A. J.; Sharma, N. P.; Jurban, B. J.; Malkowski, M. G.; Smith, W. L., Human cyclooxygenase-2 is a sequence homodimer that functions as a conformational heterodimer. *J. Biol. Chem.* **2011,** *286*, 19035-19046.

110. Prusakiewicz, J. J.; Duggan, K. C.; Rouzer, C. A.; Marnett, L. J., Differential sensitivity and mechanism of inhibition of COX-2 oxygenation of arachidonic acid and 2-arachidonoylglycerol by ibuprofen and mefenamic acid. *Biochemistry* **2009,** *48*, 7353-7355.

111. Schneider, C.; Boeglin, W. E.; Brash, A. R., Identification of two cyclooxygenase active site residues, leucine 384 and glycine 526, that control carbon ring cyclization in prostaglandin biosynthesis. *J. Biol. Chem.* **2004,** *279*, 4404-4414.

112. Smith, W. L.; Lands, W. E. M., Oxygenation of unsaturated fatty-acids by soybean lipoxygenase. *J. Biol. Chem.* **1972,** *247*, 1038-1047.

113. Losito, I.; Conte, E.; Introna, B.; Megli, F. M.; Palmisano, F., Improved specificity of cardiolipin peroxidation by soybean lipoxygenase: a liquid chromatography - electrospray ionization mass spectrometry investigation. *J. Mass Spectrom.* **2011,** *46*, 1255-1262.

114. Doderer, A.; Kokkelink, I.; van der Veen, S.; Valk, B. E.; Schram, A. W.; Douma, A. C., Purification and characterization of two lipoxygenase isoenzymes from germinating barley. *Biochim. Biophys. Acta* **1992,** *1120*, 97-104.

115. Schneider, C.; Pozzi, A., Cyclooxygenases and lipoxygenases in cancer. *Cancer Metastasis Rev.* **2011,** *30*, 277-294.

116. Mozaffarian, D.; Benjamin, E. J.; Go, A. S.; Arnett, D. K.; Blaha, M. J.; Cushman, M.; de Ferranti, S.; Despres, J. P.; Fullerton, H. J.; Howard, V. J.; Huffman, M. D.; Judd, S. E.; Kissela, B. M.; Lackland, D. T.; Lichtman, J. H.; Lisabeth, L. D.; Liu, S. M.; Mackey, R. H.; Matchar, D. B.; McGuire, D. K.; Mohler, E. R.; Moy, C. S.; Muntner, P.; Mussolino, M. E.; Nasir, K.; Neumar, R. W.; Nichol, G.; Palaniappan, L.; Pandey, D. K.; Reeves, M. J.; Rodriguez, C. J.; Sorlie, P. D.; Stein, J.; Towfighi, A.; Turan, T. N.; Virani, S. S.; Willey, J. Z.; Woo, D.; Yeh, R. W.; Turner, M. B.; Comm., A. H. A. S.; Subcomm., S. S., Heart disease and stroke statistics-2015 Update: A report from the American Heart Association. *Circulation* **2015,** *131*, E29-E322.

117. Steinberg, D.; Parthasarathy, S.; Carew, T. E.; Khoo, J. C.; Witztum, J. L., Beyond cholesterol - Modifications of low-density lipoprotein that increase its atherogenicity. *N. Eng. J. Med.* **1989,** *320*, 915-924.

118. Palinski, W.; Rosenfeld, M. E.; Ylä-Herttuala, S.; Gurtner, G. C.; Socher, S. S.; Butler, S. W.; Parthasarathy, S.; Carew, T. E.; Steinberg, D.; Witztum, J. L., Low density lipoprotein undergoes oxidative modification in vivo. *Proc. Natl. Acad. Sci. U.S.A.* **1989,** *86*, 1372-1376.

119. Steinbrecher, U. P.; Zhang, H. F.; Lougheed, M., Role of oxidatively modified LDL in atherosclerosis. *Free Radic. Biol. Med.* **1990,** *9*, 155-168.

120. Salonen, J. T.; Ylaherttuala, S.; Yamamoto, R.; Butler, S.; Korpela, H.; Salonen, R.; Nyyssonen, K.; Palinski, W.; Witztum, J. L., Autoantibody against oxidized LDL and progression of carotid atherosclerosis. *Lancet* **1992,** *339*, 883-887.

121. Vos, T.; Barber, R. M.; Bell, B., Global, regional, and national incidence, prevalence, and years lived with disability for 301 acute and chronic diseases and injuries in 188 countries, 1990-2013: a systematic analysis for the Global Burden of Disease Study 2013. *Lancet* **2015,** *386*, 743-800.

122. Jenner, P., Oxidative stress in Parkinson's disease. *Ann. Neurol.* **2003,** *53*, S26-S36.

123. Morrow, J. D.; Harris, T. M.; Roberts, L. J., Noncyclooxygenase oxidative formation of a series of novel prostaglandins: analytical ramifications for measurement of eicosanoids. *Anal. Biochem.* **1990,** *184*, 1-10.

124. Shchepinov, M. S., Reactive oxygen species, isotope effect, essential nutrients, and enhanced longevity. *Rejuvenation Res.* **2007,** *10*, 47-60.

Chapter II

DETERMINATION OF PROPAGATION RATE CONSTANTS OF STEROLS AND D-PUFAS: THE APPLICATION OF RADICAL CLOCKS

2.1. Introduction

2.1.1. Polyunsaturated Fatty Acids

Polyunsaturated fatty acids (PUFAs) contain two or more carbon-carbon double bonds. PUFAs are essential nutrients, readily taken up by cells that are unable to synthesize them. In mammalian cells, PUFAs such as linoleic acid (LA) and linolenic acid (Lnn), are converted to longer chained PUFAs which are required for life such as arachidonic acid (AA) and docosahexaenoic acid (DHA) (Figure 13).[1]

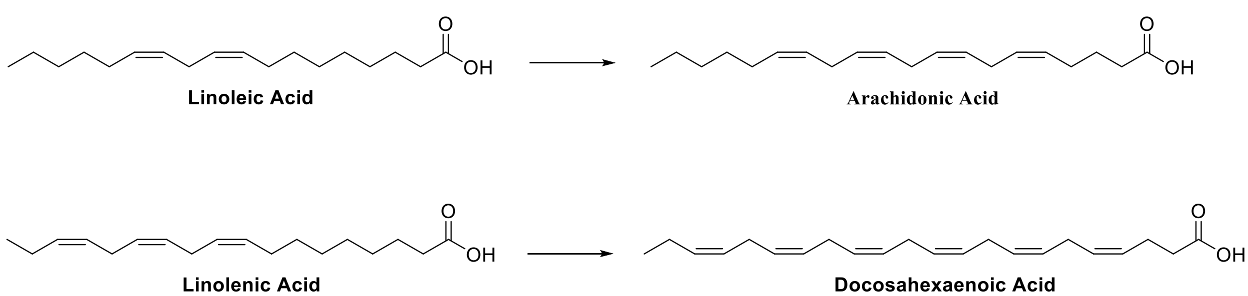

Figure 1: Linoleic and linolenic acid are essential PUFAs. Mammalian cells are able to take these PUFAs up and metabolize them to longer chained PUFAs necessary for life function.

PUFAs are important membrane constituents, and they also play an important role in cellular metabolism. Various oxidative enzymes act on PUFAs to generate prostaglandins,[2] hydroxyl-fatty acids, and leukotrienes.[3] Despite the essential need for PUFAs, these lipids are also extremely prone to peroxidation that is initiated by reactive oxygen species (ROS).[4,5] Once peroxidation is initiated, membrane permeability and fluidity are negatively affected due to accumulation of lipid peroxides[6] and *cis*- to *trans*-isomerization of PUFA double bonds.[7] Moreover, the peroxidation of PUFAs has been implicated in a number of human diseases including atherosclerosis,[8,9,10] cancer,[11,12] and acute lung injury,[13,14] as well as neurodegenerative disorders such as Alzheimer's[15,16] and Parkinson's disease.[17]

Autoxidation of PUFAs can lead to a wide variety of products, especially for the oxidation of longer chained PUFAs. Autoxidation of AA, for example, leads to the formation of distinct class of compounds known as isoprostanes (as outlined in Chapter 1).[18] In this section, the autoxidation of LA will be discussed, as will a recent strategy to diminish lipid peroxidation through isotopic reinforcement of PUFAs.

2.1.2. Autoxidation of Linoleate

The autoxidation of LA and its esters is initiated when an oxygen radical abstracts a *bis*-allylic hydrogen atom from C11 of linoleate, forming a pentadienyl radical. During propagation, oxygen adds into this radical rapidly to give peroxyl radicals at C9 or C13 in either the *trans,cis*- or *trans,trans*-conjugated diene configuration. The peroxyl radicals then abstract an H-atom from a nearby lipid or other H-atom donor, giving a hydroperoxyoctadecadienoic acid (HpODE) and a new pentadienyl radical. This free radical chain reaction will result in the buildup of HpODEs as shown in Figure 14 and as discussed in Chapter I.

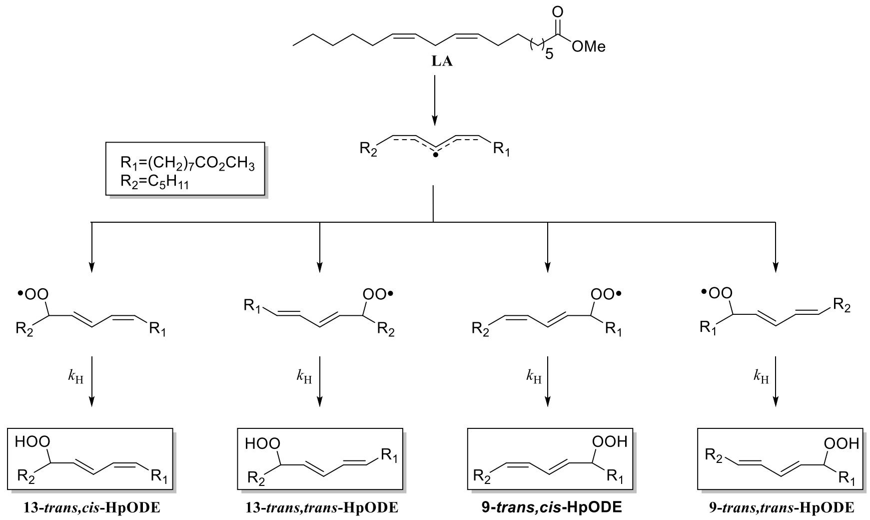

Figure 2: Autoxidation of methyl linoleate, generating HpODEs in the *trans,cis-* or *trans,trans-*diene configuration.

2.1.3. Isotopic Reinforcement of Polyunsaturated Fatty Acids

The reaction of oxygen radicals with PUFAs occurs preferentially at *bis*-allylic methylene groups. This reaction is favored by the low BDE of these C-H bonds, a consequence of the stable delocalized pentadienyl radical that is formed after H-atom abstraction.[19,20,21] A recent strategy to diminish the rate at which lipid autoxidation occurs relies on isotopic reinforcement of these *bis*-allylic sites, replacing hydrogen with deuterium to generate isotopically reinforced PUFAs such as 11,11-D_2-linoleic acid (D_2-LA, Figure 17). H- or D-abstraction at the *bis*-allylic site is the rate determining step in the autoxidation of linoleate, and substitution of a heavier D-atom results in an isotope effect for its removal. This is due to a lower zero-point energy (ZPE) for abstraction of the D-substituted linoleate which translates into a higher activation energy barrier to overcome in order for D-abstraction to occur.

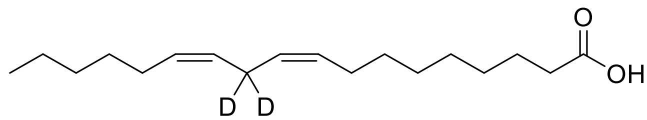

11,11-D_2-Linoleic Acid

Figure 3: Deuterated linoleic acid (D_2-LA).

Hill and coworkers have shown that supplementation of D-PUFAs into biological systems results in resistance to oxidative stress and lipid peroxide buildup.[22] In early studies, *Saccharomyces cerevisia* yeast (*S. cerevisiae*) were examined in proof of concept experiments. This strain of yeast biosynthesizes coenzyme Q (ubiquinone), the hydroquione form of which is used as a lipophilic antioxidant and electron shuttle within the respiratory chain in the mitochondria.[23] The yeasts' lipids consist primarily of saturated fatty acids but they also synthesize palmitoleic acid and oleic acid, both of which are resistant to autoxidation. These yeast also readily take up exogenous PUFAs. Wild type and mutant yeast lacking the genetic framework to produce ubiquinone and are thus more susceptible to oxidative stress, were used to study the effects natural PUFAs and D-PUFAs have during oxidative events. Workers in the Clarke group found that treatment of both wild type and mutant yeast with D-PUFAs (deuterated linoleic and linolenic acid derivatives) resulted in no overall toxicity, but natural PUFAs killed cells during incubation of up to 5 hours.[24] Furthermore, robust protection against oxidative stress was observed in both wild type and mutant yeast after treatment with D-PUFA.[24] Further studies have indicated that treatment of the same yeast with mixtures of PUFA and D-PUFA also show resistance to oxidative stress, and D-PUFA concentrations as low as 20% of the total mixture provide the same levels of protection as higher percentages of D-PUFA. This finding, named "the 20% effect", suggested that the protection against oxidative stress afforded by D-PUFAs had some minimal threshold for activity.[25]

D-PUFAs have also shown beneficial effects in diseases where oxidative stress is a primary component of pathophysiology such as Friedreich's ataxia[26] and Parkinson's disease.[27,28,29] These promising results stimulated further study of the physical aspects of autoxidation of D-PUFAs and the suppression of oxidation by these compounds.

2.2. Results

2.2.1. Measurement of the Propagation Rate Constant for Linoleate and 11,11-D_2-Linoleate

The methyl linoleate clock,[30] discussed in Chapter I, was used to determine propagation rate constants for D_2-LA. PUFAs were purified and dried under vacuum prior to experiments. A stock solution of 0.1 M 2,2'-azobis(4-methoxy-2,4-dimethyl)-valeronitrile (MeOAMVN) in benzene was used to initiate all reactions.

In a typical experiment to measure propagation rate constants for PUFAs and D-PUFAs, the concentration of LA or D_2-LA ethyl esters used ranged from 0.14 to 2.1 M. Oxidations were carried out at 37 °C for 1 h and quenched with butylated hydroxytoluene (BHT) and triphenylphosphine (PPh_3). Oxidation products (HODEs) were analyzed by HPLC-UV. The residual amount of D_1-LA and LA present in the D_2-LA ethyl ester starting material was determined using ^{1}H NMR analysis. These values were found to be 2.9 and 0.8 mol%, respectively, and these values were used to correct the data from D_2-LA assuming that 11-D_1-LA is half as reactive as LA.[31] Results for LA and D_2-LA ethyl esters are shown in Figures 4 and 5.

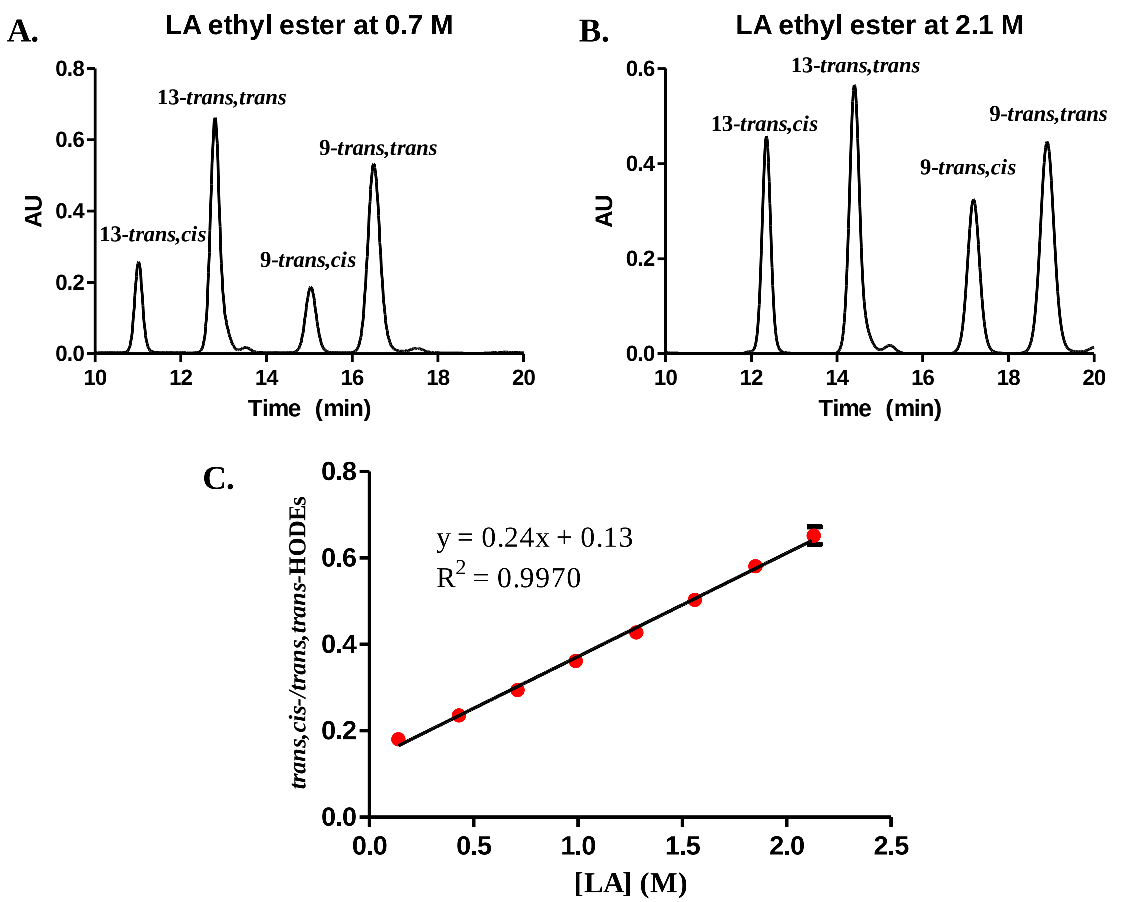

Figure 4. Determination of k_p for LA ethyl ester. **A** and **B** show typical HPLC-UV chromatograms for LA ethyl ester oxidations at 0.7 M and 2.1 M LA. **C.** Plot of the *trans*,*cis*/*trans*,*trans*-HODEs versus the concentration of LA ethyl ester for each oxidation.

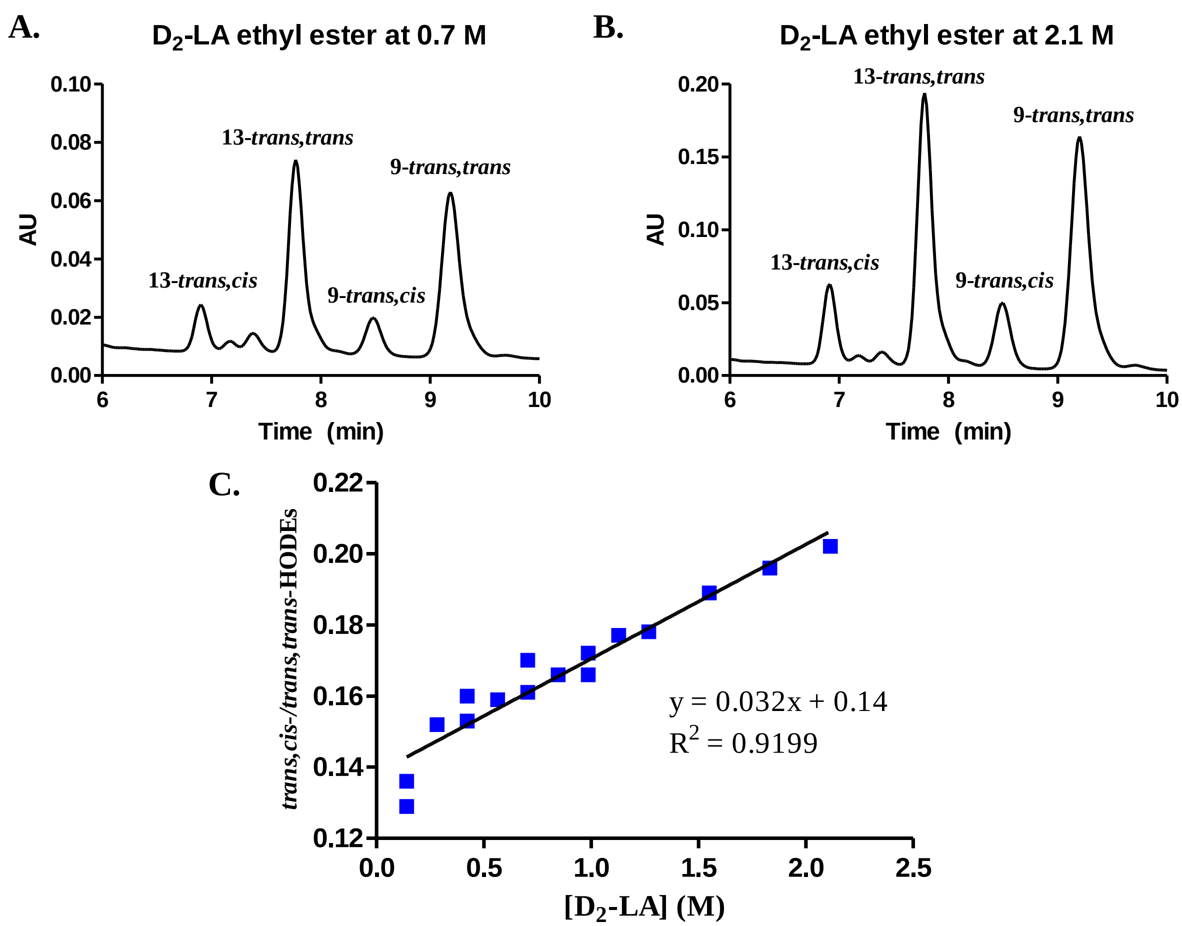

Figure 5. Determination of k_p for D_2-LA ethyl ester. **A** and **B** show typical HPLC-UV chromatograms for D_2-LA ethyl ester oxidations at 0.7 M and 2.1 M D_2-LA. **C.** Plot of the *trans,cis*/*trans,trans*-HODEs versus the concentration of D_2-LA ethyl ester for each oxidation.

In order to determine the propagation rate constant for both LA and D_2-LA ethyl ester clocking experiments, the ratios of *trans,cis*-HODEs to *trans,trans*-HODEs were plotted against the concentrations of LA or D_2-LA ethyl esters. According to Equation 1:

$$\frac{\text{trans,cis}}{\text{trans,trans}} = \sum_{i=1-n} \frac{k_p^i [R_i - H]}{214\ s^{-1}} + 0.16 \qquad (1)$$

The ratio of the *trans,cis*- to *trans,trans*-HODEs is proportional to the propagation rate constant, k_p, for the compound of interest. Therefore, the slopes from the plots above are also proportional to the k_p for both LA and D_2-LA ethyl esters.[30] The H/D kinetic isotope effect can then be calculated by direct comparison of the slopes from the two plots using Equation 2:

$$KIE = \frac{k_H}{k_D} = \frac{LA\ slope}{D_2 - LA\ Slope} \qquad (2)$$

Direct comparison of the LA and D_2-LA ethyl ester oxidation slopes is presented in Figure 6. The H/D kinetic isotope effect calculated by the application of this method was 9.3 ± 1.1.[31]

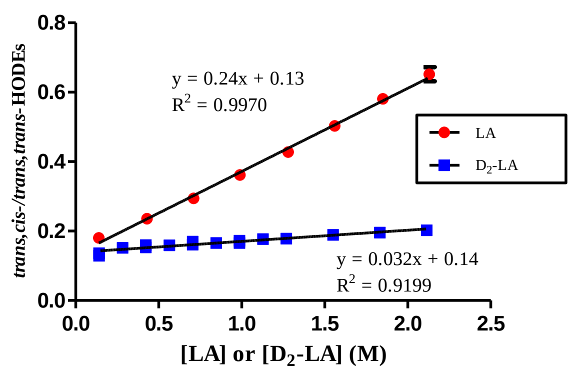

Figure 6. Direct comparison of the *trans,cis*-/*trans,trans*-HODE ratios from LA and D_2-LA ethyl ester oxidations. The slope for each data set is proportional to the k_p for the respective substrate.

2.2.2. Cooxidation Experiments

Experiments in yeast have shown that enrichment with natural PUFAs followed by the initiation of oxidative stress causes cell death. Enrichment of yeast with D-PUFAs under identical conditions as experiments with natural PUFAs resues the cells from damage and death due to oxidative stress. It was reported that levels of D-PUFA as low as 20% of the PUFAs added rescued the yeast from oxidative damage. Higher concentrations showed no effective difference in the reduction of peroxide buildup or cell survival.[25] This data suggested that the protective effect was not linear. In other words, cell survival was identical when 20% D-PUFA or 90% D-PUFA was present after enrichment.

In order to investigate these observations, cooxidation experiments were carried out in which LA and D_2-LA mixtures were oxidized together in solution. The total amount of PUFA ([LA] + [D_2-LA]) was held constant at 0.64 M with mole fraction of D_2-LA at 0.0, 0.05, 0.18, 0.30, 0.47, 0.62, 0.82, and 0.90. Free radical oxidation was initiated by MeOAMVN at 37 ˚C. Solutions were quenched after 1 h with BHT and PPh_3. The percent oxidation of pure LA after 1 h was calculated to be 2%. It can be assumed that the percent oxidation in other samples with higher mole fractions of D_2-LA will be lower than that for Lin. 4-methoxybenzyl alcohol was added as an internal standard and samples were split into two separate parts.

One part of the product mixture was analyzed by HPLC-UV to determine total HODE formation. The ratio of *trans,cis*-HODE to *trans,trans*-HODE was plotted against the percentage of D_2-LA present in solution according to Equation 3:

$$\boldsymbol{percentage\ D_2 - LA = \frac{[D_2 - LA]}{[LA + D_2 - LA]}} \qquad (3)$$

The plot from these experiments, shown in Figure 7, reveals a linear decrease in total HODE formation as a function of the mole fraction of D_2-LA present.

A.

B.

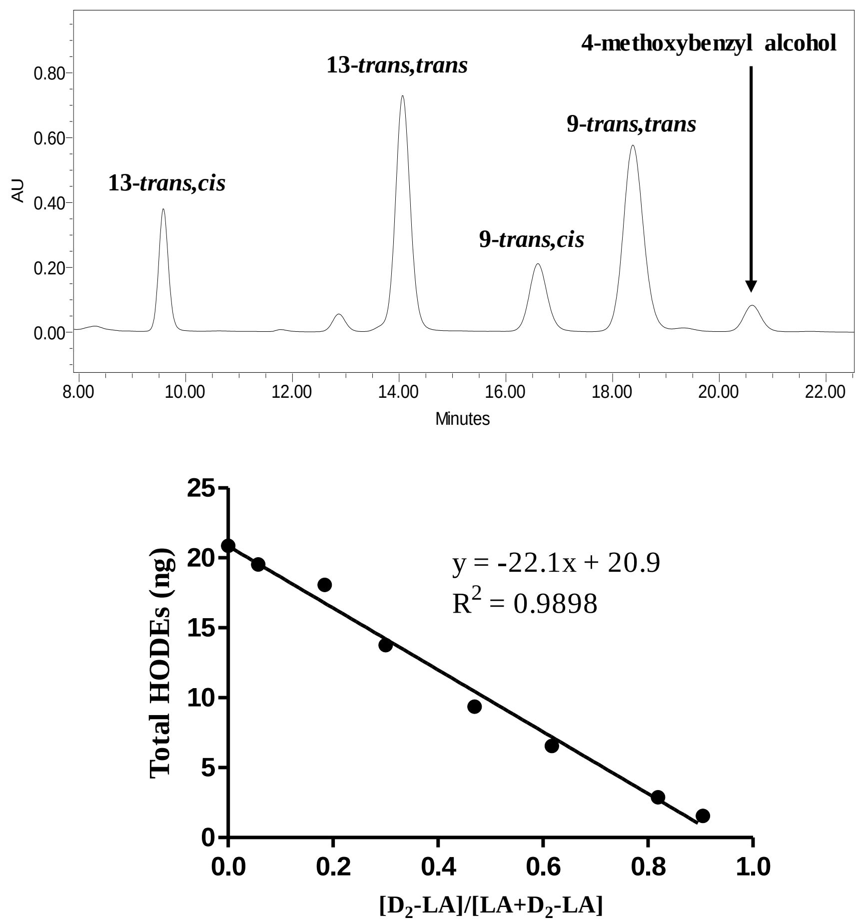

Figure 7. Results from cooxidation experiments of LA and D_2-LA. **A.** Total HODE formation was analyzed by HPLC-UV, and levels of HODEs were quantified relative to the internal standard, 4-methoxybenzyl alcohol. **B.** Total HODE formation versus the percentage of D_2-LA present in the oxidation mixtures.

To the remaining fraction of the product mixture, 13-(*S*)-D_4-HODE was added as an internal standard. The samples containing ratios of LA:D_2-LA greater than 1:5 were analyzed by LCMS in order to determine the H/D kinetic isotope effects which occur during cooxidation of the natural and deuterated substrates. Samples were introduced into the mass spectrometer by atmospheric-pressure chemical ionization (APCI) in negative mode. HODEs were analyzed by selective reaction monitoring (SRM) techniques described elsewhere.[32,4] A typical chromatogram is shown in Figure 8.

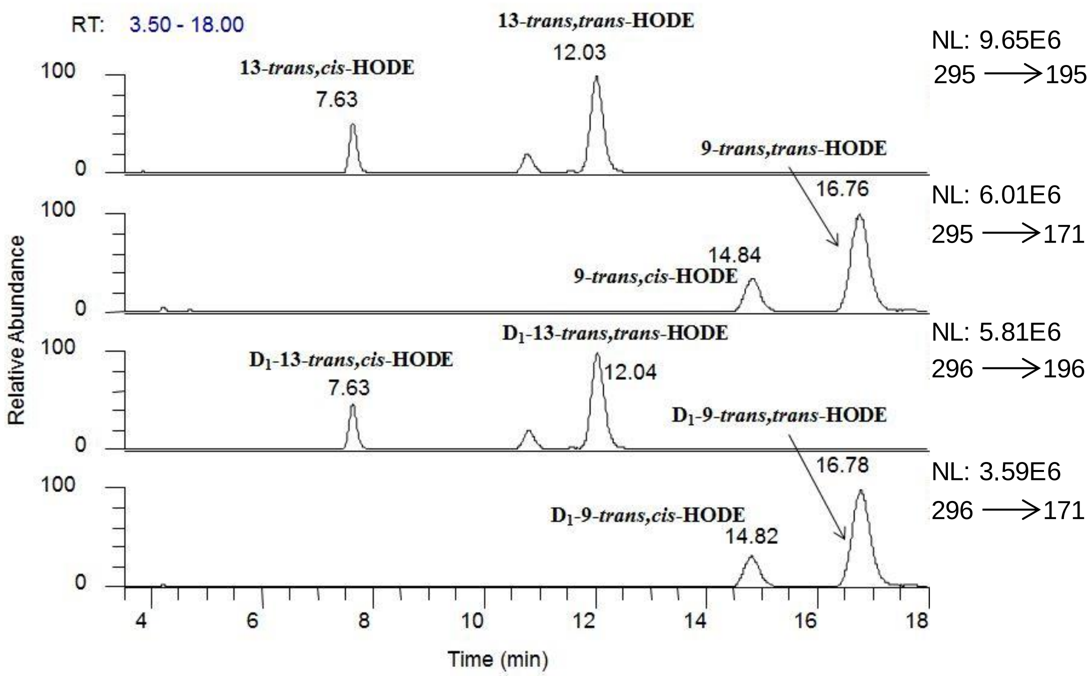

Figure 8. A typical chromatogram for analysis of cooxidations of LA and D_2-LA with ratios of LA:D_2-LA greater than 1:5. The top two panels show HODEs from LA. The bottom two panels show D_1-HODEs from D_2-LA.

During cooxidation at low conversion, the ratio of HODEs to D_1-HODEs formed reflects the relative propagation rate constants for LA and D_2-LA as shown by Equation 4:

$$\frac{[\mathbf{HODEs}]}{[\mathbf{D_1-HODEs}]} = \frac{k_{\mathbf{LA}}[\mathbf{LA}]}{k_{\mathbf{11,11-D_2-LA}}[\mathbf{11,11-D_2-LA}]} \qquad \textbf{(4)}$$

The H/D kinetic isotope effect was calculated for three separate reactions in which the ratio of LA:D_2-LA was greater than 1:5. The average KIE for these cooxidation experiments was calculated to be 12.8 ± 0.6. Results from each sample are shown in Table 1.

Sample	[LA]:[D_2-LA]	[D_0-HODEs]/[D_1-HODEs]	H/D KIE
1	1 : 5.1	2.4	12.4
2	1 : 6.5	2	13.1
3	1 : 9.5	1.3	12.8

Table 1. H/D KIE calculations from cooxidation experiments where [LA]:[D_2-LA] ratios were greater than 1:5.

2.2.3. Oxidizability Measurements of LA and D_2-LA

LA and D_2-LA were subjected to oxidation in an automatic recording gas absorption apparatus similar to those described elsewhere.[33,34] All oxidations were carried out at 37 ˚C under 760 torr of O_2. In a typical experiment, known concentrations LA (0.08 to 0.43 M) or D_2-LA (0.08 to 0.3 M) were placed into the reaction vessel along with a known concentration of 2,2'-azobis-isobutyrylnitrile (AIBN). Once autoxidation starts, a known concentration of 2,2,5,7,8-pentamethyl-6-chromanol (PMHC) was added to the reaction vessel in order to measure the induction period. A typical plot of oxygen consumption after the addition of PMHC is shown in Figure 9.

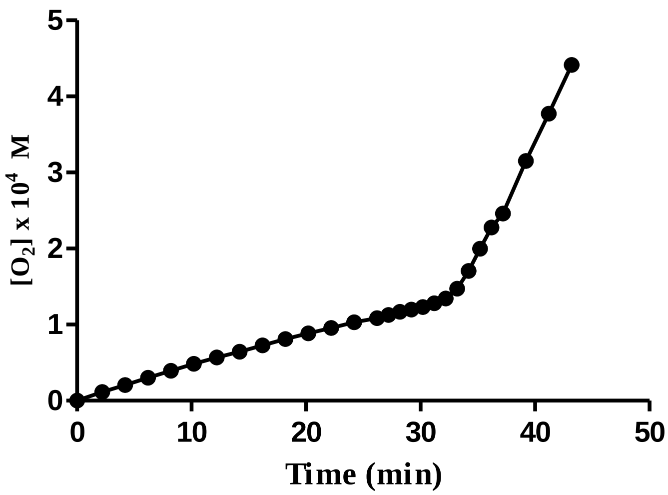

Figure 9. Typical oxygen consumption plot for LA methyl ester autoxidation.

The rate of chain initiation (R_i) was then determined using the induction period method which was discussed in length in Chapter I.[35] R_i is calculated using Equation 5:

$$\mathbf{R_i = \frac{n[ArOH]}{\tau}} \quad (5)$$

The rate of oxygen consumption during autoxidation of LA or D_2-LA was then calculated for each concentration of substrate by using Equation 6:

$$\mathbf{\frac{-d[O_2]}{dt} = \left\{\frac{k_p}{\sqrt{2k_t}}\right\}[RH]\sqrt{R_i}} \quad (6)$$

Finally, the calculated rate of oxygen consumption for each substrate was plotted against $[PUFA]\cdot R_i^{1/2}$. The slope of the resulting plots (typically designated Pryor plots) is equal to the oxidizability, or $k_p/(2k_t)^{-1/2}$, of the substrate.[36] A combined Pryor type plot is shown in Figure 10 for LA and D_2-LA. . The oxidizability for LA was calculated to be 1.96 (± 0.16) x 10^{-2} $M^{-1/2}$ $s^{-1/2}$

from the Pryor plot, in good agreement with previous values from the literature.[36,37] The oxidizability of D_2-LA was calculated to be 0.447 (± 0.04) using the same method.

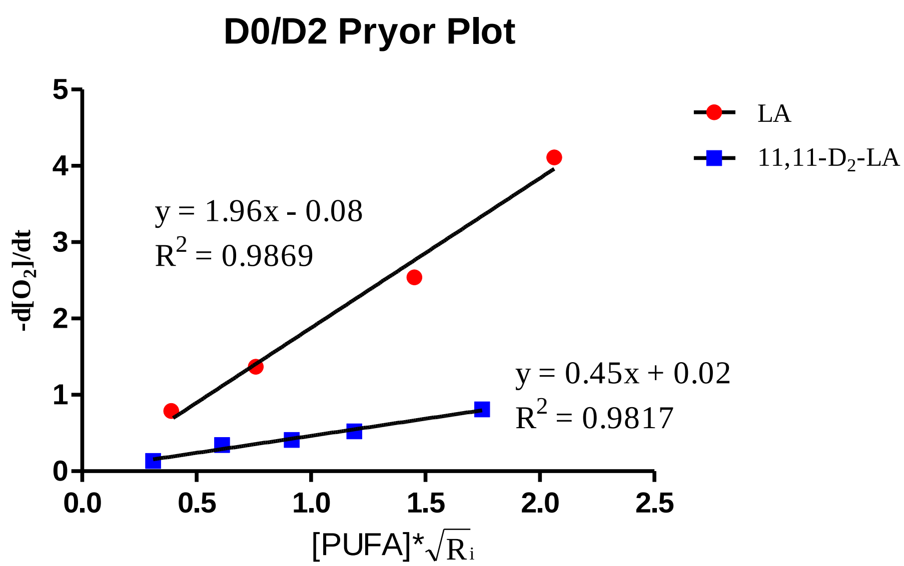

Figure 10. Pryor plots for LA and D_2-LA.

Two methods of cooxidation experiment were also carried out to once again investigate the "20% effect" described in studies of D-PUFA supplementation in yeast. In the first method The total concentration of PUFA ([LA + D_2-LA]) was held constant at 0.16 M, and the ratio of LA:D_2-LA was varied from 1:0 to 0:1. The induction method was used to measure oxygen consumption of each mixture of LA and D_2-LA. Oxygen consumption was plotted against the mole fraction of D_2-LA for each reaction. The data, shown in Figure 11, suggests that oxygen consumption decreases in linear fashion as the mole fraction of D_2-LA increases.

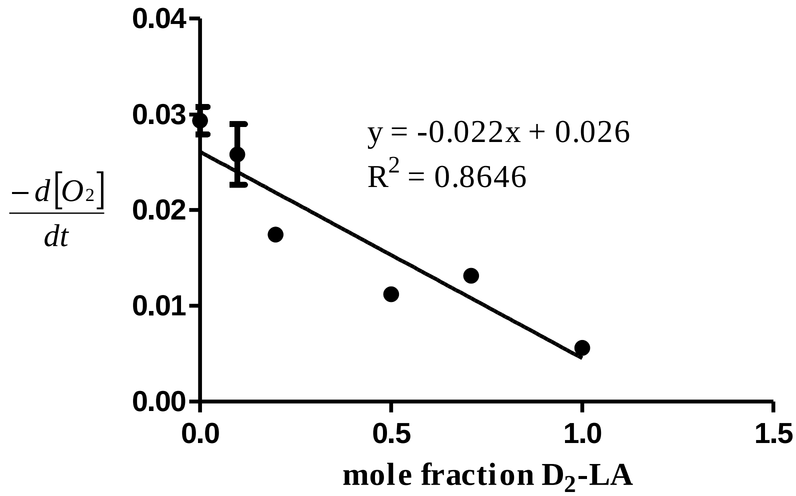

Figure 11. Oxygen consumption versus mole fraction of D_2-LA present in the reaction mixture.

The second method of cooxidation involved the incremental addition of known concentrations of D_2-LA to the reaction cell containing already autoxidizing LA. Oxygen consumption was calculated for each injection of D_2-LA, and the induction period method was used to measure R_i every other injection of D_2-LA through the addition of fresh PMHC at the same time. Oxygen consumption was again plotted versus the mole fraction of D_2-LA present. The results, shown in Figure 12, again demonstrate a linear decrease in oxygen consumption with increasing mole fraction of D_2-LA.

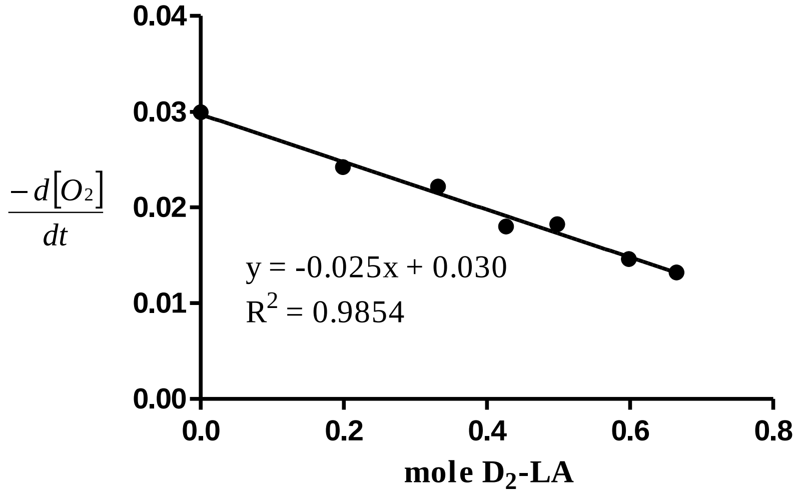

Figure 12. Oxygen consumption versus mole fraction of D_2-LA after addition of D_2-LA to already autoxidizing LA. R_i was determined every second addition of D_2-LA by the addition of fresh PMHC at a known concentration.

2.3. Discussion

Despite being essential nutrients, PUFAs are extremely prone to free radical oxidation with the *bis*-allylic hydrogen atoms being targeted for abstraction. These hydrogen atoms have a lower BDE relative to other hydrogen atoms in the molecule due to the stable, delocalized pentadienyl radical formed upon abstraction.[19,20,21] The mechanism of LA and other PUFA autoxidation is shown in Figure 14.[5]

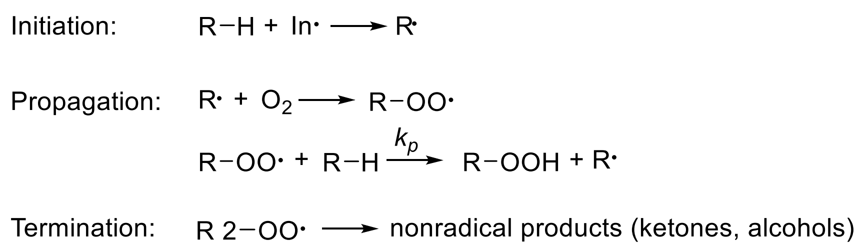

Figure 13. General scheme for the autoxidation of LA and other PUFAs.

A recent strategy to diminish autoxidation of PUFAs has focused on isotopic reinforcement of these *bis*-allylic sites, replacing hydrogen with deuterium. These D-PUFAs have been shown to lower autoxidation in yeast[22] and have beneficial effects in diseases such as Fredreich's ataxia[26] and Parkinson's disease,[77-79] both of which have oxidative stress assosciated with their pathology. In order to understand how deuterium reinforcement of the *bis*-allylic position results in protection from peroxidation, the free radical clock based on methyl linoleate[30] was used to mesure the propagation rate constant of D_2-LA.

Determination of Propagation Rate Constants and KIE for D_2-LA

The propagation rate constant for D_2-LA was calculated to be 6.8 ± 0.5 M^{-1} s^{-1} using Equation 1. This rate is roughly ten times slower than that of the natural PUFA (62 M^{-1} s^{-1}). The

H/D KIE was calculated to be 9.3 ± 1.1 using Equation 2.[31] In a typical autoxidation of LA, the *trans,cis*-HODE to *trans,trans*-HODE ratio increases as the concentration of H-atom donor increases. The *trans,cis*-HODEs become much more prevalent in the product mixture as H-atom donation competes with β-fragmentation of the *trans,cis*-peroxyl radical. In oxidations of D_2-LA however, the *trans,cis*-HODE to *trans,trans*-HODE ratio is relatively unchanged across the full concentration range of the experiments (Figure 14). This shows that D_2-LA is much less oxidizable than LA and is unable to compete with β-fragmentation of the *trans,cis*-peroxyl radical.

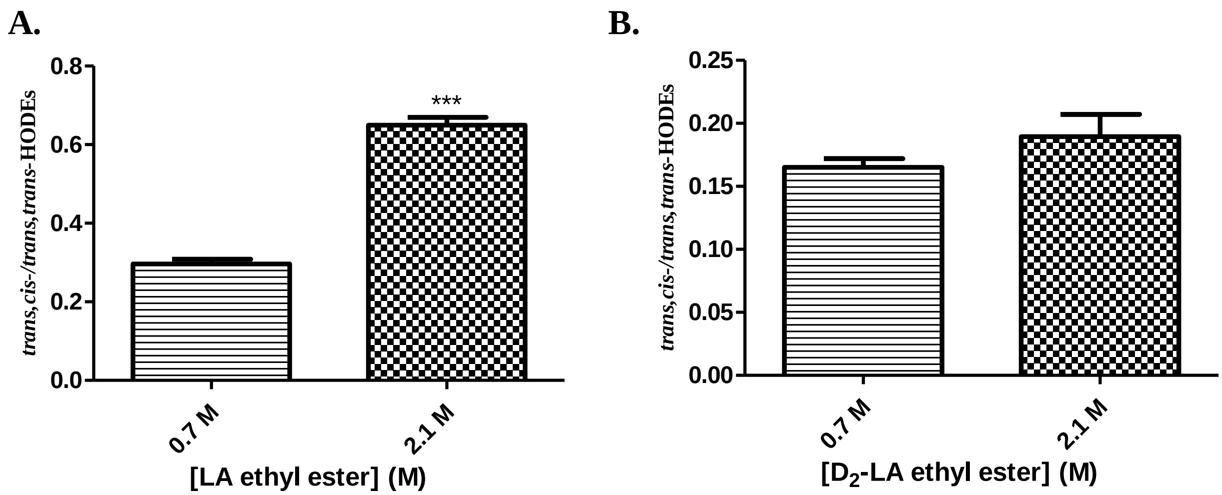

Figure 14. Histograms demonstrating the changes in *trans,cis*-HODE to *trans,trans*-HODE ratios. **A.** The *trans,cis-/trans,trans*-HODE ratio increases in the presence of a good H-atom donor such as LA ethyl ester; **B.** The *trans,cis*-/*trans,trans*-HODE ratio remains unchanged with increasing concentration of D_2-LA ethyl ester due to its poor H-atom donating capabilities.

Cooxidation of LA and D_2-LA

Cooxidation of LA and D_2-LA was carried out in order to address the reports that levels of D-PUFA as low as 20% afforded maximum protection against peroxidation in yeast. In these experiments, the overall concentration of PUFA ([LA + D_2-LA]) was held constant, and the ratio of LA:D_2-LA was varied from 1:0 to 0:1. HPLC-UV analysis of the HODEs formed during these experiments revealed that HODE formation decreased in a linear fashion as the mole fraction of D_2-LA increased in the oxidation mixtures (Figure 7B). This data shows that the 20% effect is not observed in solution cooxidations of D_2-LA, suggesting that D_2-LA does not act as an antioxidant but rather as a less reactive co-oxidant in solution[31]

A KIE of 12.8 ± 0.6 was determined in cooxidation experiments, a value that is somewhat higher than the KIE determined using the methyl linoleate clock.[31] This is likely due to error associated with the low slope for the plot of *trans,cis-*/*trans,trans-*HODEs coming from D_2-LA autoxidation. Based on the errors inherent with the low slope of the D_2-LA experiments, the KIE of 12.8 from cooxidation experiments would appear to be more reliable. Deuteration has been shown to substantially slow the rate of enzymatic oxidation of 11,11-D_2-LA, with KIE values in the range of 80-100.[38,39,40,41,42] However, the KIE for autoxidation of 11,11-D_2-LA falls in the upper range of previously reported values for other primary deuterium KIEs in autoxidation, which normally are less than 7.[43,44,45,46]

Oxygen Consumption

The autoxidation of PUFAs results in depletion of oxygen in solution and previous work has used the changes in oxygen levels to report on relative maximum rates of oxidation for fatty acids ranging from oleate to arachidonate.[47] If variables are carefully controlled (specifically R_i, Equation 5), it is possible to obtain quantitative measurements of a PUFAs' susceptibility to undergo autoxidation by measuring its oxidizability, or $k_p/(2k_t)^{1/2}$.[36] With the use of thermally labile azo initiators such as AIBN, the induction period method[35] can be used to measure R_i. This allows for the oxidizabilities of PUFAs to be determined according to Equation 6 (*vida supra*).[36]

Oxygen consumption studies were carried out in the laboratory of Ross Barclay (Mount Allison University, Sackville, New Brunswick, CA) by means of an automatic recording gas absorption apparatus. Using the induction period method, the value for oxidizability was calculated from a Pryor plot (Figure 10) to be 1.96 (± 0.16) x 10^{-2} $M^{-1/2}$ $s^{-1/2}$, in excellent agreement with previously reported values.[36] Oxidizability for D_2-LA (Figure 10) was calculated to be over four times less than LA at 0.447 (± 0.04) x 10^{-2} $M^{-1/2}$ $s^{-1/2}$. Assuming that the consumption of one molecule of oxygen is directly proportional to the formation of one peroxyl radical (and subsequently, one HpODE after hydrogen atom donation during propagation), the propagation rate constant (k_p) should also be directly proportional to the rate of oxygen consumption. If so, the KIE should be equal to the ratio of oxygen consumption as shown in Equation 7:

$$\boldsymbol{KIE = \frac{\left[\frac{-d[O_2]_H}{dt}\right]}{\left[\frac{-d[O_2]_D}{dt}\right]}} \qquad (7)$$

This assumption yields a KIE of 4.4, significantly lower than KIE values obtained by comparisons of propagation rate constants as determined through the use of the methyl linoleate clock. While the measurement of oxygen consumption is a useful tool for determining oxidizabilities of reactive substrates, the small changes in pO_2 that would be associated with the autoxidation of unreactive compounds such as D_2-LA introduce significant errors into the experiments. A recent study has also suggested that Clark-type electrodes introduce significant error into measurement of oxygen tension within a bulk liquid. Hansen and coworkers found that electrodes inserted directly into solution act as baffles, altering the hydrodynamics of the liquid as it is shaken. This results in a rise in the maximum oxygen tranfer capacity between the liquid and the electrode surface. Furthermore, low volumes of liquid in the flask may result in measurement of oxygen present in the headspace of the apparatus.[48]

Despite the shortcomings of the method, monitoring oxygen consumption during cooxidation of LA and D_2-LA was useful for again testing reports that D-PUFA concentrations as low as 20% afforded maximum protection against peroxidation in yeast. Two variations of cooxidations were carried using this technique. In the first, LA and D_2-LA were mixed in ratios from 1:0 to 0:1 (D_0:D_2). The measurement of oxidizability for the various mixtures of LA and D_2-LA revealed that oxidizability decreased in linear fashion as the mole fraction of D_2-LA present in the reaction cell increased. A linear decrease in oxidizability was also observed in the second cooxidation experiments in which D_2-LA was added incrementally added to already autoxidizing LA. These results are in agreement with cooxidations analyzed by HPLC-UV, supporting the earlier conclusions from competition experiments that D_2-LA is merely a less oxidizable substrate in solution.

2.4. Determination of Propagation Rate Constants for Sterol Intermediates from the Bloch and Kandutsch-Russell Biosynthetic Pathways to Cholesterol

Sterols are a subgroup of lipids defined as "any chiral tetracyclic isopentenoid which may be formed by cyclization of squalene oxide…and retains a polar group at C3 (hydroxyl or keto), an all-*trans,anti*-stereochemistry in the ring system and a side chain 20*R*-configuration."[49] Cholesterol (Figure 15) is present in nearly all cellular plasma membranes[50] and is biosynthesized by either the Kandutsch-Russell[51] pathway or Bloch[52] pathway, discussed in Chapter I. The free radical oxidation of cholesterol has been implicated in a number of human disorders including atherosclerosis,[53] Alzheimer's disease,[54] retinal degeneration,[55] cataracts,[56,57] and Niemann-Pick C1 disease.[58]

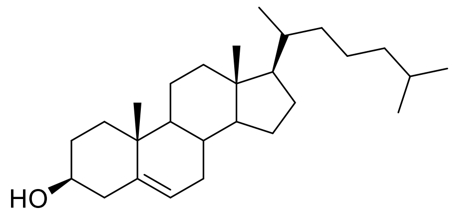

Figure 15. Cholesterol is biosynthesized *in vivo* by either the Kandutsch-Russell or Bloch pathways. The free radical oxidation of this important compound has been associated with a number of human diseases.

Breakdown of the biosynthetic pathways to cholesterol is also detrimental to human development and health. One disorder of intense interest associated with this breakdown in cholesterol biosynthesis is Smith-Lemli-Opitz syndrome (SLOS). SLOS is an autosomal recessive disorder that affects 1 in 20-60,000 individuals. It is characterized by elevated levels of 7-dehydrocholesterol (7-DHC) and by decreased levels of cholesterol. This is a direct result of mutations in the gene that encodes 7-dehydrocholesterol reductase (DHCR7), the enzyme that catalyzes the reduction of the 7,8-double bond of 7-DHC to form cholesterol (Figure 16). The consequences of mutations in DHCR7 are increased levels of 7-DHC and decreased levels of cholesterol.

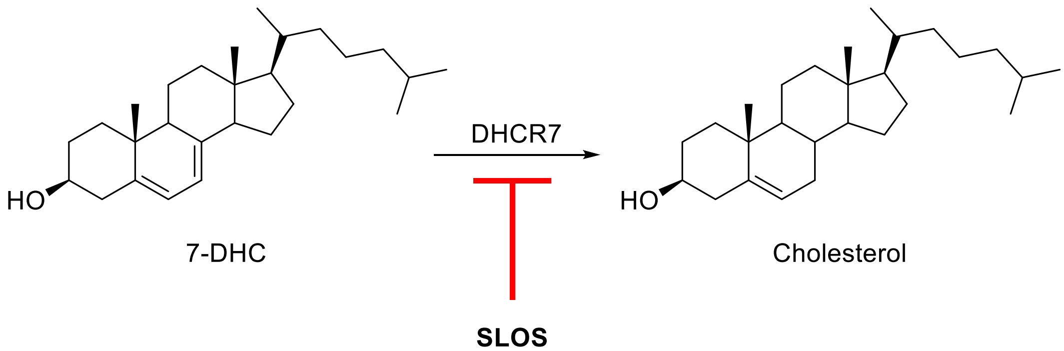

Figure 16. Cholesterol is biosynthesized from 7-DHC by the enzyme 7-dehydrocholesterol reductase (DHCR7). Patients with SLOS have deficiencies associated with DHCR7, resulting in inefficient conversion of 7-DHC to cholesterol, resulting in a buildup of 7-DHC and a number of oxysterols detrimental to cell health.

Recent work has determined propagation rate constants for both 7-DHC (2260 ± 40 M^{-1} s^{-1}) and cholesterol (11 ± 1 M^{-1} s^{-1}).[4] The unusually high propagation rate constant for 7-DHC, and the oxysterols formed during its autoxidation, have been implicated in the pathophysiology of SLOS.[59] From these studies it has become apparent that any disruption in the biosynthesis of cholesterol can have drastic effects. Indeed, other disorders associated with deficiencies in cholesterol biosynthesis have been identified including CDPX2[60,61,62] and lathosterolosis,[63,64] and oxidative stress is a component of each.

Due to the importance of the biosynthesis of cholesterol and the damage that can occur when sterol homeostasis is perturbed, the propagation rate constants for a number of sterol intermediates on the cholesterol biosynthesis pathway have been determined and are reported here.[30]

2.5. Results

Propagation rate constants for various sterols and analogs were measured using the methyl linoleate clock.[30] In a typical experiment, sterols or analogs and methyl linoleate were purified and dried under vacuum prior to oxidation. In oxidations, methyl linoleate was held constant at 0.3 M, and concentrations of the lipid cooxidant were varied depending on their reactivity and solubility. All oxidations were initiated with the thermally labile azo initiator MeOAMVN. Reactions were initiated at 37 ˚C and quenched after 1 h with the addition of BHT and PPh_3. The linoleate HODEs were analyzed by HPLC-UV, monitoring at 234 nm. Results from these experiments are presented below.

Side Chain Analog of Bloch Pathway Sterols

One pathway for cholesterol biosynthesis is the Bloch pathway,[52] in which the 20(*R*)-side chain bears a double bond between carbons C24-C25. This unit of unsaturation adds eight allylic hydrogen atoms that could potentially be abstracted by a peroxyl radical. Side chain unsaturation could increase propagation rate constants for the Bloch pathway sterol intermediates compared to their Kandutsch-Russell pathway analogs, which have a saturated C24-C25 bond. DHCR24 reduces all Bloch intermediates to the Kandutsch-Russel analogs (Figure 17).

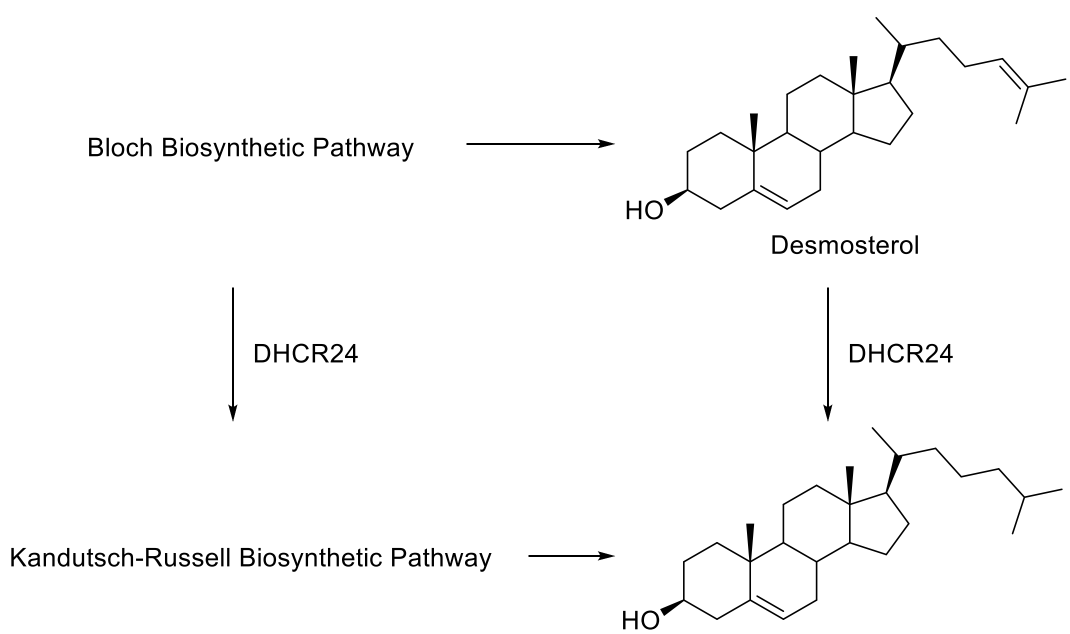

Figure 17. The Bloch and Kandutsch-Russell biosynthetic pathways are separated by the reduction of the C24-C25 double bond by 24-dehydrocholesterol reductase. This ‘crossover’ can presumably occur at any time during biosynthesis. Desmosterol to cholesterol is shown here as an example.

In order to understand the contribution of the side chain unsaturation to the overall propagation rate constant of Bloch pathway sterols, the propagation rate constant of a side chain model, 2-methyl-2-heptene, was determined (Figure 18). The propagation rate constant of this olefin was calculated to be 5.6 ± 0.2 M^{-1} s^{-1}.

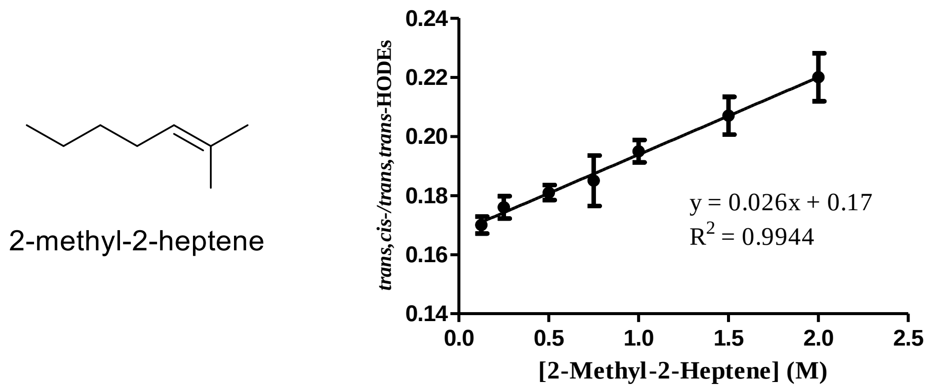

Figure 18. The propagation rate constant for 2-methyl-2-heptene was calculated at 5.6 ± 0.2 M^{-1} s^{-1} through the use of the methyl linoleate clock. The structure and plot of *trans*,*cis*/*trans*,*trans*-HODEs versus the concentration of 2-methyl-2-heptene are shown.

Desmosterol

Desmosterol is a Bloch pathway sterol intermediate which is separated from cholesterol by the reduction of the C24-C25 double bond (Figure 17, *vide supra*). As with most of the sterols, the solubility of desmosterol is low in benzene. Therefore, the concentration range spanned from 0.05 M to 0.625 M. The propagation rate constant for desmosterol was calculated to be 16 ± 5 M^{-1} s^{-1} from the results shown below in Figure 19. Due to the small range of concentrations used and the relatively low reactivity, errors in this value are particularly high.

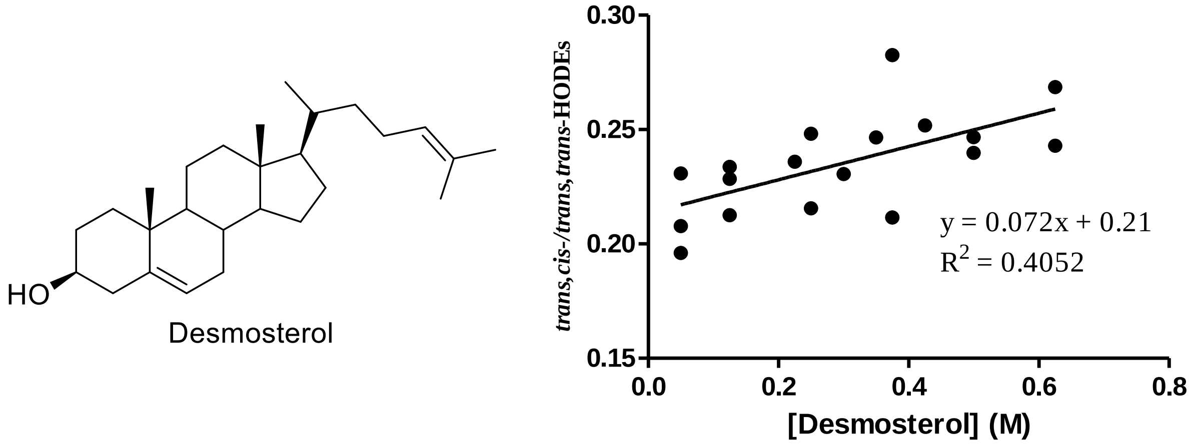

Figure 19. The propagation rate constant for desmosterol was determined over a concentration range of 0.05 to 0.625 M. k_p was calculated to be 16 ± 5 M^{-1} s^{-1} by plotting the *trans,cis-/trans,trans*-HODE ratio against the concentration of desmosterol in solution.

Lathosterol and Zymostenol

Propagation rate constants for lathosterol and zymostenol were also measured. Both sterols are a part of the Kandutsch-Russell pathway and have very low levels of solubility in benzene. Therefore, concentration ranges tested for both sterols ranged from 0.05 to roughly 0.17 M. The rate constants were calculated to be 57 ± 3 M^{-1} s^{-1} and 77 ± 5 M^{-1} s^{-1}, respectively. Structures and plots of *trans,cis-/trans,trans*-HODEs versus the concentration of sterol are shown below in Figure 20 for both compounds.

A.

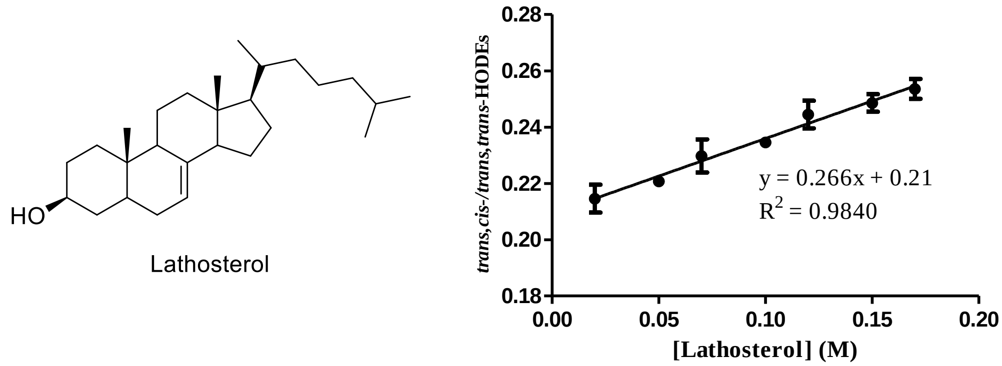

B.

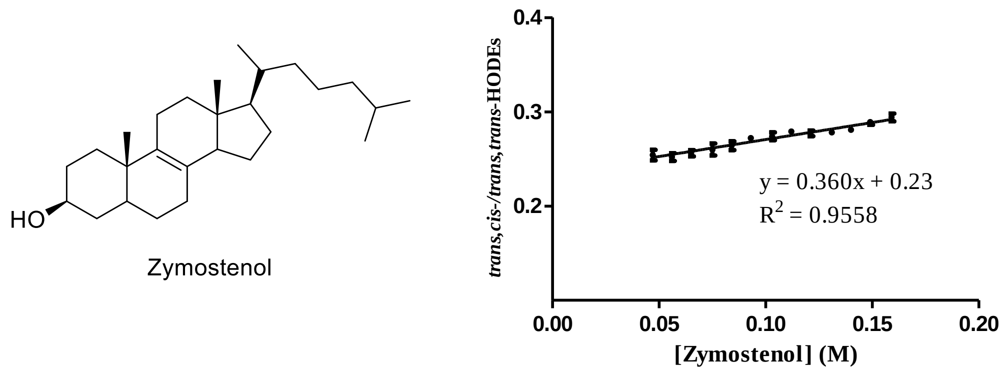

Figure 20. Results from measurement of propagation rate constants for A. Lathosterol and B. Zymostenol. Propagation rate constants were measured by plotting the ratio of *trans,cis*-/*trans,trans*-HODEs versus the concentration of the respective sterol. Propagation rate constants were calculated to be 57 ± 3 M^{-1} s^{-1} for lathosterol and 77 ± 5 M^{-1} s^{-1} for zymostenol.

2.6. *Discussion*

As discussed previously the free radical oxidation of cholesterol and 7-DHC has been implicated in a number of human diseases and disorders. Furthermore, propagation rate constants vary widely for these sterols (11 M^{-1} s^{-1} and 2260 M^{-1} s^{-1} for cholesterol and 7-DHC, respectively).[4] Inborn errors in this pathway play and important role in the pathophysiology of certain human syndromes such as SLOS, CDPX2, and lathosterolosis.

In general, sterols in the biosynthetic pathway are typically present at low levels relative to cholesterol. For instance, physiological concentrations of 7-DHC in healthy human plasma is very low (0.005 to 0.05 mg/dL)[65] compared to cholesterol (~220 mg/dL).[66] Patients with SLOS typically have much higher plasma levels of 7-DHC (10 mg/dL or greater) and substantially reduced levels of cholesterol.[65] There have also been reports of prescribed pharmaceuticals having marked effects on sterol profiles as well, even leading to elevated plasma levels of 7-DHC on par with those seen in SLOS for otherwise healthy individuals. Some drugs linked to these increases include aripiprazole, an atypical antipsychotic, and trazodone, an antidepressant(Figure 21).[67,68]

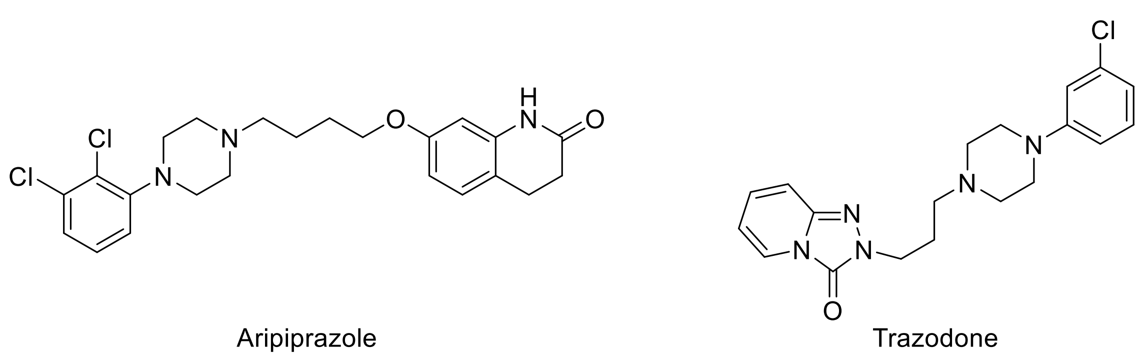

Figure 21. A number of pharmaceuticals have been shown to alter the homeostasis of sterol intermediates in the biosynthesis of cholesterol. Aripiprazole and trazodone, both pictured here, are two commonly prescribed pharmaceuticals which have such effects.

Based on the studies outlined previously, it is apparent that cholesterol biosynthesis and homeostasis can be affected by genetics, environmental exposures, and xenobiotics alike. Furthermore, certain intermediates of cholesterol biosynthesis such as 7-DHC and 8-DHC undergo autoxidation with high propagation rate constants.[4,69] Therefore, the rate constants for other intermediates in the biosynthetic pathway were determined using the methyl linoleate clock[30] in order to understand how their accumulation would affect oxidative stress.

The Bloch and Kandutsch-Russell biosynthetic pathways are separated by enzymatic reduction of the side chain C24-C25 double bond by 24-dehydrocholesterol reductase (Figure 22A). This side chain double bond has the potential to contribute to the overall propagation rate constant as it adds eight abstractable allylic hydrogen atoms to the molecule. In order to understand the contribution of this unsaturation to the propagation rate constants of sterols, the propagation rate constant of a suitable side-chain analog, 2-methyl-2-heptene (Figure 22B), was measured. Using the methyl linoleate free radical clock, the propagation rate constant for this analog was calculated to be $5.6 \pm 0.2\ M^{-1}\ s^{-1}$. This low propagation rate constant suggests that the unsaturated side chain will contribute little to the overall propagation rate constant of Bloch pathway sterol intermediates.

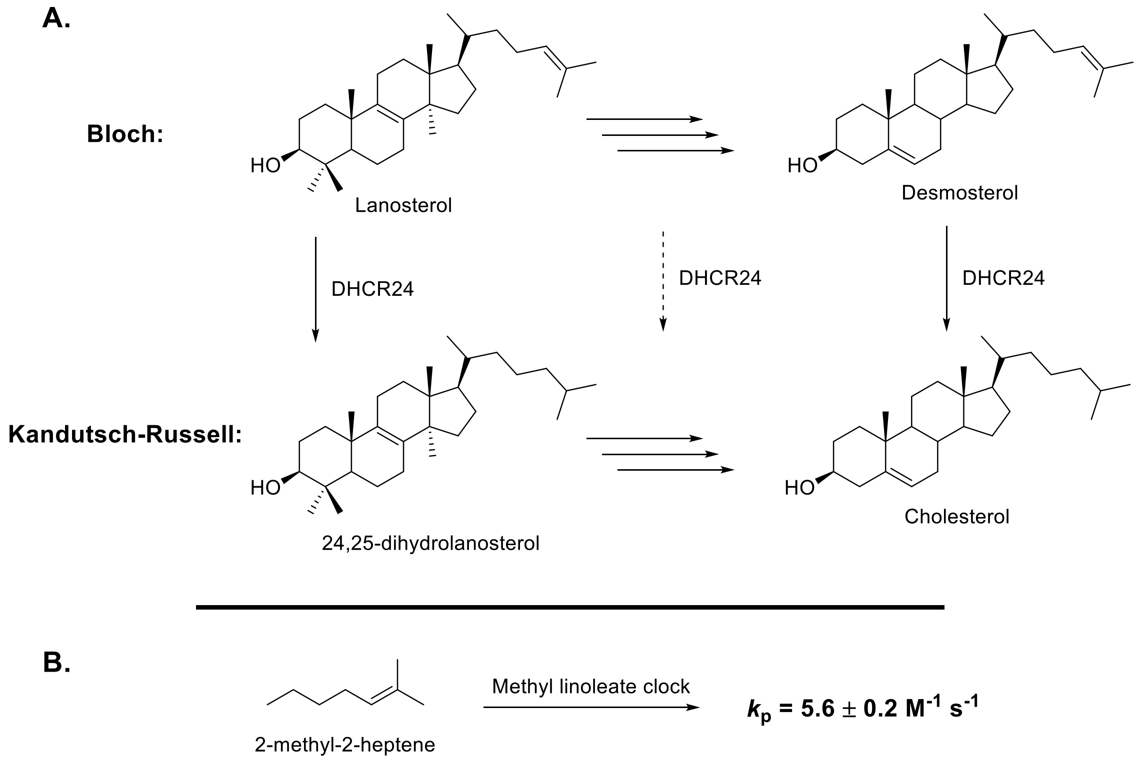

Figure 22. A. The biosynthesis of cholesterol occurs via the Bloch or Kandutsch-Russell pathways. Starting from lanosterol, the two pathways are separated by the reduction of the C24-C25 double bond. **B.** 2-methyl-2-heptene was used as an analog for the side chain unsaturation of the Bloch pathway sterols. Its propagation rate constant was calculated to be 5.6 ± 0.2 M^{-1} s^{-1} using the methyl linoleate clock.

Desmosterol is the biosynthetic precursor to cholesterol in the Bloch biosynthetic pathway.[52] The C24-C25 double bond is reduced by 24-dehydrocholesterol reductase to give cholesterol. The propagation rate constant was calculated to be 16 ± 5 M^{-1} s^{-1} for desmosterol (Figure 23), similar to that of cholesterol (11 ± 1 M^{-1} s^{-1}).[4] This result suggests that even though desmosterol contains one more double bond (C24 to C25) than cholesterol, the unsaturation in the side chain contributes little to the overall propagation rate constant. This conclusion is supported by previous results from 2-methyl-2-heptene. Based on these findings, it seems reasonable to suggest that propagation rate constants for sterol intermediate analogs in the Bloch and Kandutsch-Russell biosynthetic pathways will be similar.

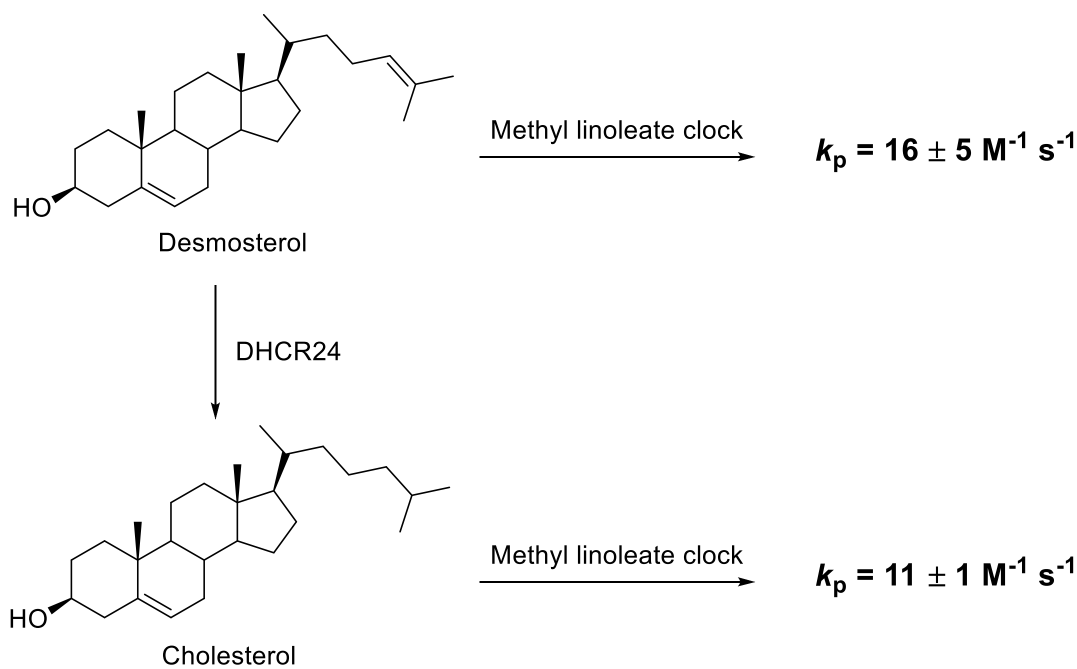

Figure 23. The C24-C25 double bond of desmosterol is reduced by 24-dehydrocholesterol reductase to give cholesterol during the last step of cholesterol biosynthesis. The propagation rate constant of desmosterol was calculated to be 16 ± 5 M^{-1} s^{-1}, similar to that of cholesterol (11 ± 1 M^{-1} s^{-1}), suggesting that the unsaturated side chain contributes little to the overall propagation rate constants of Bloch pathway sterol intermediates.

Lathosterol (Figure 24), the penultimate sterol to cholesterol in the Kandutsch-Russell pathway,[51] is oxidized by lathosterol 5-desaturase to give 7-DHC. This sterol was calculated to have a propagation rate constant of 57 ± 3 M^{-1} s^{-1}, five times faster than cholesterol (11 ± 1 M^{-1} s^{-1})[4] and similar to that of linoleate (62 $M^{-1}s^{-1}$).[36,37] Zymostenol (Figure 24), the immediate precursor to lathosterol, was also found to have a propagation rate constant on the same order of magnitude at 77 ± 5 M^{-1} s^{-1}. These propagation rate constants suggest that peroxidation and oxysterol buildup could also be issues for individuals who experience elevated levels of these sterol intermediates whether due to a genetic disorder, environmental exposure, or prescription drug usage.

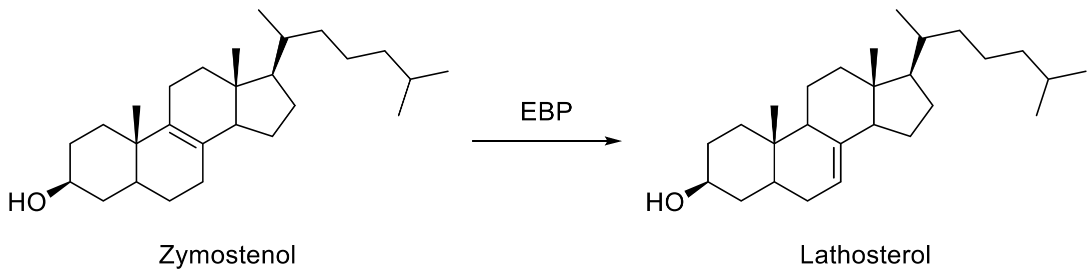

k_p = 77 ± 5 M^{-1} s^{-1} k_p = 57 ± 3 M^{-1} s^{-1}

Figure 24. Propagation rate constants were calculated for zymostenol and lathosterol using the methyl linoleate clock. Values were 77 ± 3 M^{-1} and 57 ± 3 M^{-1} s^{-1}, respectively.

The range of propagation rate constants for sterols is impressively large. Based on a comparison of rates for cholesterol (11 ± 1 M^{-1} s^{-1}) and desmosterol (16 ± 5 M^{-1} s^{-1}), it appears that the side chain unsaturation between C24-C25 contributes little to the overall propagation rate constant of Kandutsch-Russell pathway sterols. Experiments measuring the propagation rate constant for 2-methyl-2-heptene, an analog for the unsaturated side chain, confirm the small contribution to the overall rates. Therefore, the propagation rate for any sterol intermediate will be largely determined by the configuration of unsaturation located in the B-ring of the sterol. While the calculated propagation rate constants for intermediate sterols zymostenol and lathosterol fall well short of those determined for 7-DHC[4] and 8-DHC,[69] they demonstrate that disruption of cholesterol biosynthetic pathways has the potential to promote undue levels of oxidative stress through the buildup of sterols with sizeable propagation rate constants.

2.7. Conclusions

As discussed, autoxidation of lipids has been implicated in a variety of human pathologies. Some of these, including SLOS, lathosterolosis, and CPDX2, involve errors in the cholesterol biosynthetic pathway resulting in an imbalance of sterols. In SLOS patients, 7-DHC levels have been shown to be elevated with respect to unaffected individuals. 7-DHC has also been shown to be the most reactive lipid towards autoxidation with a propagation rate constant of 2260 M^{-1} s^{-1}.[4] Beyond diseases affecting cholesterol biosynthesis, small molecules have also been shown to alter the levels of various sterol intermediates along both the Bloch and Kandutsch-Russel cholesterol biosynthetic pathways.[65] Thus, rate constants for other sterols upstream of both 7-DHC and 8-DHC were determined using the methyl linoleate clock.[30] Experiments revealed propagation rate constants on par with linoleate for some of the sterols. The side chain unsaturation integral to the Bloch pathway sterols was found to contribute little to the overall rate of autoxidation, through measurement of propagation rate constants for desmosterol and 2-methyl-2-heptene, an analog for the unsaturated side chain of Bloch pathway sterols.

Fatty acids, especially PUFAs, are also very susceptible to free radical attack. Peroxyl radicals primarily attack the *bis*-allylic methylene group, abstracting hydrogen atoms at this location due to their low BDE. A new method for curbing the damage done during during these attacks – the isotopic reinforcement of the *bis*-allylic methylene groups with deuterium – was studied. The data covered in this chapter suggests a significant deuterium isotope effect for LA vs D_2-LA during propagation, and that increasing levels of D_2-LA present during autoxidation resulted in a linear decrease in HODE formation. Oxygen consumption experiments on cooxidizing mixtures of LA and D_2-LA confirmed these observations. Oxidizability was also measured for both LA and D_2-LA by using the induction method. Similar to measurement of propagation rate constants by the methyl linoleate clock, oxidizability studies demonstrated that the D_2-LA is indeed less reactive towards autoxidation LA. Therefore, isotopic reinforcement of PUFAs appears to be a plausible method for reduction of peroxide buildup during autoxidation.

In closing, Figure 25 presents the structures for every lipid whose propagation rate constant has been determined in these studies, as well as important lipids which have been studied previously.

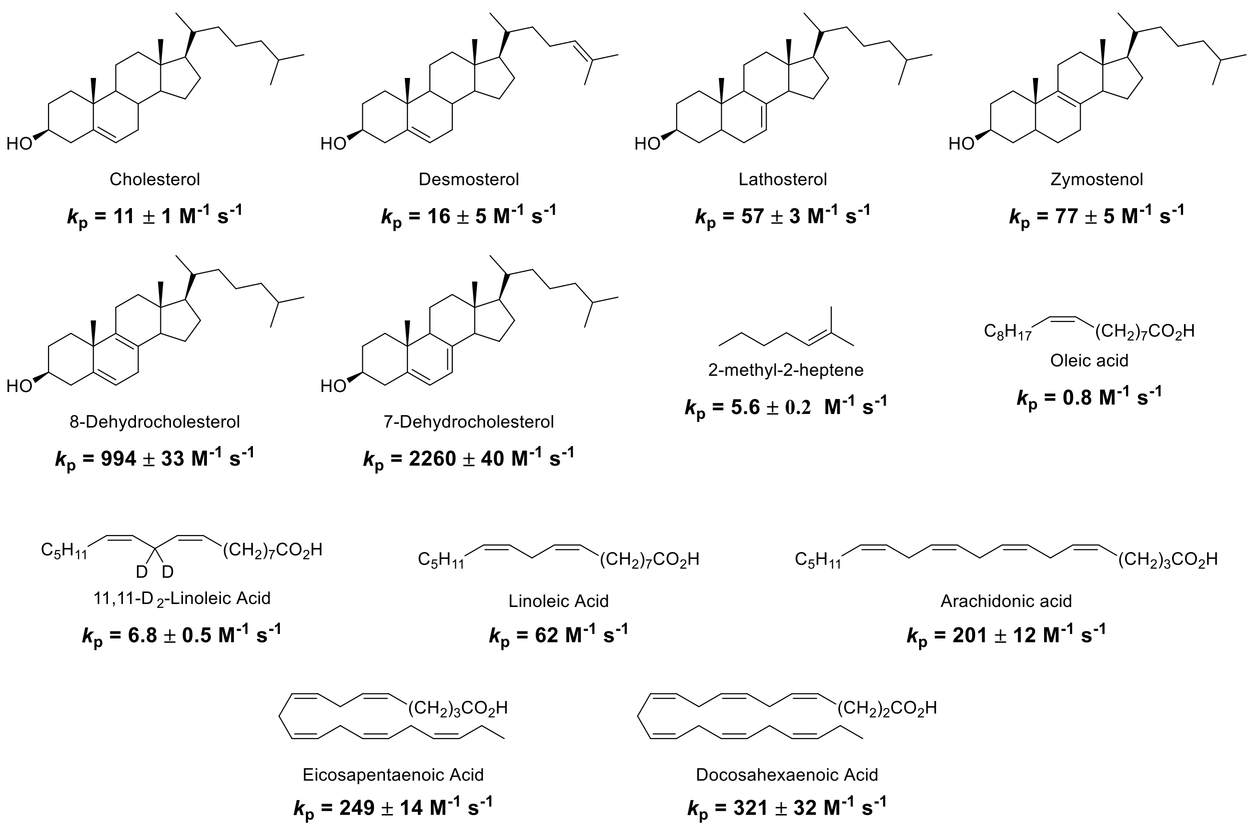

Figure 25. Catalog of propagation rate constants for select lipids.

2.8. Acknowledgements

Many thanks to Libin Xu for his help and guidance with the methyl linoleate clock, and to Dr.'s Keri Tallman and Hubert Muchalski, as well as Keri Stratton for synthesis and propagation rate constant measurement of sterol intermediates. Speical thanks to Dr. Ross Barclay for graciously hosting me at Mt. Allison University in Sackville, New Brunswick, CA and providing lab space, instrumentation, and guidance on oxidizability studies. I would also like to thank Jeremy Borque for his help in completing the oxygen consumption studies. D-PUFAs were graciously provided by Misha Shchepinov and Retrotope, Inc.

2.9. Experimental

Materials

The fatty acids used in these studies were LA, 11,11-D_2-LA, and their ethyl esters. LA and its ethyl ester (>99 % purity) were obtained from Nu-Chek Prep (Elysian, MN). 11,11-D_2-LA was obtained from Retrotope, Inc. Its synthesis has been described previously.[22] 2-methyl-2-heptene (98 %) and benzene (anhydrous, 99.8 %) were obtained from Sigma-Aldrich (St. Louis, MO). Benzene was passed through a plug of neutral alumina and stored over 4 Å molecular sieves prior to use.

Measurement of Propagation Rate Constants for LA and D_2-LA and Cooxidation Experiments

Propagation rate constants for LA and D_2-LA were measured through the use of the methyl linoleate clock.[30] Prior to all experiments, PUFAs were purified by flash column chromatography (10 % to 20 % ethyl acetate in hexanes) and dried overnight under vacuum. A stock solution of 2,2'-azobis(4-methoxy-2,4-dimethyl)-valeronitrile (MeOAMVN) in benzene (0.1 M) was used to initiate all reactions. For clocking and cooxidation of PUFAs, reagents were added in the order of: (1) benzene, (2) PUFA, (3) MeOAMVN. For sterol intermediates, reagents were added in the order of: (1) benzene, (2) sterol, (3) linoleate, (4) MeOAMVN. Reaction vials were vortexed for 5 s, followed by heating at 37 ˚C for 1 h. Each reaction was quenched by the addition of 25 μL of both 0.5 M butylated hydroxytoluene (BHT) and 0.5 M triphenylphosphine (PPh_3). All experiments were carried out in triplicate.

Ethyl esters of LA or D_2-LA were used when measuring propagation rate constants. The oxidation products, HODEs, were analyzed by normal phase HPLC-UV (250 x 4.6 mm silica column; 5 μm; elution solvent, 0.5 % 2-propanol in hexanes; monitoring wavelength 234 nm). The residual amount of D_1-LA and LA in the D_2-LA starting material were determined by ^{1}H NMR analysis to be 2.9 and 0.8 mol %, respectively. These values were used to correct data from experiments using D_2-LA, assuming that D_1-LA is half as reactive as LA.

In cooxidation (or competition) experiments, the total amount of PUFA (LA + 11,11-D_2-LA) was held constant at 0.64 M while varying the ratio of LA:D_2-LA. After quenching the reactions with BHT and PPh_3, 4-methoxybenzyl alcohol was added as an internal standard for HPLC-UV analysis. The samples were then split. One part was analyzed by HPLC-UV for total HODE formation (250 x 4.6 mm silica column; 5 μm; elution solvent, 1.4 % 2-propanol and 0.1 % acetic acid in hexanes; monitoring wavelength, 234 nm). To the other part, 500 ng of D_4-13-*trans,cis*-HODE was added as an internal standard for LCMS analysis (150 x 4.6 mm silica column; 3 μm; elution solvent, 1.4 % 2-propanol and 0.1% acetic acid in hexanes). Samples were introduced into the mass spectrometer using an atmospheric pressure chemical ionization (APCI) source in negative mode, and HODEs were monitored using selective reaction monitoring (SRM).[4,32]

LCMS analysis of cooxidation experiments with large ratios of LA:D_2-LA (>1:5) were used to calculate KIE by comparing total D_0-HODEs to D_1-HODEs. Calculations of the total D_1-

HODE formed from D_2-LA autoxidation took into account both D_1-HODEs from 11-D_1-LA oxidation as well as isotopic contribution from D_0-HODEs. The percentage of D_1-LA in the 11,11-D_2-LA starting material was 2.9 % (*vide supra*). This was used to correct the D_1-HODEs fromed from D_1-LA assuming that D_1-LA is half as reactive as LA in solution. Isotopic contribution of D_1-HODEs from LA oxidation (i.e. D_0-HODEs) was determined by running the same LCMS analysis on the autoxidation of pure LA.

Oxygen Consumption Studies

Oxygen consumption was measured using the induction period method.[35] Experiments were carried out in an automatic recording gas absorption apparatus similar to those described elsewhere.[33,34] All experiments were carried out at 37 ˚C under 760 torr of O_2. In a typical experiment, both reaction and reference cells contained known volumes (1 mL) of benzene. Known volumes of LA or D_2-LA stock solutions in benzene were injected into the reaction cell and shaken vigorously for 15-20 minutes to allow for thermal equillibrium to occur between the reaction and reference cells. A known volume of 2,2'-azobis-isobutyrylnitrile (AIBN) stock solution was then added to the reaction vessel after which autoxidation began immediately. Once a steady rate of autoxidaiton was achieved, known volumes of a stock solution of 2,2,5,7,8-pentamethyl-6-chromanol (PMHC) in chlorobenzene was added to the reaction cell.

Using n=2 for PMHC and the length of time, τ, that the oxygen uptake is inhibited, R_i was determined by the slope of a plot of 2[PMHC] versus τ. Oxidizability of the substrate, $k_p/(2k_t)^{1/2}$, is equal to the slope of the plot of oxygen consumption versus [PUFA]$R_i^{1/2}$. These plots are otherwise known as Pryor plots.

Measurement of Propagation Rate Constants for Sterols

Propagation rate constants for various sterols and the unsaturated side chain analog 2-methyl-2-heptene were carried out using the methyl linoleate clock.[30] Prior to all experiments, linoleate and sterols were purified by flash column chromatography (10% to 20% ethyl acetate in hexanes, depending on the compound) and dried overnight under vacuum. 2-methyl-2-heptene was purified by distillation at 122 ˚C. A 0.1 M stock solution of MeOAMVN in benzene was used to initiate all reactions. Reagents were added in the order of: (1) benzene, (2) sterol or 2-methyl-2-heptene, (3) linoleate, (4) MeOAMVN. Reaction vials were vortexed for 5 s, followed by heating at 37 ˚C for 1 h. Each reaction was quenched by the addition of 25 μL of both 0.5 M BHT and 0.5 M PPh_3. HODEs were monitored using HPLC-UV under the conditions described above.

Synthesis of Desmosterol

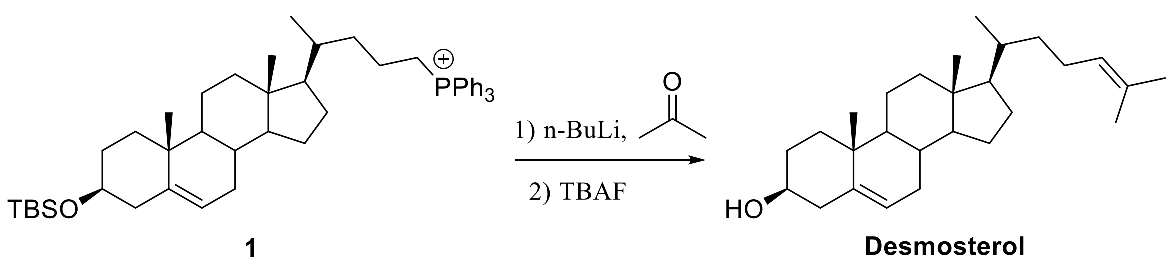

Figure 26. Synthesis of desmosterol.

The sterol phosphonium salt **1** (889.3 mg, 1.05 mmol) was dissolved in THF (10 mL). A 2.5 M solution of nBuLi in THF (0.42 mL, 1.05 mmol) was added dropwise. After turning orange, the reaction was stirred at rt for 30 min. The reaction was then cooled to -78 ˚C. Acetone (77 μL, 1.05 mmol), which was freshly distilled from crushed Dri-Rite, was slowly added. The reaction was allowed to warm to rt and stirred for 4 h. Solvent was evaporated by rotary evaporation, and the residue was purified by flash column chromatography (10 % ethyl acetate in hexanes). The resulting white solid was immediately dissolved in THF (10 mL). TBAF (1.0 M in THF) was added (0.8 mL) to the solution. The reaction was stirred overnight at rt, after which it was pouried into 10 mL of a DCM-water mixture (50:50). The aqueous layer was extracted with DCM (2 x 20 mL). The organic fractions were collected and dried over magnisum sulfate. The solvent was then removed by rotary evaporation. The residue was purified by flash column chromatography (10 % ethyl acetate in hexanes) to give a white solid (127.5 mg, 80 %). Spectral data was in agreement with previously published results.[70] ^{1}H NMR ($CDCl_3$, δ): 5.32 (d, *J* = 6.8 Hz, 1H), 5.06 (m, 1H), 3.49 (m, 1H), 2.24 (m, 2H), 1.99 (m, 3H), 1.81 (m, 4H), 1.65 (s, 3H), 1.57 (s, 3H), 1.43 (m, 8H), 1.15 (m, 6H), 0.98 (s, 3H), 0.91 (d, *J* = 8.7 Hz, 3H), 0.65 (s, 3H). ^{13}C NMR ($CDCl_3$, δ): 140.7, 130.9, 125.2, 121.7, 71.7, 56.7, 56.0, 50.1, 42.3, 42.2, 39.7, 37.2, 36.4, 36.0, 35.6, 31.8, 31.6, 28.2, 25.7, 24.7, 24.3, 21.0, 19.4, 18.6, 17.6, 11.8.

Synthesis of Lathosterol [70]

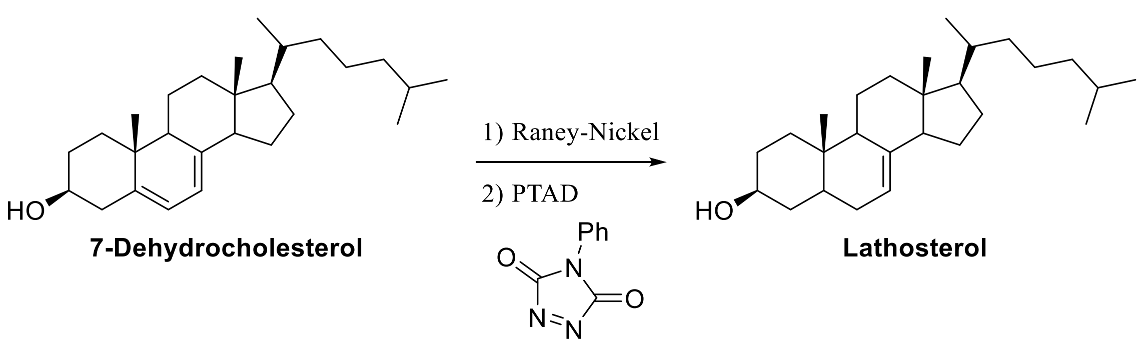

Figure 27. Synthesis of lathosterol from 7-DHC.

7-dehydrocholesterol (1.025 g, 2.67 mmol) was dissolved in a mixture of ethanol (50 mL) and dioxane (32 mL). Hydrogen was bubbled through the solution for 10 min. Raney-Nickel slurry (0.5 mL) was added to the flask. A hydrogen baloon was attached to the flask, and the reaction was allowed to run at room temperature for 5 h. The reaction was then filtered, and solvent was removed from the filtrate by rotary evaporation. Residue was purified by flash column (20 % ethyl acetate in hexanes) to yield a white flaky solid (0.85 g, 2.21 mmol, 83 %). Spectral data was in agreement with previously published results.[70] ^{1}H NMR ($CDCl_3$, δ): 5.16 (m, 1H), 3.60 (m, 1H), 2.02 (m, 1H), 1.81 (m, 6H), 1.56 (m, 9H), 1.23 (m, 12H), 0.93 (d, J = 3.6 Hz, 3H), 0.86 (dd, J = 6.6 Hz, 1.9 Hz, 6H), 0.80 (s, 3H), 0.53 (s, 3H). ^{13}C NMR ($CDCl_3$, δ): 139.6, 117.4, 71.07, 56.2, 55.0, 49.4, 43.4, 40.3, 39.6, 39.5, 38.0, 37.1, 36.2, 36.1, 34.2, 31.5, 29.6, 28.0, 27.9, 23.9, 23.0, 22.8, 22.6, 21.6, 18.8, 13.0, 11.8.

Synthesis of Zymostenol

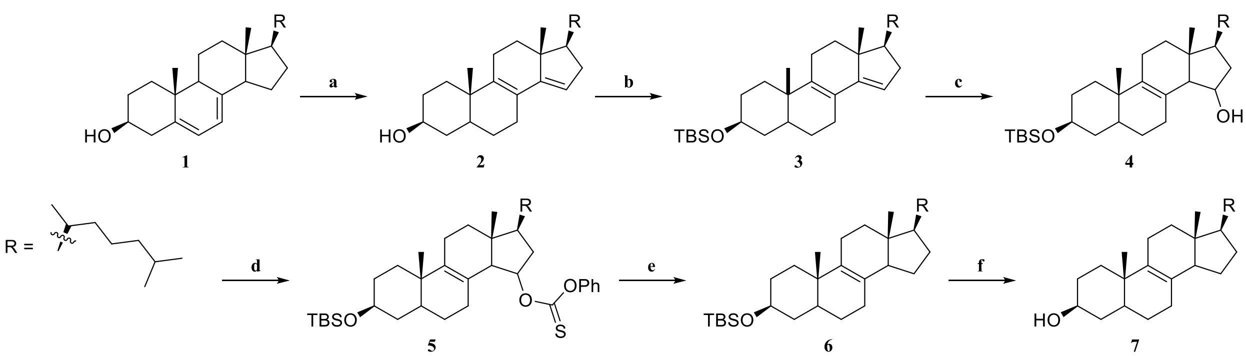

Figure 28: Synthesis of zymostenol. **a**) AcOH/HCl; **b**) TBSCl; **c**) BH_3•THF, NaOH/H_2O_2; **d**) Pyridine, phenyl chlorothionocarbonate; **e**) $(Bu)_3SnH$, AIBN; **f**) TBAF.

Synthesis of 8,14-DHC (**2**). 7-dehydrocholesterol (**1**, 2.0 g, 5.2 mmol) was dissolved in a mixture of $CHCl_3$ (20 mL) and acetic acid (5 mL). Concentrated HCl (0.5 mL, 6.0 mmol) was added and the reaction was heated to reflux. After 2 h, the reaction was cooled and diluted with ethyl acetate (20 mL). The organic layer was washed with sat. sodium bicarbonate (30 mL) and brine (30 mL), then dried over magnesium sulfate. Solvent was removed by rotary evaporation, and residue was purified by flash column (20 % ethyl acetate in hexanes) to give a yellow powder

(1.52 g, 76 %). ^{1}H NMR ($CDCl_3$, δ): 5.34 (br. s., 1H), 3.61 (m, 1H), 2.33 (m, 2H), 2.18 (m, 2H), 2.03 (m, 3H), 1.83 (m, 3H), 1.51 (m, 11H), 1.12 (m, 6H), 0.97 (s, 3H), 0.91 (d, J = 6.2 Hz, 3H), 0.84 (d, J = 6.6 Hz, 6H), 0.79 (s, 3H). ^{13}C NMR ($CDCl_3$, δ): 151.1, 140.8, 123.0, 117.4, 71.0, 57.2, 45.0, 40.9, 39.5, 38.4, 36.9, 36.5, 36.1, 35.9, 35.3, 34.0 31.7, 28.0, 36.6, 25.3, 32.7, 22.8, 22.5, 31.8, 18.8, 18.3, 15.4. HRMS (ESI) calcd $[M+H]^+$ 385.3465, found 385.3438.

Synthesis of TBS protected 8,14-DHC (**3**). 8,14-DHC (**2**, 1.52 g, 3.95 mmol) was dissoved in THF/DMF (20 mL, 1:1). TBS chloride (0.9 g, 6.0 mmol) and imidazole (0.6 g, 8.8 mmol) were added to the solution. The reaction was allowed to proceed overnight at room temperature, after which it was diluted with ethyl acetate (20 mL). The organic layer was washed with water (30 mL) and brine (30 mL). The organic layer was then dried over magnesium sulfate. Solvent was removed by rotary evaporation, and residue was purified by flash column (10% ehtyl acetate in hexanes) to give a yellow powder (1.86 g, 94 %). ^{1}H NMR ($CDCl_3$, δ): 5.34 (br. s., 1H), 3.56 (m, 1H), 2.33 (m, 2H), 2.18 (m, 2H), 2.04 (m, 3H), 1.76 (m, 2H), 1.44 (m, 11H), 1.12 (m, 6H), 0.96 (s, 3H), 0.92 (d, J = 7.9 Hz, 3H), 0.87 (s, 9H), 0.86 (d, J = 4.4 Hz, 6H), 0.79 (s, 3H), 0.04 (s, 6H). ^{13}C NMR ($CDCl_3$, δ): 151.2, 141.1, 122.9, 117.2, 71.8, 57.2, 45.0, 41.0, 39.5, 38.8, 36.9, 36.6, 36.1, 35.9, 35.5, 34.0, 32.1, 28.0, 26.6, 25.9, 25.3, 23.7, 22.8, 22.5, 21.8, 18.9, 18.4, 18.2, 15.6, -4.6. HRMS (ESI) calcd $[M+H]^+$ 499.4330, found 499.4335.

Synthesis of TBS protected Zymostenol-OH (**4**). 3-OTBS-8,14-DHC (**3**, 1.86 g, 3.73 mmol) was dissolved in THF (30 mL) and cooled to 0 ˚C. BH_3·THF was added dropwise to the solution. After 4 h, the reaction was slowly quenched with aqueous 1 N NaOH (15 mL) and H_2O_2 (15 mL) and stirred for 1 h. The reaction was then diluted with ethyl acetate (30 mL) and washed with water (3 x 30 mL), saturated sodium bicarbonate (3 x 30 mL) and brine (3 x 30 mL). The organic layer was dried over magnesium sulfate, and solvent was removed by rotary evaporation. The residue was purified by flash column (10 % ethyl acetate in hexanes) to give a white foam (1.0 g, 52 %). ^{1}H NMR ($CDCl_3$, δ): 4.05 (dt, *J* = 9.5 Hz, 3.6 Hz, 1H), 3.55 (m, 1H), 2.11 (m, 4H), 1.90 (m, 2H), 1.78 (dd, *J* = 8.8 Hz, 3.9 Hz, 1H), 1.68 (m, 2H), 1.41 (m, 20H), 1.11 (m, 8H), 0.93 (s, 3H), 0.86 (m, 19H), 0.61 (s, 3H), 0.03 (s, 6H). ^{13}C NMR ($CDCl_3$, δ): 136.3, 126.5, 72.0, 71.9, 59.5, 52.9, 43.2, 40.6, 40.5, 39.4, 38.7, 37.1, 36.0, 35.9, 35.8, 35.2, 32.0, 27.9, 27.3, 25.9, 25.5, 23.7, 22.8, 22.7, 22.5, 18.5, 18.2, 17.7, 12.4, -4.6. HRMS (ESI) calcd $[M+H]^+$ 517.4435, found 517.4422.

Synthesis of Thiocarbonate Ester (**5**). TBS Zymostenol-OH (**4**, 0.40 g, 0.77 mmol) was dissolved in CH_2Cl_2 (4 mL). Pyridine (0.12 mL, 1.48 mmol) was added, followed by thioformate (0.16 mL, 1.16 mmol). After 30 min, the reaction was diluted with ethyl acetate (10 mL) and washed with water (3 x 15 mL) and brine (3 x 15 mL) and dried over magnesium sulfate. Solvent was removed by rotary evaporation, and the resulting residue was purified by flash column (5 % ethyl acetate in hexanes) to give a white foam (0.38 g, 74 %). ^{1}H NMR ($CDCl_3$, δ): 7.27 (m, 5H), 5.38 (dt, *J* = 9.9 Hz, 3.5 Hz, 1H), 3.56 (m, 1H), 2.56 (d, *J* = 10.3 Hz, 1H), 2.06 (m, 8H), 1.71 (m, 3H), 1.42 (m, 12H), 1.10 (m, 6H), 0.95 (s, 3H), 0.92 (d, *J* = 6.1 Hz, 3H), 0.87 (m, 12H), 0.70 (s, 3H), 0.04 (s, 6H). ^{13}C NMR ($CDCl_3$, δ): 194.9, 153.4, 137.0, 129.4, 126.4, 125.5, 122.0, 121.0, 85.4, 71.9, 55.5, 53.2, 42.6, 42.5, 40.6, 39.4, 38.7, 37.0, 36.8, 35.9, 35.8, 35.2, 32.0, 28.0, 26.8, 25.9, 25.4, 23.9, 22.8, 22.7, 22.5, 18.3, 18.2, 17.7, 12.3, -4.6.

Synthesis of TBS Protected Zymostenol (**6**). A solution of the thiocarbonate ester (**5**, 0.38 g, 0.58 mmol), tributyltin hydride (0.23 mL) and azobisisobutyronitrile (10 mg) in toluene (3 mL) was sparged with argon for 20 min at rt. The reaction was then heated to 100 ˚C. After 30 min, the reaction was cooled and concentrated by rotary evaporation. The resulting residue was purified by flash column (10 % CH_2Cl_2 in hexanes) to give a white powder (0.16 g, 55 %). ^{1}H NMR ($CDCl_3$, δ): 3.55 (m, 1H), 1.89 (m, 6H), 1.57 (m, 8H), 1.25 (m, 9H), 1.15 (m, 6H), 0.92 (s, 3H), 0.90 (d, *J*

= 6.6 Hz, 3H), 0.86 (m, 12H), 0.83 (d, *J* = 1.3 Hz, 3H), 0.58 (s, 3H), 0.03 (s, 6H). ^{13}C NMR ($CDCl_3$, δ): 135.2, 128.0, 72.0, 54.8, 51.9, 42.1, 40.9, 39.5, 38.8, 37.3, 37.0, 36.2, 36.1, 35.7, 35.3, 32.1, 28.8, 28.0, 27.2, 25.9, 25.5, 23.9, 23.8, 22.8, 22.5, 18.7, 18.2, 17.9, 12.8, 11.1, -4.6.

Synthesis of Zymostenol (**7**). Tetrabutylammonium fluoride (1.0 M in THF) (1 mL, 1.0 mmol) was added to a solution of 3-OTBS-zymostenol (**6**, 0.32 g, 0.64 mmol) in THF (3 mL). Reaction proceeded overnight, after which it was diluted with ehtyl acetate (10 mL) and washed with brine (3 x 10 mL). The organic phase was dried over magnesium sulfate. Solvent was removed by rotary evaporation. Residue was then purified by column chromatography (20 % ethyl acetate in hexanes) to give a white powder (0.18 g, 74 %). The spectral data of **7** is in agreement with previously published results.[71] ^{1}H NMR ($CDCl_3$, δ): 3.58 (m, 1H), 1,98 (m, 6H), 1.74 (m, 5H), 1.55 (m, 6H), 1.34 (m, 8H), 1.15 (m, 5H), 0.92 (s, 3H), 0.0.89 (d, *J* = 6.5 Hz, 3H), 0.84 (d, *J* = 1.3 Hz, 3H), 0.82 (d, *J* = 1.3 Hz, 3H), 0.58 (s, 3H). ^{13}C NMR ($CDCl_3$, δ): 134.9, 128.2, 71.1, 60.4, 54.8, 51.9, 49.3, 44.2, 42.0, 40.7, 39.5, 38.3, 37.2, 36.9, 36.7, 36.2, 36.1, 35.9, 35.7, 35.1, 31.6, 29.6, 28.7, 28.0, 27.2, 25.8, 25.5, 23.9, 23.7, 22.8, 22.5, 19.9, 19.0, 18.7, 17.8, 14.1, 11.2. HRMS (ESI) calcd $[M+H]^+$ 387.3621, found 387.3617.

2.10. References

1. Horton, H. R.; Moran, L. A.; Scrimgeour, K. G.; Perry, M. D.; Rawn, J. D., *Principles of Biochemistry*. 4th ed.; Pearson Education, Inc.: Upper Saddle River, New Jersey, 2006.

2. Rouzer, C.; Marnett, L., Mechanism of free radical oxygenation of polyunsaturated fatty acids by cyclooxygenases. *Chem. Rev.* **2003,** *103* (6), 2239-2304.

3. Haeggstrom, J.; Funk, C., Lipoxygenase and Leukotriene Pathways: Biochemistry, Biology, and Roles in Disease. *Chem. Rev.* **2011,** *111*, 5866-5898.

4. Xu, L.; Davis, T. A.; Porter, N. A., Rate constants for peroxidation of polyunsaturated fatty acids and sterols in solution and in liposomes. *J. Am. Chem. Soc.* **2009,** *131*, 13037-13044.

5. Yin, H.; Xu, L.; Porter, N. A., Free Radical Lipid Peroxidation: Mechanisms and Analysis. *Chem. Rev.* **2011,** *111*, 5944-5972.

6. Dobretsov, G. E.; Borschevskaya, T. A.; Petrov, V. A.; Vladimirov, Y. A., The increase of phospholipidbilayer rigidity after lipid peroxidation. *FEBS Lett.* **1977,** *84*, 125-128.

7. Chatgilialoglu, C.; Ferreri, C., Trans lipids: the free radical path. *Acc. Chem. Res.* **2005,** *38*, 441-448.

8. Palinski, W.; Rosenfeld, M. E.; Ylä-Herttuala, S.; Gurtner, G. C.; Socher, S. S.; Butler, S. W.; Parthasarathy, S.; Carew, T. E.; Steinberg, D.; Witztum, J. L., Low density lipoprotein undergoes oxidative modification in vivo. *Proc. Natl. Acad. Sci. U. S. A.* **1989,** *86*, 1372-1376.

9. Steinbrecher, U. P.; Zhang, H. F.; Lougheed, M., Role of Oxidatively Modified LDL in Atherosclerosis. *Free Radic. Biol. Med.* **1990,** *9*, 155-168.

10. Salonen, J. T.; Ylaherttuala, S.; Yamamoto, R.; Butler, S.; Korpela, H.; Salonen, R.; Nyyssonen, K.; Palinski, W.; Witztum, J. L., Autoantibody against Oxidized LDL and Progression of Carotid Atherosclerosis. *Lancet* **1992,** *339*, 883-887.

11. Hammad, L. A.; Wu, G. X.; Saleh, M. M.; Klouckova, I.; Dobrolecki, L. E.; Hickey, R. J.; Schnaper, L.; Novotny, M. V.; Mechref, Y., Elevated levels of hydroxylated phosphocholine lipids in the blood serum of breast cancer patients. *Rapid Commun. Mass Spectrom.* **2009,** *23*, 863-876.

12. Wu, R. P.; Hayashi, T.; Cottam, H. B.; Jin, G.; Yao, S.; Wu, C. C.; Rosenbach, M. D.; Corr, M.; Schwab, R. B.; Carson, D. A., Nrf2 responses and the therapeutic selectivity of electrophilic compounds in chronic lymphocytic leukemia. *Proc. Natl. Acad. Sci. U. S. A.* **2010,** *107*, 7479-7484.

13. Imai, Y.; Kuba, K.; Neely, G. G.; Yaghubian-Malhami, R.; Perkmann, T.; van Loo, G.; Ermolaeva, M.; Veldhuizen, R.; Leung, Y. H.; Wang, H.; Liu, H.; Sun, Y.; Pasparakis, M.; Kopf,

M.; Mech, C.; Bavari, S.; Peiris, J. S.; Slutsky, A. S.; Akira, S.; Hultqvist, M.; Holmdahl, R.; Nicholls, J.; Jiang, C.; Binder, C. J.; Penninger, J. M., Identification of oxidative stress and Toll-like receptor 4 signaling as a key pathway of acute lung injury. *Cell* **2008,** *133*, 235-249.

14. Nonas, S.; Miller, I.; Kawkitinarong, K.; Chatchavalvanich, S.; Gorshkova, I.; Bochkov, V. N.; Leitinger, N.; Natarajan, V.; Garcia, J. G.; Birukov, K. G., Oxidized phospholipids reduce vascular leak and inflammation in rat model of acute lung injury. *Am. J. Respir. Crit. Care. Med.* **2006,** *173*, 1130-1138.

15. Montine, T. J.; Montine, K. S.; McMahan, W.; Markesbery, W. R.; Quinn, J. F.; Morrow, J. D., F2-isoprostanes in Alzheimer and other neurodegenerative diseases. *Antioxid. Redox. Signal.* **2005,** *7*, 269-275.

16. Montine, T. J.; Peskind, E. R.; Quinn, J. F.; Wilson, A. M.; Montine, K. S.; Galasko, D., Increased Cerebrospinal Fluid F-2-Isoprostanes are Associated with Aging and Latent Alzheimer's Disease as Identified by Biomarkers. *Neuromolecular Med.* **2011,** *13*, 37-43.

17. Jenner, P., Oxidative stress in Parkinson's disease. *Ann. Neurol.* **2003,** *53*, S26-S36.

18. Morrow, J. D.; Harris, T. M.; Roberts, L. J., Noncyclooxygenase oxidative formation of a series of novel prostaglandins: analytical ramifications for measurement of eicosanoids. *Anal. Biochem.* **1990,** *184*, 1-10.

19. Gardner, H. W., Oxygen radical chemistry of polyunsaturated fatty acids. *Free Radic. Biol. Med.* **1989,** *7*, 65-86.

20. Howard, J. A.; Ingold, K. U., Absolute rate constants for hydrocarbon autoxidation. V. The hydroperoxy radical in chain propagation and termination. *Can. J. Chem.* **1967,** *45*, 785-792.

21. Porter, N. A., Mechanisms for the autoxidation of polyunsaturated lipids. *Acc. Chem. Res.* **1986,** *19*, 262-268.

22. Hill, S.; Hirano, K.; Shmanai, V. V.; Marbois, B. N.; Vidovic, D.; Bekish, A. V.; Kay, B.; Tse, V.; Fine, J.; Clarke, C. F.; Shchepinov, M. S., Isotope-reinforced polyunsaturated fatty acids protect yeast cells from oxidative stress. *Free Radic. Biol. Med.* **2011,** *50*, 130-138.

23. Bentinger, M.; Brismar, K.; Dallner, G., The antioxidant role of coenzyme Q. *Mitochondrion* **2007,** *7*, S41-S50.

24. Hill, S.; Hirano, K.; Shmanai, V. V.; Marbois, B. N.; Vidovic, D.; Bekish, A. V.; Kay, B.; Tse, V.; Fine, J.; Clarke, C. F.; Shchepinov, M. S., Isotope-reinforced polyunsaturated fatty acids protect yeast cells from oxidative stress. *Free Radic. Biol. Med.* **2011,** *50*, 130-138.

25. Hill, S.; Lamberson, C. R.; Xu, L.; To, R.; Tsui, H. S.; Shmanai, V. V.; Bekish, A. V.; Awad, A. M.; Marbois, B. N.; Cantor, C. R.; Porter, N. A.; Clarke, C. F.; Shchepinov, M. S.,

Small amounts of isotope-reinforced polyunsaturated fatty acids suppress lipid autoxidation. *Free Radic. Biol. Med.* **2012,** *53*, 893-906.

26. Cotticelli, M. G.; Crabbe, A. M.; Wilson, R. B.; Shchepinov, M. S., Insights into the role of oxidative stress in the pathology of Friedreich ataxia using peroxidation resistant polyunsaturated fatty acids. *Redox Biol.* **2013,** *1*, 398-404.

27. Andreyev, A. Y.; Tsui, H. S.; Milne, G. L.; Shmanai, V. V.; Bekish, A. V.; Fomich, M. A.; Pham, M. N.; Nong, Y.; Murphy, A. N.; Clarke, C. F.; Shchepinov, M. S., Isotope-reinforced polyunsaturated fatty acids protect mitochondria from oxidative stress. *Free Radic. Biol. Med.* **2015,** *82*, 63-72.

28. Shchepinov, M.; Chou, V.; Pollock, E.; Langston, P.; Cantor, C.; Molinari, R.; Manning-Bog, A., Isotopic reinforcement of essential polyunsaturated fatty acids diminishes nigrostriatal degeneration in a mouse model of Parkinson's disease. *Toxicol. Lett.* **2011,** *207*, 97-103.

29. Angelova, P. R.; Horrocks, M. H.; Klenerman, D.; Gandhi, S.; Abramov, A. Y.; Shchepinov, M. S., Lipid peroxidation is essential for a-synuclein-induced cell death. *J. Neurochem.* **2015,** *133*, 582-589.

30. Roschek, B.; Tallman, K.; Rector, C.; Gillmore, J.; Pratt, D.; Punta, C.; Porter, N., Peroxyl radical clocks. *J. Org. Chem.* **2006,** *71*, 3527-3532.

31. Hill, S.; Lamberson, C. R.; Xu, L.; To, R.; Tsui, H. S.; Shmanai, V. V.; Bekish, A. V.; Awad, A. M.; Marbois, B. N.; Cantor, C. R.; Porter, N. A.; Clarke, C. F.; Shchepinov, M. S., Small amounts of isotope-reinforced polyunsaturated fatty acids suppress lipid autoxidation. *Free Radic. Biol. Med.* **2012,** *53*, 893-906.

32. Liu, W.; Yin, H.; Akazawa, Y. O.; Yoshida, Y.; Niki, E.; Porter, N. A., Ex vivo oxidation in tissue and plasma assays of hydroxyoctadecadienoates: Z,E/E,E stereoisomer ratios. *Chem. Res. Toxicol.* **2010,** *23*, 986-995.

33. Howard, J. A.; Ingold, K. U., Absolute rate constants for hydrocarbon autoxidation. XVII. The oxidation of some cyclic ethers. *Can. J. Chem.* **1969,** *47*, 3809-3815.

34. Yamamoto, Y.; Haga, S.; Niki, E.; Kamiya, Y., Oxidation of lipids. V. Oxidation of methyl linoleate in aqueous dispersion. *Bull. Chem. Soc. Jpn.* **1984,** *57*, 1260-1264.

35. Boozer, C. E.; Hammond, G. S.; Hamilton, C. E.; Sen, J. N., Air oxidation of hydrocarbons. II. The stoichiometry and fate of inhibitors in benzene and chlorobenzene. *J. Am. Chem. Soc.* **1955,** *77*, 3233-3237.

36. Cosgrove, J. P.; Church, D. F.; Pryor, W. A., The Kinetics of the Autoxidation of Polyunsaturated Fatty Acids. *Lipids* **1987,** *22*, 299-304.

37. Howard, J. A.; Ingold, K. U., Absolute Rate Constants for Hydrocarbon Autoxidation. 6. Alkyl Aromatic and Olefinic Hydrocarbons. *Can. J. Chem.* **1967,** *45*, 793-802.

38. Glickman, M. H.; Wiseman, J. S.; Klinman, J. P., Extremely Large Isotope Effects in the Soybean Lipoxygenase-Linoleic Acid Reaction. *J. Am. Chem. Soc.* **1994,** *116*, 793-794.

39. Hwang, C. C.; Grissom, C. B., Unusually Large Deuterium Isotope Effects in Soybean Lipoxygenase Are Not Caused by a Magnetic Isotope Effect. *J. Am. Chem. Soc.* **1994,** *116*, 795-796.

40. Glickman, M. H.; Klinman, J. P., Nature of Rate-Limiting Stepts in the Soybean Lipoxygenase-1 Reaction. *Biochemistry* **1995,** *34*, 14077-14092.

41. Glickman, M. H.; Klinman, J. P., Lipoxygenase Reaction Mechanism: Demonstration That Hydrogen Abstraction from Substrate Precedes Dioxygen Binding during Catalytic Turnover. *Biochemistry* **1996,** *35*, 12882-12892.

42. Lewis, E. R.; Johansen, E.; Holman, T. R., Large Competitive Kinetic Isotope Effects in Human 15-Lipoxygenase Catalysis Measured by a Novel HPLC Method. *J. Am. Chem. Soc.* **1999,** *121*, 1395-1396.

43. Russell, G. A., Deuterium-Isotope Effects in the Autoxidation of Aralkyl Hydrocarbons. Mechanism of the Interaction of Peroxy Radicals. *J. Am. Chem. Soc.* **1957,** *79*, 3871-3877.

44. Howard, J. A.; Ingold, K. U., Absolute rate constants for hydrocarbon autoxidation. IV. Tetralin, cyclohexene, diphenylmethane, ethylbenzene, and allylbenzene. *Can. J. Chem.* **1966,** *44*, 1113-1118.

45. Howard, J. A.; Ingold, K. U.; Symonds, M., Absolute Rate Constants for Hydrocarbon Oxidation. 8. The Reactions of Cumylperoxy Radicals. *Can. J. Chem.* **1968,** *46*, 1017-1022.

46. Kitaguchi, H.; Ohkubo, K.; Ogo, S.; Fukuzumi, S., Additivity rule holds in the hydrogen transfer reactivity of unsaturated fatty acids with a peroxyl radical: mechanistic insight into lipoxygenase. *Chem. Commun. (Camb.)* **2006**, 979-81.

47. Holman, R. T.; Elmer, O. C., The rates of oxidation of unsaturated fatty acids and esters. *J. Am. Oil Chem. Soc.* **1947,** *24*, 127-129.

48. Hansen, S.; Kensy, F.; Kaser, A.; Buchs, J., Potential errors in conventional DOT measurement techniques in shake flasks and verification using a rotating flexitube optical sensor. *BMC Biotechnol.* **2011,** *11*, 1-7.

49. Parker, S. R.; Nes, W. D., Regulation of Sterol Biosynthesis and Its Phylogenetic Implications. *Regulation of Isopentenoid Metabolism*, American Chemical Society: 1992; Vol. 497, pp 110-145.

50. van Meer, G.; Voelker, D. R.; Feigenson, G. W., Membrane lipids: where they are and how they behave. *Nat. Rev. Mol. Cell. Biol.* **2008,** *9*, 112-124.

51. Kandutsch, A. A.; Russell, A. E., Preputial gland tumor sterols. 3. A metabolic pathway from lanosterol to cholesterol. *J. Biol. Chem.* **1960,** *235*, 2256-2261.

52. Bloch, K., Sterol molecule: structure, biosynthesis, and function. *Steroids* **1992,** *57*, 378-383.

53. Brown, A. J.; Jessup, W., Oxysterols and atherosclerosis. *Atherosclerosis* **1999,** *142*, 1-28.

54. Vaya, J.; Schipper, H. M., Oxysterols, cholesterol homeostasis, and Alzheimer disease. *J. Neurochem.* **2007,** *102*, 1727-1737.

55. Rodriguez, I. R.; Fliesler, S. J., Photodamage generates 7-keto- and 7-hydroxycholesterol in the rat retina via a free radical-mediated mechanism. *Photochem. Photobiol.* **2009,** *85*, 1116-1125.

56. Girao, H.; Mota, M. C.; Ramalho, J.; Pereira, P., Cholesterol oxides accumulate in human cataracts. *Exp. Eye Res.* **1998,** *66*, 645-652.

57. Vejux, A.; Samadi, M.; Lizard, G., Contribution of cholesterol and oxysterols in the physiopathology of cataract: Implication for the development of pharmacological treatments. *J. Ophthalmol.* **2011,** *2011*, 1-6.

58. Porter, F. D.; Scherrer, D. E.; Lanier, M. H.; Langmade, S. J.; Molugu, V.; Gale, S. E.; Olzeski, D.; Sidhu, R.; Dietzen, D. J.; Fu, R.; Wassif, C. A.; Yanjanin, N. M.; Marso, S. P.; House, J.; Vite, C.; Schaffer, J. E.; Ory, D. S., Cholesterol oxidation products are sensitive and specific blood-based biomarkers for Niemann-Pick C1 disease. *Sci. Transl. Med.* **2010,** *2*, 56ra81.

59. Korade, Z.; Xu, L.; Shelton, R.; Porter, N. A., Biological activities of 7-dehydrocholesterol-derived oxysterols: implications for Smith-Lemli-Opitz syndrome. *J. Lipid Res.* **2010,** *51*, 3259-3269.

60. Kelley, R. I.; Wilcox, W. G.; Smith, M.; Kratz, L. E.; Moser, A.; Rimoin, D. S., Abnormal sterol metabolism in patients with Conradi-Hunermann-Happle syndrome and sporadic lethal chondrodysplasia punctata. *Am. J. Med. Genet.* **1999,** *83*, 213-219.

61. Martanova, H.; Krepelova, A.; Baxova, A.; Hansikova, H.; Cansky, Z.; Kvapil, M.; Gregor, V.; Magner, M.; Zeman, J., X-linked Dominant Chondrodysplasia Punctata (CDPX2): Multisystemic Impact of the Defect in Cholesterol Biosynthesis. *Prague Med. Rep.* **2007,** *108*, 263-269.

62. Porter, F. D.; Herman, G. E., Malformation syndromes caused by disorders of cholesterol synthesis. *J. Lipid Res.* **2011,** *52*, 6-34.

63. Herman, G. E., Disorders of cholesterol biosynthesis: prototypic metabolic malformation syndromes. *Hum. Molec. Genet.* **2003,** *12*, R75-R88.

64. Krakowiak, P. A.; Wassif, C. A.; Kratz, L.; Cozma, D.; Kovarova, M.; Harris, G.; Grinberg, A.; Y., Y.; Hunter, A. G. W.; Tsokos, M.; Kelley, R. I.; Porter, F. D., Lathosterolosis: an inborn error of human and murine cholesterol synthesis due to lathosterol 5-desaturase deficiency. *Hum. Mol. Genet.* **2003,** *12*, 1631-1641.

65. Korade, Z.; Kim, H. H.; Tallman, K. A.; Liu, W.; Koczok, K.; Balogh, I.; Xu, L.; Mirnics, K.; Porter, N. A., The Effect of Small Molecules on Sterol Homeostasis: Measuring 7-Dehydrocholesterol in Dhcr7-Deficient Neuro2a Cells and Human Fibroblasts. *J. Med. Chem.* **2016,** *59*, 1102-1115.

66. Castelli, W. P.; Garrison, R. J.; Wilson, P. W. F.; Abbott, R. D.; Kalousdian, S.; Kannel, W. B., Incidence of coronary heart disease and lipoprotein cholesterol levels. *J. Am. Med. Soc.* **1986,** *256*, 2835-2838.

67. Canfran-Duque, A.; Casado, M. E.; Pastor, O.; Sanchez-Wandelmer, J.; de la Pena, G.; Lerma, M.; Mariscal, P.; Bracher, F.; Lasuncion, M. A.; Busto, R., Atypical antipsychotics alter cholesterol and fatty acid metabolism in vitro. *J. Lipid Res.* **2013,** *54*, 310-324.

68. Hall, P.; Michels, V.; Gavrilov, D.; Matern, D.; Oglesbee, D.; Raymond, K.; Rinaldo, P.; Tortorelli, S., Aripiprazole and trazodone cause elevations of 7-dehydrocholesterol in the absence of Smith-Lemli-Opitz Syndrome. *Mol. Genet. Metab.* **2013,** *110*, 176-178.

69. Xu, L.; Porter, N. A., Unpublished results. 2011.

70. Eguchi, S.; Yamaguchi, S.; Mitsuko, F.; Morisaki, M., Epoxide Cleavage of 7a,8a- and 7B,8B-Epoxycholestanol Acetates. *Chem. Pharm. Bull.* **1988,** *36*, 2813-2818.

71. Wilson, W. K.; Sumpter, R. M.; Warren, J. J.; Rogers, P. S.; Ruan, B.; Schroepfer Jr., G. J., Analysis of unsaturated C27 sterols by nuclear magnetic resonance spectroscopy. *J. Lipid Res.* **1996,** *37*, 1529-1555.

Chapter III

TOCOPHEROL-MEDIATED PEROXIDATION

3.1. Introduction

The free radical oxidation of sterols and fatty acids has attracted attention in recent years due to the association of lipid peroxidation and oxidized lipid products with a number of human pathologies including atherosclerosis,[1,2,3] cancer,[4,5] acute lung injury[6,7] and neurodegenerative disorders such as Alzheimer's[8,9] and Parkinson's disease.[10] Exposure to reactive oxygen species (ROS) from normal cellular metabolism or environmental toxicants is a common part of life. Aerobic organisms have a number of integrated enzymatic and nonenzymatic antioxidant systems to counteract ROS damage. In pathological conditions listed above, the antioxidant systems are often overwhelmed.[11]

Enzymatic antioxidant systems play an important role in counterbalancing the effect of ROS on biological systems. One of the major enzymatic systems is the superoxide dismutase (SOD)/catalase (CAT) couple. SOD, largely considered to be a bulk scavenger of superoxide radicals in biological systems, catalyzes the breakdown of superoxide through Equation 1, shown below.

$$O_2^- + 2H^+ \rightarrow H_2O_2 \qquad (1)$$

The hydrogen peroxide formed during SOD action is then reduced to water by catalase (CAT) as shown in Equation 2.

$$2H_2O_2 \rightarrow 2H_2O + O_2 \quad (2)$$

While enzymatic antioxidant systems such as the SOD/CAT couple play a large role in protecting organisms from rampant oxidative stress, small molecule antioxidants are also heavily utilized for the same purpose in biological systems. One of the most prevalent and highly studied of these antioxidants is α-tocopherol, commonly referred to as Vitamin E (Figure 1).

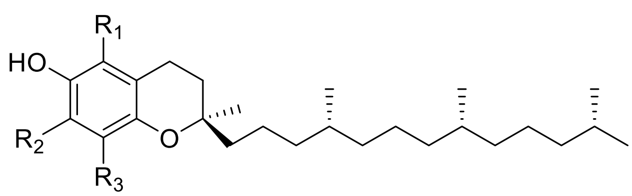

- α-Tocopherol : $R_1=R_2=R_3=CH_3$
- β-Tocopherol : $R_1=R_3=CH_3$; $R_2=H$
- γ-Tocopherol : $R_1=R_2=CH_3$; $R_3=H$
- δ-Tocopherol : $R_1=CH_3$; $R_2=R_3=H$

Figure 1. The basic phenolic framework of all tocopherols is pictured on the left, with designations for R_1, R_2, and R_3 for α, β, γ, and δ-tocopherols on the right.

Tocopherol is the most prevalent and efficient antioxidant in Nature.[12] It exists in four different structures shown in Figure 1, with α-tocopherol (TocH) being the most potent free radical chain breaking antioxidant. The free radical chain oxidation of lipids propagates through a rate-limiting hydrogen atom transfer (k_p) to lipid peroxyl radicals (Equation 1, Figure 2). TocH inhibits this propagation step through hydrogen atom donation to the chain carrying peroxyl radical species, generating a tocopheryl radical (Toc·) during the process (Equation 3, Figure 2). The phenolic Toc· is highly stabilized through resonance delocalization, making it relatively inert and unlikely to continue the chain reaction.[12] This species will eventually trap a second peroxyl radical to terminate the chain sequence (Equation 4, Figure 2).

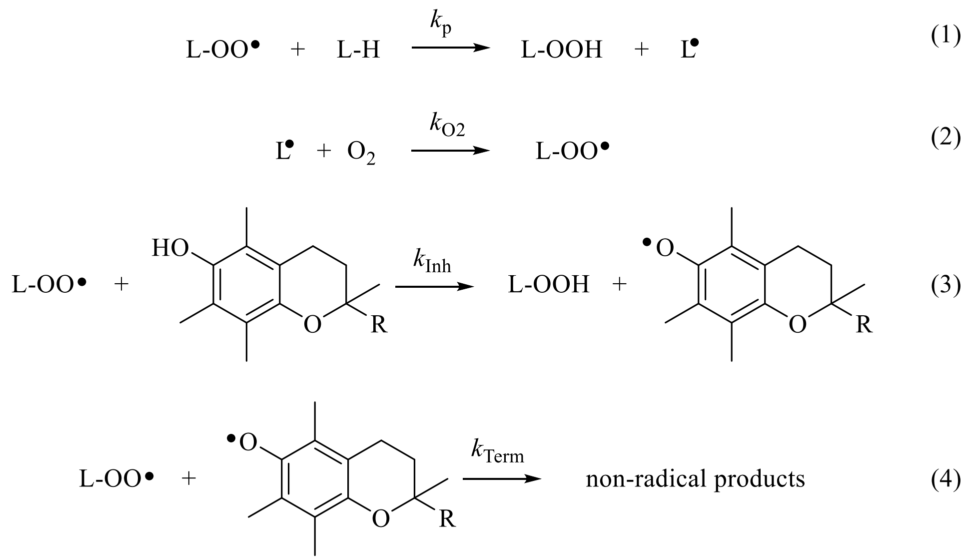

Figure 2. Lipid peroxidation (k_p) and inhibition (k_{inh}) by α-tocopherol or other free radical chain-breaking antioxidants.

While all of the tocopherols are good chain breaking antioxidants, α-tocopherol has the fastest inhibition rate constant ($k_{inh} = 3.5 \times 10^6\ M^{-1}\ s^{-1}$),[13,14,15] even faster than numerous synthetic phenolic antioxidants. TocH also has a thermodynamic advantage for breaking free radical chain reactions. The BDE of the phenolic O-H is 77.1 kcal mol^{-1},[16] at least 11 kcal mol^{-1} lower than that of a typical alkyl hydroperoxide O-H bond (82-89 kcal mol^{-1}).[17] This results in favorable thermodynamic conditions in which TocH readily transfers a hydrogen atom to a peroxyl radical as the new bond being formed is stronger than the bond being broken.

TocH is the major lipid-soluble radical trapping antioxidant in Nature.[12] It is present at concentrations higher than any other antioxidant in plasma lipoproteins, including human low-density lipoprotein (LDL).[12,18,19] The LDL particle, shown in Figure 3, is composed of three major components. The outer shell of this particle is comprised of Apoprotein B100 embedded in a coat of polar lipids, 85% of which are phosphatidylcholine (40% containing PUFA). The core of the particle is comprised mainly of cholesterol esters, 40% of which are cholesteryl linoleate, as well as TocH (6 mol/mol of LDL), ubiquinol ($CoQH_2$), and assorted carotenoids.[18,19,20]

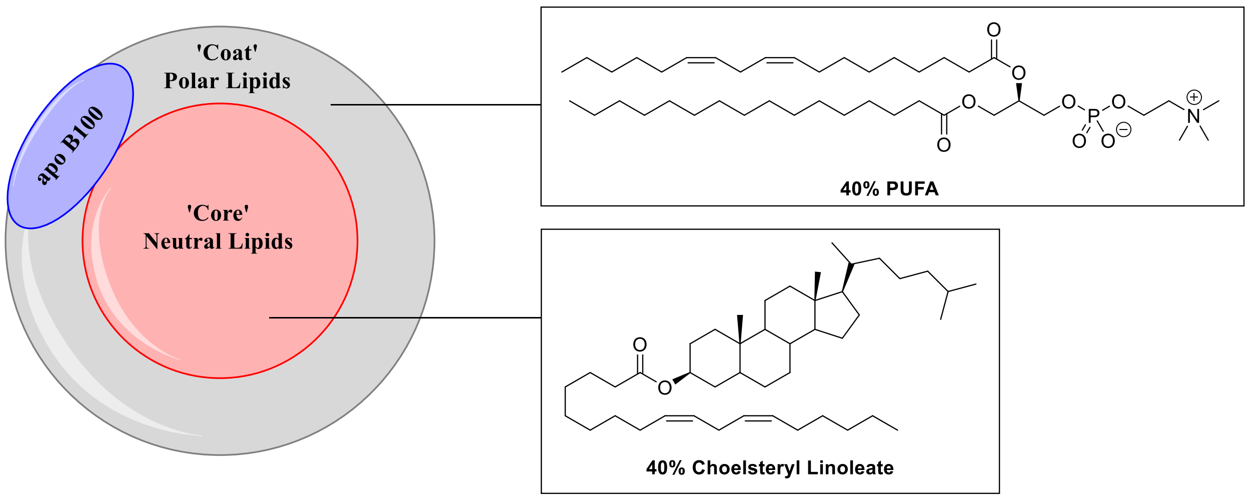

Figure 3. Basic structure of the LDL particle. Apoprotein B100 is embedded in the polar coat lipids, which consists of roughly 85% phosphatidylcholine. The neutral core lipids are comprised primarily of cholesterol esters, 40% of which are cholesteryl linoleate. TocH, $CoQH_2$, and other carotenoids also reside in this region.[12,18,19]

LDL is one of the five major groups of lipoprotein. The main function of LDL and others is to shuttle lipids around the body for cells to take up as needed, with LDL being the major cholesterol-bearing lipoprotein in human blood plasma. Congruent with its physical composition, LDL is also susceptible to attack from reactive oxygen species (ROS). Indeed, oxidative modification of LDL has been implicated as an initiator of atherosclerosis,[21,22] as oxidative modification can lead to increased and uncontrolled uptake of cholesterol by macrophages.[23] This is largely thought to be an early step in a number of cellular responses leading to the formation of fatty streaks in arterial walls and the eventual formation of atherosclerotic lesions.[21] A great deal of research has been devoted to the prevention of lipid peroxidation in LDL by natural antioxidants but cell, animal, and clinical studies have been largely disappointing.[24]

While studying the oxidation of LDL under a steady flux of peroxyl radicals, Bowry and coworkers found that rates of peroxidation decreased as TocH was consumed.[25] The slowest rates of lipid peroxidation were recorded when one or fewer molecules of TocH remained in the LDL particle.[25] Additional experiments showed that enrichment with exogenous TocH accelerated peroxidation rates.[25] In other words, rates of lipid peroxidation within the LDL particle were higher when the concentration of TocH is high. Further studies on the oxidation of LDL by both lipid- and water-soluble peroxyl radicals showed that TocH can actually act as a prooxidant in LDL when rates of initiation are low and concentrations of TocH are high.[26]

The result of these studies was a new hypothesis on how TocH can act under the constraints discussed in the previous paragraph. When TocH acts as a chain-breaking antioxidant, it is able to scavenge peroxyl radicals at a rate (k_{inh}) of 3.5 x 10^6 M^{-1} s^{-1},[13,14,15] leading to a decrease in concentration of the propagating peroxyl radical species (Equation 3, Figure 2). The tocopheryl radical (Toc$^{\cdot}$) generated after H-atom donation then rapidly reacts with other peroxyl radicals in solution (*ca.* 3 x 10^8 M^{-1} s^{-1}) to give non-radical products (Equation 4, Figure 2).[27] When TocH concentrations are high *or* rates of initiation are low, the steady state concentration of the tocopheryl radical becomes orders of magnitude greater than peroxyl radicals in solution. The tocopheryl radical becomes the main propagating species despite its low rate constant for abstracting a hydrogen atom (k_{TMP} = 0.1 M^{-1} s^{-1}) (Equation 5, Figure 4).[28] This results in suppression of Toc· termination reactions (Equation 4, Figure 2). The end result is an acceleration in rates of lipid peroxidation.[29] This process has been named tocopherol-mediated peroxidation (TMP, Figure 4).[29]

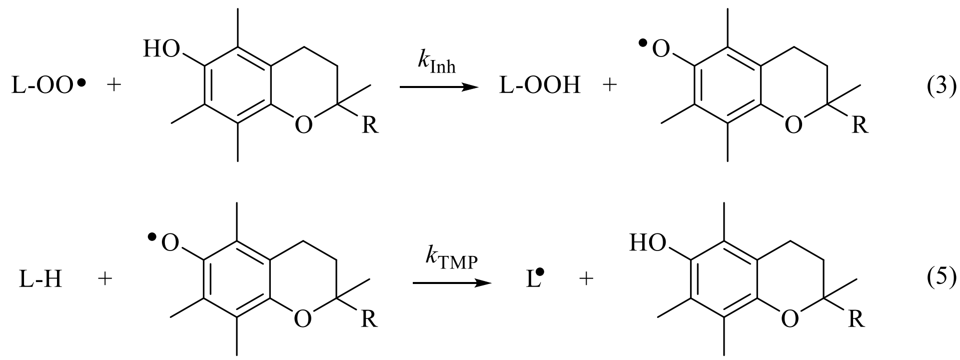

Figure 4. Tocopherol-mediated peroxidation.

As reported in Chapter II of this dissertation, the deuterated polyunsaturated fatty acid 11,11-D_2-linoleic acid (D_2-LA) is 10-fold less reactive than the natural polyunsaturated fatty acid (PUFA) via comparison of their propagation rate constants.[30] The H/D isotope effects measured were outside of the typical range of k_H/k_D (<10) that has been reported for other H/D-atom transfers from hydrocarbons to peroxyl radicals.[31,32,33,34] These findings led to an expanded study of isotope effects in C-H/C-D free radical transfer reactions. Here, we report the results of studies of tocopherol-mediated oxidations of several D-PUFAs which are shown in Figure 5.

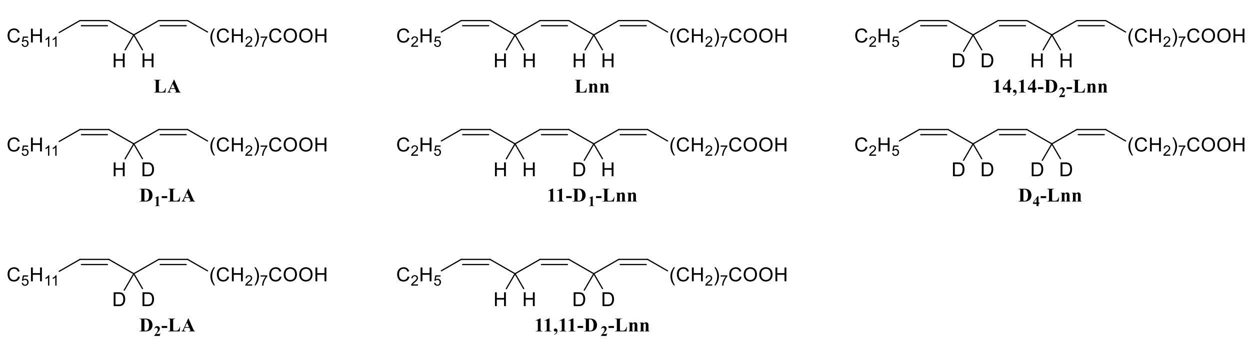

Figure 5. Library of PUFAs and D-PUFAs used for studies of tocopherol-mediated oxidations in solution.

3.2. Results

Linoleic acid (LA), α-linolenic acid (Lnn), and deuterated derivatives of these fatty acids were subjected to azo-initiated free radical oxidations in benzene in the presence of TocH in concentrations of 0.05 to 0.5 M. The fatty acid concentration was 0.64 M, and a 0.1 M stock solution of 2,2'-azobis(4-methoxy-2,4-dimethyl)-valeronitrile (MeOAMVN) in benzene was used to initiate the oxidations (final concentration of 0.005 M) at 37 ˚C. As previously reported, these conditions resulted in a relatively simple mixture of *trans,cis*-conjugated diene products.[35,36,37] Peroxides formed during oxidations were reduced to the corresponding alcohols using PPh_3 prior to analysis. HPLC-UV and HPLC-MS were used to analyze products as previously described.[38,39,30] High resolution mass spectrometry (HRMS) was also used to measure products formed during Lnn/11,11,14,14-D_4-Lnn cooxidations.

Tocopherol-Mediated Oxidations of LA and D_2-LA Mixtures

Cooxidations of LA and D_2-LA were carried out in the presence of 0.5 M TocH. The ratio of LA:D_2-LA was greater than 1:5 in all experiments due to the low reactivity of D_2-LA towards autoxidation.[30] The extent of oxidation after 1 hr was measured to be approximately 2% for LA in the absence of TocH,[40] therefore the concentration of LA (or D_2-LA) will essentially remain constant over the course of an oxidation with TocH in solution. The presence of TocH results in the formation of a simple mixture of 9-*trans,cis*- and 13-*trans,cis*-HODEs which were analyzed by HPLC-MS. A typical chromatogram for these experiments is shown in Figure 6. The k_H/k_D was calculated to be 29.2 ± 2.9 in the presence of 0.5 M TocH and 24.4 ± 2.4 in the presence of 0.05 M TocH.

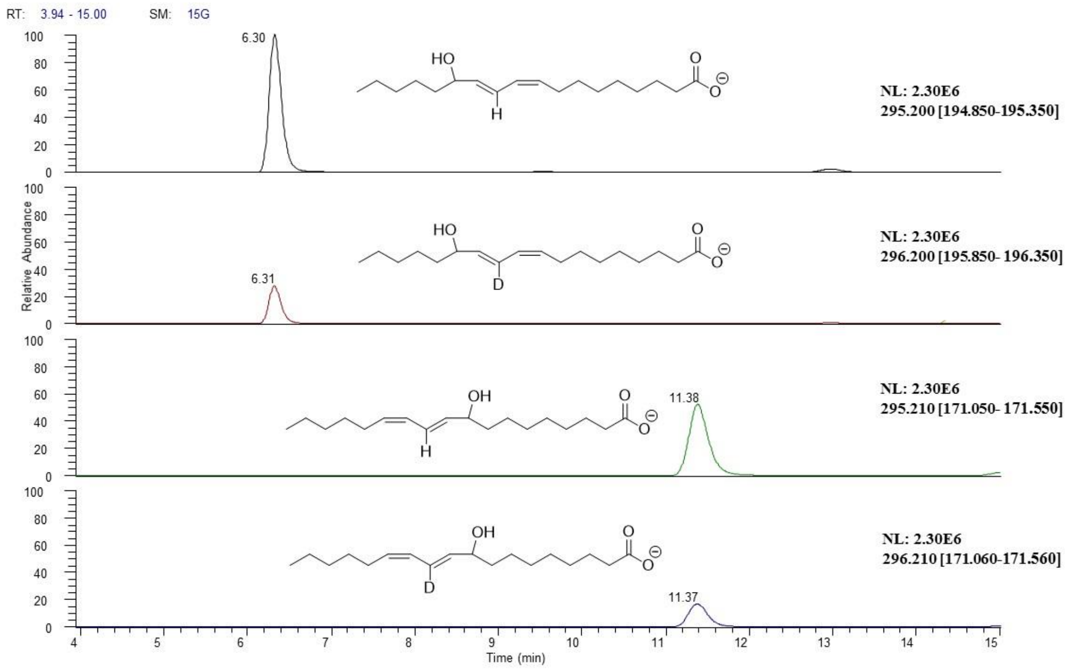

Figure 6. Typical chromatogram for HPLC-MS analysis of the cooxidation of LA and D_2-LA. From top to bottom panel are: 13-*trans,cis*-HODE, 13-*trans,cis*-D_1-HODE, 9-*trans,cis*-HODE, and 9-*trans,cis*-D_1-HODE.

The HODEs from the cooxidation experiments above were also collected by HPLC-UV. High resolution mass spectrometry (HRMS) was completed for each HODE on a Waters Synapt G2 time of flight (TOF) instrument using direct liquid introduction (DLI). Typical mass spectra from these experiments are shown below in Figure 7. The HODEs from LA autoxidation and D_1-HODEs from D_2-LA autoxidation differed in m/z = 1 Da. Using data obtained from these experiments, KIE (k_H/k_D) was calculated to be 23.0 ± 2.3 after correction of the D_1-HODEs for isotopic contribution from HODEs.

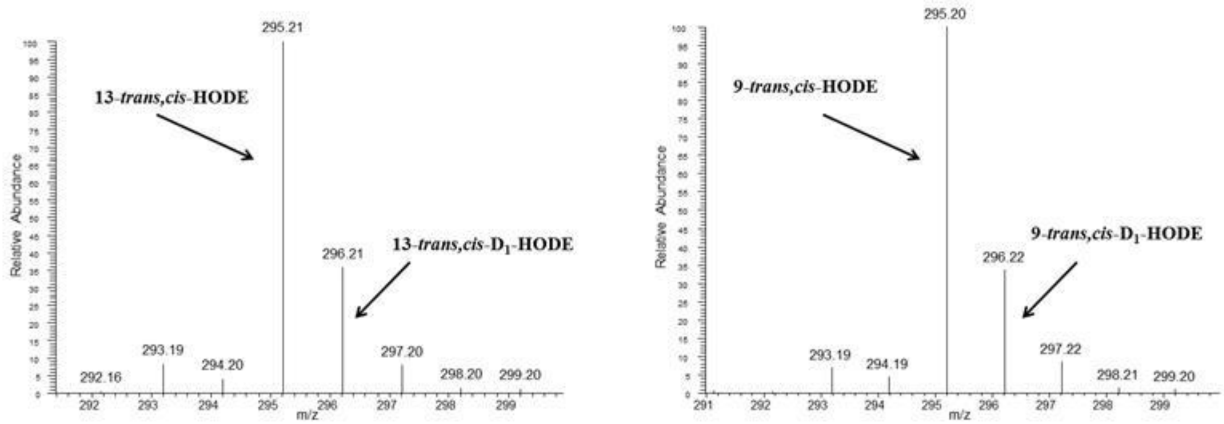

Figure 7. Typical high resolution mass spectra for 13-*trans*,*cis*-HODE and 9-*trans*,*cis*-HODE after HPLC-UV separation and collection. Samples were introduced into the ion source (- APCI) by DLI.

Tocopherol-Mediated Oxidations of D_1-LA

D_1-LA was also oxidized in the presence of 0.5 M TocH. In these experiments the attacking peroxyl or tocopheryl radical will have the option of abstracting either H or D from the reactive *bis*-allylic carbon atom. This results in a product mixture where H-atom abstraction results in products still containing deuterium at the *bis*-allylic center and *vice versa* for D-atom abstraction (Figure 8). HODEs were analyzed using LC-MS. The value of k_H/k_D for this experiment was calculated to be 8.9 ± 0.9. A typical chromatogram for LC-MS analysis of the product mixture is shown in Figure 9.

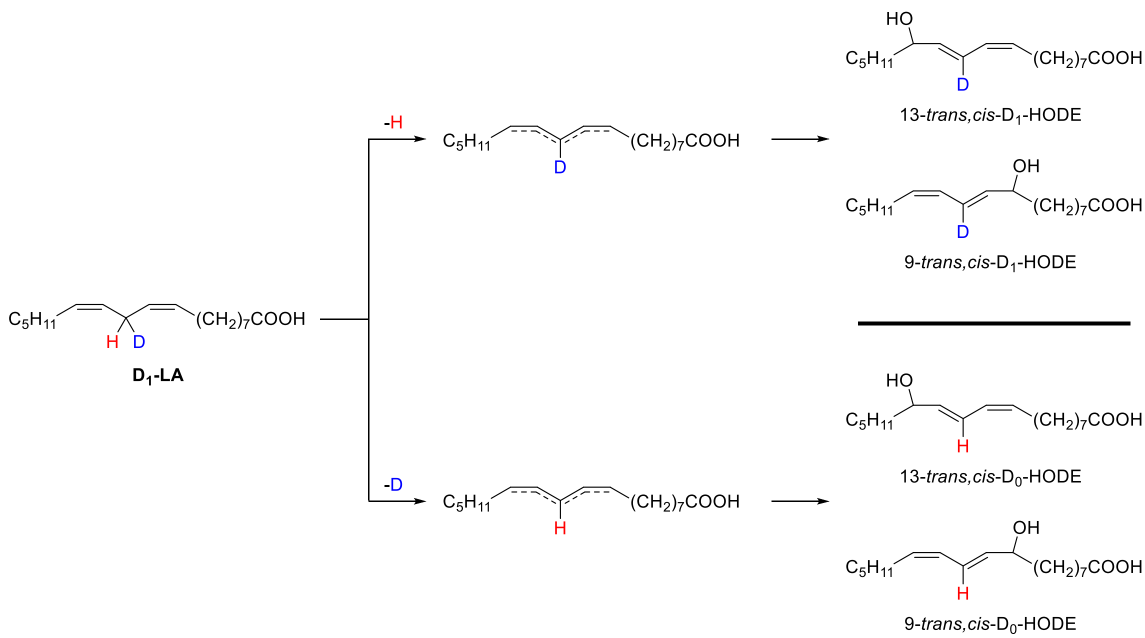

Figure 8. The free radical oxidation of D_1-LA in the presence of TocH results in a simple mixture of *trans*,*cis*-HODEs. H-atom abstraction gives HODEs that still contain deuterium at the *bis*-allylic carbon atom, with the opposite being true for D-atom abstraction.

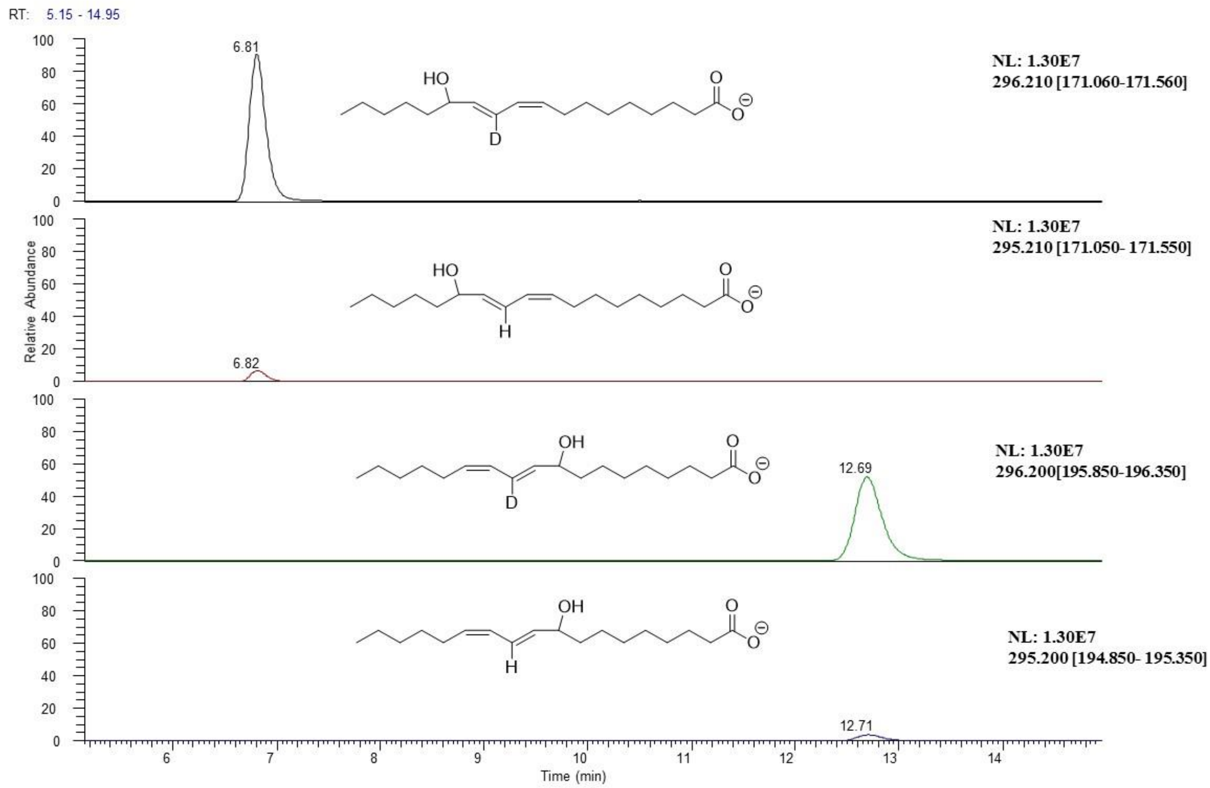

Figure 9. Typical chromatogram from HPLC-MS analysis for oxidations of D_1-LA in the presence of 0.5 M TocH. The top two panels show *trans,cis*-D_1-HODEs from H-atom abstraction. The bottom two panels show *trans,cis*-D_0-HODEs from D-atom abstraction.

Tocopherol-Mediated Oxidations of Lnn and its Deuterated Derivatives

When oxidized in the presence of TocH, Lnn gives four conjugated diene hydroperoxides with -OOH substitution at carbons 9, 12, 13, and 16. Hydrogen atom abstraction from C11 gives the 9- and 13-hydroperoxides. The 13- and 16-hydroperoxides come from hydrogen atom abstraction at C14. Reduction of the product mixture with PPh_3 after oxidation gives the corresponding alcohols (Figure 10).

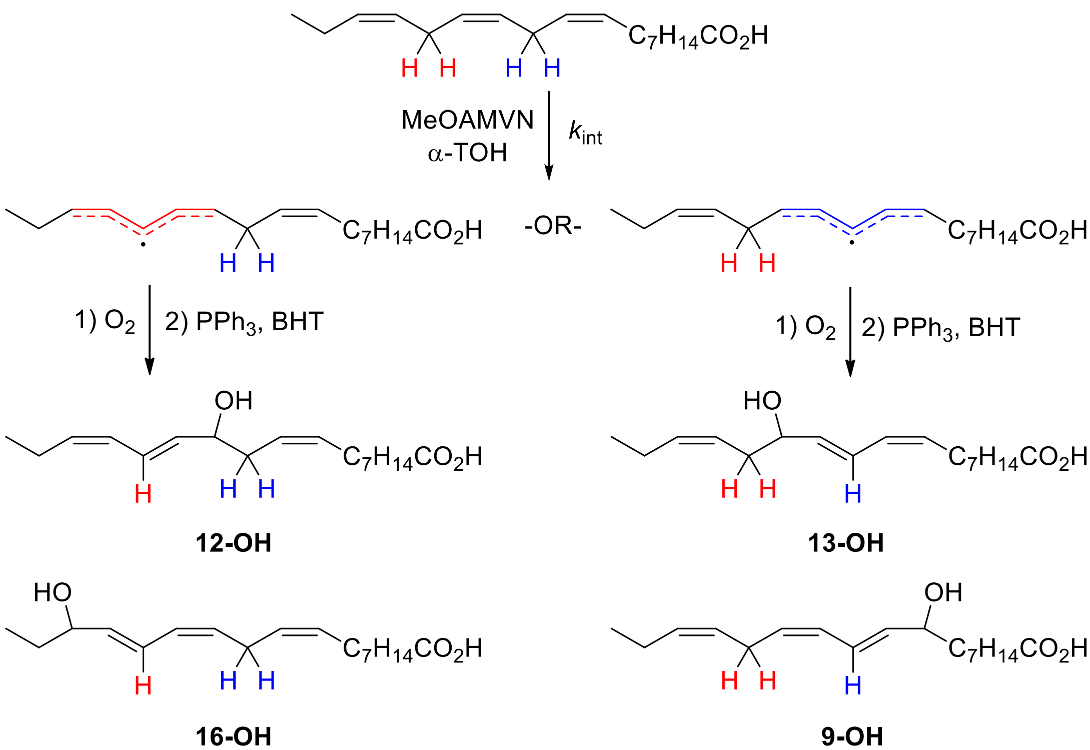

Figure 10. Free radical oxidation of Lnn in the presence of TocH. The products arising from hydrogen atom abstraction at the two bis-allylic methylene groups (C11 and C14) are shown after PPh_3 reduction.

Analysis of these products by HPLC-UV shows a slight preference for H-atom abstraction at C11 over C14 (1.05 to 1.00). This preference was factored in to calculations of k_H/k_D for all of the experiments in this section. A typical HPLC-UV chromatogram of the product mixture are shown in Figure 11.

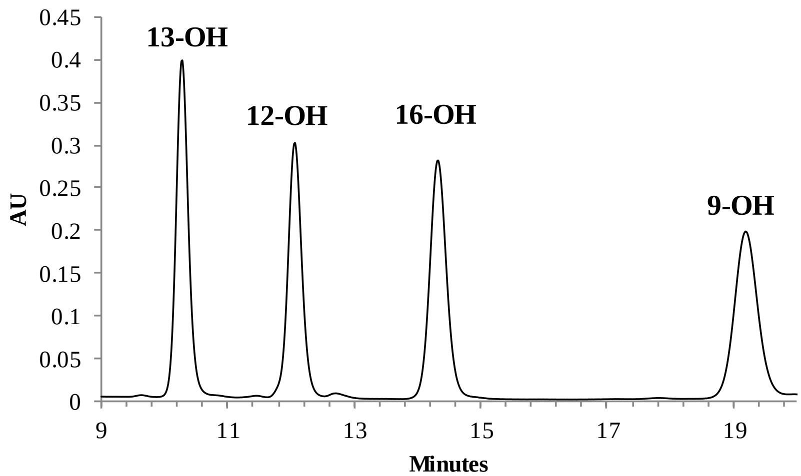

Figure 11. A typical HPLC-UV chromatogram of the product mixture from Lnn oxidations in the presence of TocH after PPh_3 reduction.

Cooxidations of Lnn and D_4-Lnn were carried out in the presence of 0.5 M TocH, with ratios of PUFA to D-PUFA at 1 to 4 respectively. The extent of oxidation was kept below 5% by allowing oxidation to occur for only 1 hr. The four oxidation products were individually collected using the same HPLC-UV conditions described for LA and D_2-LA cooxidations. Samples were then analyzed using a Waters Synapt G2 by DLI. Figure 12 shows typical mass spectra for each of the oxidation products (9-, 12-, 13-, and 16-OH). The D_0- and D_3-products differ by m/z = 3 Da, therefore minimal corrections were needed to account for isotopic overlap. The value of k_H/k_D for these experiments was calculated to be 32.3 ± 3.2. Oxidations were also carried out in the presence of 0.05 M TocH, resulting in a k_H/k_D value of 36.3 ± 3.6.

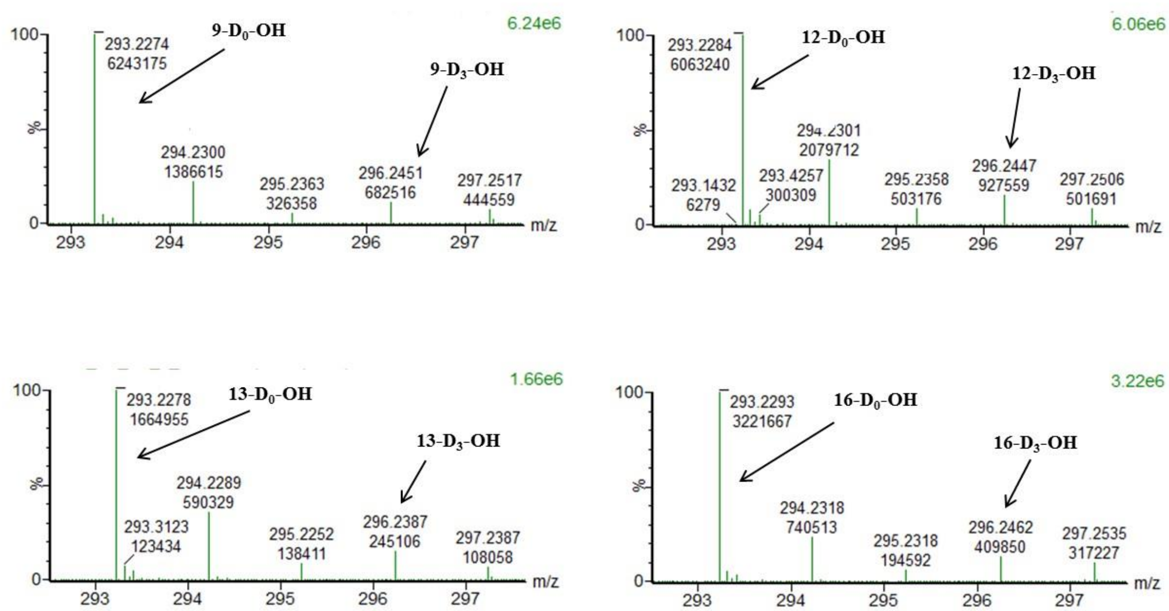

Figure 12. Typical mass spectra acquired by HRMS for the 9-, 12-, 13-, and 16-OH products from Lnn and D_4-Lnn cooxidations.

The selectively deuterated Lnn series (11,11-D_2-Lnn, 14,14-D_2-Lnn, and 11-D_1-Lnn) were oxidized individually in the presence of 0.5 M and 0.05 M TocH. Oxidations were analyzed by HPLC-UV. An overlay of typical chromatograms for each compound oxidized in the presence of 0.5 M TocH is shown in Figure 13. The oxidation of 11,11-D_2-Lnn resulted mainly in products derived from hydrogen atom abstraction at C14. Oxidation of 14,14-D_2-Lnn resulted in products from hydrogen atom abstraction at C11. 11-D_1-Lnn gave products from either hydrogen or deuterium atom abstraction at C11 and hydrogen atom abstraction at C14. Products arising from hydrogen or deuterium abstraction at C11 equaled 47% of the products formed by abstraction of hydrogen at C14. The k_H/k_D for 11,11-D_2-Lnn was calculated to be 36.1 ± 3.6, and 35.9 ± 3.6 for 14,14-D_2-Lnn. The same compounds oxidized in the presence of 0.05 M TocH gave lower k_H/k_D values of 30.9 ± 3.1 for 11,11-D_2-Lnn and 31 ± 3.1 for 14,14-D_2-Lnn.

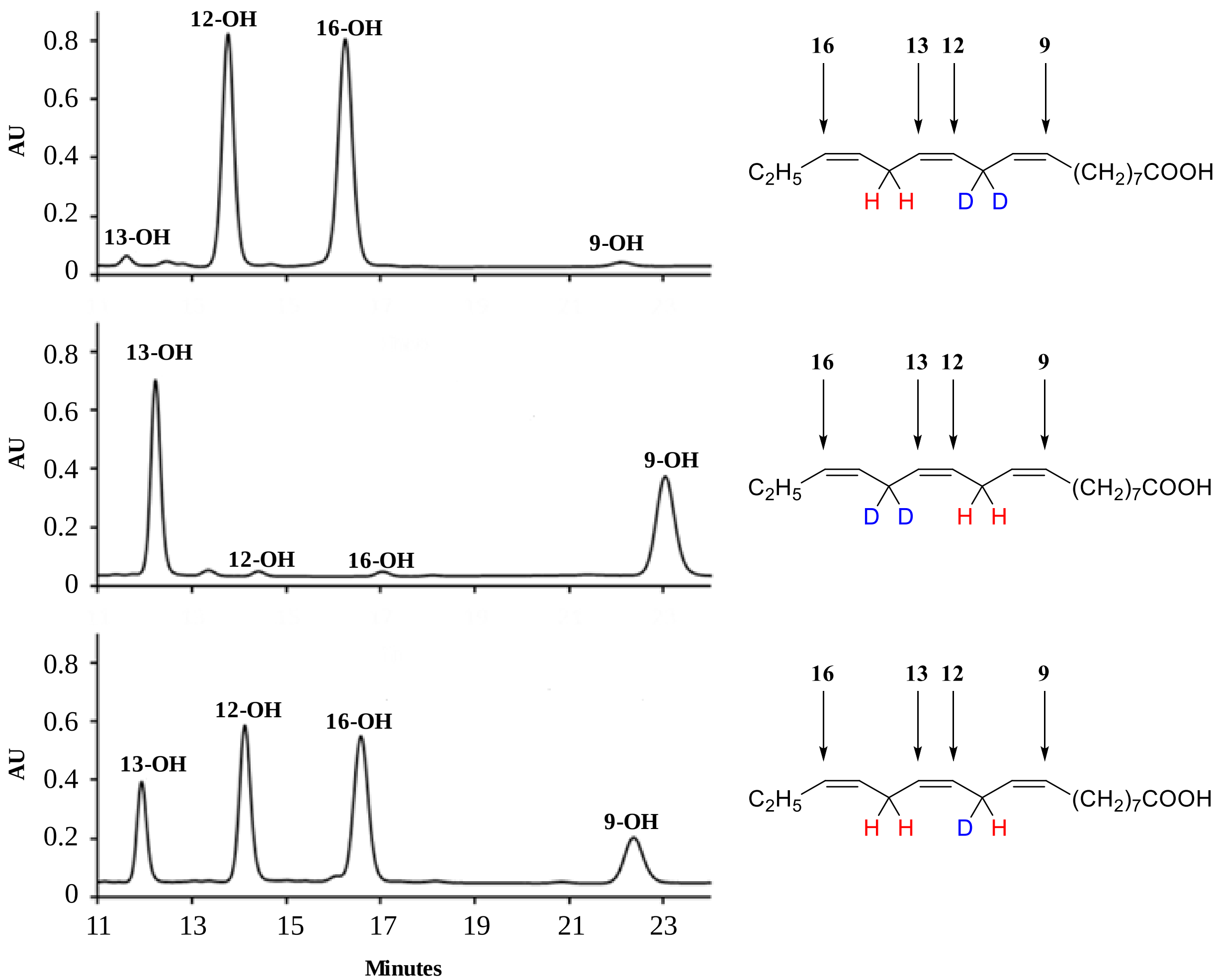

Figure 13. Typical HPLC-UV chromatograms for oxidations of 11,11-D_2-Lnn, 14,14-D_2-Lnn, and 11-D_1-Lnn (top to bottom) in the presence of 0.5 M TocH.

3.3. Discussion

TMP was first discovered while studying LDL oxidation under a steady flux of peroxyl radicals.[25] Bowry and coworkers noted that rates of lipid peroxidation were higher within the LDL particle early on when concentrations of TocH were at their highest, suggesting that TocH was acting in a prooxidant capacity. These results were surprising since TocH is generally recognized as an excellent chain breaking antioxidant.

While the prooxidant activity of TocH was surprising, this behavior is not entirely unexpected for phenolic antioxidants and inhibitors. It has long been understood that unhindered phenols will increase oxidation rates of hydrocarbons. For example, addition of phenol to already oxidizing solutions of cumene results in the acceleration of oxidation rates while the addition of the more hintered 2,6-*tert*-butyl phenol has no influence (Figure 14A). These studies indicated that unhindered phenolic radicals are able to propagate radical reactions. This propagation reaction can interfere with typical termination reactions of phenolic radicals (Figure 14B).[41,42]

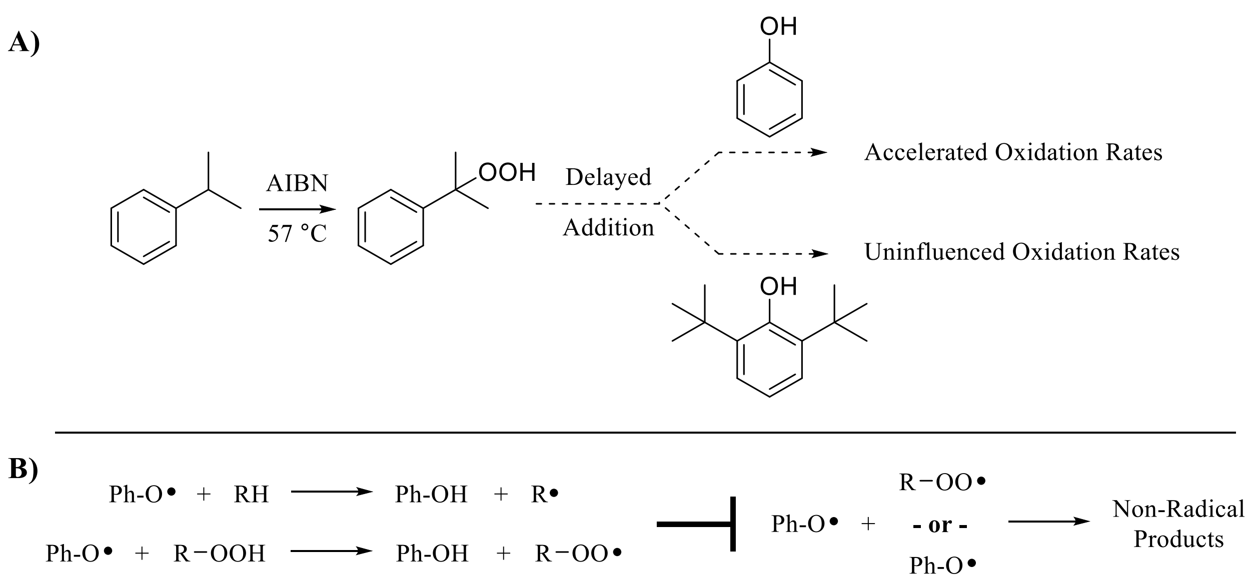

Figure 14. Effects of phenolic antioxidants on rates of oxidation. **A)** Addition of phenol or 2,6-tert-butyl phenol to already autoxidizing solutions of cumene shows that the unhindered phenol accelerates the rate of oxidation. **B)** Propagation by the phenolic radical inhibits typical termination reactions.[40,41]

As discussed in Chapter II, primary deuterium KIEs for H/D atom transfers are less than 10 for hydrocarbons.[31,32,33,34] Previous work has shown that in the absence of any antioxidants, the propagation rate constant for D_2-LA is some 10-fold less than the propagation rate constant of the natural fatty acid, and that KIEs for the H or D atom transfer to a propagating peroxyl radical are as high as 12.8.[30] These results stimulated an expanded study of the D-PUFAs under conditions in which tocopherol mediated peroxidation (TMP) will occur.

Table 1 shows KIEs calculated from the tocopherol-mediated oxidations of a number of D-PUFAs (shown in Figure 5). The KIEs measured under conditions where tocopherol-mediated oxidation predominates[43] were substantially higher than those previously reported in the absence of antioxidants[30] for D-PUFAs containing two or more deuterium atoms. The finding of KIEs (k_H/k_D) greater than 20 for autoxidation in the presence of TocH does not have precedence in the literature. These large KIEs are only observed for geminal H_2/D_2 substitution (i.e. 11,11-D_2-LA vs LA). The KIE observed for D_1-LA (-CHD-) is unexceptional.

	0.5 M TocH	0.05 M TocH	
PUFA	k_H/k_D	k_H/k_D	**Method of Analysis**
11,11-D_2-Lnn	36.1 ± 3.6	30.9 ± 3.1	**HPLC-UV**
14,14-D_2-Lnn	35.9 ± 3.6	31.0 ± 3.1	**HPLC-UV**
Lnn/11,11,14,14-D_4-Lnn Cooxidation	32.3 ± 3.2	36.3 ± 3.6	**DLI-HRMS**
LA/11,11-D_2-LA Cooxidation	29.2 ± 2.9	24.4 ± 2.4	**LCMS**
LA/11,11-D_2-LA Cooxidation	23.0 ± 2.3	NA	**DLI-HRMS**
11-D_1-LA	8.9 ± 0.9	NA	**LCMS**

Table 1. List of KIEs ± 10% variance, along with the method of analysis.

For both 11,11-D_2-Lnn and 14,14-D_2-Lnn, intermolecular competition between H and D-atom abstraction was set up between CH_2 and CD_2 *bis*-allylic methylene groups. Both compounds were oxidized in the presence of TocH at low (0.05 M) or high (0.5 M) concentrations and k_H/k_D was determined at each TocH concentration by comparison of products arising from H- or D-atom abstraction (Figure 15).

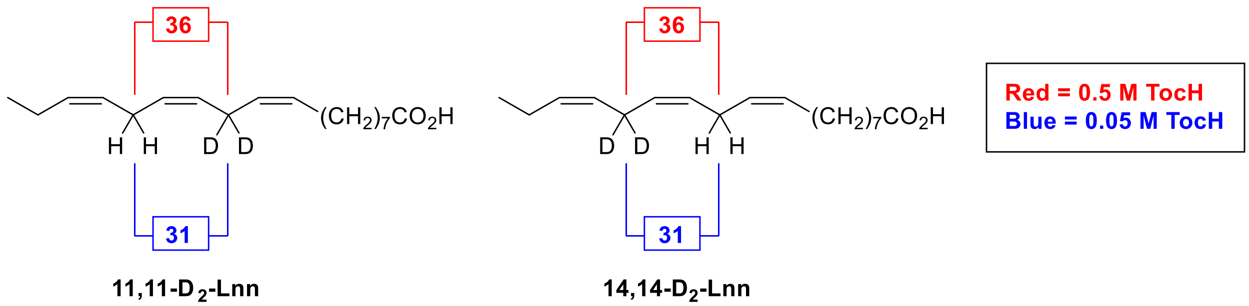

Figure 15. Values calculated for k_H/k_D for both 11,11-D_2-Lnn and 14,14-D_2-Lnn at low and high concentrations of TocH.

The k_H/k_D values calculated for both 11,11-D_2-Lnn and 14,14-D_2-Lnn were notably larger at the higher concentrations of TocH. Previous work by Bowry and Stocker noted that when TocH concentrations are high the tocopheryl radical is the main propagating species. This occurs despite the slow rate of H-atom abstraction by the tocopheryl radical (k_{TMP}) because termination reactions of Toc· (k_{Term}) are suppressed by the Toc· forming reaction (k_{inh}). As the concentration of TocH decreases the peroxyl radical begins to play a larger role in propagation and normal termination reactions of Toc· occur (Figure 16).[29] Propagation by peroxyl radicals results in lower k_H/k_D values for D-PUFAs in the absence of antioxidants,[40] suggesting that the decrease in KIE at lower TocH concentrations is due to participation by this species.

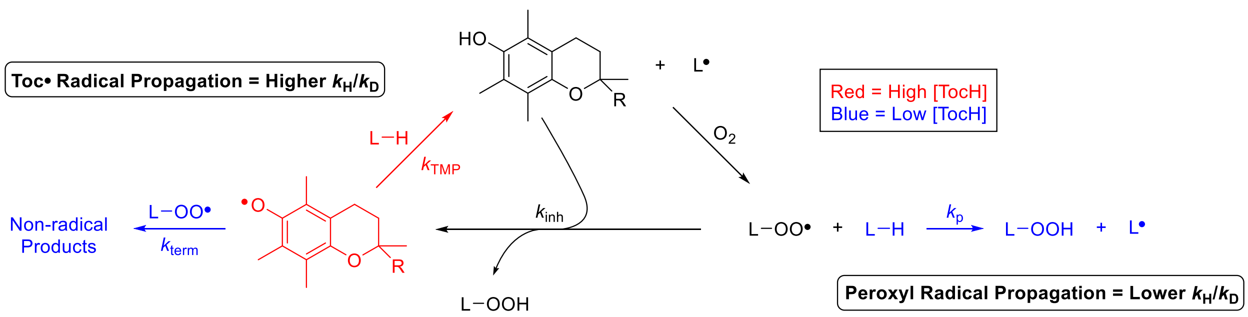

Figure 16. Free radical oxidation of PUFAs at low (blue) and high (red) concentrations of TocH, and the relationship to k_H/k_D values.

Cooxidations of Lnn/D_4-Lnn and LA/D_2-LA gave similarly high k_H/k_D values (Figure 17). Products from the Lnn and D_4-Lnn cooxidations were collected individually by HPLC-UV and analyzed using HRMS. The products from Lnn versus D_4-Lnn oxidation differed by m/z = 3 Da, so values for k_H/k_D needed minimal corrections for isotopic overlap. Cooxidations of LA and D_2-LA analyzed by LCMS also showed decreased k_H/k_D values at lower TocH concentrations (Figure 17).

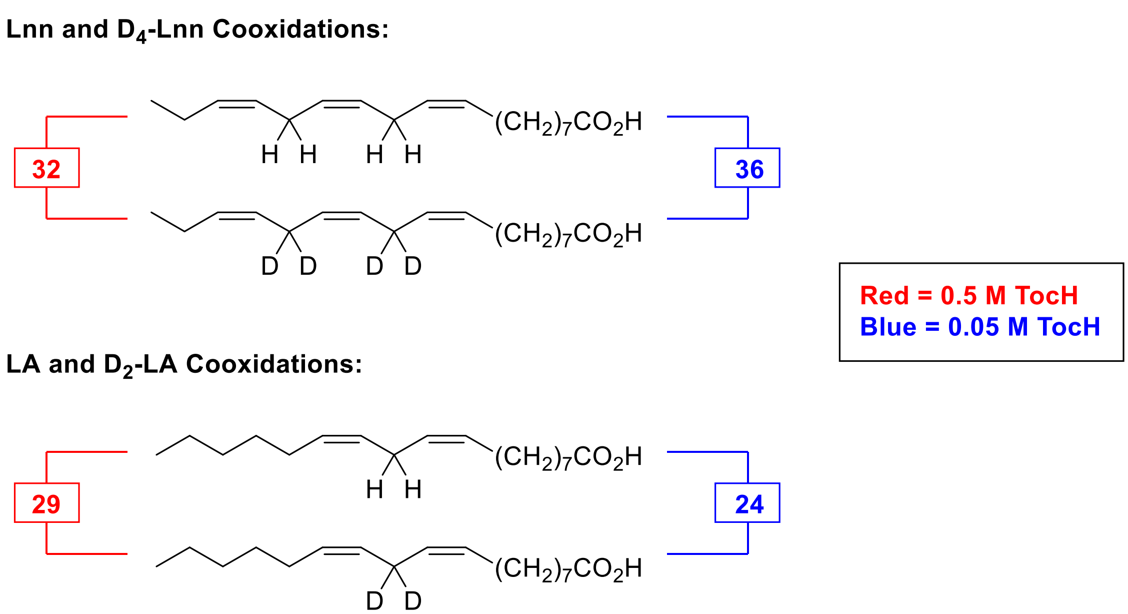

Figure 17. k_H/k_D values calculated for cooxidations of Lnn/D_4-Lnn and LA/D_2-LA cooxidations at high (red) and low (blue) concentrations of TocH.

Mono-deuterated 11-D_1-Lnn and D_1-LA were also oxidized in the presence of 0.5 M TocH. HPLC-UV analysis of 11-D_1-Lnn oxidations showed that products arising from H- or D-atom abstraction at C-11 were equal to 47% of the products formed from abstraction of either H-atom at C-14 (Figure 18). This suggests that no secondary isotope effects are present. Products from D_1-LA were analyzed by LCMS and k_H/k_D was calculated to be 8.9 (Figure 18). This significantly decreased KIE suggests that geminal substitution of D and H (-CHD-) does not offer the same resistance towards H- or D-atom abstraction as *bis*-allylic carbons substituted with two D-atoms (-CD_2-).

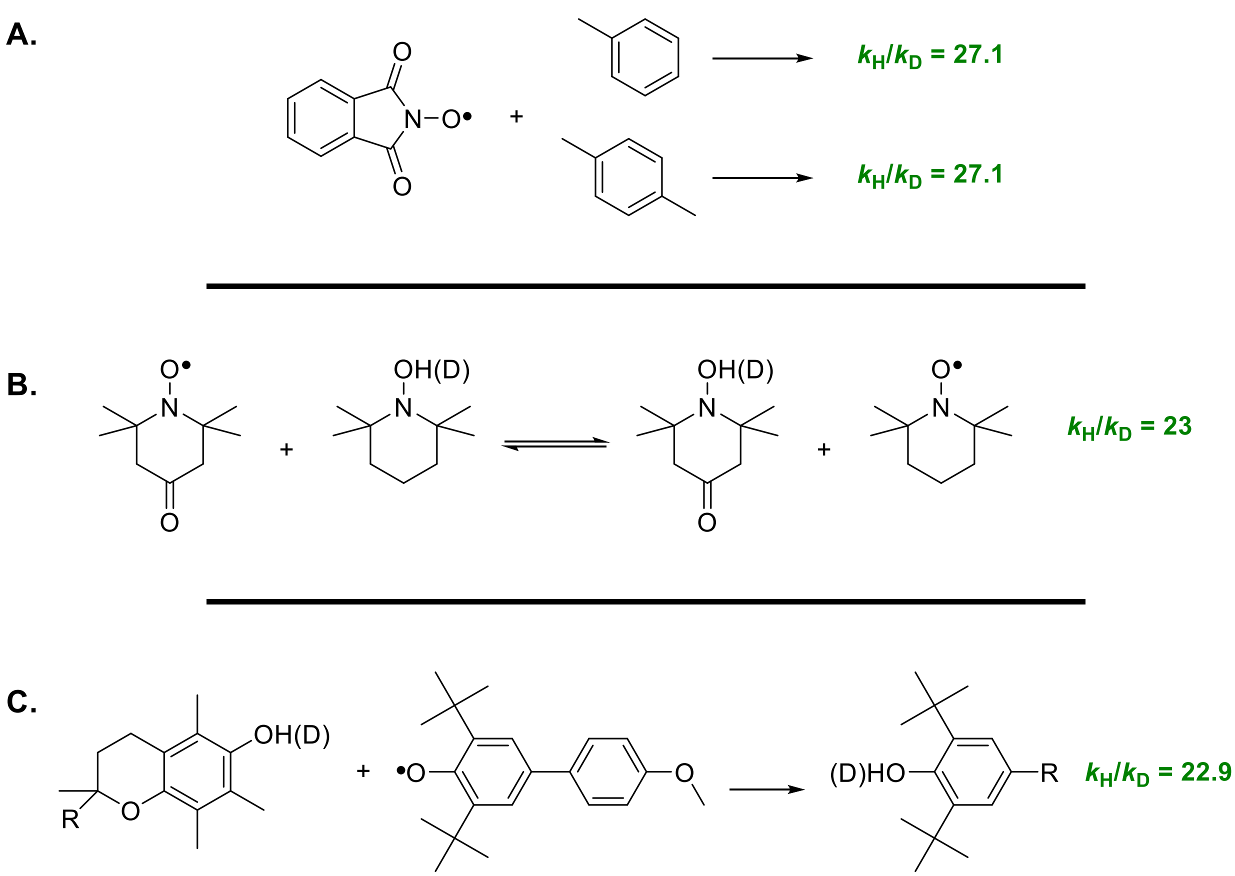

Figure 18. Large KIEs calculated for H or D atom transfer to other stabilized oxygen-centered radicals. **A.** H(D) atom transfer from hydrocarbons to phthalimide N-oxyl radicals[44-46]; **B.** KIE for H(D) atom transfer from hydroxyl amines to nitroxides[47]; **C.** H(D) atom transfer from tocopherol to oxygen centered radicals such as 2,6-di-*tert*-butyl-4-(4'-methoxyphenyl)phenoxyl.[48]

Although the high KIEs reported here are unprecedented for PUFA autoxidation, previous studies of KIEs have reported k_H/k_D values in excess of 10 in the presence a stabilized oxygen-centered radical. For instance, KIEs of 27 have been reported for H or D atom transfers from carbon to phthalimide *N*-oxyl radicals, shown below in Figure 18A.[44,45,46] Other large KIEs (k_H/k_D = 20-25) have been reported for the self-exchange of H or D from hydroxylamines to nitroxides (Figure 18B).[47] Mukai and coworkers carried out exhaustive studies of reactions in which the tocopheryl radical is involved and found similarly high KIEs for hydrogen atom transfer from TocH (k_{inh}) to oxygen centered radicals (k_H/k_D = 22.9) as shown in Figure 18C.[48] These studies suggest that hydrogen atom tunneling is important in the process of H or D atom transfer to oxygen-centered radicals.

The results reported in this chapter are of interest not only because of the high KIEs measured, but also because tocopherol-mediated peroxidation (TMP) has been suggested to play an important role in the oxidative modification of human LDL.[49,50,51] It is hypothesized that the LDL particle provides an excellent setting for this type of oxidation to occur due to its size and composition.[29] The following arguments describe how TMP is able to oxidatively modify LDL:[29]

1) Only one radical at a time may persist in an LDL particle for longer time intervals.
2) Lipophilic radicals formed in LDL (i.e. tocopheryl radical) cannot diffuse freely between particles.
3) LDL particles are struck by aqueous peroxyl radicals at a very low rate (10^{-3} s^{-1}, or roughly 1 strike every 17 minutes).
4) Despite the slow rate for k_{TMP} (0.1 M^{-1} s^{-1}), the TMP reaction could occur around 100 times over the peroxyl radical strike intervals.

There is substantial evidence in the literature to suggest that these arguments are indeed a plausible description of how TMP occurs within the LDL particle. The tocopheryl radical has been observed by electron paramagnetic resonance (EPR) spectroscopy in peroxidizing LDL.[52] Other experiments have revealed that the tocopheryl radical does not rapidly escape lipid particles such as liposomes,[53] membrane fragments,[53,54] and micelles[55,56] in aqueous dispersions. These studies as a whole suggest that the tocopheryl radical persists (on EPR time scales) within the LDL particle, and is able to propagate free radical chain oxidation of PUFAs once antioxidant activity has been exhausted.

The effect of isotopic substitution on the rate of tocopherol-mediated oxidations of linoleate and linolenate suggest that hydrogen atom tunneling plays a significant role in the particularly high KIEs reported here.[43] Therefore, it may also play an important role in the oxidative modification of LDL when TMP is occuring. The kinetics of TMP have been the subject of numerous publications, and the involvment of TocH in the oxidative modification of LDL has been a hotly debated topic.[50,51,57] The results presented in this chapter by no means settle the score on the ultimate function of TocH within the LDL particle. However, they do provide an important look into how TocH is able to act as a prooxidant under certain circumstances as opposed to a chain-breaking antioxidant.

3.4. Acknowledgements

Many thanks to Dr. John McLean for the gracious use of his mass spectrometers and laboratory space, as well as Dr. Rafael Montenegro for his help and guidance in experimental procedures. We are also greatful to Misha Shchepinov and Retrotope, Inc. for providing D-PUFA analogs and helpful discussions.

3.5. Experimental

General Methods and Materials:

Deuterium reinforced PUFAs were synthesized as described previously. The synthesis of novel deuterated PUFAs are described below. All other PUFAs were purchased from Nu-Chek, Prep. MeOAMVN was purchased from Wako Chemicals. α-Tocopherol (α-Toc) was purchased from Sigma-Aldrich Co. and purified by flash column chromatography (10% ethyl acetate in hexanes). All HPLC solvents were purchased from Sigma-Aldrich Co.

HPLC analyses were carried out with a Waters 717plus Autosampler coupled to a Waters 1525 Binary HPLC Pump, both of which were interfaced to a Waters 2996 Photodiode Array Detector. Mass spectrometry was carried out on a Thermo Scientific TSQ Quantum Ultra Triple Stage Quadrupole mass spectrometer. Atmospheric-pressure chemical ionization in negative mode was used for the ionization of PUFAs and their oxidation products. Samples were introduced by direct liquid infusion (DLI) and monitored by full-scan in order to minimize any isotope effects which may occur during ionization and fragmentation of oxidation products.[58]

For oxidations where the products differ by 1 m/z (e.g. D1-LA oxidations and D0/D2-LA co-oxidations), analyses of products containing one deuterium had to be corrected for normal isotope contribution from D0-products. This was done by subtracting 13.1% of the value of the integrated D0 product peak from the peak area of the D1 product peak. This isotopic distribution was determined by injections of a standard mixture of D0-LA oxidation products.

High resolution mass spectrometry isotope ratio analysis:

For isotope ratio analysis it is crucial to have unbiased sensitivity for isotopic labeled molecules. Also, integration functions capable of calculating peak areas are needed in order to compare the abundance (concentrations) of these molecules.

A Synapt G2 equipped with MassLynx (Waters, Milford, MA) was used to analyze H4/D4-αLn cooxidations. Three functions are available to obtain integration values for peaks of interest depending on the instrumentation used: Integrate (predominately for quadrupole mass analyzers), Center (for TDC data) and Automatic Peak Detection (for ADC data). Data was collected utilizing a combination of all three approaches thus a comparison of the three strategies is warranted. All three functions were used to calculate the KIE values for the H0/D4-αLn Cooxidation. They provided the results shown in Figure S1 and are summarized in Table 1, where the results do not vary significantly from function to function and all fall within a 10 % variance. Using a 1-sample t-test with a hypothesis mean of 32.9 no significant difference between these three K_{IE} values is found (p-value of 0.968 with $\alpha = 0.05$).

The data in the Synapt G2 was acquired with DLI (15 µL/min) (11 Plus, Harvard Apparatus, Holliston, MA) in negative ion mode with an ESI source (T 80º C and capillary voltage of 2.7kV).

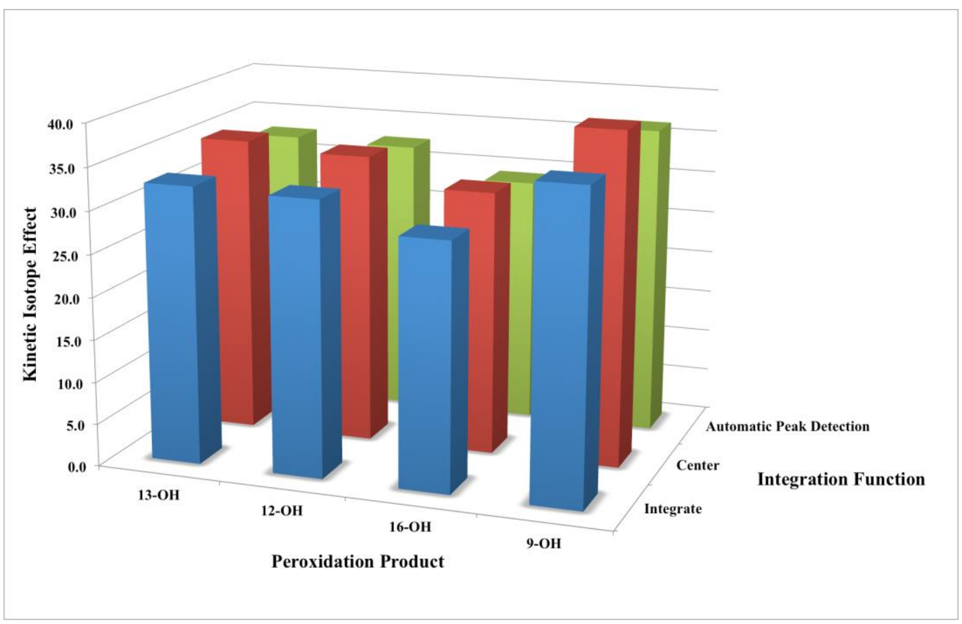

Figure 8. k_H/k_D for Lnn oxidation products using three different integration functions for HRMS data.

Function	Average K_{IE}	Standard Deviation	Percent Error
Integrate	**32.1**	**1.7**	**5.3**
Center	**34.4**	**3.1**	**8.9**
Automatic Peak Detection	**32.3**	**1.8**	**5.5**

Table 2. Average k_H/k_D, standard deviation, and percent error for the three integration functions.

IR spectra were recorded with Vertex 70 spectrometer. ^{1}H and ^{13}C NMR spectra were obtained with a Bruker AC 400 instrument at 400 and 100 MHz respectively, in $CDCl_3$ (TMS at $\delta = 0.00$ or $CHCl_3$ at $\delta = 7.26$ for ^{1}H and $CHCl_3$ at $\delta = 77.0$ for ^{13}C as an internal standard).

General Oxidation Procedure:

All PUFAs were purified by flash column chromatography (10 % EtOAc in hexanes to 20 % EtOAc in hexanes) and dried for 2 to 3 hours under vacuum before use. Stock solutions of 2,2'-azobis(4-methoxy-2,4-dimethyl)-valeronitrile (MeOAMVN, 0.1 M) and α-Toc (1.0 M) were prepared in benzene. For all experiments, reagents were added in the order of: (1) benzene, (2) PUFA, (3) α-Toc (if appropriate), (4) MeOAMVN. Reaction vials were vortexed for 5 s and heated at 37 °C for 1 h. Each reaction was quenched by the addition of 25 µL of both 0.5 M butylated hydroxytoluene (BHT) and 0.5 M PPh_3. All experiments were carried out in triplicate. Additionally, t=0 samples were prepared by dispensing purified PUFA into a vial and quenching via procedure outlined above without being oxidized, done concurrently with the corresponding experiment.

HPLC Separations:

Oxidation products of PUFAs (as the free acid) were separated by HPLC-UV (250 x 4.6 mm silica column; 5 µm; elution solvent, 1.4 % isopropanol, 0.1 % acetic acid in hexanes; 1.0 ml/min; monitoring wavelength, 234 nm). For samples where mass spectrometry was used, oxidation products were collected using HPLC-UV (same conditions as above) into vials contianing BHT. Collected products were introduced to the ion source (- APCI) by direct liquid introduction (DLI) using the same solvent conditions listed above.

Oxidation products of PUFA methyl esters were separated by HPLC-UV (250 x 4.6 mm silica column; 5 µm; elution solvent, 0.5 % isopropanol in hexanes; 1.0 ml/min; monitoring wavelength, 234 nm).

Synthesis of 11-D₁-linolenic acid

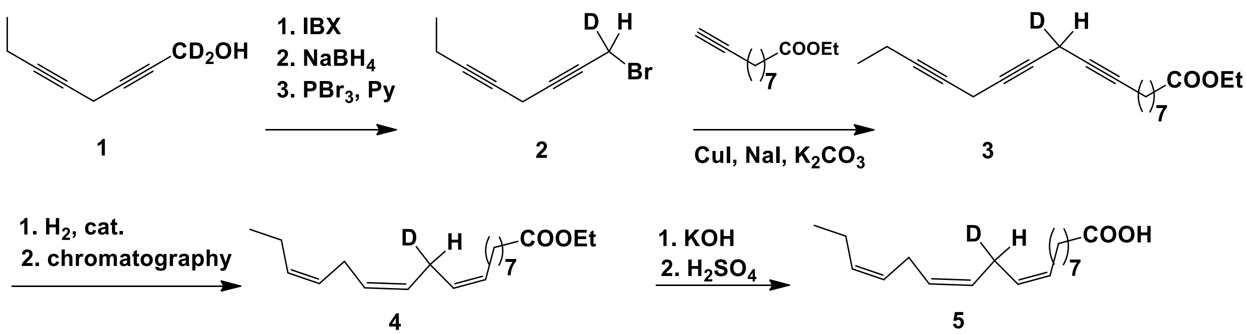

Figure 20. Synthetic route to 11-D_1-linolenic acid (11-D_1-Lnn).

1-Deutero-1-bromo-octa-2,5-diyne (**2**) 2-Iodoxybenzoic acid (IBX, 35.0 g) was added in one portion to a solution of 1,1-dideuteroocta-2,5-diyn-1-ol (**1**) [1] (5.50 g) in ethyl acetate (400 ml) (1,2-dichloroethane can be applied alternatively). The reaction mixture was stirred with simultaneous heating under reflux for 15 h until disappearance of (**1**) (TLC control). The reaction mixture was diluted with pentane (300 ml) and kept at 0^{o}C for 3 h. The reaction mixture was filtered, and precipitate additionally washed with pentane. Methanol (20 ml) was added to the filtrate followed by $NaBH_4$ (0.60 g). After stirring for 15 min (TLC control) the reaction mixture was washed with brine (50 ml). The organic layer was dried over Na_2SO_4 and solvent was gently removed under reduced pressure. The residue was purified by flash column (*n*-pentane/diethyl ether 10:1) to yield 1-deuteroocta-2,5-diyn-1-ol (3.02 g, 55 %). IR (CCl_4): $\tilde{\nu}$ = 3622 cm^{-1}. ^1H NMR ($CDCl_3$, δ): 4.25 (m, 1H, CHD), 3.19 (m, 2H, CH_2), 2.16 (m, 2H, CH_2), 1.63 (br. s., 1H, OH), 1.09 (t, J = 7.5 Hz, 3H, CH_3). ^{13}C NMR ($CDCl_3$, δ): 82.3, 80.6, 78.2, 72.7, 51.0 (t, J = 23 Hz), 13.7, 12.2, 9.7.

To a solution of 1-deuteroocta-2,5-diyn-1-ol (3.00 g, 24.2 mmol) and pyridine (0.15 ml) in dry diethyl ether (15 ml), a solution of PBr_3 (0.8 ml, 8.5 mmol) in diethyl ether (3 ml) was added dropwise with stirring over 10 min at -15°C under argon. The reaction mixture was allowed to gradually warm up to r.t. and then refluxed for 3.5 h with stirring. The reaction mixture was then cooled down to -10°C and 10 ml of cold water was added. When the residue dissolved, saturated NaCl (10 ml) and pentane (25 ml) were added, and the organic layer was separated. The aqueous fraction was washed with pentane (2 x 10 ml), and the combined organic fractions were washed with saturated $NaHCO_3$ (5 ml), saturated NaCl (5 ml) and dried over Na_2SO_4 in the presence of traces of hydroquinone. The solvent was removed under reduced pressure. The residue was dissolved in pentane and filtered through silica gel (10 ml). Removal of the solvent gave the product (3.21 g, 71 %, 39 % starting from 1,1-dideuteroocta-2,5-diyn-1-ol (**1**)). IR (CCl_4): $\tilde{\nu}$ = 2255 cm^{-1}. ^1H NMR ($CDCl_3$, δ): 3.90 (m, 1H, CHD), 3.21 (q, J = 2.3 Hz, 2H, CH_2), 2.16 (m, 2H, CH_2), 1.12 (t, J = 7.5 Hz, 3H, CH_3). ^{13}C NMR ($CDCl_3$, δ): 82.6, 81.9, 75.2, 72.0, 14.8 (t, J = 24 Hz), 13.7, 12.3, 9.8.

11-Deuterooctadeca-9,12,15-triynoic acid ethyl ester (**3**) was synthesized as described for the synthesis of 11,11-dideuterooctadeca-8,12,15-triynoic acid methyl ester [1, 2]. CuI (6.40 g) was quickly added to 15 ml of stirred DMF (freshly distilled over CaH_2), followed by dry NaI (5.10 g) and K_2CO_3 (7.20 g). Dec-9-ynoic acid ethyl ester (3.10 g) was then added in one portion, followed by bromide (**2**) (3.20 g). Additional 10 ml of DMF was used to rinse the reagents off the flask walls into the bulk of reaction mixture, which was then stirred for 16 h at r.t. Saturated aqueous NH_4Cl (25 ml) was then added with stirring, followed in a few minutes by saturated aqueous NaCl (15 ml) and then by a 5:1 mixture of hexane : ethyl acetate (30 ml). The mixture was further stirred for 15 min and then filtered through a fine mesh Schott glass filter. The residue was washed with hexane : ethyl acetate mixture several times. The organic fraction was separated, and the aqueous phase was additionally extracted with hexane (3 x 20 ml). The combined organic fractions were dried (Na_2SO_4), traces of hydroquinone were added, and the solvent was evaporated under reduced pressure. The residue was purified by flash column (hexane/ethyl acetate 25:1) to give compound **3** (4.53 g, 95 %) of the title compound. ^{1}H NMR ($CDCl_3$, δ): 4.11 (q, J = 7.2 Hz, 2H, OCH_2), 3.12 (m, 3H, CH_2 and CHD), 2.28 (t, J = 7.5 Hz, 2H, CH_2CO), 2.15 (m, 4H, CH_2), 1.61 (m, 2H, CH_2), 1.48 (m, 2H, CH_2), 1.31 (m, 6H, CH_2), 1.24 (t, J = 7.2 Hz, 3H, CH_3), 1.11 (t, J = 7.4 Hz, 3H, CH_3).

11-Deutero-cis,cis,cis-octadeca-9,12,15-trienoic acid ethyl ester (**4**) was synthesized as described for the synthesis of 11,11-dideutero-*cis,cis,cis*-octadeca-9,12,15-trienoic acid methyl ester [1, 2]. A suspension of nickel acetate tetrahydrate (1.87 g) in 96 % EtOH (25 ml) was heated with stirring to approx. 60 - 70°C until the salt dissolved. The flask was flushed with hydrogen, and then 7.7 ml of $NaBH_4$ solution (prepared by a 15 min stirring of $NaBH_4$ suspension (0.43 g) in EtOH (10 ml) followed by filtering) was added dropwise over 5-10 min with stirring. In 5 min ethylenediamine (2.3 ml) was added in one portion, followed in 5 min by an addition of (**3**) (4.50 g) in EtOH (15 ml). The reaction mixture was vigorously stirred under hydrogen (1 atm). The absorption of hydrogen stopped in about 2 h. To the reaction mixture, 70 ml of hexane and 3.3 ml of acetic acid were added, followed by water (6 ml) and the mixture was allowed to separate. Aqueous fractions were extracted by 5:1 mixture of hexane : ethyl acetate. The completion of extraction was monitored by TLC. The combined organic fractions were washed with diluted solution of HCl, followed by saturated NaCl and saturated $NaHCO_3$, and then dried over Na_2SO_4. The solvent was removed at reduced pressure. Silica gel (Silica gel 60, Merck; 162 g) was added to a solution of silver nitrate (43 g) in anhydrous MeCN (360 ml), and the solvent removed on a rotavap. The obtained impregnated silica gel was dried for 3 h at 50°C (aspiration pump) and then 8 h on an oil pump. 30 g of this silica was used per gram of product. The reaction mixture was dissolved in a small volume of hexane and applied to the silver-modified silica gel, eluted with gradient of hexane: ether (from 50:1 to 20:1). When the non-polar contaminants were washed off (control by $AgNO_3$-impregnated TLC), the product was eluted with ether and the solvent evaporated under reduced pressure to give ester **4** (1.91 g, 42 %). IR (CCl_4): $\tilde{\nu}$ = 1740 cm^{-1}. ^1H NMR ($CDCl_3$, δ): 5.36 (m, 6H, CH-double bonds), 4.12 (q, 2H, J = 7.2 Hz, OCH_2), 2.81 (m, 3H, CH_2 and CHD), 2.28 (t, J = 7.5 Hz, 2H, CH_2CO), 2.06 (m 4H, CH_2), 1.59 (m, 2H, CH_2), 1.30 (m, 8H, CH_2), 1.25 (t, J = 7.2 Hz, 3H, CH_3), 0.97 (t, J = 7.5 Hz, 3H, CH_3). ^{13}C NMR ($CDCl_3$, δ): 173.9, 131.9, 130.3, 128.3, 128.2, 127.6, 127.1, 60.1, 34.4, 29.5, 29.1, 29.08, 29.06, 27.2, 25.5, 25.3 (t, J = 19.5 Hz), 24.9, 20.5, 14.25, 14.23.

11-Deutero-cis,cis,cis-octadeca-9,12,15-trienoic acid (**5**) To a solution of (**4**) (1.20 g, 3.9 mmol) in ethanol (8 ml), a solution of KOH (1.10 g, 19.6 mmol) in water (2.5 ml) was added in one portion. The reaction mixture was stirred at 40-50 °C for 15 min (control by TLC) and then diluted with water (20 ml). Diluted sulfuric acid was added to pH 2, followed by diethyl ether (15 ml) and hexane (15 ml). The organic layer was separated and the aqueous layer washed with diethyl ether/hexane mixture (3 x 10 ml). The combined organic fractions were washed with saturated aqueous NaCl and then dried over Na_2SO_4. The solvent was removed under reduced pressure and the residue was filtered through silica gel (2 ml, eluent: ethyl acetate/hexane 1:1). Evaporation of the solvent gave compound **5** (1.08 g, 98 %). HRMS (ESI-QTOF) *m/z*: $[M-H]^-$ Calcd for

$C_{18}H_{29}DO_2$ 278.2230; Found 278.2227. IR (CCl_4): $\tilde{\nu}$ = 1741, 1711 cm^{-1}. ^1H NMR ($CDCl_3$, δ): 11.4 (br. s., 1 H, COOH), 5.36 (m, 6H, CH-double bonds), 2.81 (m, 3H, CH_2 and CHD), 2.35 (t, J = 7.5 Hz, 2H, CH_2), 2.06 (m, 4H, CH_2), 1.63 (m, 2H, CH_2), 1.31 (m, 8H, CH_2), 0.97 (t, J = 7.5 Hz, 3H, CH_3). ^{13}C NMR ($CDCl_3$, δ): 180.3, 131.9, 130.2, 128.3, 128.1, 127.7, 127.1, 34.0, 29.5, 29.1, 29.04, 28.99, 27.2, 25.5, 25.3 (t, J = 19.5 Hz), 24.6, 20.5, 14.2.

3.6. References

1. Palinski, W.; Rosenfeld, M. E.; Ylä-Herttuala, S.; Gurtner, G. C.; Socher, S. S.; Butler, S. W.; Parthasarathy, S.; Carew, T. E.; Steinberg, D.; Witztum, J. L., Low density lipoprotein undergoes oxidative modification in vivo. *Proc. Natl. Acad. Sci. U.S.A.* **1989,** *86*, 1372-1376.

2. Steinbrecher, U. P.; Zhang, H. F.; Lougheed, M., Role of oxidatively modified LDL in atherosclerosis. *Free Radic. Biol. Med.* **1990,** *9*, 155-168.

3. Salonen, J. T.; Ylaherttuala, S.; Yamamoto, R.; Butler, S.; Korpela, H.; Salonen, R.; Nyyssonen, K.; Palinski, W.; Witztum, J. L., Autoantibody against oxidized LDL and progression of carotid atherosclerosis. *Lancet* **1992,** *339*, 883-887.

4. Hammad, L. A.; Wu, G. X.; Saleh, M. M.; Klouckova, I.; Dobrolecki, L. E.; Hickey, R. J.; Schnaper, L.; Novotny, M. V.; Mechref, Y., Elevated levels of hydroxylated phosphocholine lipids in the blood serum of breast cancer patients. *Rapid Commun. Mass Spectrom.* **2009,** *23*, 863-876.

5. Wu, R. P.; Hayashi, T.; Cottam, H. B.; Jin, G.; Yao, S.; Wu, C. C.; Rosenbach, M. D.; Corr, M.; Schwab, R. B.; Carson, D. A., Nrf2 responses and the therapeutic selectivity of electrophilic compounds in chronic lymphocytic leukemia. *Proc. Natl. Acad. Sci. U.S.A.* **2010,** *107*, 7479-7484.

6. Imai, Y.; Kuba, K.; Neely, G. G.; Yaghubian-Malhami, R.; Perkmann, T.; van Loo, G.; Ermolaeva, M.; Veldhuizen, R.; Leung, Y. H.; Wang, H.; Liu, H.; Sun, Y.; Pasparakis, M.; Kopf, M.; Mech, C.; Bavari, S.; Peiris, J. S.; Slutsky, A. S.; Akira, S.; Hultqvist, M.; Holmdahl, R.; Nicholls, J.; Jiang, C.; Binder, C. J.; Penninger, J. M., Identification of oxidative stress and Toll-like receptor 4 signaling as a key pathway of acute lung injury. *Cell* **2008,** *133*, 235-249.

7. Nonas, S.; Miller, I.; Kawkitinarong, K.; Chatchavalvanich, S.; Gorshkova, I.; Bochkov, V. N.; Leitinger, N.; Natarajan, V.; Garcia, J. G.; Birukov, K. G., Oxidized phospholipids reduce vascular leak and inflammation in rat model of acute lung injury. *Am. J. Respir. Crit. Care. Med.* **2006,** *173*, 1130-1138.

8. Montine, T. J.; Montine, K. S.; McMahan, W.; Markesbery, W. R.; Quinn, J. F.; Morrow, J. D., F2-isoprostanes in Alzheimer and other neurodegenerative diseases. *Antioxid. Redox. Signal.* **2005,** *7*, 269-275.

9. Montine, T. J.; Peskind, E. R.; Quinn, J. F.; Wilson, A. M.; Montine, K. S.; Galasko, D., Increased cerebrospinal fluid F2-isoprostanes are associated with aging and latent Alzheimer's disease as identified by biomarkers. *Neuromol. Med.* **2011,** *13*, 37-43.

10. Jenner, P., Oxidative stress in Parkinson's disease. *Ann. Neurol.* **2003,** *53*, S26-S36.

11. Birben, E.; Sahiner, U. M.; Sackesen, C.; Erzurum, S.; Kalayci, O., Oxidative stress and antioxidant defense. *World Allergy Organ. J.* **2012,** *5*, 9-19.

12. Burton, G. W.; Ingold, K. U., Vitamin E: Application of the Principles of Physical Organic Chemistry to the Exploration of Its Structure and Function. *Acc. Chem. Res.* **1986,** *19*, 194-201.

13. Burton, G. W.; Hughes, L.; Ingold, K. U., Antioxidant Activity of Phenols Related to Vitamin E. Are there Chain-Breaking Antioxidants Better than alpha-Tocopherol? *J. Am. Chem. Soc.* **1983,** *105*, 5950-5951.

14. Burton, G. W.; Doba, T.; Gabe, E. J.; Hughes, L.; Lee, F. L.; Prasad, L.; Ingold, K. U., Autoxidation of Biological Molecules. 4. Maximizing the Antioxidant Activity of Phenols. *J. Am. Chem. Soc.* **1985,** *107*, 7053-7065.

15. Pratt, D. A.; DiLabio, G. A.; Brigati, G.; Pedulli, G. F.; Valgimigli, L., 5-Pyrimidinols: novel chain-breaking antioxidants more effective than phenols. *J. Am. Chem. Soc.* **2001,** *123*, 4625-4626.

16. Pratt, D. A.; Mills, J. H.; Porter, N. A., Theoretical calculations of carbon-oxygen bond dissociation enthalpies of peroxyl radicals formed in the autoxidation of lipids. *J. Am. Chem. Soc.* **2003,** *125*, 5801-5810.

17. Simmie, J. M.; Black, G.; Curran, H.; Hinde, J. P., Enthalpies of Formation and Bond Dissociation Energies of Lower Alkyl Hydroperoxides and Related Hydroperoxy and Alkoxy Radicals. *J. Phys. Chem. A* **2008,** *112*, 5010-5016.

18. Esterbauer, H.; Dieber-Rotheneder, M.; Striegl, G.; Waeg, G., Role of Vitamin-E in Preventing the Oxidation of Low-Density Lipoprotein. *Am. J. Clin. Nutr.* **1991,** *53*, S314-S321.

19. Suarna, C.; Hood, R. L.; Dean, R. T.; Stocker, R., Comparative Antioxidant Activity of Tocotrienols and other Natural Lipid-Soluble Antioxidants in a Homogenous System, and in Rat and Human Lipoproteins. *Biochim. Biophys. Acta* **1993,** *1166*, 163-170.

20. Mohr, D.; Bowry, V. W.; Stocker, R., Dietary Supplementation with Coenzyme Q_{10} Results in Increased Levels of Ubiquinol-10 within Circulating Lipoproteins and Increased Resistance of Human Low-Density Lipoprotein to the Initiation of Lipid Peroxidation. *Biochim. Biophys. Acta* **1992,** *1126*, 247-254.

21. Steinberg, D.; Parthasarathy, S.; Carew, T. E.; Khoo, J. C.; Witztum, J. L., Beyond Cholesterol. *N. Engl. J. Med.* **1989,** *320*, 915-924.

22. Palinski, W.; Rosenfeld, M. E.; Ylä-Herttuala, S.; Gurtner, G. C.; Socher, S. S.; Butler, S. W.; Parthasarathy, S.; Carew, T. E.; Steinberg, D.; Witztum, J. L., Low density lipoprotein undergoes oxidative modification in vivo. *Proc. Natl. Acad. Sci. U.S.A.* **1989,** *86*, 1372-1376.

23. Steinbrecher, U. P.; Lougheed, M.; Kwan, W. C.; Dirks, M., Recognition of Oxidized Low Density Lipoprotein by the Scavenger Receptor of Macrophages Results from Derivatization of Apolipoprotein B by Products of Fatty Acid Peroxidation. *J. Biol. Chem.* **1989,** *264*, 15216-15223.

24. Kamat, C. D.; Gadal, S.; Mhatre, M.; Williamson, K. S.; Pye, Q. N.; Hensley, K., Antioxidants in central nervous system diseases: Preclinical promise and translational challenges. *J. Alzheimers Dis.* **2008,** *15*, 473-493.

25. Bowry, V. W.; Ingold, K. U.; Stocker, R., Vitamin-E in human low-density lipoprotein - When and how this antioxidant becomes a prooxidant. *Biochem. J.* **1992,** *288*, 341-344.

26. Bowry, V. W.; Stocker, R., Tocopherol-mediated peroxidation. The prooxidant effect of vitamin-E on the radical-initiated oxidation of human low-density lipoprotein. *J. Am. Chem. Soc.* **1993,** *115*, 6029-6044.

27. Remorova, A. A.; Roginskii, V. A., Rate Constants for the Reaction of alpha-Tocopherol Phenoxyl Radicals with Unsaturated Fatty Acid Esters and Contribution of that Reaction to the Kinetics of the inhibited Oxidation of Lipids. *Kinet. Catal.* **1991,** *32*, 726-731.

28. Ingold, K. U.; Bowry, V. W.; Stocker, R.; Walling, C., Autoxidation of Lipids and Antioxidation by alpha-Tocopherol and Ubiquinol in Homogenous Solution and in Aqueous Dispersions of Lipids: Unrecognized Consequences of Lipid Particle Size as Exemplified by Oxidation of Human Low Density Lipoprotein. *Proc. Natl. Acad. Sci. U.S.A.* **1993,** *90*, 45-49.

29. Bowry, V. W.; Stocker, R., Tocopherol-Mediated Peroxidation. The Prooxidant Effect of Vitamin E on the Radical-Initiated Oxidation of Human Low-Density Lipoprotein. *J. Am. Chem. Soc.* **1993,** *115*, 6029-6044.

30. Hill, S.; Lamberson, C. R.; Xu, L.; To, R.; Tsui, H. S.; Shmanai, V. V.; Bekish, A. V.; Awad, A. M.; Marbois, B. N.; Cantor, C. R.; Porter, N. A.; Clarke, C. F.; Shchepinov, M. S., Small amounts of isotope-reinforced polyunsaturated fatty acids suppress lipid autoxidation. *Free Radic. Biol. Med.* **2012,** *53*, 893-906.

31. Russell, G. A., Deuterium-Isotope Effects in the Autoxidation of Aralkyl Hydrocarbons. Mechanism of the Interaction of Peroxy Radicals. *J. Am. Chem. Soc.* **1957,** *79*, 3871-3877.

32. Howard, J. A.; Ingold, K. U., Absolute rate constants for hydrocarbon autoxidation. IV. Tetralin, cyclohexene, diphenylmethane, ethylbenzene, and allylbenzene. *Can. J. Chem.* **1966,** *44*, 1119-1130.

33. Howard, J. A.; Ingold, K. U.; Symonds, M., Absolute Rate Constants for Hydrocarbon Oxidation. 8. The Reactions of Cumylperoxy Radicals. *Can. J. Chem.* **1968,** *46*, 1017-1022.

34. Kitaguchi, H.; Ohkubo, K.; Ogo, S.; Fukuzumi, S., Additivity rule holds in the hydrogen transfer reactivity of unsaturated fatty acids with a peroxyl radical: mechanistic insight into lipoxygenase. *Chem. Commun. (Camb.)* **2006**, 979-81.

35. Roschek, B.; Tallman, K.; Rector, C.; Gillmore, J.; Pratt, D.; Punta, C.; Porter, N., Peroxyl radical clocks. *J. Org. Chem.* **2006,** *71*, 3527-3532.

36. Tallman, K. A.; Pratt, D. A.; Porter, N. A., Kinetic products of linoleate peroxidation: Rapid beta-fragmentation of nonconjugated peroxyls. *J. Am. Chem. Soc.* **2001,** *123*, 11827-11828.

37. Tallman, K. A.; Rector, C. L.; Porter, N. A., Substituent Effects on Regioselectivity in the Autoxidation of Nonconjugated Dienes. *J. Am. Chem. Soc.* **2009,** *131*, 5635-5641.

38. Xu, L.; Davis, T. A.; Porter, N. A., Rate Constants for Peroxidation of Polyunsaturated Fatty Acids and Sterols in Solution and in Liposomes. *J. Am. Chem. Soc.* **2009,** *131*, 13037-13044.

39. Liu, W.; Yin, H.; Akazawa, Y. O.; Yoshida, Y.; Niki, E.; Porter, N. A., Ex vivo oxidation in tissue and plasma assays of hydroxyoctadecadienoates: Z,E/E,E stereoisomer ratios. *Chem. Res. Toxicol.* **2010,** *23*, 986-995.

40. Hill, S.; Lamberson, C. R.; Xu, L.; To, R.; Tsui, H. S.; Shmanai, V. V.; Bekish, A. V.; Awad, A. M.; Marbois, B. N.; Cantor, C. R.; Porter, N. A.; Clarke, C. F.; Shchepinov, M. S., Small amounts of isotope-reinforced polyunsaturated fatty acids suppress lipid autoxidation. *Free Radic. Biol. Med.* **2012,** *53*, 893-906.

41. Thomas, J. R., Influence of Cumene Hydroperoxide upon the Inhibited Oxidation of Cumene. *J. Am. Chem. Soc.* **1963,** *85*, 2166-2167.

42. Mahoney, L. R., Antioxidants. *Angew. Chem., Int. Ed. Engl.* **1969,** *8*, 547-555.

43. Lamberson, C.; Xu, L.; Muchalski, H.; Montenegro-Burke, J.; Shmanai, V.; Bekish, A.; McLean, J.; Clarke, C.; Shchepinov, M.; Porter, N., Unusual Kinetic Isotope Effects of Deuterium Reinforced Polyunsaturated Fatty Acids in Tocopherol-Mediated Free Radical Chain Oxidations. *J. Am. Chem. Soc.* **2014,** *136* (3), 838-841.

44. Koshino, N.; Cai, Y.; Espenson, J. H., Kinetic Study of the Phthalimide N-Oxyl (PINO) Radical in Acetic Acid. Hydrogen Abstraction from C−H Bonds and Evaluation of O−H Bond Dissociation Energy of N-Hydroxyphthalimide. *J. Phys. Chem. A* **2003,** *107*, 4262-4267.

45. Koshino, N.; Saha, B.; Espenson, J. H., Kinetic Study of the Phthalimide N-Oxyl Radical in Acetic Acid. Hydrogen Abstraction from Substituted Toluenes, Benzaldehydes, and Benzyl Alcohols. *J. Org. Chem.* **2003,** *68*, 9364-9370.

46. Amorati, R.; Lucarini, M.; Mugnaini, V.; Pedulli, G. F.; Minisci, F.; Recupero, F.; Fontana, F.; Astolfi, P.; Greci, L., Hydroxylamines as Oxidation Catalysts: Thermochemical and Kinetic Studies. *J. Org. Chem.* **2003,** *68*, 1747-1754.
47. Wu, A.; Mader, E. A.; Datta, A.; Hrovat, D. A.; Borden, W. T.; Mayer, J. M., Nitroxyl Radical Plus Hydroxylamine Pseudo Self-Exchange Reactions: Tunneling in Hydrogen Atom Transfer. *J. Am. Chem. Soc.* **2009,** *131*, 11985-11997.

48. Nagaoka, S.; Kuranska, A.; Tsuboi, H.; Nagashima, U.; Mukai, K., Mechanism of Antioxidant Reaction of Vitamin E. Charge Transfer and Tunneling Effect in Proton-Transfer Reaction. *J. Phys. Chem.* **1992,** *96*, 2754-2761.

49. Upston, J. M.; Terentis, A. C.; Stocker, R., Tocopherol-mediated peroxidation of lipoproteins: implications for vitamin E as a potential antiatherogenic supplement. *FASEB J.* **1999,** *13*, 977-994.

50. Upston, J. M.; Terentis, A. C.; Morris, K.; Keaney, J. F. J.; Stocker, R., Oxidized Lipid Accumulates in the Presence of alpha-Tocopherol in Atherosclerosis. *Biochem. J.* **2002,** *363*, 753-760.

51. Thomas, S. R.; Stocker, R., Molecular Action of Vitamin E in Lipoprotein Oxidation: Implications for Atherosclerosis. *Free Radic. Biol. Med.* **2000,** *28*, 1795-1805.

52. Kalyanaraman, B.; Darley-Usmar, V. M.; Wood, J.; Joseph, J.; Parthasarathy, S., Synergistic Interaction Between the Probucol Phenoxyl Radical and Ascorbic Acid in Inhibiting the Oxidation of Low Density Lipoprotein. *J. Biol. Chem.* **1992,** *267*, 6789-6795.

53. Mehlhorn, R. J.; Sumida, S.; Packer, L., Tocopheroxyl Radical Persistence and Tocopherol Consumption in Liposomes and in Vitamin E-enriched Rat Liver Mitochondria and Microsomes. *J. Biol. Chem.* **1989,** *264*, 13448-13452.

54. Erin, A. N.; Skrypin, V. K.; Kagan, V. E., Formation of alpha-Tocopherol Complexes with Fatty Acids. Nature of Complexes. *Biochim. Biophys. Acta* **1985,** *815* (209-214).

55. Bisby, R. H.; Parker, A. W., Reactions of the α-tocopheroxyl radical in micellar solutions studied by nanosecond laser flash photolysis. *FEBS Lett.* **1991,** *290*, 205-208.

56. Mukai, K.; Nishimura, M.; Kikuchi, S., Stopped-flow Investigation of the Reaction of Vitamin C with Tocopheroxyl Radical in Aqueous Triton X-100 Miceller Solutions. The Structure-activity Relationship of the Regeneration Reaction of Tocopherol by Vitamin C. *J. Biol. Chem.* **1991,** *266*, 274-278.

57. Kathir, K.; Dennis, J. M.; Croft, K. D.; Mori, T. A.; Lau, A. K.; Adams, M. R.; Stocker, R., Equivalent lipid oxidation profiles in advanced atherosclerotic lesions of carotid endarterectomy plaques obtained from symptomatic type 2 diabetic and nondiabetic subjects. *Free Radic. Biol. Med.* **2010,** *49*, 481-486.

58. Wheelan, P.; Zirrolli, J. A.; Murphy, R. C., Low-energy fast-atom-bombardment tandem mass-spectrometry of monohydroxy substituted unsaturated fatty-acids. *Biol. Mass Spectrom.* **1993,** *22*, 465-473.

Chapter IV

IN-VIVO EFFECTS OF D-PUFAS ON OXIDATIVE STRESS

4.1. Introduction

4.1.1. Lipid Peroxidation, Oxidative Stress, and D-PUFAs

Polyunsaturated fatty acids (PUFAs) are essential nutrients avidly taken up by cells, incorporated into phospholipid pools and used as one of the primary building blocks of membrane bilayers with more than 30 phospholipid molecules per every protein anchored in the bilayer being typical.[1] Beyond their importance in imparting membrane structural integrity, PUFAs are also metabolized into several signaling compounds or hormones via enzymes such as the cyclooxygenases[2] and lipoxygenases.[3,4] Despite their importance in function, PUFAs are also extremely susceptible to attack by peroxyl and hydroxyl radical species.[5,6] These oxygen centered radicals readily attack the *bis*-allylic hydrogen atoms, initiating a free radical chain reaction which can result in damage to lipid bilayers and related structures through the buildup of peroxides and via *cis*- to *trans*-isomerization of PUFA double bonds.[7,8] This process, known as lipid peroxidation, has been implicated in a number of diseases including atherosclerosis,[9,10] cancer,[11] acute lung injury,[12,13] and neurodegenerative disorders such as Parkinson's[14,15] and Alzheimer's disease.[16]

A common link between these diseases is oxidative stress arising from inflammation. Inflammation is generally described by heat, redness, swelling, and pain.[17] It can be viewed as a classic biological stimulation-response system, or as an organisms' response to invading microorganisms or other environmental exposures.[17] Inflammation can also be triggered by physical trauma. Regardless of the initiating event, the processes driving inflammation are complex and diverse with a number of proteins and small molecules playing specific roles in the inflammatory process.[18] Lipid peroxidation has also been directly associated with the inflammatory process and can lead to significant cellular damage if left unchecked.[18]

A recent strategy has emerged to diminish lipid peroxidation *in vivo* based on isotopic reinforcement of the *bis*-allylic methylene, replacing hydrogen atoms with deuterium atoms at vulnerable sites.[19] These deuterated PUFAs (D-PUFAs) have been shown to increase resistance of yeast to oxidative stress,[20] to diminish neurodegeneration in a mouse model of Parkinson's disease,[21] and to rescue a mammalian cell model for Friedreich ataxia from succumbing to oxidative stress.[22] Recent work has shown that in the absence of antioxidants, the free radical oxidation of 11,11-D_2-linoleic acid (11,11-D_2-LA) proceeds with a propagation rate constant some 10-fold less than the propagation rate constant of the natural fatty acid, linoleic acid (LA).[23] When oxidized in the presence of alpha-tocopherol (TocH) under conditions in which tocopherol-mediated oxidation predominates,[24] D-PUFAs underwent autoxidation at rates of up to 36-fold lower than the natural compounds.[25] The high kinetic isotope effects (KIEs) measured in these experiments coupled with the demonstrated protective effects seen in various disease models suggest that D-PUFAs are much more resistant to autoxidation than natural PUFAs. Therefore these compounds may be well suited to protect against excessive lipid peroxidation during inflammatory processes.

4.1.2. Inflammation

As discussed above, inflammation is a biological process marked by five distinct physical features: heat, redness, swelling, pain, and loss of function.[17] Inflammation accompanies or causes numerous human diseases including atherosclerosis,[26] cancer,[27] lung,[28,29] kidney,[30,31] and fatty liver diseases,[32] as well as general bacterial infections. It is also a common driving feature of neurodegenerative disorders such as Parkinson's and Alzheimer's disease and amyotrophic lateral sclerosis.[33] Macrophages play a prominent and complex role in inflammation since they are part of an organism's innate immune system.

The innate immune response relies on the identification of conserved features of pathogens, otherwise known as pathogen-associated molecular patterns (PAMPs).[34] A prime example is lipopolysaccharide (LPS), a common structural feature of Gram-negative bacteria. Macrophages are able to detect LPS and initiate inflammatory signaling through toll-like receptor 4 (TLR4), releasing a cascade of downstream responses to the pathogen.[35,36] The response can manifest itself in a number of different ways including engulfment of the pathogen or the production of reactive oxygen species (ROS) and reactive nitrogen species (RNS) to kill the pathogen.[37,38] Signaling molecules such as prostaglandins (PGs),[39] leukotrienes,[40] and interleukins[41] are also released to recruit leukocytes in an effort to intensify the inflammatory response to the pathogen.[42] Although macrophages are commonly associated with an invading pathogen, other environmental factors can induce an inflammatory response. Some of these factors include cigarette smoke[43,44] and exposure to other air pollutants.[45]

4.1.3. Lipid Peroxidation, Lipid Electrophiles, and Enzymatic Oxidation

Oxidized PUFAs are generated during the inflammatory response through a number of different pathways. The PUFAs associated with lipid bilayers and other structural components of cells are susceptible to free radical oxidation, and the generation of ROS and RNS exacerbates the formation of lipid hydroperoxides and other oxidized species. Linoleic (LA) and arachidonic (AA) acids are primary targets of peroxidation. The free radical oxidation of these lipids proceeds through an identical first step in which a hydrogen atom is abstracted at a *bis*-allylic methylene group. A delocalized pentadienyl radical is formed in this step and oxygen will rapidly add to this radical to give a lipid hydroperoxyl radical. The mechanism of free radical oxidation of LA has been discussed at length in previous chapters – typical products formed include HpODEs in either *trans*,*cis*- or *trans*,*trans*-configurations. The corresponding HODEs are formed after reduction of these hydroperoxides, and keto-octadecadienoic acids (KODEs) are formed through termination reactions.

The free radical oxidation of AA is much more complex than LA. AA is more susceptible to free radical oxidation than linoleate due to the presence of three *bis*-allylic sites as compared to one on LA. As a consequence, the propagation rate constant for AA (201 ± 12 M^{-1} s^{-1})[46] is roughly three times greater than that of LA (62 M^{-1} s^{-1}).[47,48] The two additional *bis*-allylic centers offer extra options for initial hydrogen atom abstraction and open up a much more diverse chemistry leading to oxidized products.

In the presence of good hydrogen atom donors such as TocH, autoxidation of AA results in the formation of six major hydroperoxide products known as hydroperoxyeicosatetraenoates (HpETEs, Figure 1).[49]

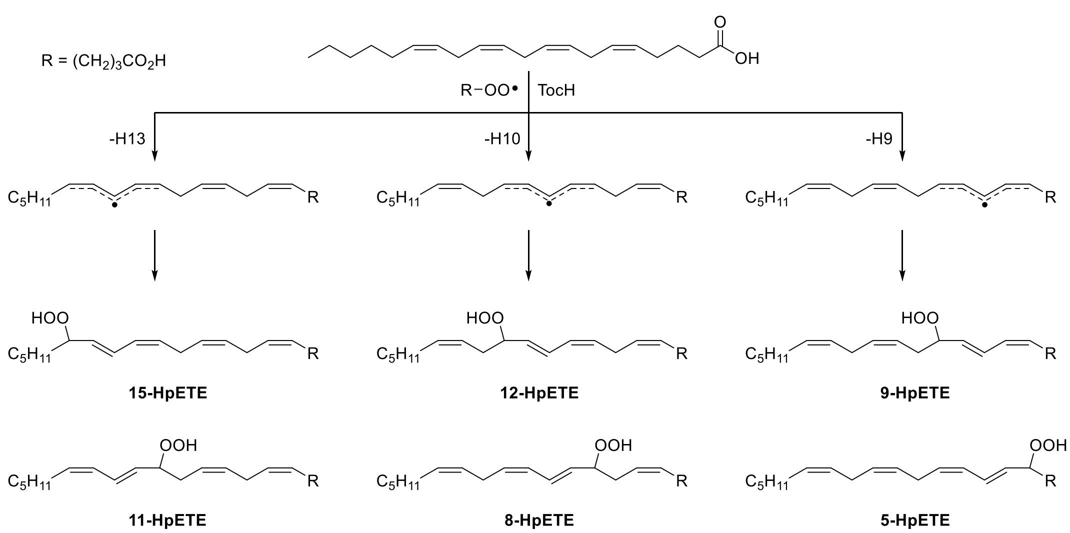

Figure 1. Autoxidation of AA in the presence of a TocH gives 6 HpETE products, all with *trans*,*cis*-conjugated diene configuration.

When TocH is not present, autoxidation still produces the six *trans,cis*-HpETEs shown in Figure 1, yet little or none of the *trans,trans*-HpETEs are observed. This is in stark contrast to the major products from linoleate autoxidation in which the *trans,trans*-HpODEs are formed after β-fragmentation of the *trans,cis*-peroxyl radical. This fragmentation proceeds at a rate of roughly 700 s^{-1}. However, PUFAs containing three or more double bonds are capable of undergoing peroxyl radical cyclization, which directly competes with β-fragmentation that occurs at a rate from 500 to 1000 s^{-1}. This process, shown in Figure 2, accounts for the fact that little or no *trans,trans*-HpETEs are observed during autoxidation of AA.[49]

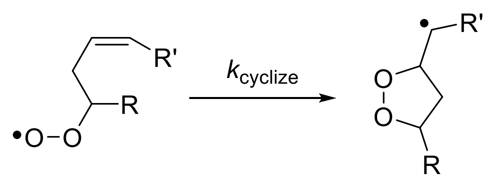

Figure 2: When a PUFA has three or more double bonds, cyclization of the peroxyl radical is able to out-compete β-fragmentation. Little to none of the *trans,trans*-conjugated diene HpETEs are seen for this reason.

The ability of AA to undergo the cyclization reaction discussed above results in a much more complex mixture of products during autoxidation. As cyclization of the initial peroxyl radical proceeds, four different regioisomers of isoprostanes are formed. Isoprostanes were first reported in 1990,[16] and these compounds have since been used as biomarkers of endogenous lipid peroxidation[50] as evidenced by a number of animal and clinical studies.[51,52] The major regioisomers of isoprostanes are shown in Figure 3.

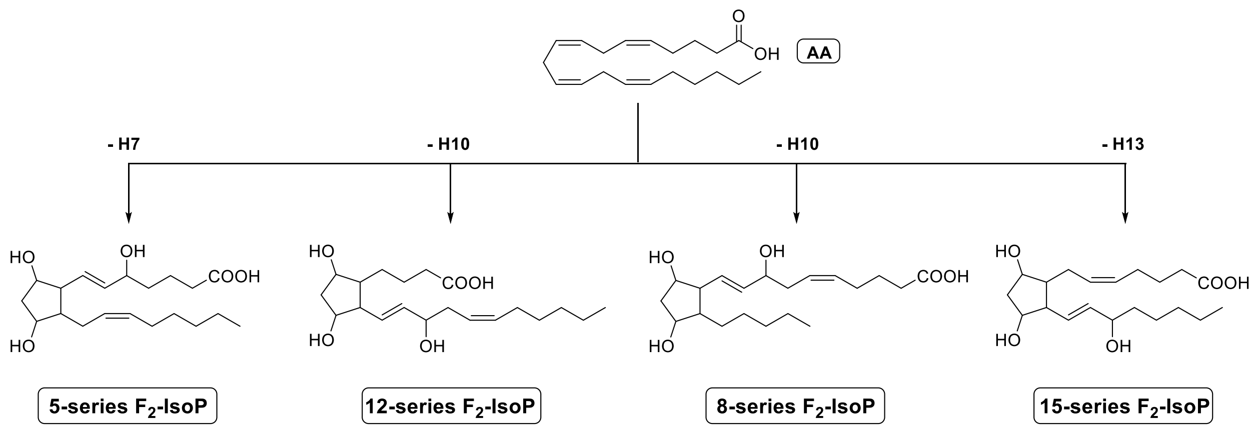

Figure 3. During autoxidation of arachidonic acid, peroxyl radicals at every position except for C5 and C15 are able to cyclize and form four sets of regioisomers of isoprostanes. These isoprostanes are often used as biomarkers of oxidative stress in biological systems.

The inflammatory process generates oxygen radical species that not only attack PUFAs, but also target lipids that have already been oxidized. This secondary oxidation can lead to the formation of α,β-unsaturated aldehydes of differing electrophilicity, three of which have been extensively studied (4-hydroxy-2-nonenal (HNE), 4-oxo-2-nonenal (ONE), and malondialdehyde (MDA)).[53]

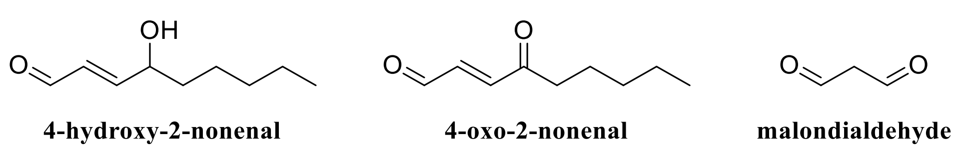

Figure 4. Lipid electrophiles HNE, ONE, and MDA. Such electrophiles are formed during secondary oxidation of LA and AA.

HNE is capable of mediating a wide variety of biological processes through protein modification. This modification is thought to occur primarily through Michael addition to nucleophilic amino acids such as histidine (His), cysteine (Cys), and lysine (Lys) residues.[54] Once this adduction occurs, the function of the protein may be altered or lost all together. For instance, studies have shown that electrophilic modification of IκB kinase (IKK) results in altered function of the NF-κB (Figure 5) signaling pathway which plays an important role in the regulation of immune response to infection.[55] Keap1, important for protection from oxidative injury through regulation of the transcription of antioxidant response element (ARE) genes, also shows altered function in the presence of lipid electrophiles.[56,57]

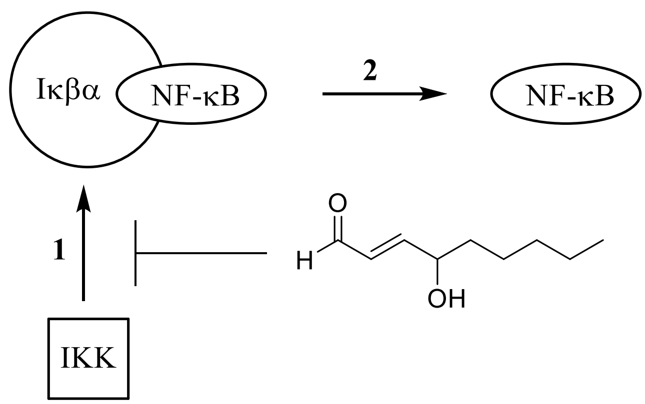

Figure 5. HNE inhibition of IκB Kinase (IKK). NF-κB is retained in the cytoplasm by the inhibitory protein Iκβα, released only when Iκβα is phosphorylated, ubiquinated, or degraded. IKK phosphorylates Iκβα which leads to its degradation (**1**), after which NF-κB is released and translocates to the nucleus to modulate gene expression. HNE adducts IKK (**2**), inhibiting the degradation of Iκβα and in turn the translocation of NF-κB to the nucleus.

While LA and AA are both subject to free radical oxidation reactions during inflammation, enzymatic oxidation also occurs when the inflammatory response is activated. Cyclooxygenase-2 (COX-2), discussed in depth in Chapter 1, is expressed after activation of the TLR-4 signaling pathway.[58] COX-2 acts on AA that has been released from the lipid bilayer by cytosolic phospholipase A_2 ($cPLA_2$), generating prostaglandin H_2 (PGH_2) via *bis*-oxygenation and cyclization. Other eicosanoid signaling molecules such as PGE_2 and PGD_2 are then formed from PGH_2 by various synthases.[2,59,60] COX-2 also generates monooxygenated species of AA such as 11-(*R*)-HpETE and 15-(*S*)-HpETE, analogous to the HpETEs that are formed by peroxidation.[61] In circumstances where these HpETEs are of interest, chiral chromatography is essential in determining whether the HpETEs were generated by a free radical (racemic) or enzymatic process (optically enriched). Figure 6 shows the complexity of products derived from COX-2 activity.

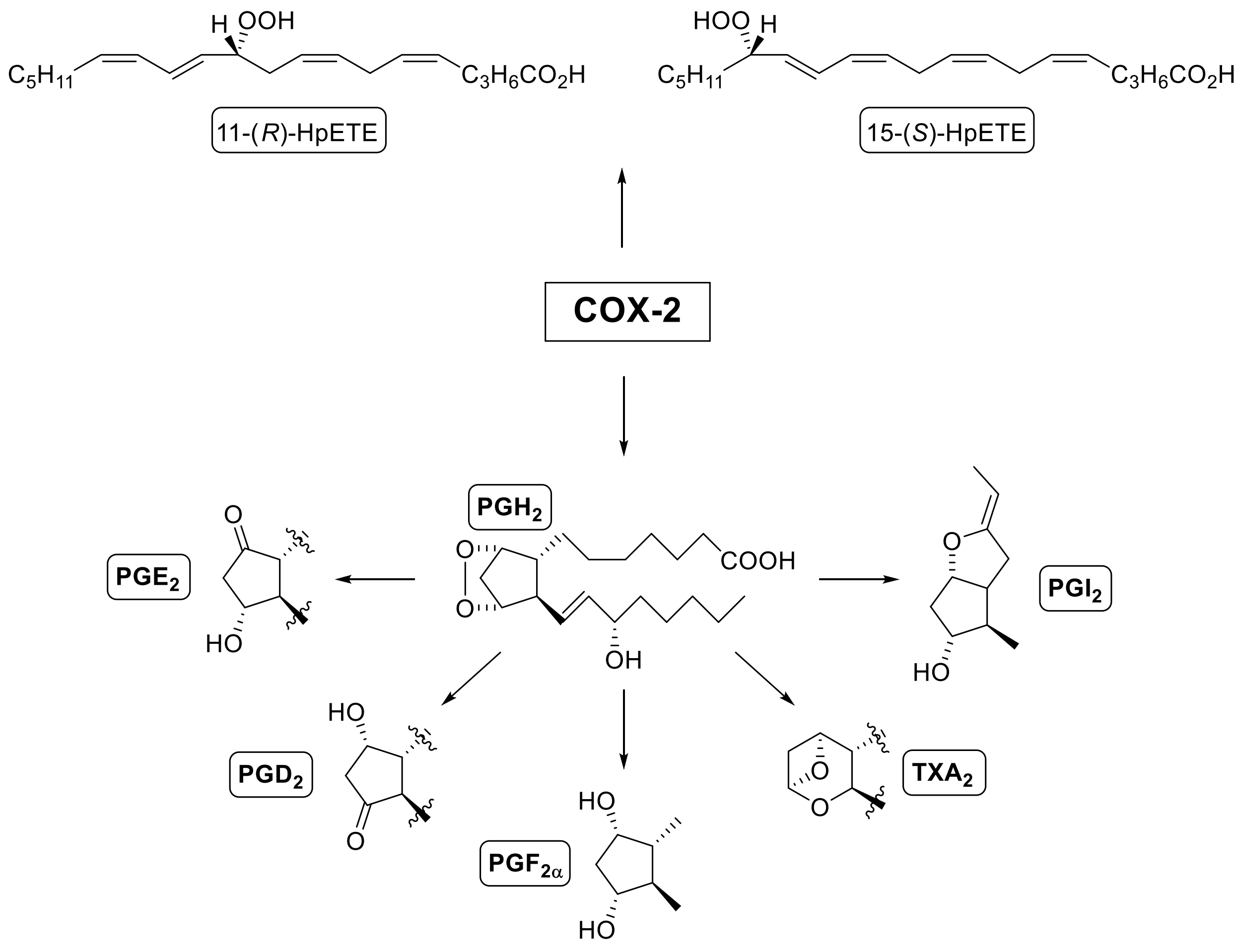

Figure 6. After expression, COX-2 acts on AA released from the lipid bilayer by cPLA2. The major product is PGH_2, which is used by other synthases to produce a more diverse array of signaling eicosanoids. COX-2 is also able to synthesize monooxygenated AA products 11-(*R*)-HpETE and 15-(*S*)-HpETE.

4.1.4. *"Click Chemistry"*

Due to the extent of damage cause from protein adduction by lipid electrophiles, there has been interest in identifying the proteins that are adducted and the responsible electrophilic species. Early studies identified HNE adducts using Anti-HNE antibodies[55,57,62,63,64] but in spite of the utility of those antibodies, cross reactivity with other lipid electrophiles has also been an issue.[65,66]

Other methods have also been used in an attempt to identify lipids, electrophiles, and protein adducts in cellular systems. Stable isotope derivatives of lipids have seen use in tracking distribution of lipid classes in organelles,[67] and powerful mass spectrometry techniques have been leveraged towards the identification of specific lipid electrophile adducts.[68] Attempting to track specific lipids, metabolites, and decomposition products has proven to be difficult despite all of these efforts. Recently, new developments have emerged and shaped the way in which lipids and their metabolites are tracked throughout cellular systems. Affinity tags consisting of terminal alkynyl functionality on lipids have been successfully used to monitor the distribution of lipids throughout cellular membranes.[69] Stable but reversible alkyne-cobalt complexes on phosphine-modified silica were used to isolate lipid species containing the alkynyl tag, followed by mass spectrometry.[70,69]

This terminal alkynyl tag can also be used to visualize and identify lipid electrophile-protein adducts using "click chemistry".[71] "Click chemistry" refers to the copper-catalyzed Huisgen 1,3-dipolar cycloaddition reaction in which an azide is coupled to a terminal alkyne (Figure 7A).[72] In initial studies, human colorectal cancer (RKO) cells were enriched with either terminally tagged azido-HNE (Az-HNE) or alkynyl-HNE (Al-HNE) in order to label proteins in intact cells. This was followed by conjugation to the appropriate biotin conjugated alkynyl (aBiotin) or azido (N_3-Biotin) compounds, respectively (Figure 7B). Streptavidin beads were used to pull down proteins, which had been adducted by aHNE or N_3-HNE and conjugated to biotin following the click reaction. The beads were subsequently washed to release the proteins that were pulled down. Western blotting was used to verify that adducted proteins had indeed been captured by the streptavidin beads. Finally, proteomic analysis of the captured proteins revealed that a number of interesting proteins were adducted by the tagged lipid electrophiles and successfully captured by streptavidin bead purification.[71] Basic workflow for these experiments, along with streptavidin Western blots for aHNE are shown in Figure 7C.

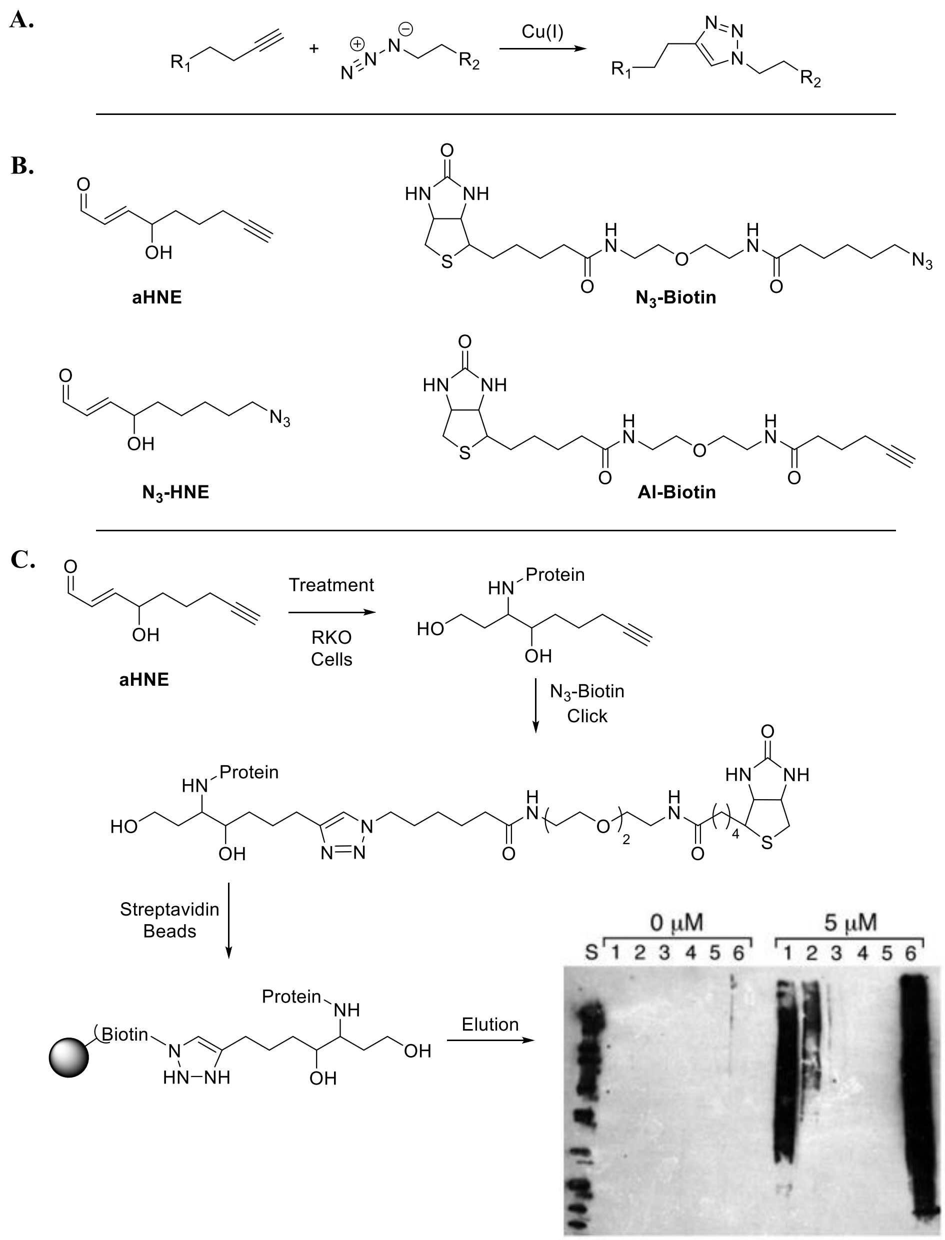

Figure 7. Click chemistry. **A.** Copper(I) catalyzed Huisgen 1,3-dipolar cycloaddition reaction between an azide and terminal alkyne; **B.** Variations of terminally-tagged alkynyl- or azido- HNE and biotin; **C.** General workflow of experiments using aHNE as the lipid electrophile. The Western blot shows protein pull-downs of vehicle (untreated) versus 5 μM treatment of aHNE. Cellular lysates (lane 1), breakthrough after washing streptavidin beads (lane 2), and successive washes (lanes 3,4,5), with final wash eluting the adducted proteins (lane 6).[71]

4.2. Experimental Design

Inflammation accompanies a number of human diseases and disorders and is a significant source of oxidative stress in biological systems. The continual production of ROS and RNS results in an oxidative assault on lipids. As discussed in the introduction, D-PUFAs have been shown to provide protection from oxidative stress in a number of disease models. They have also been shown in solution to be less prone to free radical chain oxidation than their corresponding natural substrates. These findings stimulated the exploration of D-PUFAs in biological models of inflammation.

In the experiments described here, macrophages were used as a model for inflammation. As discussed above, macrophages play an important role in innate immune response to the invasion of pathogens. Macrophages are found in nearly every body system including the liver, lungs, blood, and lymph nodes. The specific cell line used herein is RAW 264.7 macrophage-like cells. This line was derived from BALB/c mice transfected with the Abelson leukemia virus. This particular cell type is arguably one of the most studied cell lines in terms of lipidomics. It is the official cell of the Lipid Metabolites and Pathways Strategy (LIPID MAPS) project. A large compilation of data has been gathered in this cell line including lipid content, mechanisms of lipid metabolism, lipid metabolite profiles, and extensive signaling pathway data.

The RAW 264.7 macrophages were enriched with a number of different PUFAs, D-PUFAs, and alkynyl PUFAs, all shown in Figure 8. The macrophages were activated using Kdo2-Lipid A (KLA), which is a chemically defined analog of lipopolysaccharide (LPS) that also activates the TLR-4 signaling pathway.

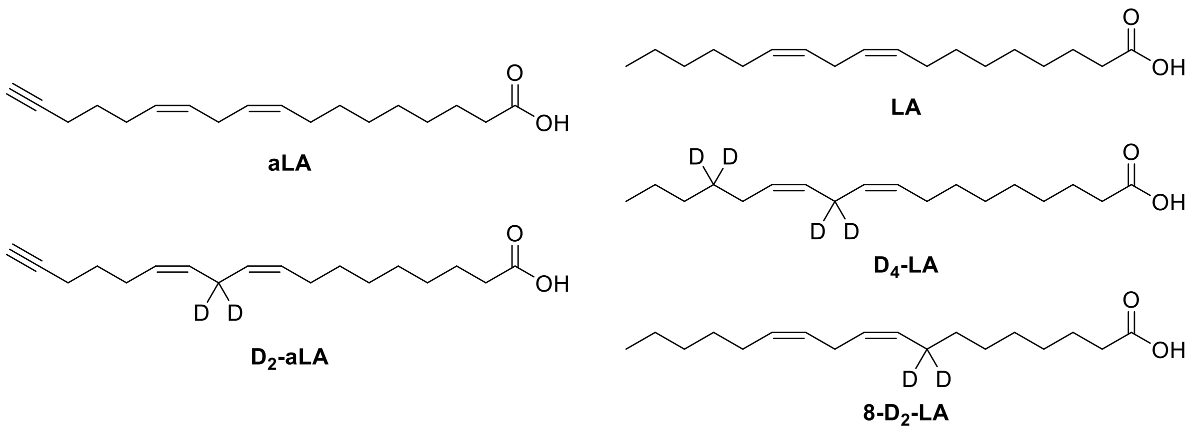

Figure 8. PUFAs used throughout RAW 264.7 macrophage experiments.

Experiments were designed to address specific questions. The first question was how levels of protein adduction (from lipid electrophile formation) were affected by the presence of D-PUFAs. Click chemistry and streptavidin Western blotting was used extensively to address this question. In a typical experiment RAW 264.7 macrophages were plated, enriched with a mixture of PUFAs (see Figure 8), allowed to grow, and activated using KLA, with 24 h between each step. Cells were collected, lysed, and treated with streptavidin beads to remove any biotinylated proteins. Click chemistry was then carried out using Az-Biotin, and proteins were separated by tris-glycine polyacrylamide gels (SDS-PAGE) and visualized by streptavidin Western blotting.

The second question addressed was how levels of lipid metabolites – both from peroxidation reactions and enzymatic reactions – were affected by the presence of D-PUFAs. In these experiments, macrophages were plated and enriched with either PUFA or D-PUFA, allowed to grow, and activated with KLA (again with 24 h between each step). Cells were subsequently collected and lipids were extracted by Folch extraction. The lipid extracts were then hydrolyzed and analyzed by LCMS using both normal-phase and chiral columns. Reverse-phase methods were also utilized to monitor the extent of enrichment for the D-PUFAs and alkynyl analogs as needed.

4.3. Results

Griess Assay

Nitric oxide (NO), produced by nitric oxide synthase (iNOS), is a prevalent physiological messenger and effector molecule that is associated with oxidative stress.[73] Nitrite (NO_2^-), a stable decomposition product of NO, is commonly measured using the Griess assay. The assay relies on a diazotization reaction (Figure 9) that was originally discovered by Peter Griess in 1879.[74]

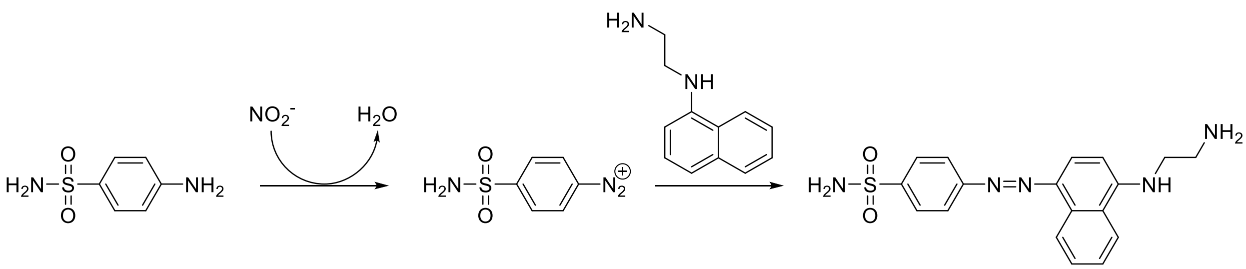

Figure 9. The diazotization reaction used in the Griess assay to measure nitrite concentrations in cellular media.

Macrophages were plated and enriched with 15 μM LA, 8-D_2-LA, or D_4-LA. Unenriched controls were also plated. After +/- KLA treatment, 1 mL of media was removed from each plate. 100 μL of each media sample was dispensed in a 96-well plate. 50 μL of sulfanilamide solution (10 mg/mL in aqueous 5% phosphoric acid) was added to each well. The plate was allowed to develop for 10 minutes in the dark at room temperature. 50 μL of NED solution (N-1-napthylethylenediamine dihydrochloride in water, 1 mg/mL) was then added to each well. The plate was again developed at room temperature in the dark for 20 minutes. After incubation, absorbance of each well was measured using a plate reader at 550 nm. Absorbance values were plotted against a nitrite standard reference curve that was plated and exposed to Griess reagents at the same time. Data from this experiment (Figure 10) shows that enrichment with LA or D-PUFA does not affect the activity iNOS since NO_2^- levels are relatively stable across all enrichment conditions. This suggests that the presence of D-PUFA does not negatively affect the TLR-4 signaling pathway.

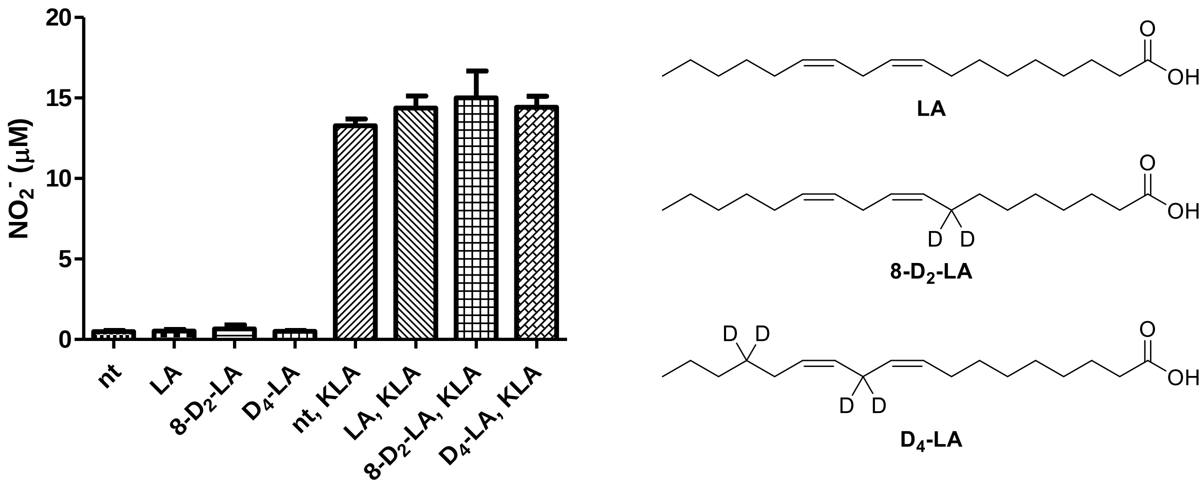

Figure 10. Griess assay results, comparing untreated and treated RAW 264.7 macrophages with and without KLA activation after no treatment or enrichment with LA, 8-D_2-LA, or D_4-LA.

Cyclooxygenase-2 Expression Levels

Similar to iNOS, cyclooxygenase-2 (COX-2) expression is induced when the TLR-4 signaling pathway is activated. In order to determine if D-PUFAs had an effect on COX-2 expression, macrophages were plated and enriched with 15 μM LA, 8-D_2-LA, or D_4-LA. Unenriched controls were also plated. After +/- KLA treatment the macrophages were pelleted, lysed, and proteins were separated using SDS-PAGE. Gels were transferred to 0.45 μm nitrocellulose, probed with a COX-2 antibody, and visualized using an Odyssey scanner. Bands corresponding to COX-2 were digitized using UN-SCAN-IT gel 6.1 in order to quantify any changes in expression level. Results from this experiment (Figure 11) indicate again that the TLR-

4 signaling pathway is not affected by the presence of D-PUFAs as expression levels of COX-2 are relatively stable across all enrichment conditions.

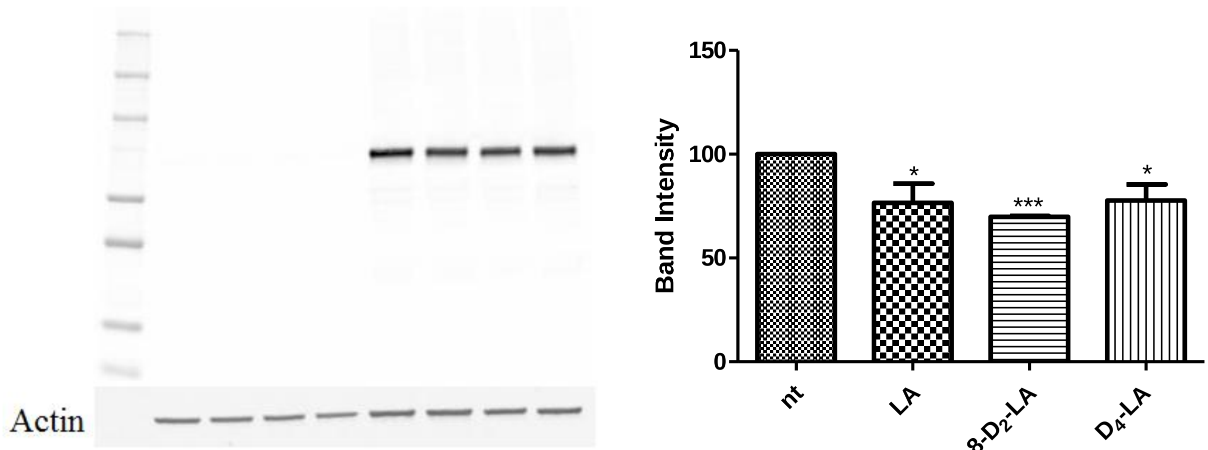

KLA	-	-	-	-	-	+	+	+	+
LA	-	-	+	-	-	-	+	-	-
8-D_2-LA	-	-	-	+	-	-	-	+	-
D_4-LA	-	-	-	-	+	-	-	-	+

Figure 11. COX-2 expression levels after various PUFA enrichments. Proteins were separated by SDS-PAGE, transferred to 0.45 μM nitrocellulose, and probed with a COX-2 antibody. Experimental conditions are found below the blot on the left. Band intensity for COX-2 for each enrichment conditions after KLA activation is shown on the right.

Protein Adduction Assays

In order to gauge the effects of D-PUFAs on protein adduction in activated macrophages, a number of experiments were conducted using click methods to detect adducted proteins. In the first experiment, macrophages were enriched with 15 µM alkynyl linoleic acid (aLA), 15 µM 11,11-D_2-alkynyl linoleic acid (D_2-aLA), or a 15 µM mixture of aLA and D_2-aLA (7.5 µM each). Macrophages were treated with +/- KLA and pelleted, lysed, then ligated to N_3-Biotin. Proteins were separated using SDS-PAGE and the gels were transferred to 0.45 µm nitrocellulose. The blots were probed with the appropriate antibodies and visualized using an Odyssey scanner. The results are shown below in Figure 12.

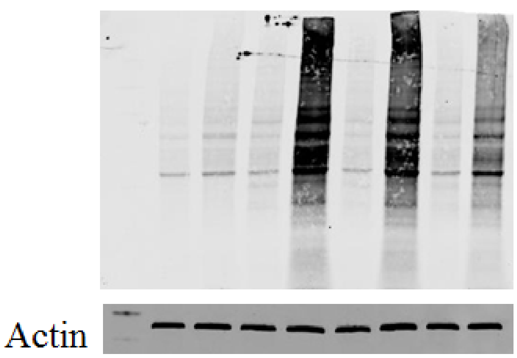

KLA	-	-	+	-	+	-	+	-	+
aLA	-	-	-	+	+	+	+	-	-
D_2-aLA	-	-	-	-	-	+	+	+	+

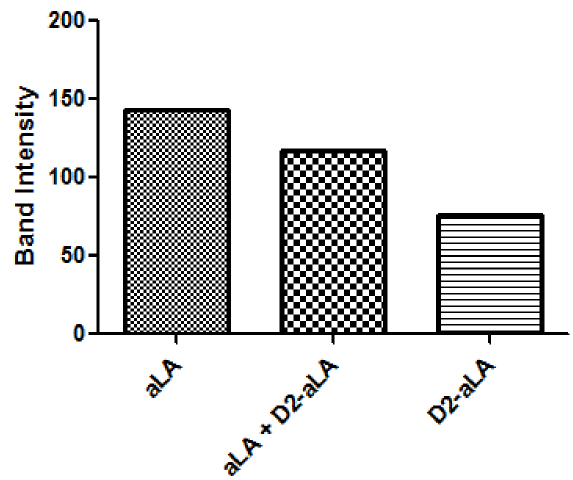

Figure 12. Western blot for aLA vs D_2-aLA comparison. Macrophages were plated and enriched with 15 µM aLA, 15 µM mixture of aLA and D_2-aLA (7.5 µM each), or 15 µM D_2-aLA. Macrophages were treated with +/- KLA. Lysates were ligated to N_3-Biotin and visualized using streptavidin Western blotting. The histogram (right) shows a comparison of band intensity for the three alkynyl PUFA treatments.

Decreases in protein adduction were observed in macrophages enriched with the mixture of aLA and D_2-aLA as well as D_2-aLA enrichment alone. A different approach was attempted in which macrophages were enriched with 15 μM aLA, a 15 μM mixture of aLA and D_4-LA (7.5 μM aLA, 7.5 μM D_4-LA), a 30 μM mixture of aLA and D_4-LA (15 μM aLA, 15 μM D_4-LA), or 15 μM D_4-LA. Under these conditions, streptavidin Western blotting would only identify protein adducts arising from aLA peroxidation as deuterium reinforcement had been moved to D_4-LA (which bears no alkynyl functionality). Clear decreases in protein adduction were observed in cells that had been enriched with the mixtures of aLA and D_4-LA. A Western blot from this experiment that shows decreased protein adduction in the presence of D_4-LA is presented in Figure 13.

Actin

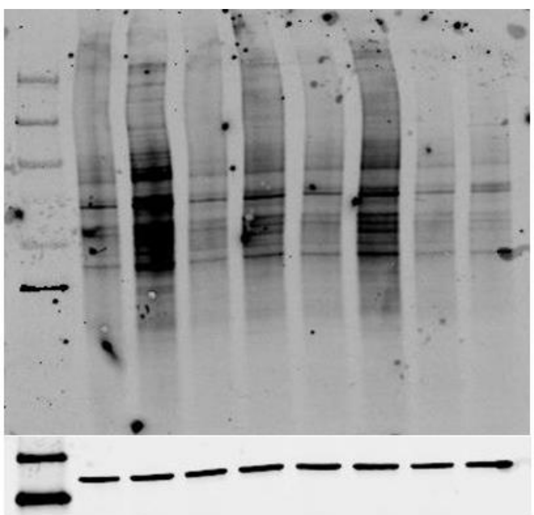

KLA	-	-	+	-	+	-	+	-	+
aLA	-	+	+	+	+	+	+	-	-
D_4-LA	-	-	-	+	+	+	+	+	+
				15 μM		30 μM			

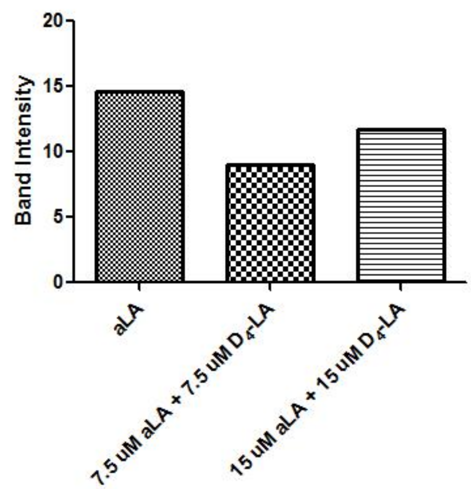

Figure 13. Click blots for aLA and D_2-aLA enriched macrophages. Macrophages were enriched with 15 μM aLA, a 15 μM mixture of aLA and D_4-LA (7.5 μM of each), a 30 μM mixture of aLA and D_4-LA (15 μM of each), or 15 μM D_4-LA and treated with +/- KLA. The histogram (right) compares band intensity after enrichment with aLA or either concentration of aLA and D_4-LA

Prostaglandin Formation

Activation of RAW 264.7 macrophages by KLA induces the expression of COX-2, an enzyme that catalyzes the formation of prostaglandins. In order to assess the activity level of COX-2, levels of PGE_2 and PGD_2 in the media were determined. Cells were plated and enriched with 15 μM LA or 15 μM D_4-LA. After the activation step (+/- KLA), 4 mL of media was collected from each plate. Media was delivered directly into a falcon tube holding 4 mL of ethyl acetate containing the internal standard D_4-prostaglandin E_2. The media was extracted, and the organic layer blown dry. Residue was resuspended in methanol and analyzed by LC-MS. The levels these prostaglandins, displayed in Figure 14, decreased significantly in macrophages treated with D_4-LA.

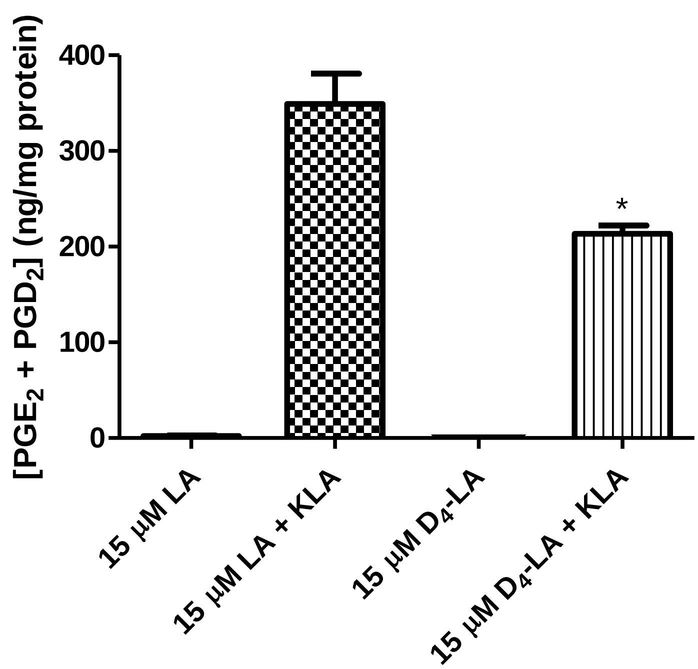

Figure 14. Prostaglandin formation in macrophages enriched with either LA or D_4-LA. After activation, prostaglandin levels were significantly lower in macrophages, which had been enriched with D_4-LA.

Incorporation and Metabolism of D_4-LA

Evidence has been presented that RAW 264.7 macrophages enriched with D_4-LA reduced levels of protein adduction as well as prostaglandin (PGE_2) formation. The presence of D-PUFA appeared, however, to have no negative effect on expression of various elements of the TLR-4 pathway (iNOS and COX-2). In order to better understand these observations, an understanding of the ultimate fate and the level of incorporation of D_4-LA was sought. To carry out these experiments, macrophages were plated and enriched with 15 μM LA or 15 μM D_4-LA and comparisons of the activated and unactivated macrophages were made. Macrophages were pelleted and lipids were extracted using Folch extraction. The lipid fraction was subjected to hydrolysis, and free fatty acids were analyzed by LC-MS using reverse-phase chromatography.

LC-MS analysis was carried out in negative mode using an atmospheric-pressure chemical ionization (APCI) source. RAW 264.7 macrophages are able to synthesize longer chained PUFAs from LA and linolenic acid. Therefore, the molecular ions for LA and D_4-LA were monitored, as were arachidonic acid (AA) and 13,13,17,17-D_4-arachidonic acid (D_4-AA). Selective reaction monitoring was used with a low voltage in the collision cell, monitoring the parent molecular ion in both Q1 and Q3 (279.2 -> 279.2 for LA, etc.). Heptadecanoic acid (C17:0) was used as an internal standard. A typical chromatagram is shown in Figure 15.

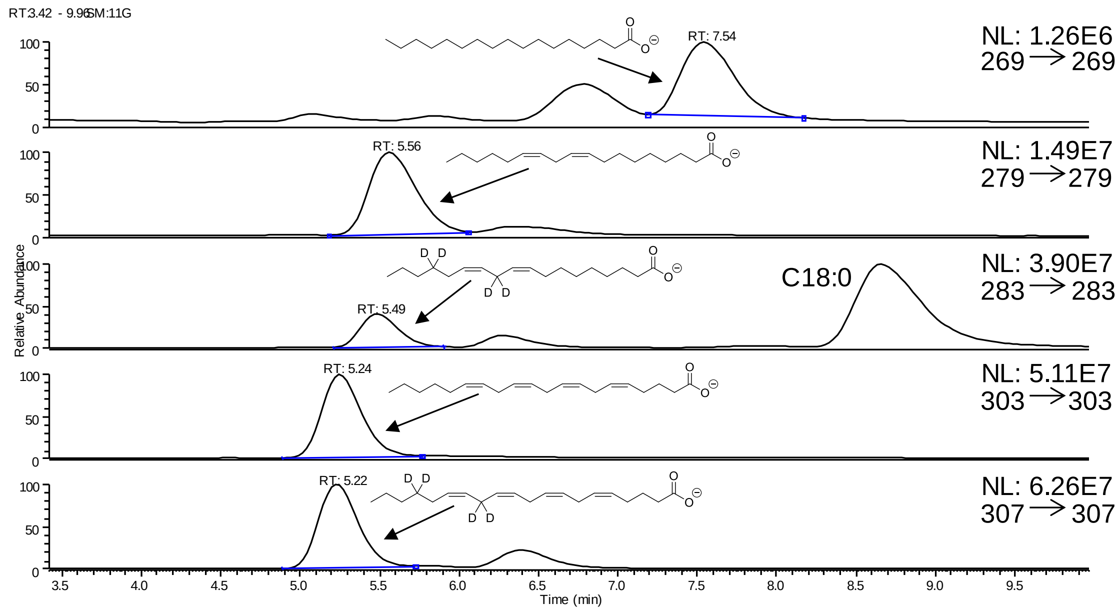

Figure 15. Typical HPLC-MS chromatogram for the analysis of D_4-LA and D_4-AA in unactivated RAW 264.7 macrophages. Aside from the four main fatty acids and internal standard, stearic acid (C18:0) is also observed in the 283 -> 283 panel.

Levels of LA, D_4-LA, AA, and D_4-AA were analyzed for both unactivated and activated macrophages. The histogram in Figure 16 shows the total PUFA profile ([LA + AA] for untreated macrophages, [LA + AA + D_4-LA + D_4-AA] for treated macrophages) divided into fractions of the four major species of interest for all four treatment conditions listed above.

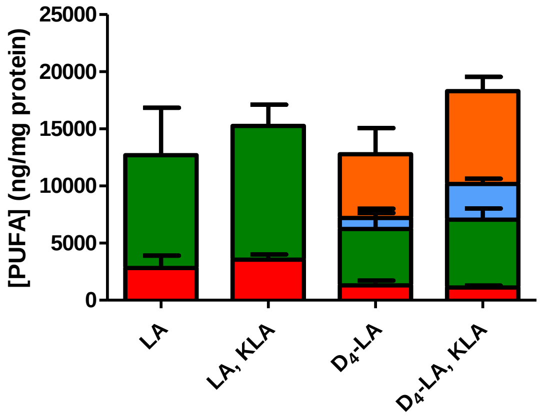

Treatment	15 µM LA		15 µM D_4-LA	
KLA	-	+	-	+
LA	2820 ± 1090	3550 ± 460	1300 ± 420	1120 ± 170
AA	9890 ± 4150	11700 ± 1860	4950 ± 1760	5940 ± 960
D_4-LA	0 ± 0	0 ± 0	960 ± 440	3110 ± 460
D_4-AA	0 ± 0	0 ± 0	5580 ± 2290	8120 ± 1250

Figure 16. Total PUFA profiles for macrophages enriched with 15 µM LA or 15 µM D_4-LA, both unactivated and activated. The table on the right presents the legend for the histogram as well as the observed levels of each PUFA monitored (in ng/mg protein).

Analysis of HODEs and HETEs

RAW 264.7 macrophages were enriched with 15 µM LA or 15 µM D_4-LA and activated with KLA. After 24 h, the macrophages were pelleted, 13(S)-D_4-HODE was added as an internal standard, and lipids were extracted using the Folch method. The lipid fraction was hydrolyzed and analyzed by LCMS using negative mode APCI and normal-phase chromatography. The products monitored included hydroxyoctadecadienoic acids (HODEs), and hydroxyeicosatetraenoic acids (HETEs), products which arise after PPh_3 reduction of their hydroperoxide parents HpODEs and HpETEs, respectively.

The 13- and 9-HODEs were monitored using an established SRM technique that had been previously reported.[75,46] Typical chromatograms are shown in Figure 17A (15 µM LA enrichment) and 17B (15 µM D_4-LA enrichment).

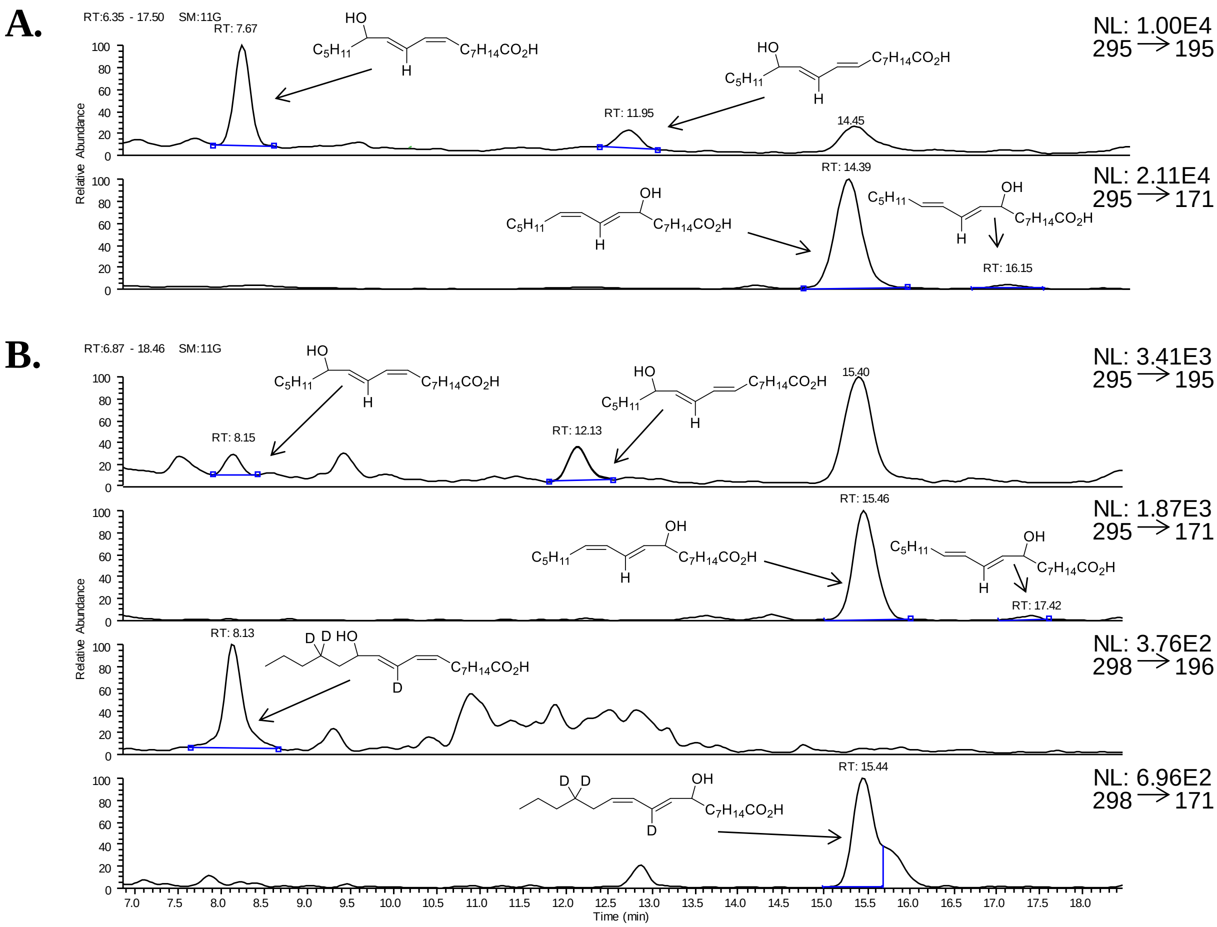

Figure 17. Typical normal-phase HPLC-MS chromatograms monitoring HODE formation in RAW 264.7 macrophages after KLA activation. Enrichments were either **A.** 15 µM LA; or **B.** 15 µM D_4-LA.

Experiments were run in triplicate, and both D_0-HODE and D_3-HODE levels were monitored. As can be seen in the bottom two panels of Figure 16B, D_3-HODEs are difficult to analyze. These products arise from oxidation of D_4-LA, and previous work suggests that linoleic acid containing deuterium at the *bis*-allylic center undergoes autoxidation with a propagation rate constant roughly 10-fold slower compared to the natural compound.[23] Thus, these D-HODE products are formed in low yields. Data from all of the analyses is included throughout this chapter, but the amounts recorded for the D_3-HODEs should be considered as the upper limit for these compounds that constitute only a minor fraction of products formed. Comparisons of the HODE distribution (both D_0- and D_3-HODEs) from LA and D_4-LA enriched macrophages were obtained, and total HODEs were compared for each enrichment condition. Macrophages enriched with D_4-LA showed a significant decrease in HODE levels compared to LA enriched macrophages. Data from these analyses is shown in Figure 18.

A.

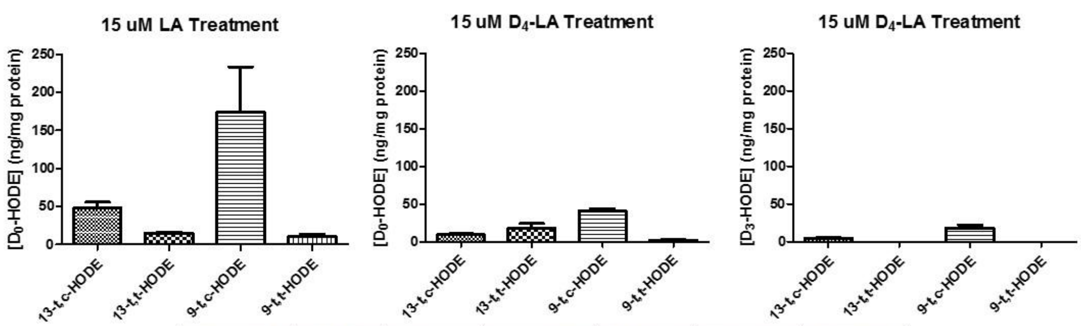

Treatment	HODE	13-trans,cis	13-trans,trans	9-trans,cis	9-trans,trans	Total HODE
15 µM LA	D_0-HODE	48 ± 6	15 ± 1	174 ± 49	11 ± 3	247 ± 67
15 µM D_4-LA	D_0-HODE	10 ± 1	18 ± 7	41 ± 4	2 ± 1	70 ± 3
15 µM D_4-LA	D_3-HODE	5 ± 1	0	19 ± 6	0	24 ± 6

B.

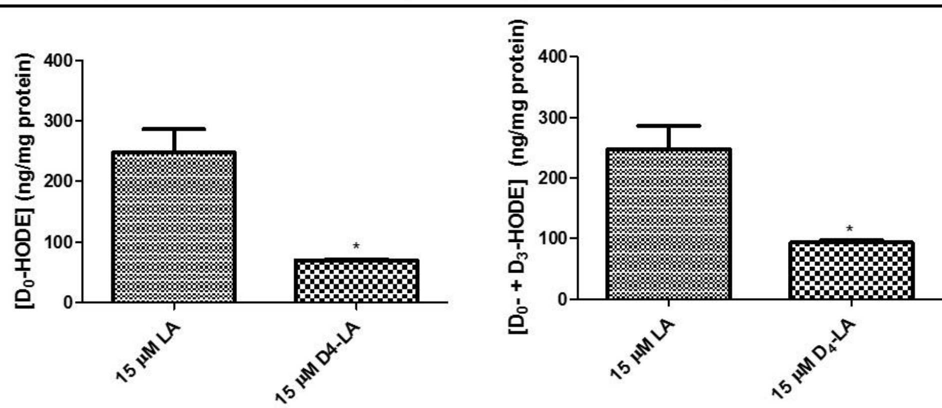

Figure 18. Analysis of HODEs from macrophages enriched with 15 µM LA or 15 µM D_4-LA. **A.** Histograms show the distribution of D_0-HODE regioisomers after LA enrichment (+ KLA), and D_0-/D_3-HODE regioisomers after D_4-LA enrichment (+ KLA); **B.** Comparison of D_0-HODE levels (left) and D_0- + D_3-HODE levels (right) after LA or D_4-LA treatment and KLA activation.

HETEs were also analyzed at the same time. Specifically, the 5-, 11-, and 15-HETEs were monitored. Both 5-HETE and 15-HETE are considered to be good markers for peroxidation of arachidonic acid since peroxyl radicals formed at those centers (5-OO· and 15-OO·) are not able to undergo direct cyclization to give isoprostane-like products.[76] The presence of 5-HETE and 15-HETE were too low for consistent analysis, a result that is likely due to β-fragmentation of the peroxyl radical and readdition of oxygen to give the 9-peroxyl radical (9-OO·) or 11-peroxyl radical (11-OO·), leading ultimately to the formation of isoprostanes (IsoP's).[76] The 11-peroxyl radical (11-OO·) is able to form IsoP's, but can also form 11-HETE after hydrogen atom donation if good donors are present. 11-HETE may also be formed through COX-2 activity (i.e. inefficient conversion of AA to PGE_2).[2,61] A typical chromatogram for the analysis of 11-HETE and its D_3-11-HETE compounds is shown in Figure 19.

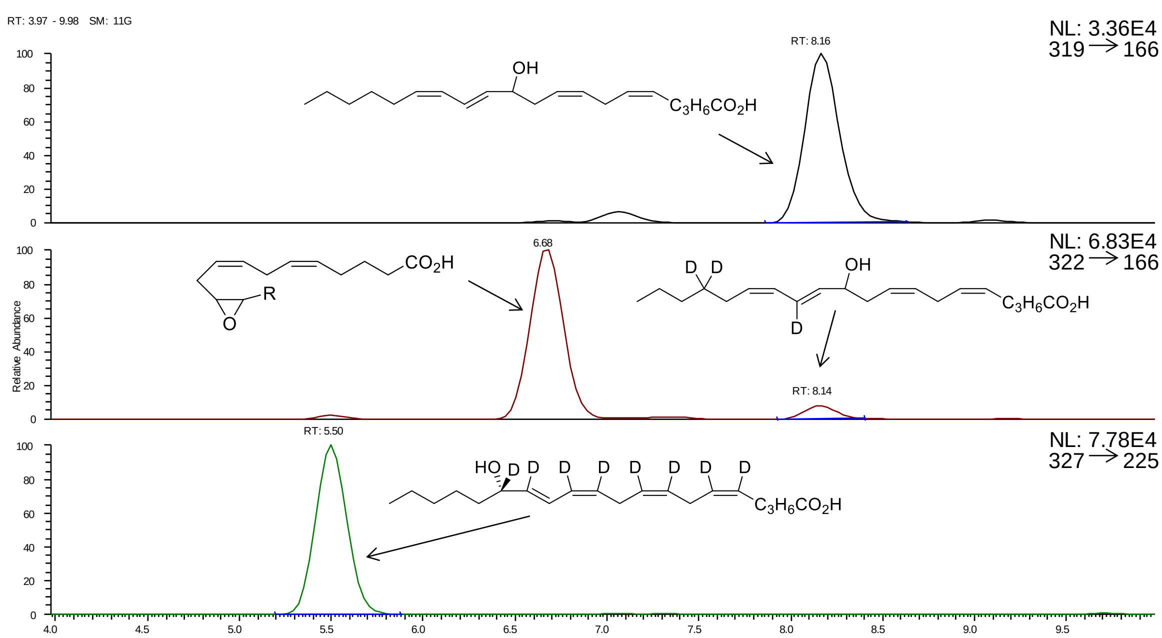

Figure 19. Analysis of 11-HETE and D_3-11-HETE after activation of macrophages enriched with 15 μM D_4-LA by normal-phase HPLC-MS. The peak in the panel analyzing D_3-11-HETE is possibly an epoxide product. Its identity is speculative at this time as authentic standards are needed for confirmation. 15(*S*)-D_8-HETE was used as the internal standard (bottom panel).

Analysis of HODEs and HETEs by Chiral Chromatography

Chiral analysis was carried out on HODE and HETE products to determine whether products observed were from free radical or enzymatic oxidation. Due to low levels of oxidation in D_4-LA enriched macrophages, multiple plates of cells were combined to gain an acceptable signal. The HODEs from LA and D_4-LA oxidation were monitored, as well as the 15-, 11-, and 5-HETEs. Determination of the enantiomers present in macrophage samples was completed by comparison to enantiopure standards for each compound. A more in depth discussion is presented in the following Discussion section.

4.4. Discussion

Inflammation is a complex process that results in a wide array of physiological responses. Macrophages are often seen as the first line of defense against invading pathogens, recognizing lipopolysaccharide (LPS) or other pathogen-associated molecular patterns (PAMPs) and initiating a coordinated oxidative response and the recruitment of other immune cells. One consequence of inflammation is lipid peroxidation in proximate areas to the assault, a process that can result in significant oxidative damage. Isotopically reinforced PUFAs have recently been shown to be resistant towards free radical autoxidation with propagation rate constants some 10-fold less than that of the natural PUFAs.[23] The observed kinetic isotope effect arises due to the replacement of the reactive H-atoms located at *bis*-allyic methylene groups by deuterium. This demonstrated isotopic resistance to free radical oxidation stimulated the exploration of how D-PUFAs would affect inflammatory processes *in vivo*. Thus, RAW 264.7 macrophages enriched with D-PUFAs were studied to enquire how the inflammatory process was affected by their presence in these cells.

Our first experiments focused on the effect of D-PUFAs on protein adduction. Since D-PUFAs are resistant to autoxidation, we hypothesized that lipid electrophile formation would be reduced. The first experiments were carried out comparing protein adduction in macrophages which had been enriched with aLA, D_2-aLA, or a mixture of both. The blots from this experiment, presented previously in Figure 12, show reduced protein adduction in macrophages treated with D_2-aLA compared to aLA treated controls. A decrease in protein adduction was seen for the mixed treatment of aLA and D_2-aLA as well. This experiment demonstrated that isotopic reinforcement of PUFAs does indeed lower protein adduction.

In followup experiments, mixtures of aLA and D_4-LA were used for these studies. Macrophages were enriched with aLA at 15 μM or the mixture of aLA and D_4-LA at total concentrations of either 15 μM (7.5 μM of each) or 30 μM (15 μM of each). Western blots from these experiments showed decreases in protein adduction for macrophages enriched with both 15 μM and 30 μM of the aLA/D_4-LA mixture (Figure 20). This suggests that the presence of D-PUFAs lowers levels of lipid peroxidation within the macrophage during activation and results in decreased protein adduction. Furthermore, reduction in protein adduction for both concentrations of the aLA/D_4-LA mixture shows that this decrease is not simply due to the effects of dilution of the aLA in the original treatment conditions. In other words, a decrease in protein adduction is seen regardless of the concentration of aLA present during enrichment.

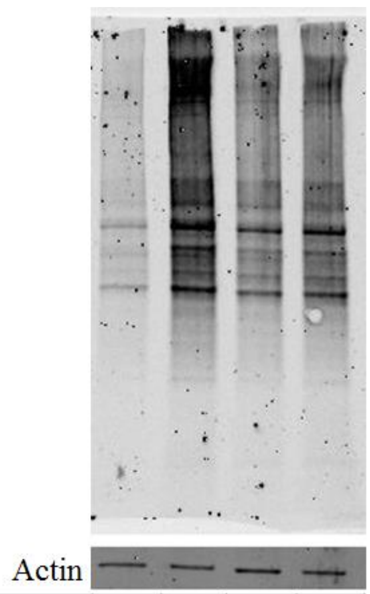

KLA	+	+	+	+
15 µM aLA	-	+	-	-
7.5 µM aLA/7.5 µM D_4-LA	-	-	+	-
15 µM aLA/15 µM D_4-LA	-	-	-	+

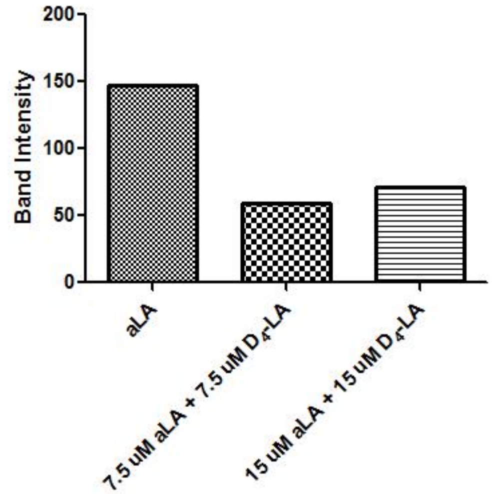

Figure 20. Comparison of protein adduction after KLA activation of RAW 264.7 macrophages treated with aLA or mixtures of aLA and D_2-aLA. The histogram (right) shows a comparison of band intensity from each enrichment condition.

Other experiments were carried out to investigate if expression levels and/or activity of proteins that are activated by the TLR-4 pathway were altered. The first set of experiments looked specifically at iNOS activity. iNOS is responsible for the production of nitric oxide, an important physiological messenger during immune response. Nitric oxide decomposes to nitrite (NO_2^-), and the Griess assay is used to measure its levels in media. Sampling of media from macrophages subjected to different enrichment conditions showed that levels of nitrite, and thus the activity of iNOS, were not affected by the presence of D-PUFAs (presented previously in Figure 10). Similarly, COX-2 expression was found to decrease slightly after enrichment with LA as well as

D-PUFAs (Figure 21). However, expression levels between macrophages which had been enriched with any of the lipids showed no statistical difference. These data suggest that major signaling and response pathways associated with the TLR-4 cascade suffered no significant changes after macrophages were enriched with D-PUFAs.

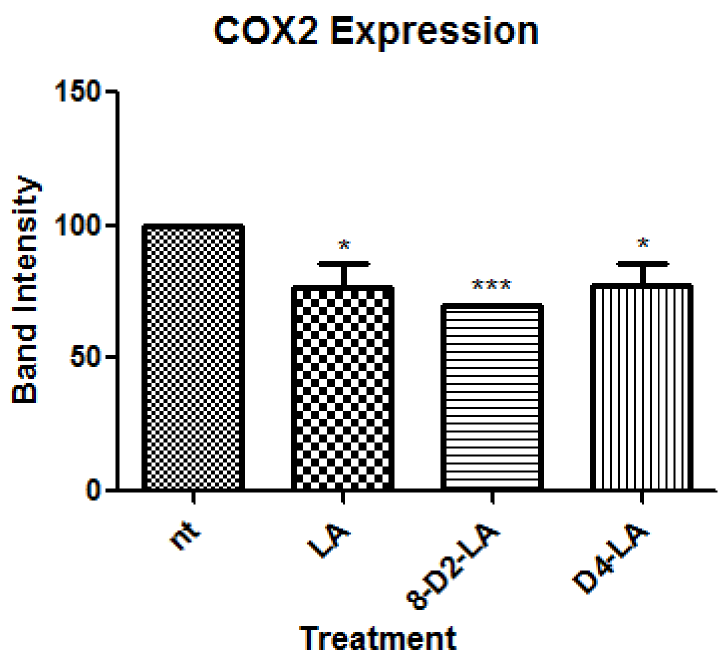

Figure 21. COX-2 expression levels as determined by Western blotting. Blots were digitized using UN-SCAN-IT gel 6.1, and bands corresponding to COX-2 were quantified and normalized to the actin band.

In order to better understand the metabolic fate of D-PUFAs, analysis of the PUFA profile of macrophages after enrichment with LA or D_4-LA was carried out by LCMS. The results show that macrophages biosynthesize D_4-AA from D_4-LA, with deuterium atoms presumably at carbons C13 and C17. D-PUFAs as a whole were found to comprise 50-60% of the total PUFA content of the macrophage after enrichment with 15 μM D_4-LA. Furthermore, D_4-AA was the major D-PUFA present in both unactivated and activated macrophages comprising roughly 86% and 72% of the total D-PUFA present, respectively (see Results, Figure 16).

By monitoring PGE_2 levels in media, COX-2 activity was found to decrease 40-50% in macrophages that had been treated with D_4-LA (see Results, Figure 14) even though COX-2 expression levels were relatively unaffected by the presence of D-PUFAS (Figure 21). This suggests that the decrease in PGE_2 formation must be the result of deuterium substitution in D_4-AA at C13. The first step in prostaglandin biosynthesis involves hydrogen atom abstraction at C13 by the tyrosyl radical in the COX-2 active site,[2] and isotopic substitution at that center is consistent with decreased PGE_2 formation. Abstraction of deuterium at C13 apparently involves a significant isotope effect.

Analysis of Linoleic Acid Oxidation Products (HODEs)

Analysis of LA and AA oxidation products derived from free radical oxidation (HODEs and HETEs) was also carried out to provide mechanistic insight. Oxidation products from activated macrophages were analyzed by LCMS using previously described methods.[75,46] Analysis showed that the total level of D_0-HODEs from LA oxidation were reduced by over 70% in D_4-LA enriched macrophages, dropping to 70 ± 3 ng/mg protein compared to 247 ± 67 ng/mg protein in LA enriched macrophages. When including the D_3-HODEs from D_4-LA oxidation, total HODE levels still saw a significant drop to 94 ± 6 ng/mg protein (a roughly 60% reduction). This data is shown in Figure 22.

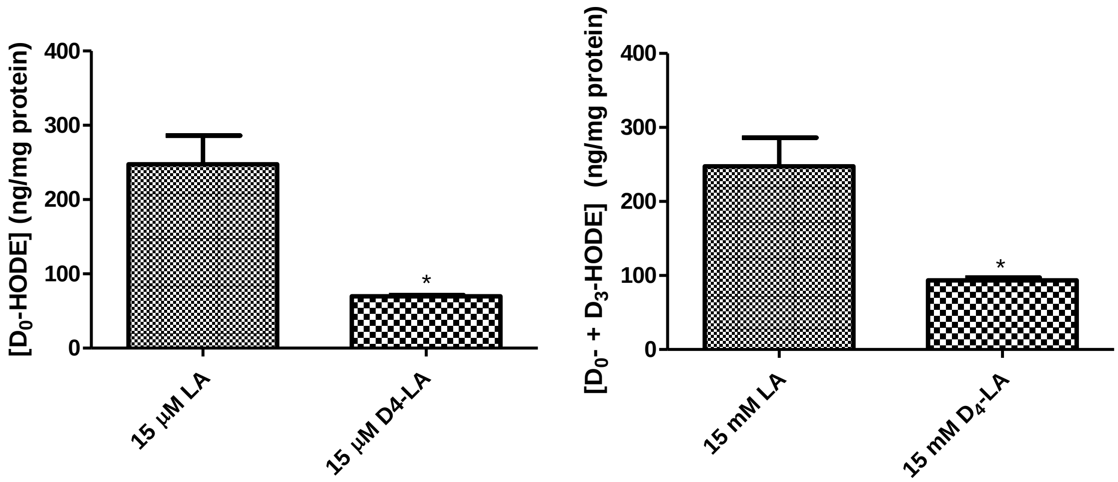

Treatment	KLA	$[D_0$-HODE] (ng/mg protein)	$[D_0 + D_3$-HODE] (ng/mg protein)
15 µM LA	+	247 ± 67	247 ± 67
15 µM D_4-LA	+	70 ± 3	94 ± 6

Figure 22. Comparison of D_0-HODEs (left) and D_0- + D_3-HODEs (right) from LA and D_4-LA treated macrophages.

One possible explanation for the reduction in total D_0-HODE levels in this study could be due to the fact that incorporation of D_4-LA results in an overall reduction of LA levels in the macrophages. Indeed, LA levels after KLA activation in D_4-LA enriched macrophages do decrease from roughly 23% to about 6% of the LA in the total PUFA pool (see Figure 16). To address this explanation, analysis of the data to determine the fraction of oxidation of the total LA can be done using Equation 1:

$$\frac{[D_0 - HODE]}{[LA]} = Oxidized\ Fraction\ of\ LA \qquad (1)$$

Using Equation 1, the fraction of oxidized LA was calculated to be unchanged when macrophages were treated with D_4-LA. This data, along with the concentration of LA for each enrichment condition are shown below in Figure 23.

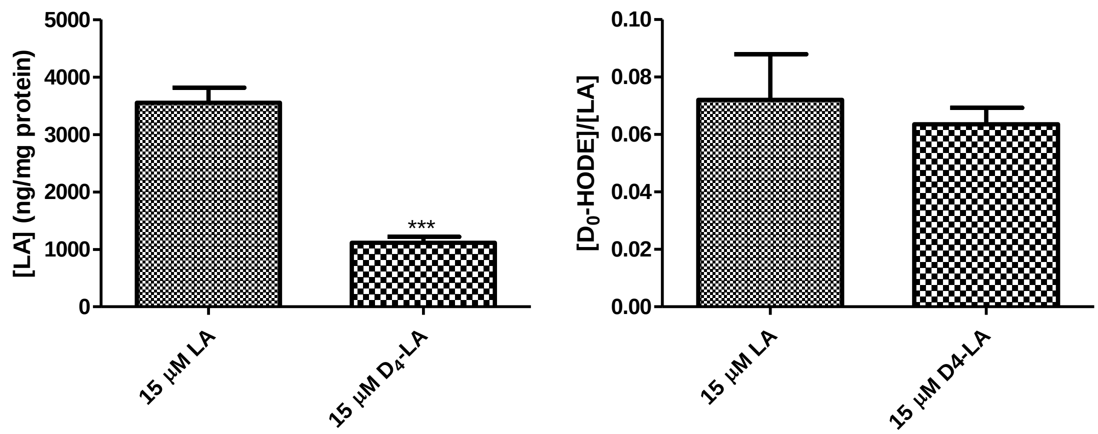

Treatment	KLA	[LA] (ng/mg protein)	[D_0-HODE] (ng/mg protein)	[D_0-HODE]/[LA]
15 µM LA	+	3550 ± 460	247 ± 67	0.07 ± 0.03
15 µM D_4-LA	+	1116 ± 174	70 ± 3	0.06 ± 0.01

Figure 23. Data showing the concentration of LA (ng/mg protein) (left) and the oxidized fraction of LA (right), calculated using Equation 1, for KLA activated RAW 264.7 macrophages enriched with 15 µM LA or 15 µM D_4-LA. The table gives absolute values for these data points.

According to these data, D_0-HODE formation was unchanged after enrichment with D_4-LA. However, D_4-LA treatment results in a roughly 69% decrease in the total endogenous LA in the macrophages. The drop in LA is accounted for by the incorporation of D_4-LA. Our observations suggest that 'total LA' levels, or [LA] + [D_4-LA], in macrophages enriched with 15 µM D_4-LA are similar to LA levels in macrophages after enrichment with 15 µM LA (Figure 24).

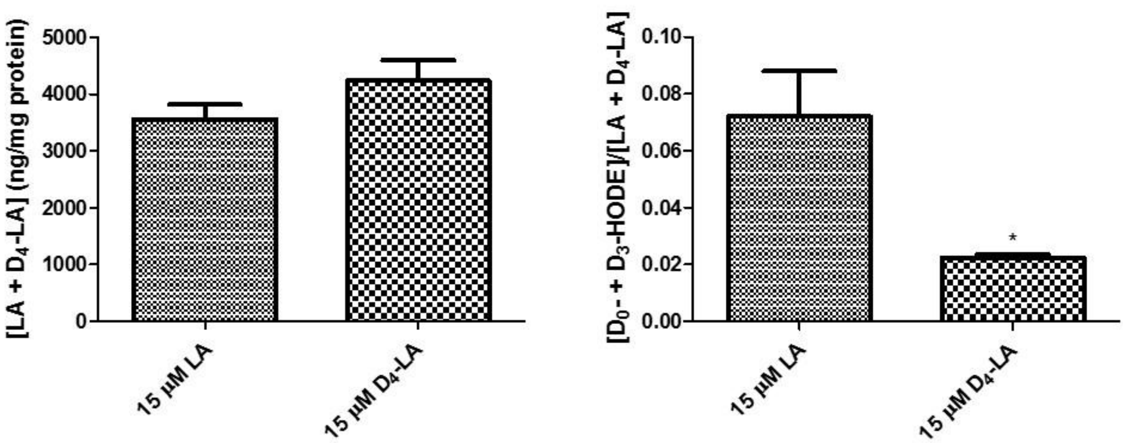

Treatment	KLA	[LA] (ng/mg protein)	[D_4-LA] (ng/mg protein)	[D_0- + D_3-HODE] (ng/mg protein)	[D_0- + D_3-HODE]/[LA +D_4-LA]
15 µM LA	+	3550 ± 460	N/A	247 ± 67	0.07 ± 0.02
15 µM D_4-LA	+	1120 ± 170	3110 ± 460	94 ± 6	0.02 ± 0.001

Figure 24. Data showing the concentration of total LA ([LA] + [D_4-LA], ng/mg protein) (left) and the oxidized fraction of total LA (right), calculated using Equation 2, for KLA activated RAW 264.7 macrophages enriched with 15 µM LA or 15 µM D_4-LA. The table gives absolute values for these data points.

The oxidized fraction of total LA was calculated using Equation 2:

$$\frac{[D_0-HODE+D_3-HODE]}{[LA+D_4-LA]} = Oxidized\ Fraction\ of\ Total\ LA \qquad \textbf{(2)}$$

Taking into account the total LA present, including the natural and deuterated forms, the oxidized fraction (D_0-HODEs + D_3-HODEs) of the total LA measured in the macrophages enriched with 15 µM D_4-LA is significantly decreased in comparison to LA enriched macrophages.

The distribution of HODEs between the four isomers also provides valuable insight into how peroxidation is affected after D_4-LA enrichment (Table 1). In macrophages enriched with LA the *trans,cis*-HODEs are formed preferrentially over the *trans,trans*-HODEs. The 9-*trans,cis*-HODE dominates the mixture. The same trend in HODE distribution is seen in macrophages treated with D_4-LA. Solution oxidations of LA at high concentrations give the 9- and 13-HODE regioisomers in more comparable amounts. A similar distortion in the HODE distribution has been noted previously during the autoxidation of 1-palmitoyl-2-linoleoyl-*sn*-glycero-3-phosphocholine (PLPC) in liposomes. At high concentrations of PLPC (0.5 M) the *trans,cis*- to *trans,trans*-HODE ratio (0.70) was found to favor the *trans,cis*-HODE products. In this instance, the asymmetrical product distribution was attributed to different local environments for the 9- and 13-peroxyl radicals.[46]

	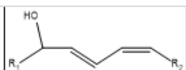	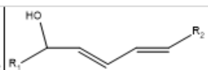	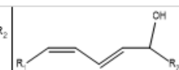	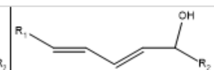	
Conditions	**13-*trans,cis* -HODE**	**13-*trans,trans* -HODE**	**9-*trans,cis* -HODE**	**9-*trans,trans* -HODE**	***trans,cis-/trans,trans* -HODE**
0.64 M in soltuion	0.12	0.37	0.12	0.39	0.32
15 μM LA + KLA	0.19	0.06	0.70	0.04	8.74
15 μM D_4-LA + KLA	0.14	0.25	0.58	0.03	2.58

Table 1. Distribution of HODEs after free radical oxidation of linoleic acid in solution, and in activated RAW 264.7 macrophages following enrichment with LA or D_4-LA.

An additional complication to the interpretation of the macrophage HODE data is the fact that COX-2 can convert LA into 9-*trans,cis*-HODE, providing another explanation for the asymmetrical product distribution. When LA is the substrate taken into the COX-2 active site, the expected product resulting from enzymatic activity is the 9-(*R*)-HODE based on the enzyme mechanism for hydrogen atom abstraction at the *bis*-allylic carbon (C11).[77,78,79] In order to understand whether or not COX-2 was a contributing factor in the preference for 9-*trans,cis*-HODE formation, the enantiomeric purity of the HODE products was analyzed using chiral chromatography mass spectrometry. The 9-*trans,cis*-HODE was of particular interest due to its prevalence HODE mixtures from both LA and D_4-LA enriched macrophages. In macrophages enriched with D_4-LA, the 9-(*R*)-HODE was found to be preferred by 4 to 1 over the 9-(*S*)-HODE

(Figure 25). This observation is consistent with the notion that roughly two-thirds of the 9-HODE product is formed enzymatically via the COX pathway, with the remainder of this product being formed by a non-enzymatic free radical mechanism.

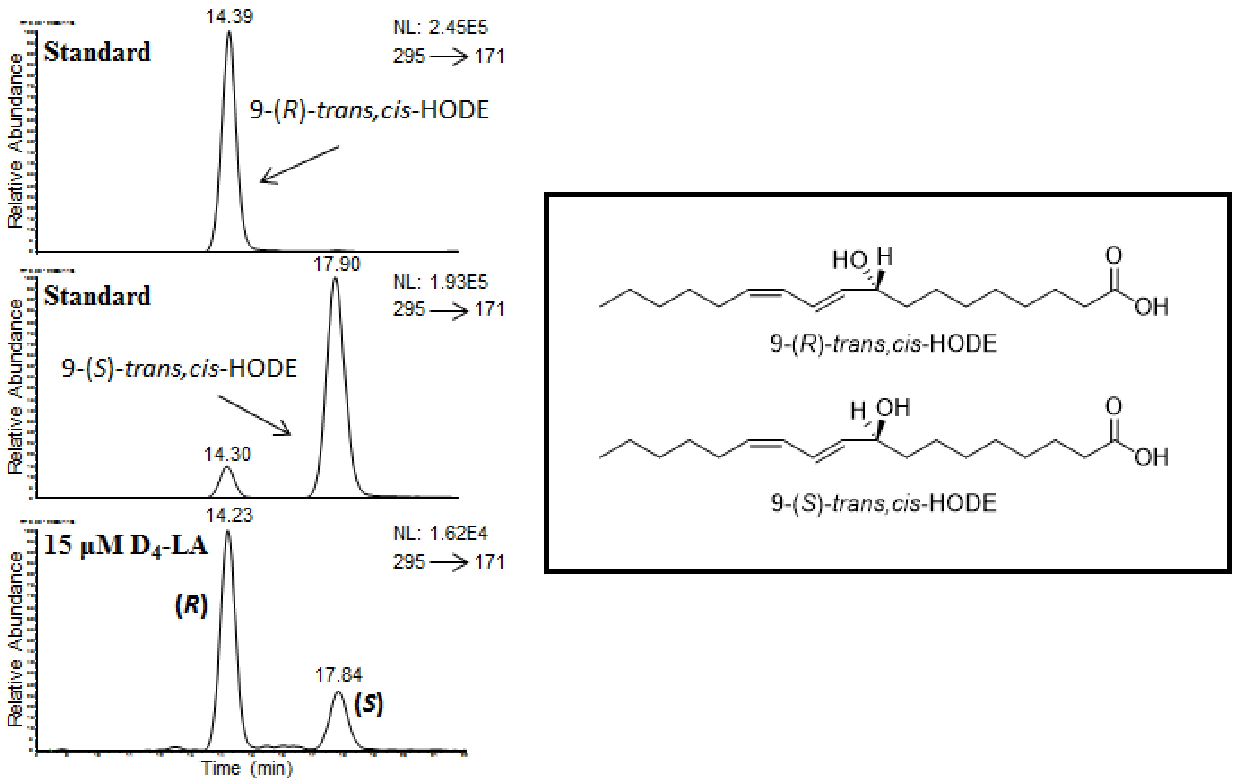

Figure 25. Analysis of D_0-9-*trans,cis*-HODE to determine enantiomeric distribution (R vs. S) in activated macrophages after enrichment with 15 μM D_4-LA. The HPLC-MS chromatograms on the left show enantiopure standards for 9-(R)-*trans,cis*-HODE, 9-(S)-*trans,cis*-HODE, and D_0-9-*trans,cis*-HODE extracted from the macrophages.

Chromatograms of lipid metabolite extracts from LA enriched macrophages were more complex than those from D_4-LA enriched macrophages and this complexity makes analysis of the optical purity of lipid metabolites formed in these incubations difficult. LA supplemented macrophages are subjected to a much more oxidative environment than D_4-LA enriched cells. The presence of D-PUFA lowers levels of peroxidation significantly, gives a clean chromatogram of LA oxidation products and allows for the enzymatic oxidation profile of LA to be observed.

Analysis of Arachidonic Acid Oxidation Products (HETEs)

11-HETE was found to be the major hydroxyeicosatetraenoic acid product formed and efforts were focused on the analysis and quantitation of D_0- and D_3-11-HETEs. The levels of 11-HETE were reduced significantly after enrichment with D_4-LA, and calculation of the percentage of oxidation of the entire AA pool ([AA + D_4-AA]) showed once again that this decrease in HETE formation was not purely due to dilution of AA by the presence of D_4-AA (Figure 26).

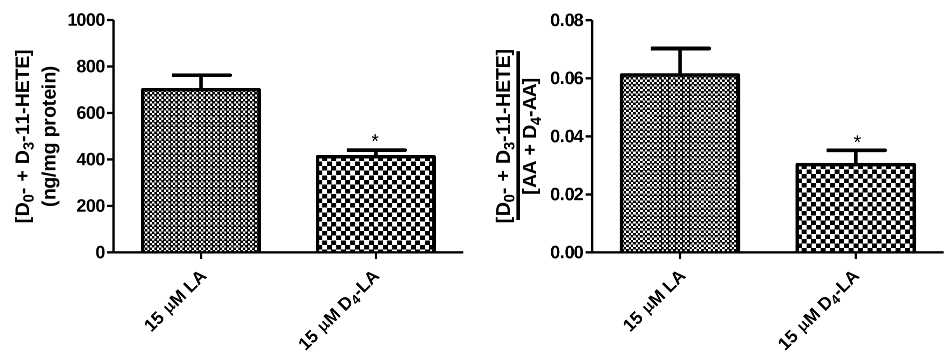

Treatment	[AA] (ng/mg protein)	[D_4-AA] (ng/mg protein)	[D_0-11-HETE] (ng/mg protein)	[D_3-11-HETE] (ng/mg protein)	[D_0- + D_3-HETE]/[AA + D_4-AA]
15 µM LA	11700 ± 1860	N/A	700 ± 110	0	0.06 ± 0.01
15 µM D_4-LA	5940 ± 960	8120 ± 1250	406 ± 50	7 ± 1	0.03 ± 0.01

Figure 26. Total HETE formation in activated macrophages. Histograms showing the level of total HETEs on the left ([D_0 + D_3-11-HETE]) and the oxidized fraction of total AA pool ([AA + D_4-AA]) on the right.

Analysis of HETEs on a chiral column was carried out to determine the optical purity of the products formed during macrophage activation. RAW 264.7 macrophages were enriched with LA or D_4-AA and the 5-, 11-, and 15-D_0-HETEs were analyzed. Chromatograms from the LCMS analysis of metabolites from D_4-LA enriched macrophages are presented below in Figure 27.

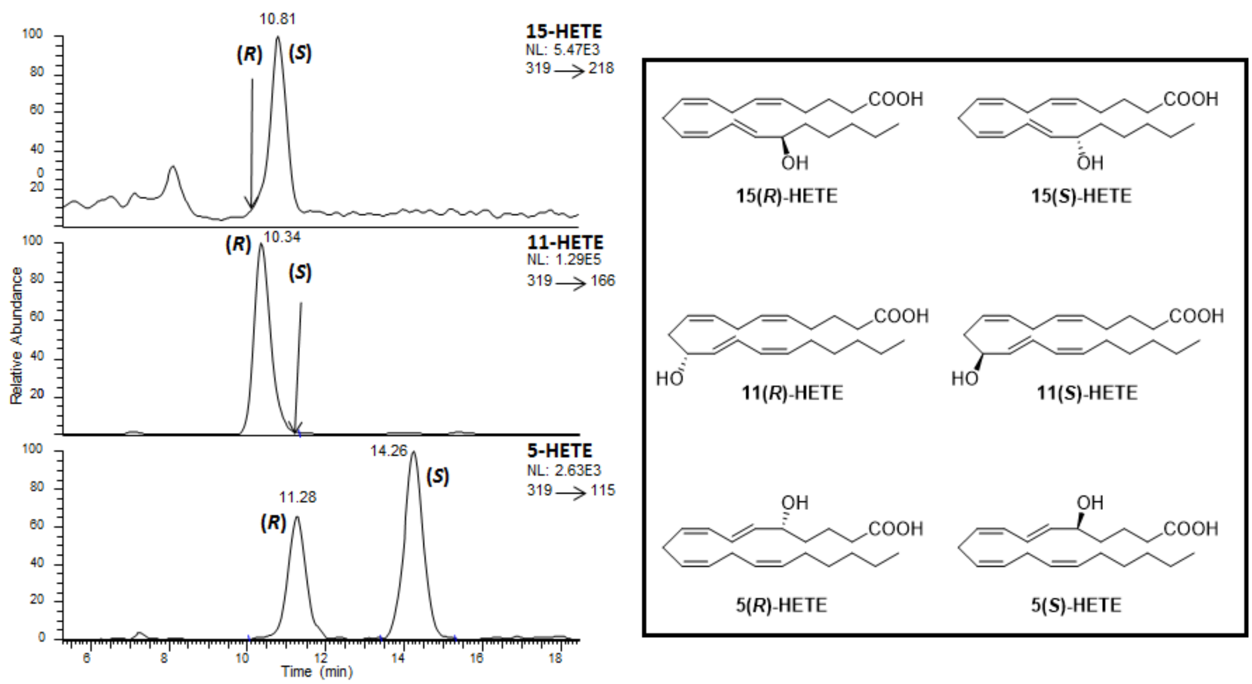

Figure 27. Analysis of 5-, 11-, and 15-D_0-HETEs to determine enantiomeric distribution (*R* vs *S*) in activated macrophages after enrichment with 15 µM D_4-LA. Analysis was carried out using chiral chromatography and HPLC-MS.

Again the chromatograms of lipid metabolite extracts from LA enriched macrophages were of lower quality than macrophages enriched with D_4-LA, likely due to the reasons mentioned previously. In macrophages enriched with D_4-LA the 15-D_0-HETE is found largely in the *S*-configuration, with small amounts of *R*-enantiomer falling in the shoulder of the peak. The 11-D_0-HETE is found in primarily the *R*-configuration as expected from COX-2 activity. The 5-D_0-HETE shows a modest preference for the *S*-enantiomer over the *R*-enantiomer. The formation of 15(*S*)-

D_0-HETE and 11(*R*)-D_0-HETE suggests that enrichment of macrophages with D_4-LA (and subsequent metabolism to D_4-AA) has no negative effect on COX-2 activity with respect to the formation of the expected HETE enantiomers. It does however lower total levels of HETEs (Figure 26) and PGE_2 (Figure 14 in Results).

4.5. Conclusions

Incorporation of D-PUFAs into several cellular systems and animal disease models has shown that these compounds have the ability to alleviate oxidative stress. Physical data on the fate of these D-PUFAs, including oxidation products, has not previously been reported in biological systems. The studies herein offer an in depth look at D-PUFA interactions in macrophages where an inflammatory response is easily induced by KLA.

The D_4-LA is rapidly taken up by the macrophages and metabolized to D_4-AA, both of which comprise 50-60% of the total LA and AA pools depending on activation state of the macrophage. The presence of these D-PUFAs significantly reduces lipid peroxidation as evidenced by the reduction in HODE levels. Furthermore, the percent oxidation of the total LA pool is significantly reduced which suggests that D-PUFAs are responsible for the reduction in lipid peroxidation as opposed to merely diluting the oxidizable substrates to give the appearance of reduced lipid peroxidation. Enrichment with D_4-LA also resulted in significant reductions in protein adduction by lipid electrophiles as seen in Western blots. Finally, significant cellular functions associated with the TLR-4 pathway are not negatively affected. Nitric oxide formation was unaffected by the presence of D-PUFAs, meaning that its expression was not negatively affected. In the same way, COX-2 expression was unaffected by D-PUFA supplementation. Despite normal expression levels, the production of PGs was significantly reduced, as were levels of 11-HETE.

The data presented in this chapter suggests that D_4-LA and other D-PUFAs may be excellent candidates as small molecules that can reduce oxidative stress in systems where chronic inflammation exists while allowing normal cellular processes to operate as usual. This suggests that levels of systematic inflammation may be reduced by the presence of these D-PUFAs, reducing the need for treatments using selective COX-2 inhibitors which are commonly associated with a number of undesirable side effects,[80,81] and by providing protection from free radical oxidation in diseases where free radical damage is heavily associated with progression such as Friedreich's ataxia and Parkinson's disease.

4.6. Acknowledgements

Many thanks to Dr. William Beavers, Dr. James Galligan, and Michelle Mitchner for their help and support with tissue culture, Western blotting, and other biological assays. Their help was invaluable and truly appreciated. I would also like to thank Dr. Lawrence Marnett for his willingness to allow me access to his lab space and resources throughout this project. Finally, thank you to Misha Shchepinov and Retrotope, Inc. for graciously synthesizing and providing the D-PUFAs used during these studies.

4.7. Experimental

Materials

All reagents were obtained from Sigma-Aldrich, St. Louis, MO, unless otherwise noted. Natural fatty acids and internal standards were purchased from Cayman Chemical, Ann Arbor, MI. Alkynyl linoleic acid (aLA) was synthesized as previously described.[82] Deuterated fatty acids were provided by Retrotope, Inc., Los Altos, CA. 100 mM stock solutions of PUFAs (natural, alkynyl, and deuterated) in ethanol were made prior to experiments and stored at -80 ˚C. RAW 264.7

macrophages were obtained from American Type Culture Collection (ATCC), Manassas, VA. Invitrogen Dulbecco's Modified Eagle Media - GlutaMAX (DMEM+GlutaMAX) was purchased from ThermoFiscer Scientific, Waltham, MA. Fetal bovine serum (FBS) was purchased from Atlas Biologicals, Fort Collins, CO.

Mass Spectrometry

PGE_2 was analyzed according to a previously published method.[83] HODE and HETE analysis was also carried out according to the literature.[46, 75] Analysis of *R* and *S* distribution for HODEs and HETEs was carried out using the same mass spectrometry settings identical to that of HODE and HETE analysis. Chromatography was carried out on a Chiracel AD-H column (250 x 4.6 mm, 5 μm, 1.0 mL/min, elution solvent: 3% ethanol, 0.1% acetic acid in hexanes). Free fatty acids were separated on a Discovery C18 column (150 x 2.1 mm, 5 μm, 0.2 mL/min, elution solvent: 0.1% acetic acid in methanol).

RAW 264.7 Culture

RAW 264.7 macrophages were plated at 1 x 10^6 cells in 8 mL of DMEM+GlutaMAX and 10% FBS in 100 mm plates or 3.5 x 10^6 cells in 20 mL of DMEM+GlutaMAX and 10% FBS in 150 mm plates. Macrophages were incubated for 24 h at 37 ˚C. The old media was removed. DMEM+GlutaMAX and 10% FBS containing desired concentration of alkynyl, deuterated, or natural PUFA was added to each plate. After incubation for 24 h, the old media was removed and DMEM+GlutaMAX +/- Kdo_2-Lipid A (100 ng/mL) was added. After a final incubation for 24 h, cells were scraped into fresh media and pelleted at 1000 rpm for 5 min. 100 μL of a BHT and PPh_3 solution (10 mg BHT and 25 mg PPh_3 in 10 mL ethanol) was immediately added to the cell pellet. Pellets were stored at -80 ˚C until further analysis.

Biotin Conjugation and Western Blotting

Cells were lysed in 1 mL lysis buffer (1% IGEPAL + 50 mM HEPEs + 100 mM NaCl + 0.5% PIC). Debris were pelleted at 16000g at 4 ˚C for 10 min. The supernatant was transferred to a new microcentrifuge tube and $NaBH_4$ (5 mM in H_2O) was added. Samples were turned end over end for 1 h at room temperature. Reduction was quenched by the addition of 10 µL of acetone. 50 µL of streptavidin beads were added to each sample, again turning end over end for 2 hr at room temperature. Beads were pelleted at 100g for 1 min. Supernatant was transferred to a new microcentrifuge tube. A bicinchoninic acid assay (BCA assay) was performed to determine total protein concentration of each sample. Samples were diluted accordingly to 240 µL total volume with water togive a final protein concentration of 0.5 µg/µL.

Stock solutions of 100 mM TCEP, 100 mM $CuSO_4$, 10 mM TBTA, and 20 mM N_3-Biotin were made, and 2.5 µL of each was added to each sample, resulting in a final sample volume of 250 µL and 1 mM TCEP, 1 mM $CuSO_4$, 0.1 mM TBTA and 0.2 mM N_3-Biotin. Samples were turned end over at room temperature overnight. Samples were then diluted 1:1 with 95:5 Laemli:BME loading buffer and boiled for 10 min.

Samples were then loaded on 4-20% Biorad gel with 4 µL (4 µg protein) loaded to each lane. Gels were run at 140V until completion. The gel was transferred to a 0.45 µM nitrocellulose membrane at 100V for 1 hr. The membrane was then rocked in Odyssey blocking buffer for 30 min at room temperature. The membrane was then rocked in 5 mL enhancced Odyssey blocking buffer (10 µL Tween 20, 10 µL SDS) with Actin (goat, 1:500) and SAIRDye 800 CW (streptavidin, 1:5000) at 4 ˚C overnight. Blots were washed with TBST (3 x 5 min.) at room temperature. Membrane was then rocked in 5 mL enhanced Odyssey blocking buffer containing 2˚ antibody (donkey anti-goat IRDie 680LT, 1:5000) for 45 min. at room temperature. Blot was again washed with TBST (3 x 5 min.) and scanned on Odyssey scanner.

Analysis of Free Fatty Acids and Lipid Metabolites

After treatment and activation, cells were scraped and pelleted according to the procedure outlined above. Excess media was removed. 100 μL of a solution containing BHT and PPh_3 (10 mg and 25 mg, respectively, in 10 mL EtOH) was added immediately. 100 μL of 17:0 standard (10 μg/mL) and 40 μL D_8-15(*S*)-HETE (10 μg/mL) were added. Cells were taken up in 2 mL 5% HCl (aq.) and extracted with 3 mL Folch solvent (2:1 $CHCl_3$/MeOH with 50 mg/L BHT). The organic layer was collected, blown dry, and resuspended in methanol (1 mL). 3M LiOH (1 mL) was added, after which samples were incubated at 37 ˚C for 1 hr. Samples were acidified with con HCl and extracted with 1 mL of 4:1 ethyl acetate:$CHCl_3$. The organic layer was blown dry. Samples were stored at -80 ˚C until analysis.

Griess Assay

In order to assess iNOS activity, nitrite (NO_2^-) present in the media after activation was quantified using the Griess assay. Macrophages were plated according to the 'RAW 264.7 Macrophage Culture' section above and enriched with 15 μM LA, 8-D_2-LA, or D_4-LA. Unenriched controls were also plated. After +/- KLA treatment, 1 mL of media was removed from each plate. 100 μL of each media sample was dispensed in a 96-well plate. 50 μL of sulfanilamide solution (10 mg/mL in aqueous 5% phosphoric acid) was added to each well. The plate was allowed to develop for 10 minutes in the dark at room temperature. 50 μL of NED solution (N-1-napthylethylenediamine dihydrocholride in water, 1 mg/mL) was then added to each well. The plate was again developed at room temperature in the dark for 20 minutes. After incubation, absorbance of each well was measured using a plate reader at 550 nm. Absorbance values were plotted against a nitrite standard reference curve which was plated and exposed to Griess reagents at the same time.

Cyclooxygenase-2 Expression

Macrophages from the Griess Assay were collected and lysed according to the 'RAW 264.7 Macrophage Culture' section. A BCA assay was run to determine protein concentration, and samples were diluted to 4 mg protein/mL in water (100 μL total volume). Samples were diluted 1:1 in Laemli:BME (95:5) loading buffer and boiled for 10 min. Samples were then loaded onto a 4-20% precast gel, with 15 μL (7.5 mg total protein) into each well. Gels were run at 150V until completion, followed by transfer to 0.45 μM nitrocellulose membrane at 100V for 1 hr. Blots were rocked in Odyssey blocking buffer for 1.5 hr at room temperature, followed by rocking in 5 mL of 1:1 TBST:Odyssey blocking buffer with 10 μL SDS, COX-2 antibody (1:1000) and actin (goat, 1:2500) overnight at 4 ˚C.

Blots were washed with TBST (2 x 15 min) at room temperature, then rocked in 5 mL of 1:1 TBST:Odyssey blocking buffer with 10 μL SDS and donkey anti-rabbit IR Dye 680LT (1:5000) and donkey anti-goat 800CW (1:5000) for 1 hr at room temperature. Blots were once again washed in TBST (2 x 15 min) and scanned using the Odyssey scanner.

Prostaglandin Formation

In order to assess the activity level of COX-2, levels of PGE_2 in the media were determined. Macrophages were plated according to the 'RAW 264.7 Macrophage Culture' section and enriched with 15 μM LA or 15 μM D_4-LA. After the activation step (+/- KLA), 4 mL of media was collected from each plate. Media was delivered directly into a falcon tube holding 4 mL of ethyl acetate containing the internal standard D_4-prostaglandin E_2. The media was extracted, and the organic layer blown dry. Residue was resuspended in methanol and analyzed by LC-MS.

4.8. References

1. Jain, M. K.; Wagner, R. C., *Introduction to Biological Membranes*. 1 ed.; John Wiley and Sons: New York, 1980; p 382.

2. Rouzer, C. A.; Marnett, L. J., Mechanism of free radical oxygenation of polyunsaturated fatty acids by cyclooxygenases. *Chem. Rev.* **2003,** *103,* 2239-2304.

3. Smith, W. L.; Lands, W. E. M., Oxygenation of unsaturated fatty-acids by soybean lipoxygenase. *J. Biol. Chem.* **1972,** *247*, 1038-1047.

4. Losito, I.; Conte, E.; Introna, B.; Megli, F. M.; Palmisano, F., Improved specificity of cardiolipin peroxidation by soybean lipoxygenase: a liquid chromatography - electrospray ionization mass spectrometry investigation. *J. Mass Spectrom.* **2011,** *46*, 1255-1262.

5. Porter, N. A., A perspective on free radical autoxidation: The physical organic chemistry of polyunsaturated fatty acid and sterol peroxidation. *J. Org. Chem.* **2013,** *78*, 3511-3524.

6. Pratt, D. A.; Tallman, K. A.; Porter, N. A., Free radical oxidation of polyunsaturated lipids: New mechanistic insights and the development of peroxyl radical clocks. *Acc. Chem. Res.* **2011,** *44*, 458-467.

7. Dobretsov, G. E.; Borschevskaya, T. A.; Petrov, V. A.; Vladimirov, Y. A., The increase of phospholipidbilayer rigidity after lipid peroxidation. *FEBS Lett.* **1977,** *84*, 125-128.

8. Chatgilialoglu, C.; Ferreri, C., Trans lipids: the free radical path. *Acc. Chem. Res.* **2005,** *38*, 441-448.

9. Berliner, J. A.; Heinecke, J. W., The role of oxidized lipoproteins in atherogenesis. *Free Radic. Biol. Med.* **1996,** *20*, 707-727.

10. Berliner, J. A.; Leitinger, N.; Tsimikas, S., The role of oxidized phospholipids in atherosclerosis. *J. Lipid Res.* **2009,** *50*, S207-S212.

11. Hammad, L. A.; Wu, G. X.; Saleh, M. M.; Klouckova, I.; Dobrolecki, L. E.; Hickey, R. J.; Schnaper, L.; Novotny, M. V.; Mechref, Y., Elevated levels of hydroxylated phosphocholine lipids in the blood serum of breast cancer patients. *Rapid Commun. Mass Spectrom.* **2009,** *23*, 863-876.

12. Imai, Y.; Kuba, K.; Neely, G. G.; Yaghubian-Malhami, R.; Perkmann, T.; van Loo, G.; Ermolaeva, M.; Veldhuizen, R.; Leung, Y. H.; Wang, H.; Liu, H.; Sun, Y.; Pasparakis, M.; Kopf, M.; Mech, C.; Bavari, S.; Peiris, J. S.; Slutsky, A. S.; Akira, S.; Hultqvist, M.; Holmdahl, R.; Nicholls, J.; Jiang, C.; Binder, C. J.; Penninger, J. M., Identification of oxidative stress and Toll-like receptor 4 signaling as a key pathway of acute lung injury. *Cell* **2008,** *133*, 235-249.

13. Nonas, S.; Miller, I.; Kawkitinarong, K.; Chatchavalvanich, S.; Gorshkova, I.; Bochkov, V. N.; Leitinger, N.; Natarajan, V.; Garcia, J. G.; Birukov, K. G., Oxidized phospholipids reduce

vascular leak and inflammation in rat model of acute lung injury. *Am. J. Respir. Crit. Care. Med.* **2006,** *173*, 1130-1138.

14. McGeer, P. L.; McGeer, E. G., Inflammation and neurodegeneration in Parkinson's disease. *Parkinsonism Relat. Disord.* **2004,** *10*, S3-S7.

15. Dexter, D. T.; Carter, C. J.; Wells, F. R.; Javoy-Agid, F.; Agid, Y.; Lees, A.; Jenner, P.; Marsden, C. D., Basal lipid peroxidation in substantia nigra is increased in Parkinson's disease. *J. Neurochem.* **1989,** *52*, 381-389.

16. Morrow, J. D.; Harris, T. M.; Roberts, L. J., Noncyclooxygenase oxidative formation of a series of novel prostaglandins: analytical ramifications for measurement of eicosanoids. *Anal. Biochem.* **1990,** *184*, 1-10.

17. Tracy, R. P., The five cardinal signs of inflammation: Calor, Dolor, Rubor, Tumor ... and Penuria (apologies to Aulus Cornelius Celsus, *De medicina*, c. A.D. 25). *J. Gerontol. A Biol. Sci. Med. Sci.* **2006,** *61*, 1051-1052.

18. Nathan, C.; Ding, A., Nonresolving inflammation. *Cell* **2010,** *140*, 871-882.

19. Shchepinov, M. S., Reactive oxygen species, isotope effect, essential nutrients, and enhanced longevity. *Rejuvenation Res.* **2007,** *10*, 47-60.

20. Hill, S.; Hirano, K.; Shmanai, V. V.; Marbois, B. N.; Vidovic, D.; Bekish, A. V.; Kay, B.; Tse, V.; Fine, J.; Clarke, C. F.; Shchepinov, M. S., Isotope-reinforced polyunsaturated fatty acids protect yeast cells from oxidative stress. *Free Radic. Biol. Med.* **2011,** *50*, 130-138.

21. Shchepinov, M.; Chou, V.; Pollock, E.; Langston, P.; Cantor, C.; Molinari, R.; Manning-Bog, A., Isotopic reinforcement of essential polyunsaturated fatty acids diminishes nigrostriatal degeneration in a mouse model of Parkinson's disease. *Toxicol. Lett.* **2011,** *207*, 97-103.

22. Cotticelli, M. G.; Crabbe, A. M.; Wilson, R. B.; Shchepinov, M. S., Insights into the role of oxidative stress in the pathology of Friedreich ataxia using peroxidation resistant polyunsaturated fatty acids. *Redox Biol.* **2013,** *1*, 398-404.

23. Hill, S.; Lamberson, C. R.; Xu, L.; To, R.; Tsui, H. S.; Shmanai, V. V.; Bekish, A. V.; Awad, A. M.; Marbois, B. N.; Cantor, C. R.; Porter, N. A.; Clarke, C. F.; Shchepinov, M. S., Small amounts of isotope-reinforced polyunsaturated fatty acids suppress lipid autoxidation. *Free Radic. Biol. Med.* **2012,** *53*, 893-906.

24. Bowry, V. W.; Stocker, R., Tocopherol-mediated peroxidation. The prooxidant effect of vitamin-E on the radical-initiated oxidation of human low-density lipoprotein. *J. Am. Chem. Soc.* **1993,** *115*, 6029-6044.

25. Lamberson, C. R.; Xu, L. B.; Muchalski, H.; Montenegro-Burke, J. R.; Shmanai, V. V.; Bekish, A. V.; McLean, J. A.; Clarke, C. F.; Shchepinov, M. S.; Porter, N. A., Unusual kinetic

isotope effects of deuterium reinforced polyunsaturated fatty acids in tocopherol-mediated free radical chain oxidations. *J. Am. Chem. Soc.* **2014,** *136*, 838-841.

26. Libby, P., Inflammation in atherosclerosis. *Nature* **2002,** *420*, 868-874.

27. Coussens, L. M.; Werb, Z., Inflammation and cancer. *Nature* **2002,** *420*, 860-867.

28. Balough, K.; McCubbin, M.; Weinberger, M.; Smits, W.; Ahrens, R.; Fick, R., The relationship between infection and inflammation in the early stages of lung disease from cystic fibrosis. *Pediatr. Pulmonol.* **1995,** *20*, 63-70.

29. Chmiel, J. F.; Berger, M.; Konstan, M. W., The role of inflammation in the pathophysiology of CF lung disease. *Clin. Rev. Allergy Immunol.* **2002,** *23*, 5-27.

30. Himmelfarb, J., Poor nutritional status and inflammation: Linking oxidative stress and inflammation in kidney disease: Which is the chicken and which is the egg? *Sem. Dialysis* **2004,** *17*, 449-454.

31. Oberg, B. P.; McMenamin, E.; Lucas, F. L. E. E.; McMonagle, E.; Morrow, J.; Ikizler, T. A. L. P.; Himmelfarb, J., Increased prevalence of oxidant stress and inflammation in patients with moderate to severe chronic kidney disease. *Kidney Int.* **2004,** *65*, 1009-1016.

32. Reddy, J. K.; Rao, M. S., Lipid metabolism and liver inflammation. II. Fatty liver disease and fatty acid oxidation. *Am. J. Physiol. Gastrointest. Liver Physiol.* **2006,** *290*, G852-G858.

33. Gao, H.; Hong, J., Why neurodegenerative diseases are progressive: uncontrolled inflammation drives disease progression. *Trends Immunol.* **2008,** *29*, 357-365.

34. Zhang, X.; Mosser, D. M., Macrophage activation by endogenous danger signals. *J. Pathol.* **2008,** *214*, 161-178.

35. Park, J. S.; Svetkauskaite, D.; He, Q.; Kim, J. Y.; Strassheim, D.; Ishizaka, A.; Abraham, E., Involvement of toll-like receptors 2 and 4 in cellular activation by high mobility group box 1 protein. *J. Biol. Chem.* **2004,** *279*, 7370-7377.

36. West, A. P.; Koblansky, A. A.; Ghosh, S., Recognition and signaling by toll-like receptors. *Annu. Rev. Cell Dev. Biol.* **2006,** *22*, 409-437.

37. West, A. P.; Brodsky, I. E.; Rahner, C.; Woo, D. K.; Erdjument-Bromage, H.; Tempst, P.; Walsh, M. C.; Choi, Y.; Shadel, G. S.; Ghosh, S., TLR signalling augments macrophage bactericidal activity through mitochondrial ROS. *Nature* **2011,** *472*, 476-480.

38. MacMicking, J. D.; North, R. J.; LaCourse, R.; Mudgett, J. S.; Shah, S. K.; Nathan, C. F., Identification of nitric oxide synthase as a protective locus against tuberculosis. *Proc. Natl. Acad. Sci. U.S.A.* **1997,** *94*, 5243-5248.

39. Rouzer, C. A.; Scott, W. A.; Kempe, J.; Cohn, Z. A., Prostaglandin synthesis by macrophages requires a specific receptor-ligant interaction. *Proc. Natl. Acad. Sci. U.S.A.* **1980,** *77*, 4279-4282.

40. Rouzer, C. A.; Scott, W. A.; Cohn, Z. A.; Blackburn, P.; Manning, J. M., Mouse peritoneal macrophages release leukotriene C in response to phagocytic stimulus. *Proc. Natl. Acad. Sci. U.S.A.* **1980,** *77*, 4928-4932.

41. Bozinovski, S.; Seow, H. J.; Chan, S. P. J.; Anthony, D.; McQualter, J.; Hansen, M.; Jenkins, B. J.; Anderson, G. P.; Vlahos, R., Innate cellular sources of interleukin-17A regulate macrophage accumulation in cigarette-smoke-induced lung inflammation in mice. *Clin. Sci.* **2015,** *129*, 785-796.

42. O'Shea, J. J.; Murray, P. J., Cytokine signaling modules in inflammatory responses. *Immunity* **2008,** *28*, 477-487.

43. Barnes, P. J.; Shapiro, S. D.; Pauwels, R. A., Chronic obstructive pulmonary disease: Molecular and cellular mechanisms. *Eur. Respir. J.* **2003,** *22*, 672-688.

44. Churg, A.; Wang, R. D.; Tai, H.; Wang, X.; Xie, C.; Dai, J.; Shapiro, S. D.; Wright, J. L., Macrophage metalloelastase mediates acute cigarette smoke-induced inflammation via tumor necrosis factor-alpha release. *Am. J. Respir. Crit. Care Med.* **2003,** *167*, 1083-1089.

45. Hiraiwa, K.; van Eeden, S. F., Contribution of lung macrophages to the inflammatory responses induced by exposure to air pollutants. *Mediators Inflamm.* **2013,** *2013*, 1-10.

46. Xu, L.; Davis, T. A.; Porter, N. A., Rate constants for peroxidation of polyunsaturated fatty acids and sterols in solution and in liposomes. *J. Am. Chem. Soc.* **2009,** *131*, 13037-13044.

47. Howard, J. A.; Ingold, K. U., Absolute rate constants for hydrocarbon autoxidation. VI. Alkyl aromatic and olefinic hydrocarbons. *Can. J. Chem.* **1967,** *45*, 793-802.

48. Cosgrove, J. P.; Church, D. F.; Pryor, W. A., The kinetics of the autoxidation of polyunsaturated fatty acids. *Lipids* **1987,** *22*, 299-304.

49. Yin, H.; Xu, L.; Porter, N. A., Free radical lipid peroxidation: mechanisms and analysis. *Chem. Rev.* **2011,** *111*, 5944-5972.

50. Milne, G. L.; Dai, Q.; Roberts II, L. J., The isoprostanes—25 years later. *Biochim. Biophys. Acta* **2015,** *1851*, 433-445.

51. Il'yasova, D.; Spasojevic, I.; Wang, F.; Tolun, A. A.; Base, K.; Young, S. P.; Marcom, P. K.; Marks, J.; Mixon, G.; DiGiulio, R.; Millington, D. S., Urinary biomarkers of oxidative status in a clinical model of oxidative assault. *Cancer Epidemiol. Biomarkers Prev.* **2010,** *19*, 1506-1510.

52. Masoodi, M.; Nicolaou, A., Lipidomic analysis of twenty-seven prostanoids and isoprostanes by liquid chromatography/electrospray tandem mass spectrometry. *Rapid Commun. Mass Spectrom.* **2006,** *20*, 3023-3029.

53. Esterbauer, H.; Schaur, R. J.; Zollner, H., Chemistry and biochemistry of 4-hydroxynonenal, malonaldehyde and related aldehydes. *Free Radic. Biol. Med.* **1991,** *11*, 81-128.

54. Sayre, L. M.; Lin, D.; Yuan, Q.; Zhu, X.; Tang, X., Protein adducts generated from products of lipid oxidation: Focus on HNE and ONE. *Drug Metab. Rev.* **2006,** *38*, 651-675.

55. Ji, C.; Kozak, K. R.; Marnett, L. J., IkB kinase, a molecular target for inhibition by 4-hydroxy-2-nonenal. *J. Biol. Chem.* **2001,** *276*, 18223-18228.

56. Dinkova-Kostova, A. T.; Holtzclaw, W. D.; Cole, R. N.; Itoh, K.; Wakabayashi, N.; Katoh, Y.; Yamamoto, M.; Talalay, P., Direct evidence that sulfhydryl groups of Keap1 are the sensors regulating induction of phase 2 enzymes that protect against carcinogens and oxidants. *Proc. Natl. Acad. Sci. U.S.A.* **2002,** *99*, 11908-11913.

57. Levonen, A. L.; Landar, A.; Ramachandran, A.; Ceaser, E. K.; Dickinson, D. A.; Zanoni, G.; Morrow, J. D.; Darley-Usmar, V. M., Cellular mechanisms of redox cell signalling: role of cysteine modification in controlling antioxidant defences in response to electrophilic lipid oxidation products. *Biochem. J.* **2004,** *378*, 373-382.

58. von Knethen, A.; Brune, B., Cyclooxygenase-2: An essential regulator of NO-mediated apoptosis. *FASEB J.* **1997,** *11*, 887-895.

59. Dong, L.; Vecchio, A. J.; Sharma, N. P.; Jurban, B. J.; Malkowski, M. G.; Smith, W. L., Human cyclooxygenase-2 is a sequence homodimer that functions as a conformational heterodimer. *J. Biol. Chem.* **2011,** *286*, 19035-19046.

60. Prusakiewicz, J. J.; Duggan, K. C.; Rouzer, C. A.; Marnett, L. J., Differential sensitivity and mechanism of inhibition of COX-2 oxygenation of arachidonic acid and 2-arachidonoylglycerol by ibuprofen and mefenamic acid. *Biochemistry* **2009,** *48*, 7353-7355.

61. Schneider, C.; Boeglin, W. E.; Brash, A. R., Identification of two cyclooxygenase active site residues, leucine 384 and glycine 526, that control carbon ring cyclization in prostaglandin biosynthesis. *J. Biol. Chem.* **2004,** *279*, 4404-4414.

62. Hartley, D. P.; Kroll, D. J.; Petersen, D. R., Prooxidant-initiated lipid peroxidation in isolated rat hepatocytes: Detection of 4-hydroxynonenal- and malondialdehyde-protein adducts. *Chem. Res. Toxicol.* **1997,** *10*, 895-905.

63. Neely, M. D.; Sidell, K. R.; Graham, D. G.; Montine, T. J., The lipid peroxidation product 4-hydroxynonenal inhibits neurite outgrowth, disrupts neuronal microtubules, and modifies cellular tubulin. *J. Neurochem* **1999,** *72*, 2323-2333.

64. Carbone, D. L.; Doorn, J. A.; Kiebler, Z.; Ickes, B. R.; Petersen, D. R., Modification of heat shock protein 90 by 4-hydroxynonenal in a rat model of chronic alcoholic liver disease. *J. Pharmacol. Exp. Ther.* **2005,** *315*, 8-15.

65. Uchida, K.; Szweda, L. I.; Chae, H. Z.; Stadtman, E. R., Immunochemical detection of 4-hydroxynonenal protein adducts in oxidized hepatocytes. *Proc. Natl. Acad. Sci. U.S.A.* **1993,** *90* (8742-8746).

66. Uchida, K.; Itakura, K.; Kawakishi, S.; Hiai, H.; Toyokuni, S.; Stadtman, E. R., Characterization of epitopes recognized by 4-hydroxy-2-nonenal specific antibodies. *Arch. Biochem. Biophys.* **1995,** *324*, 241-248.

67. Myers, D. S.; Ivanova, P. T.; Milne, S. B.; Brown, H. A., Quantitative analysis of glycerophospholipids by LC–MS: Acquisition, data handling, and interpretation. *Biochim. Biophys. Acta* **2011,** *1811*, 748-757.

68. Rouzer, C.; Ivanova, P.; Byrne, M.; Milne, S.; Marnett, L.; Brown, H., Lipid profiling reveals arachidonate deficiency in RAW264.7 cells: Structural and functional implications. *Biochemistry* **2006,** *45* (49), 14795-14808.

69. Tallman, K. A.; Armstrong, M. D.; Milne, S. B.; Marnett, L. J.; Brown, H. A.; Porter, N. A., Cobalt carbonyl complexes as probes for alkyne-tagged lipids. *J. Lipid Res.* **2013,** *54*, 859-868.

70. Milne, S. B.; Tallman, K. A.; Serwa, R.; Rouzer, C. A.; Armstrong, M. D.; Marnett, L. J.; Lukehart, C. M.; Porter, N. A.; Brown, H. A., Capture and release of alkyne-derivatized glycerophospholipids using cobalt chemistry. *Nat. Chem. Biol.* **2010,** *6*, 205-207.

71. Vila, A.; Tallman, K. A.; Jacobs, A. T.; Liebler, D. C.; Porter, N. A.; Marnett, L. J., Identification of protein targets of 4-hydroxynonenal using click chemistry for ex vivo biotinylation of azido and alkynyl derivatives. *Chem. Res. Toxicol.* **2008,** *21*, 432-444.

72. Kolb, H. C.; Sharpless, K. B., The growing impact of click chemistry on drug discovery. *Drug Discov. Today* **2003,** *8*, 1128-1137.

73. Bredt, D. S.; Snyder, S. H., Nitric oxide: A physiologic messenger molecule. *Annu. Rev. Biochem.* **1994,** *63*, 175-195.

74. Griess, P., Bemerkungen zu der Abhandlung der HH. Weselsky und Benedikt "Ueber einige azoverbindungen.". *Chem. Ber.* **1879,** *12*, 426-428.

75. Liu, W.; Yin, H.; Akazawa, Y. O.; Yoshida, Y.; Niki, E.; Porter, N. A., Ex vivo oxidation in tissue and plasma assays of hydroxyoctadecadienoates: Z,E/E,E stereoisomer ratios. *Chem. Res. Toxicol.* **2010,** *23*, 986-995.

76. Yin, H. Y.; Havrilla, C. M.; Gao, L.; Morrow, J. D.; Porter, N. A., Mechanisms for the formation of isoprostane endoperoxides from arachidonic acid - "Dioxetane" intermediate versus beta-fragmentation of peroxyl radicals. *J. Biol. Chem.* **2003,** *278*, 16720-16725.

77. Funk, C. D.; Powell, W. S., Release of prostaglandins and monohydroxy and trihydroxy metabolites of linoleic and arachidonic acids by adult and fetal aortae and ductus arteriosus. *J. Biol. Chem.* **1985,** *260*, 7481-7488.

78. Daret, D.; Blin, P.; Larrue, J., Synthesis of hydroxy fatty acids from linoleic acid by human blood platelets. *Prostaglandins* **1989,** *38*, 203-214.

79. Fujimoto, Y.; Yonemura, T.; Sakuma, S., Role of linoleic acid hydroperoxide preformed by cyclooxygenase-1 or -2 on the regulation of prostaglandin formation from arachidonic acid by the respective enzyme. *J. Clin. Biochem. Nutr.* **2008,** *43*, 65-68.

80. Khurana, P.; Jachak, S. M., Chemistry and biology of microsomal prostaglandin E_2 synthase-1 (mPGES-1) inhibitors as novel anti-inflammatory agents: Recent developments and current status. *RSC Adv.* **2016,** *6*, 28343-28369.

81. Melnikova, I., Future of COX2 inhibitors *Nat. Rev. Drug Discov.* **2005,** *4*, 453-454.

82. Windsor, K.; Genaro-Mattos, T. C.; Y., K. H.; Liu, W.; Tallman, K. A.; Miyamoto, S.; Korade, Z.; Porter, N. A., Probing lipid-protein adduction with alkynyl surrogates: Application to Smith-Lemli-Opitz syndrome. *J. Lipid Res.* **2013,** *54*, 2842-2850.

83. Kingsley, P. J.; Rouzer, C. A.; Saleh, S.; Marnett, L. J., Simultaneous analysis of prostaglandin glyceryl esters and prostaglandins by electrospray tandem mass spectrometry. *Anal. Biochem.* **2005,** *343*, 203-211.